

LOW-ORDER MULTI-PORT ARRAYS WITH REDUCED  
ELEMENT SPACING FOR DIGITAL BEAM-FORMING  
AND DIRECTION-FINDING

CHUA PING TYNG

NATIONAL UNIVERSITY OF SINGAPORE

2004

LOW-ORDER MULTI-PORT ARRAYS WITH REDUCED ELEMENT SPACING  
FOR DIGITAL BEAM-FORMING AND DIRECTION-FINDING

CHUA PING TYNG

*(B.Eng. (Hons.), NUS)*

A THESIS SUBMITTED  
FOR THE DEGREE OF MASTER OF ENGINEERING  
DEPARTMENT OF ELECTRICAL AND COMPUTER ENGINEERING  
NATIONAL UNIVERSITY OF SINGAPORE

2004

## SUMMARY

An array of three monopole elements with reduced element spacing of  $\lambda/20$  to  $\lambda/6$  is considered for application in digital beam-forming and direction-finding. The small element spacing introduces strong mutual coupling between the array elements, which affects the signal-to-noise-ratio performance of the array. A decoupling network can compensate for the mutual coupling effects so that simultaneous matching can be achieved at all the ports. This thesis discusses decoupling for arrays with three or more elements and describes the realization of decoupling networks using Kuroda's identities. Design equations for the decoupling network are presented. Experimental results show close agreement with the theoretical predictions. The decoupled prototype array has a bandwidth of 1% and a superdirective radiation pattern. This narrowband and superdirective antenna may find application for frequency selectivity in digital beam-forming and direction-finding.

## ACKNOWLEDGEMENTS

I would like to express special thanks to Dr. Jacob Carl Coetzee for his invaluable guidance and supervision in this project. I am indebted to him for his understanding and patience in times when problems were faced. It has been an enjoyable experience working with him. No words can ever fully express the gratitude that I have for Dr. Coetzee for the valuable experiences and knowledge that he has shared with me. Thank you.

My thanks also go to the following people who have helped to make this project a success:

- (a) Mr. Kevin Ho Ming Jiang – for his important and helpful advice.
- (b) Mr. Jalil – for his valuable advice on fabrication of the microstrip network.
- (c) Mr. Victor Liang and Mr. Chin (SQ Engineering & Trading Pte Ltd) – for manufacturing the antenna structures.
- (d) Mr. Chan (NUS ECE Workshop) – for manufacturing the antenna structures.
- (e) Mr. Quek and Mr. Sim (INTERHORIZON Corporation Pte Ltd) – for fabricating the microstrip networks.
- (f) Mr. Sing (NUS Microwave Lab) – for his help in the measurement of the antenna.
- (g) Mdm. Lee (NUS Microwave Lab) – for her help in the procurement of materials required.
- (h) My boyfriend, Jialong – for his love, support and encouragement.

# CONTENTS

<b>SUMMARY</b>	<b>I</b>
<b>ACKNOWLEDGEMENTS</b>	<b>II</b>
<b>CONTENTS</b>	<b>III</b>
<b>LIST OF FIGURES</b>	<b>VII</b>
<b>LIST OF TABLES</b>	<b>X</b>
<b>CHAPTER 1</b>	<b>1</b>
<b>INTRODUCTION</b>	<b>1</b>
1.1. Background	1
1.2. Objectives of the project	3
1.3. Outline of the project	3
1.4. Organization of the thesis	3
1.5. Publications	4
<b>CHAPTER 2</b>	<b>5</b>
<b>THEORETICAL BACKGROUND</b>	<b>5</b>
2.1. Introduction	5
2.2. Smart antennas and digital beam forming	5
2.3. Theory of mutual coupling	9
2.3.1. Mutual impedance between two linear elements	9
2.3.2. Mutual coupling in a circular array	11
2.4. Conclusion	13

<b>CHAPTER 3</b>	<b>14</b>
<b>MODELLING OF AN ARRAY ELEMENT</b>	<b>14</b>
3.1. Introduction	14
3.2. Antenna elements	14
3.3. IE3D modelling	16
3.3.1. About IE3D software	16
3.3.2. Construction of a monopole in IE3D	16
3.3.3. IE3D simulation settings	17
3.3.4. Radiation patterns from IE3D	18
3.3.5. Troubleshooting for IE3D modelling	20
3.4. HFSS modelling	21
3.4.1. About HFSS software	21
3.4.2. Construction of monopole in HFSS	21
3.4.3. HFSS simulation settings	22
3.4.4. Troubleshooting for HFSS modelling	25
3.5. Conclusion	25
<b>CHAPTER 4</b>	<b>26</b>
<b>DECOUPLING OF ARRAY</b>	<b>26</b>
4.1. Introduction	26
4.2. The need for a decoupled array	26
4.3. Theory of eigenmode analysis	29
4.4. A design for decoupling an array by modifying element length	31
4.4.1. Example A1	34
4.4.2. Example A2	41
4.5. A generalized design for the decoupling network of an array	44
4.5.1. Eigenmode analysis	45
4.5.2. Network analysis	47
4.5.3. Matching network	49

4.5.4. Example B1	50
4.5.5. Example B2	52
4.5.6. Example B3	53
4.6. Analytical solutions for array with more elements	55
4.7. Conclusion	55
<b>CHAPTER 5</b>	<b>57</b>
<b>DECOUPLING NETWORK IMPLEMENTATION</b>	<b>57</b>
5.1. Introduction	57
5.2. Realization of lumped elements	57
5.2.1. Kuroda's identities	57
5.2.2. Realization of series inductors	59
5.2.3. Realization of series capacitors	60
5.2.4. Realization of shunt inductors and capacitors	61
5.2.5. Summary of realization of ideal components	62
5.3. Preservation of symmetry in decoupling network	63
5.4. Interdigital capacitors as series capacitors	64
5.5. Conclusion	67
<b>CHAPTER 6</b>	<b>68</b>
<b>EXPERIMENTAL RESULTS</b>	<b>68</b>
6.1. Introduction	68
6.2. Construction of antenna hardware	68
6.2.1. Specifications of array element	68
6.2.2. Specifications of antenna support structure	70
6.2.3. The complete array	71
6.2.4. Specifications of microstrip network	73
6.2.5. Specifications of stripline network	76

6.3. Results	78
6.3.1. Verification of array element modelling	78
6.3.2. Results of microstrip design	81
6.3.3. Results of stripline design	84
6.4. Applications of decoupled array	87
6.5. Conclusion	87
<b>CHAPTER 7</b>	<b>88</b>
<b>CONCLUSION</b>	<b>88</b>
<b>REFERENCES</b>	<b>89</b>
<b>APPENDIX A</b>	<b>93</b>
<b>PROGRAM CODE FOR EIGENMODE ANALYSIS</b>	<b>93</b>
<b>APPENDIX B</b>	<b>99</b>
<b>PROGRAM CODE FOR NETWORK ANALYSIS</b>	<b>99</b>
<b>APPENDIX C</b>	<b>103</b>
<b>PROGRAM CODE FOR VERIFYING EIGENMODE AND NETWORK ANALYSES</b>	<b>103</b>
<b>APPENDIX D</b>	<b>110</b>
<b>PROGRAM CODE FOR 3-ELEMENT ARRAY</b>	<b>110</b>
<b>APPENDIX E</b>	<b>112</b>
<b>PROGRAM CODE FOR 4-ELEMENT ARRAY</b>	<b>112</b>
<b>APPENDIX F</b>	<b>114</b>
<b>PROGRAM CODE FOR 5-ELEMENT ARRAY</b>	<b>114</b>
<b>APPENDIX G</b>	<b>116</b>
<b>PROGRAM CODE OF 6-ELEMENT ARRAY</b>	<b>116</b>
<b>APPENDIX H</b>	<b>118</b>
<b>PROGRAM CODE FOR INTERDIGITAL CAPACITORS</b>	<b>118</b>
<b>APPENDIX I</b>	<b>129</b>
<b>CAD DRAWINGS OF THE ARRAY STRUCTURES</b>	<b>129</b>



## LIST OF FIGURES

Figure 2.1	A 120° sectorized cell pattern [11].	7
Figure 2.2	Independently steered beams at same frequency to each user [11].	7
Figure 2.3	A generic DBF antenna system [11].	8
Figure 2.4	A two-element antenna array.	9
Figure 2.5	A circular array of $M$ -elements.	11
Figure 3.1	A 3-element array.	15
Figure 3.2	Azimuth radiation pattern of array with port 1 excited.	18
Figure 3.3	Azimuth radiation pattern of array with port 2 excited.	19
Figure 3.4	Azimuth radiation pattern of array with port 3 excited.	19
Figure 3.5	Elevation radiation pattern of array with any one port excited.	20
Figure 3.6	Radiation patterns over grounds with finite and infinite conductivity.	21
Figure 4.1	Equivalent circuit for $m$ th eigenmode of array in receive mode.	27
Figure 4.2	Decoupling network for array with modified element length.	33
Figure 4.3	Radiation pattern of eigenmode A.	35
Figure 4.4	Radiation pattern of eigenmode B.	35
Figure 4.5	Radiation pattern of eigenmode C.	36
Figure 4.6	Plot of mode admittances over a range of frequencies (Example A1).	37
Figure 4.7	Point of intersection, F1 (Example A1).	38
Figure 4.8	An array with its decoupling network.	40
Figure 4.9	Radiation pattern of a decoupled array.	40
Figure 4.10	Plot of mode admittances over a range of frequencies (Example A2).	42
Figure 4.11	Point of intersection, F1 (Example A2).	43
Figure 4.12	A generalized decoupling network for a 3-element array.	45

Figure 4.13	Equivalent circuits for different eigenmodes of a 3-element array.....	46
Figure 4.14	A matching network section for a decoupled array. ....	49
Figure 4.15	A 3-element array with its decoupling and matching network. ....	51
Figure 5.1	Kuroda's identities [26]. ....	58
Figure 5.2	Kuroda's identity applied to a series inductor. ....	59
Figure 5.3	Steps involved in the transformation of a series inductor. ....	60
Figure 5.4	Steps to realize a series capacitor.....	61
Figure 5.5	Transformation for inductor to maintain symmetry.....	63
Figure 5.6	A typical interdigital capacitor.....	64
Figure 5.7	An equivalent circuit for a unit cell of two fingers of an interdigital capacitor.....	65
Figure 5.8	An equivalent circuit for the whole interdigital capacitor with $N$ fingers. ....	65
Figure 5.9	Implementation of a series capacitor as an interdigital capacitor. ....	66
Figure 6.1	Array elements. Monopoles: (a) Ideal. (b) Tapered. (c) Stepped. ....	69
Figure 6.2	Dimensions of the monopole manufactured. ....	69
Figure 6.3	A cross-section of a monopole and the supporting structure. ....	70
Figure 6.4	Picture showing the elements of the array. ....	72
Figure 6.5 (a)	Picture showing the top of the supporting structure. ....	72
Figure 6.5 (b)	Picture showing the bottom of the supporting structure. ....	73
Figure 6.6 (a)	Lumped components of the network for microstrip design. ....	74
Figure 6.6 (b)	Network after Kuroda's transformation for microstrip design. ....	75
Figure 6.6 (c)	Layout of the network for microstrip design. ....	75
Figure 6.7	Picture showing the fabricated microstrip network. ....	76
Figure 6.8	Layout of the network for stripline design.....	77

Figure 6.9	Picture showing the fabricated stripline network.....	77
Figure 6.10 (a)	Comparison of measured and simulation $S_{11}$ results of the array. ....	79
Figure 6.10 (b)	Comparison of measured and simulation $S_{11}$ results of the array. ....	79
Figure 6.10 (c)	Comparison of measured and simulation $S_{21}$ results of the array. ....	80
Figure 6.10 (d)	Comparison of measured and simulation $S_{21}$ results of the array. ....	80
Figure 6.11	Schematic drawing of microstrip circuit in ADS.....	82
Figure 6.12 (a)	Measured and theoretical $S_{11}$ results for microstrip design. ....	83
Figure 6.12 (b)	Measured and theoretical $S_{21}$ results for microstrip design. ....	83
Figure 6.13	Schematic drawing of stripline circuit in ADS.....	85
Figure 6.14 (a)	Measured and simulation $S_{11}$ results for stripline design.....	86
Figure 6.14 (b)	Measured and simulation $S_{21}$ results for stripline design. ....	86

## LIST OF TABLES

Table 3.1	Parameters of the 3-element array. ....	15
Table 3.2	HFSS simulation setup parameters. ....	24
Table 4.1	Parameters of the array for example A1. ....	34
Table 4.2	Parameters of the array for example A2. ....	41
Table 4.3	Parameters of the array for example B1. ....	50
Table 4.4	Admittance parameters of the array (Example B1). ....	51
Table 4.5	Decoupling and matching network configurations (Example B1). ....	51
Table 4.6	Parameters of the array for Example B2. ....	52
Table 4.7	Admittance parameters of the array (Example B2). ....	52
Table 4.8	Decoupling and matching network configurations (Example B2). ....	53
Table 4.9	Parameters of the array for Example B3. ....	53
Table 4.10	Admittance parameters of the array (Example B3). ....	54
Table 4.11	Decoupling and matching network configurations (Example B3). ....	54
Table 5.1	Transformation of ideal components to microstrip stubs. ....	62

# CHAPTER 1

## INTRODUCTION

### 1.1. Background

Arrays with reduced element spacing of  $\lambda/20$  to  $\lambda/6$  are applicable for digital beam-forming and direction-finding. However, the small element spacing introduces strong mutual coupling between the array elements. Mutual coupling effects are significant even for inter-element spacing of more than half a wavelength [1], and the effects are more severe when the spacing is reduced beyond that. If mutual coupling is not properly accounted for, there is significant degradation of the signal-to-interference-plus-noise ratio (SINR) [1, 2]. The decrease in the SINR reduces the detection range and increases the minimum detectable velocity of the target in space-time adaptive processing [2]. The presence of mutual coupling decreases the eigenvalues of the covariance matrix of the signal, which controls the response time of an adaptive array [1]. It is therefore vital that mutual coupling be taken into consideration during the design of arrays with small element spacing.

Various compensation techniques have been proposed. In shaped beam antennas, modifying the excitation vector compensates for the mutual coupling effect [3]. In digital beam-forming antenna arrays, a matrix multiplication technique may be performed on the received signal vector to restore the signals at the isolated elements in the absence of coupling [4 – 7]. Determination of the coupling matrix can be achieved by the method of Fourier decomposition, method of least-squares solution or the method of moments [7].

However, it has been shown in [8, 9] that signal-to-noise maximization can only be achieved if all mode admittances of the array are identical, which necessitates the use of a decoupling network. Without a decoupling network, the mode admittances cannot be simultaneously matched to the optimum source admittance, and some modes will be badly noise-matched. If these modes are needed for forming the desired radiation characteristic, the signal-to-noise-ratio (SNR) will be reduced substantially. This effect cannot be compensated for by means of digital signal processing.

It has been suggested that by connecting simple reactive elements between the input ports and antenna ports, the mutual coupling between the antenna elements can be completely removed [10]. However, this can only be implemented in cases where the off-diagonal elements of the admittance matrix are all purely imaginary. For a 3-element array, this can be achieved by adjusting the distances between the antenna elements [10], or by modifying the length of the antenna elements [8, 9].

In this thesis, a new way of decoupling the antenna elements is explored. This approach does not require the mutual admittances of the antenna to be purely susceptible. Instead, an array with any complex mutual admittance can be analytically decoupled with the help of a lossless network without having to modify the length of the antenna elements or the spacing between the elements. The lossless decoupling network can then be realized using Kuroda's identities, and implemented on microstrip and stripline.

## **1.2. Objectives of the project**

This project aims to develop design concepts for compact arrays with considerably reduced element spacing. It investigates the different ways of achieving decoupling between the ports. These include modification of the radiating part of the antenna and the inclusion of special decoupling networks in front of the element ports. Procedures for the design and realization of the decoupling technique used are to be developed and verified with experimental results.

## **1.3. Outline of the project**

The project involved the modelling of the array to extract the parameters of the antenna. Different methods of achieving decoupling between the array ports were designed and investigated analytically. The decoupling network was then realized and the array structure manufactured. The theoretical performance of the decoupled array was verified with the experimental results.

## **1.4. Organization of the thesis**

This thesis consists of seven chapters, including this introductory chapter. Chapter 2 provides the background on the applications of such an array for digital beam-forming and the theory of mutual coupling. Chapter 3 describes the modelling of the array element using commercial simulation software. Chapter 4 discusses the different methods of achieving decoupling between the array ports and provides analytical solutions for arrays with not more than six elements. Chapter 5 illustrates the realization of the decoupling and matching networks. Chapter 6 covers the construction procedures and specifications of the array structure and presents a

discussion on the experimental and theoretical results obtained. Chapter 7 gives some concluding remarks on this project.

## **1.5. Publications**

Conference papers

- J. C. Coetzee and P. T. Chua, “Realization of Decoupling Networks for Low-Order Multi-Port Arrays with Reduced Element Spacing”, *Progress in Electromagnetics Research Symposium (PIERS), Pisa, Italy*, March 28 – 31, 2004.
  
- P. T. Chua and J. C. Coetzee, “Microstrip Implementation of Decoupling Networks for Multi-Port Arrays with Reduced Element Spacing”, *IEEE AP-S/URSI International Symposium on Antennas and Propagation, Monterey, California, USA*, June 20 – 26, 2004.



## **CHAPTER 2**

### **THEORETICAL BACKGROUND**

#### **2.1. Introduction**

This chapter provides the theoretical background to the project. It describes smart antennas and digital beam-forming and its applications. It also describes the theory of mutual coupling for a linear array and a circular array.

#### **2.2. Smart antennas and digital beam forming**

With the increasing demand for wireless services, telecommunications has evolved from the traditional wired phone to personal communication services (PCS). This brings about an increase in the type of wireless services provided, such as fixed, mobile, outdoor and indoor, and satellite communications. As PCS provides pervasive communication services, it will require much higher levels of system capacity than the current mobile systems.

The capacity of a communications system can be increased directly by enlarging the bandwidth of the existing communications channels or by allocating new frequencies to the service. However, since the electromagnetic spectrum is limited and becoming congested with a proliferation of unintentional and intentional sources of interference, it may not be feasible to increase system capacity by opening new spectrum space for wireless communications applications. Instead, efficient use of the existing frequency resources is critical.

There are currently many existing multiple access techniques that serve to maximize the capacity of the existing frequency resources. These include frequency-division multiple access (FDMA), time-division multiple access (TDMA), code-division multiple access (CDMA) and space-division multiple access (SDMA). In FDMA, the frequency spectrum is divided into segments that are shared among different users. In TDMA, each user is given access to the whole frequency spectrum for an allocated period of time. In CDMA, each transmitted signal is modulated with a unique code that identifies each user, and each user has access to the entire frequency spectrum. In SDMA, the geographical coverage area is divided into a large number of cells. The same frequency can be reused in different cells that are separated by a spatial distance to reduce the level of co-channel interference. However, for a given amount of base-station transmission power, there is a limit on the number of cells that can be served in a particular geographical area, and hence a limit on the capacity that the base-station can support. Therefore, to further increase the capacity, advanced forms of SDMA are needed.

The advanced forms of SDMA call for the use of smart antennas, or more commonly known as adaptive antennas. These antennas are capable of beam-forming. For example, 120° sectorial beams at different carrier frequencies can be used within a cell and each sectorial beam can be used to serve the same number of users as are served in the case of ordinary cells [11], as illustrated in Figure 2.1. This technique triples the capacity of the cell. The ultimate form of SDMA is to use independently steered high-gain beams at the same carrier frequency to provide service to an individual user within a cell [11], as shown in Figure 2.2.

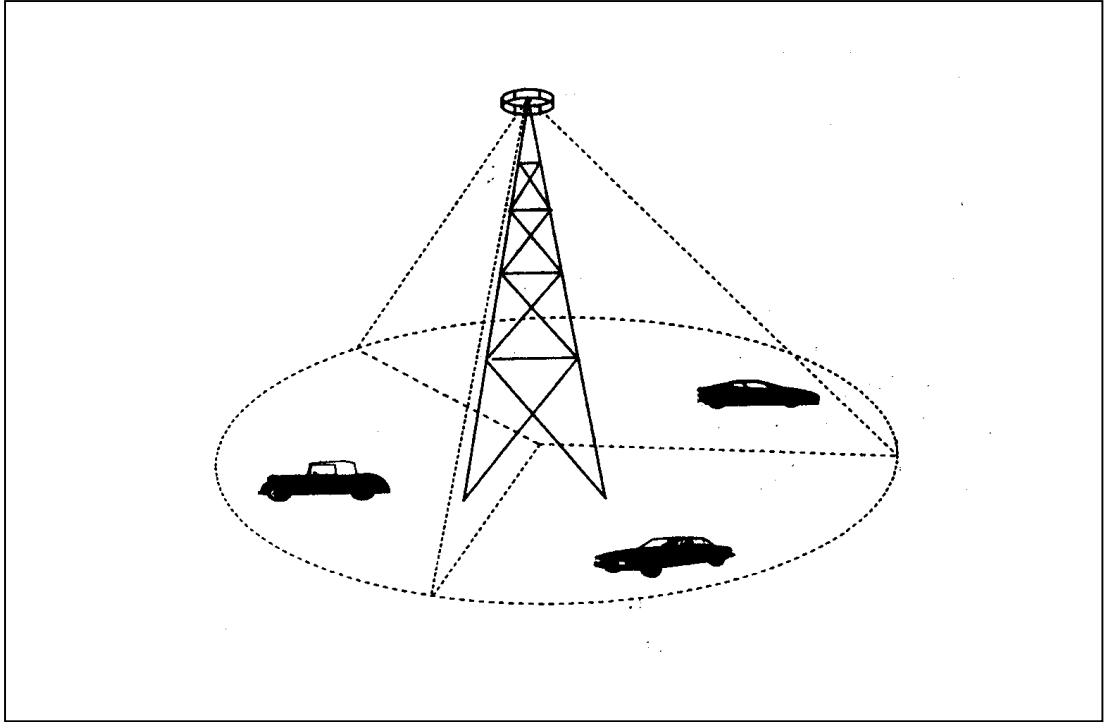


Figure 2.1 A 120° sectorized cell pattern [11].

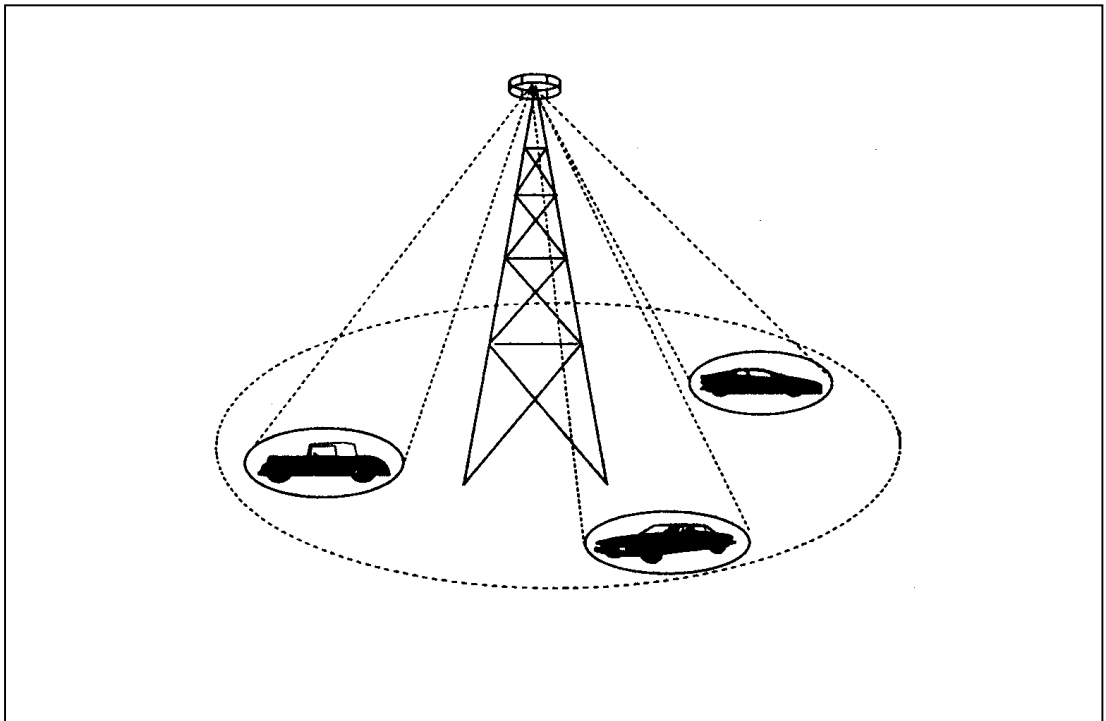


Figure 2.2 Independently steered beams at same frequency to each user [11].

With advancement in computing power, more flexibility and control can be achieved from smart antennas by employing digital beam-forming (DBF) techniques. A DBF antenna can be considered as the ultimate antenna, since it has the ability to capture all the information incident on the antenna and apply appropriate signal processing to make the information useful to the observer. DBF is a marriage between antenna technology and digital technology. Figure 2.3 shows a generic DBF antenna system. It consists of three major components, namely the antenna array, the digital transceivers, and the digital signal processor [11]. DBF is a system in which the RF signal received by the antenna array is digitized and processed digitally. The radiation patterns of the antenna can be controlled by digital signal processing techniques to achieve the desired performance [11 – 19].

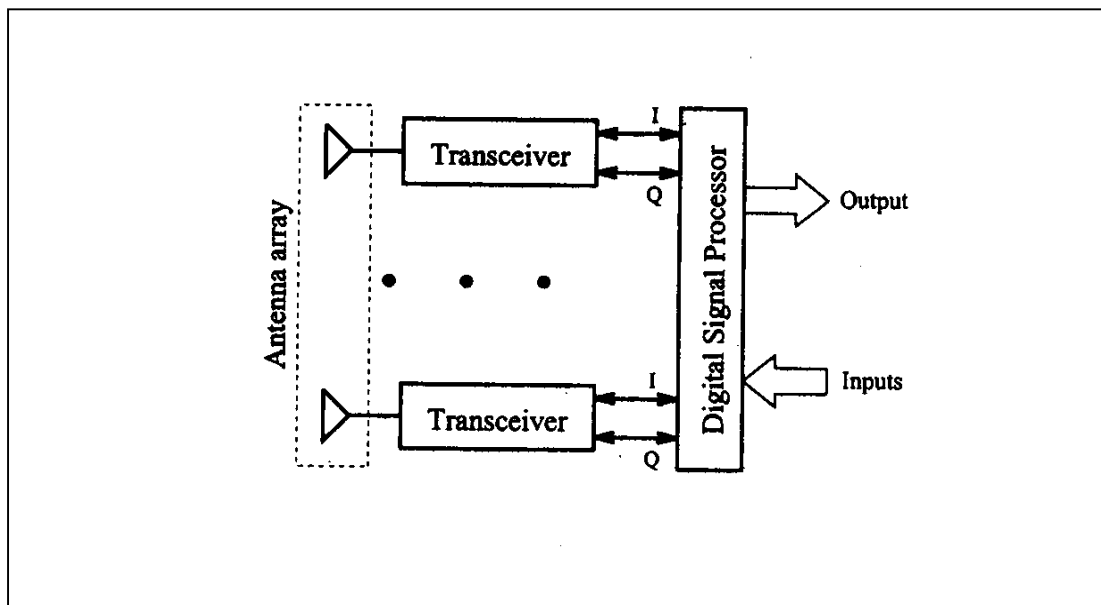


Figure 2.3 A generic DBF antenna system [11].

## **2.3. Theory of mutual coupling**

### **2.3.1. Mutual impedance between two linear elements**

When two antennas are in close proximity of each other, there is an interchange of energy between them. This interchange of energy constitutes mutual coupling between the antenna elements. The presence of a nearby element alters the current distribution, radiated field and input impedance of an antenna. Therefore, the performance of the antenna depends not only on its own current but also on the current of neighbouring elements.

For an antenna element, there are two types of impedance associated with it. The first type is the driving-point impedance. This depends on the self-impedance, that is, the input impedance in the absence of other elements. The second type is the mutual impedance between the driven element and other elements. Consider a two-element antenna system as shown in Figure 2.4.

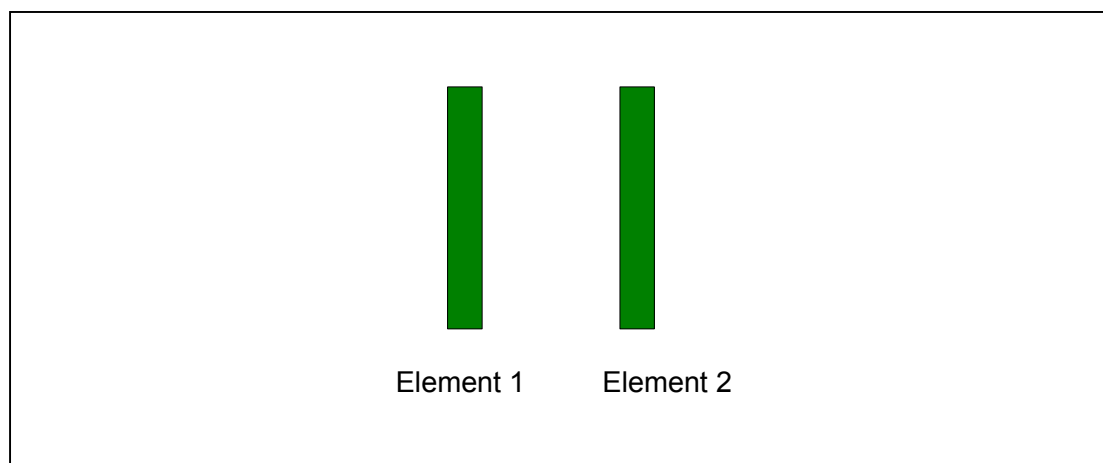


Figure 2.4 A two-element antenna array.

The two-element system is equivalent to a two-port network. The voltage-current relations can be written as:

$$\begin{aligned} V_1 &= Z_{11}I_1 + Z_{12}I_2 \\ V_2 &= Z_{21}I_1 + Z_{22}I_2 \end{aligned} \quad , \quad (2.1)$$

where

$$\begin{aligned} Z_{11} &= \left. \frac{V_1}{I_1} \right|_{I_2=0} \\ Z_{12} &= \left. \frac{V_1}{I_2} \right|_{I_1=0} \\ Z_{21} &= \left. \frac{V_2}{I_1} \right|_{I_2=0} \\ Z_{22} &= \left. \frac{V_2}{I_2} \right|_{I_1=0} \end{aligned} \quad . \quad (2.2)$$

$Z_{11}$  and  $Z_{22}$  are the self-impedances of antenna elements 1 and 2 respectively;  $Z_{12}$  and  $Z_{21}$  are the mutual impedances. From (2.1),

$$\begin{aligned} Z_{1d} &= \frac{V_1}{I_1} = Z_{11} + Z_{12} \frac{I_2}{I_1} \\ Z_{2d} &= \frac{V_2}{I_2} = Z_{22} + Z_{21} \frac{I_1}{I_2} \end{aligned} \quad , \quad (2.3)$$

where  $Z_{1d}$  and  $Z_{2d}$  represent driving-point impedances of antenna elements 1 and 2 respectively.

When attempting to match any antenna, it is the driving-point impedance that must be matched. Since mutual impedance affects the driving-point impedance, it plays an important role in the performance of the array.

### 2.3.2. Mutual coupling in a circular array

Consider a circular array of  $M$ -elements as shown in Figure 2.5. The mutual impedance and mutual admittance between the elements  $i$  and  $j$  are  $Z_{ij}$  and  $Y_{ij}$  respectively. For an array with  $M$ -elements,

$$[\mathbf{I}] = [\mathbf{Y}][\mathbf{V}]. \quad (2.4)$$

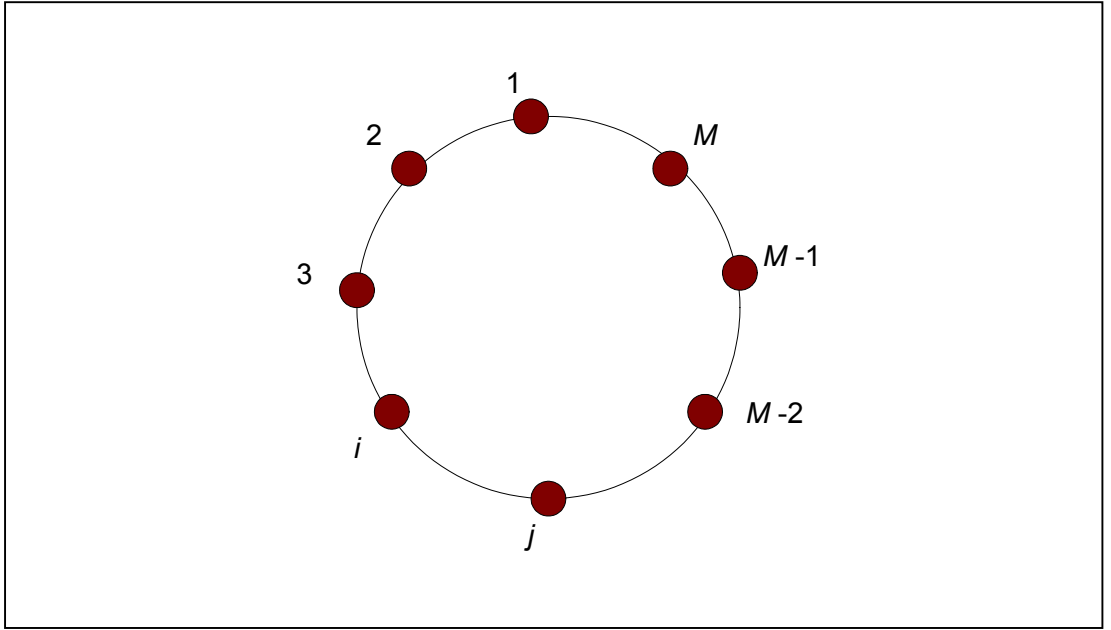


Figure 2.5 A circular array of  $M$ -elements.

The  $Y$ -matrix characterizes the mutual admittances or mutual coupling between the array elements. By applying reciprocity and symmetry, the  $Y$ -matrix can be simplified. From reciprocity,

$$Y_{ij} = Y_{ji}. \quad (2.5)$$

From symmetry,

$$Y_{12} = Y_{1M}, Y_{13} = Y_{1(M-1)}, \dots, Y_{ij} = Y_{i(M-j+2)}. \quad (2.6)$$

Therefore, the generalized  $Y$ -matrix for a circular array is:

$$\begin{bmatrix} Y_{11} & Y_{12} & Y_{13} & \cdots & Y_{1(N-1)} & Y_{1N} & Y_{1(N-1)} & \cdots & Y_{12} \\ Y_{12} & Y_{11} & Y_{12} & \cdots & Y_{1(N-2)} & Y_{1(N-1)} & Y_{1N} & \cdots & Y_{13} \\ Y_{13} & & & \ddots & & & & & \vdots \\ \vdots & & & & & & & & \vdots \\ Y_{1(N-1)} & & & & & & & & Y_{1N} \\ Y_{1N} & & & & \ddots & & & & Y_{1(N-1)} \\ Y_{1(N-1)} & & & & & & & & Y_{1(N-2)} \\ \vdots & & & & & & & & \vdots \\ Y_{12} & Y_{13} & \cdots & \cdots & Y_{1N} & Y_{1(N-1)} & Y_{1(N-2)} & \cdots & Y_{11} \end{bmatrix}$$

for  $M$  even, or

$$\begin{bmatrix} Y_{11} & Y_{12} & Y_{13} & \cdots & Y_{1(N-1)} & Y_{1N} & Y_{1N} & Y_{1(N-1)} & \cdots & Y_{12} \\ Y_{12} & Y_{11} & Y_{12} & \cdots & Y_{1(N-2)} & Y_{1(N-1)} & Y_{1N} & Y_{1N} & \cdots & Y_{13} \\ Y_{13} & & & & & & & & & \vdots \\ \vdots & & & & & & & & & \vdots \\ Y_{1(N-1)} & & & & & & & & & Y_{1N} \\ Y_{1N} & & & & \ddots & & & & & Y_{1N} \\ Y_{1N} & & & & & & & & & Y_{1(N-1)} \\ Y_{1(N-1)} & & & & & & & & & Y_{1(N-2)} \\ \vdots & & & & & & & & & \vdots \\ Y_{12} & Y_{13} & \cdots & \cdots & Y_{1N} & Y_{1N} & Y_{1(N-1)} & Y_{1(N-2)} & \cdots & Y_{11} \end{bmatrix}$$

for  $M$  odd, where  $N = \text{Floor}\left(\frac{M}{2}\right) + 1$  for all  $M$ .

For example, for a three-element array,  $M = 3$ ,  $N = \text{Floor}\left(\frac{3}{2}\right) + 1 = 2$ .

Therefore

$$\mathbf{Y} = \begin{bmatrix} Y_{11} & Y_{12} & Y_{12} \\ Y_{12} & Y_{11} & Y_{12} \\ Y_{12} & Y_{12} & Y_{11} \end{bmatrix}. \quad (2.7)$$



## **2.4. Conclusion**

The theoretical background on smart antennas, digital beam-forming and its applications are described in this chapter. Also the mutual coupling properties between elements of a linear array and a circular array is discussed.

## **CHAPTER 3**

### **MODELLING OF AN ARRAY ELEMENT**

#### **3.1. Introduction**

This chapter presents the modelling of an array element using commercial software such as IE3D by Zeland Inc. and HFSS by Hewlett-Packard. The array element is a quarter-wavelength monopole with finite thickness. The modelling is extended to encompass an array of three elements.

#### **3.2. Antenna elements**

The array element used in this project is a quarter-wavelength monopole of finite thickness. Monopole antennas are the most commonly used antennas in mobile communications and they have the simplest structure [11]. The monopole is usually mounted vertically above a ground plane. If the ground plane were a perfect conductor and infinite in size, the radiation pattern and bandwidth characteristics of the monopole would be the same as those of a dipole antenna, due to the image effect [20]. An advantage that a monopole has over a dipole is that the directivity of the monopole is 3 dB higher than that of the dipole, since the radiation power is radiated only to the upper half space of the ground plane. It is reported in [11] that an antenna with a larger diameter supports more broadband operations, and that monopole elements used in a circular array result in an array pattern that is not stable as frequency changes, that is, the array has a narrow bandwidth.

For this project, an array of three monopoles is considered. Figure 3.1 shows the 3-element array, where each monopole element has a height that is quarter of a

wavelength, and the inter-element spacing is a tenth of a wavelength. This is very small compared to the conventional half-wavelength element spacing. Table 3.1 summarizes the parameters of the array.

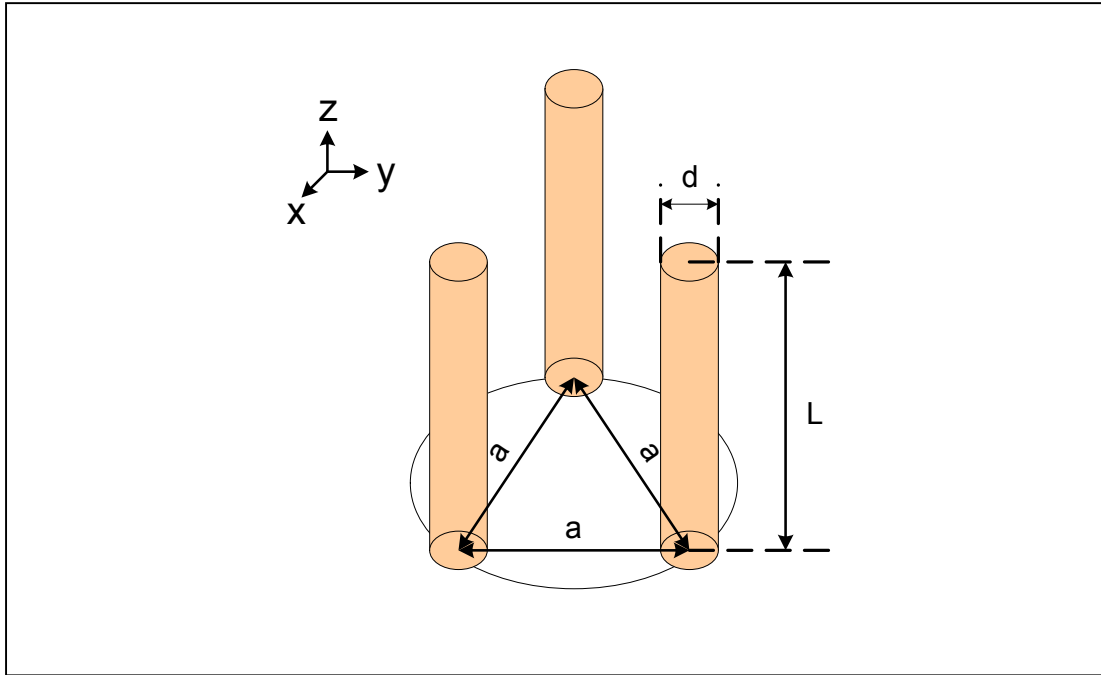


Figure 3.1 A 3-element array.

Table 3.1 Parameters of the 3-element array.

Operational frequency, $f_0$	2.45 GHz
Wavelength, $\lambda_0$	$c/f_0 = 122.4$ mm
Height of monopole, $L$	$\lambda_0 / 4 = 30.6$ mm
Diameter of monopole, $d$	$\lambda_0 / 40 = 3.06$ mm
Array element spacing, $a$	$\lambda_0 / 10 = 12.24$ mm

### **3.3. IE3D modelling**

#### **3.3.1. About IE3D software**

IE3D is an integrated full-wave electromagnetic simulation and optimization package for the analysis and design of 3-dimensional antennas and high frequency printed circuits [21]. IE3D has been adopted as an industrial standard in planar and 3D electromagnetic simulation. The primary formulation of IE3D is an integral equation obtained through the use of Green's functions. Both the electric current on a metallic structure and the magnetic current representing the field distribution on a metallic aperture are modelled [21].

#### **3.3.2. Construction of a monopole in IE3D**

There are many different ways to build a monopole structure in IE3D. The geometry construction is carried out in the MGRID application window in IE3D. One way of building a monopole is to use a *wire path*. The coordinates of the centres of the top and bottom surfaces of the monopole have to be entered, and a 3D wire path with a specified radius will be constructed between the entered points.

Another way of constructing a monopole is the *edge via* method. In this method, a circle is first drawn for the top surface of the monopole. The vertices of the circle are then selected and via edges are added to them.

A third method is the *connect path* method. Circles are first drawn for both the top and bottom surfaces of the monopole. These circles lie on different layers, separated by the height of the monopole. The vertices of both the circles are selected and a connecting path is built between the two layers.

It should be noted that in the *wire path* method, there is no metallic surfaces at the top or bottom of the monopole. Metal only covers the cylindrical surface of the monopole. For the latter two methods, there is at least a metallic surface at either or both ends of the monopole. It was observed that the simulation results given by each of the three methods are in close agreement. Hence, any of the three ways of constructing the monopole can be used. To model the physical monopole as closely as possible and to simplify the geometry of the model, the *edge via* method is adopted for the project. This produces a monopole with a metallic surface at the top and is much simpler to build in MGRID.

### **3.3.3. IE3D simulation settings**

There are a few important parameters to take note for simulations in IE3D. They are:

- *Meshing Frequency* – This is the highest application frequency. For the project, it is recommended to set the meshing frequency to 3 GHz, which is the upper limit of the operating frequency band. The centre operating frequency is 2.45 GHz.
- *Cells Per Wavelength* – This specifies the number of cells per wavelength, and is a measure of the finest of a mesh. For the project, this is set to 20.
- *Meshing Optimization* – This option has to be enabled to optimize the meshing done to the structure.
- *Automatic Edge Cells (AEC)* – This is a feature to add small cells along edges for guaranteed simulation accuracy. It has to be within 10% to 15% of a cell size. The cell size can be obtained from the meshing properties.

- *Ground plane* – The ground is modelled as a perfect conductor with conductivity of  $1e+15$  S/m.
- *Vertical Localized Port* – This is the type of port defined to excite the monopole. The height of the port has to be less than 5% of the guided wavelength. It should be noted that the height of the monopole is inclusive of the height of the port.

### 3.3.4. Radiation patterns from IE3D

The radiation patterns of the 3-element array are shown below. Figures 3.2 to 3.4 show the radiation pattern on the horizontal plane for cases where only one port is excited. Figure 3.5 shows the radiation pattern on the vertical plane. These radiation patterns are the characteristics of the array alone, without any external networks. It is noted that the array has a linear directivity of 7.40 dBi and a 3-dB beamwidth of  $34.9^\circ$ .

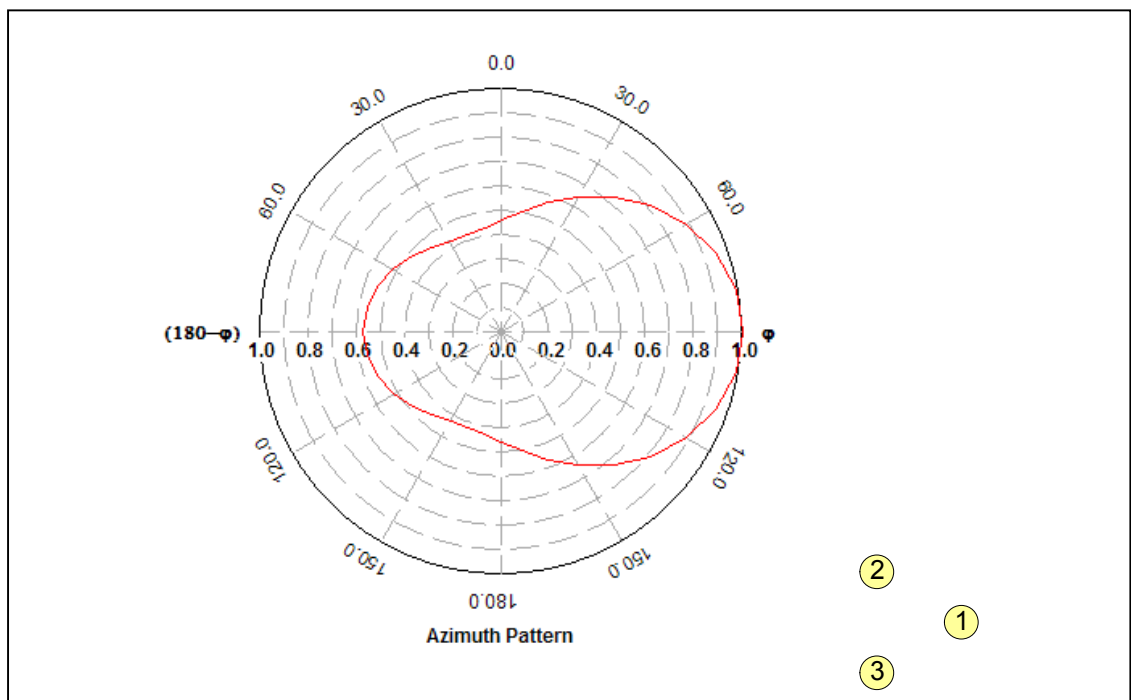


Figure 3.2 Azimuth radiation pattern of array with port 1 excited.

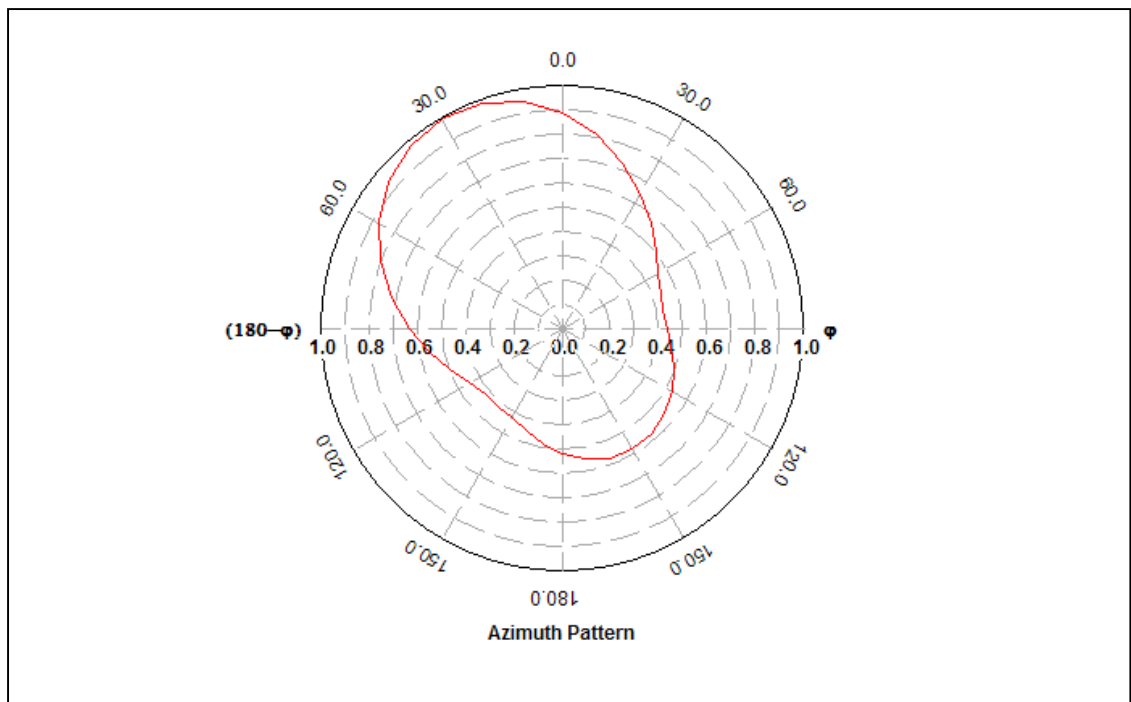


Figure 3.3 Azimuth radiation pattern of array with port 2 excited.

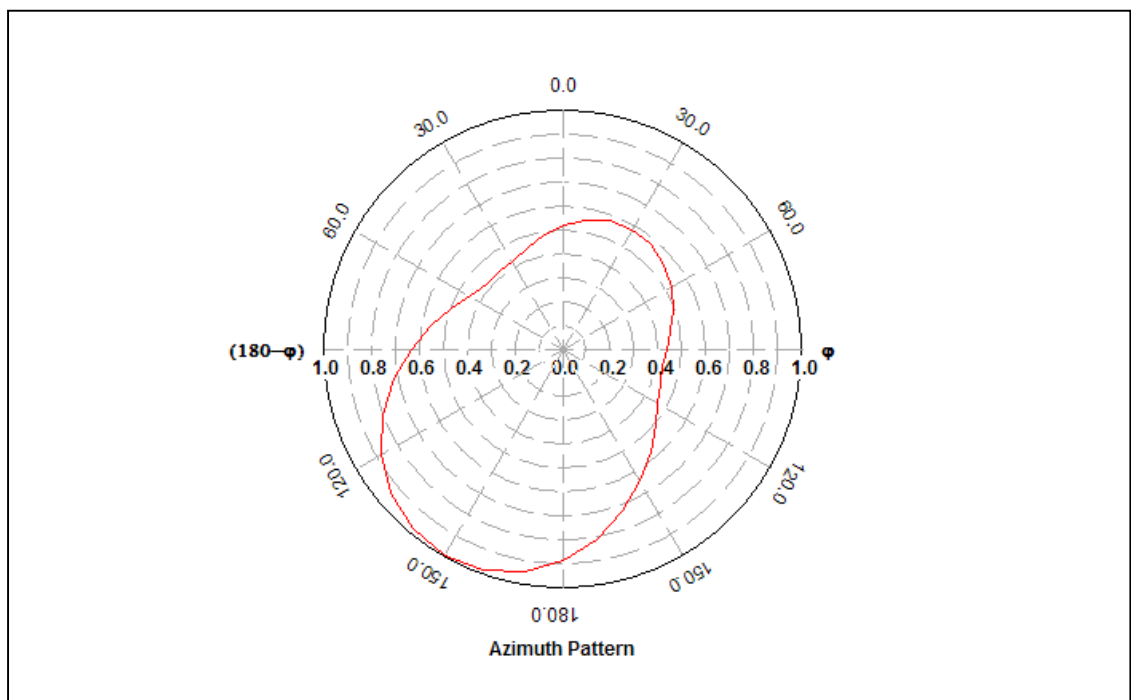


Figure 3.4 Azimuth radiation pattern of array with port 3 excited.

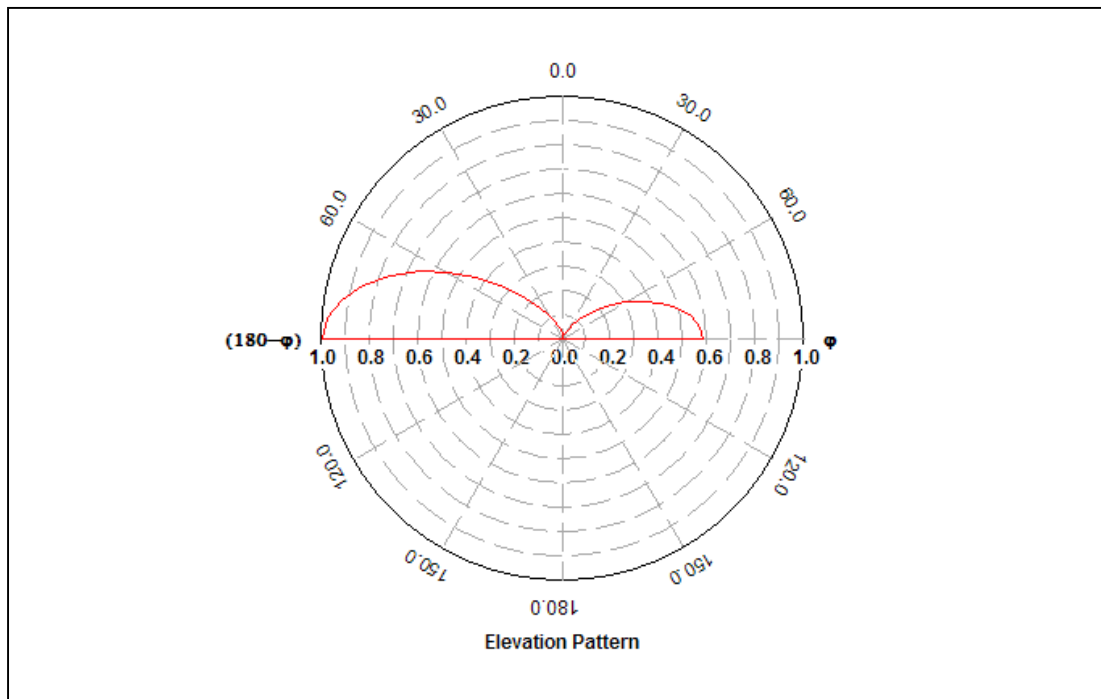


Figure 3.5 Elevation radiation pattern of array with any one port excited.

### 3.3.5. Troubleshooting for IE3D modelling

Generally, the modelling in IE3D is relatively easy to learn. However, there are a few pitfalls that one should take note of. For example, to construct an array from a single monopole in MGRID, if the Copy-and-Reflect command from the Edit menu were executed, it would give incorrect element spacing, because the command measures the distance to the edge of the monopole and not to its centre. Instead, the Copy-at-an-angle command from the Edit menu should be used. This command allows the angle and distance of the copied object to be specified. It allows the object as well as the defined ports to be copied.

Another point to note is the definition of the ground plane. By default, the ground plane is defined as having finite conductivity. If this were used in simulations, the radiation patterns in the direction of maximum radiation would show a slight tilt



upwards from the horizontal plane, as shown in Figure 3.6. To get ideal radiation patterns, the ground has to be defined as a perfect ground with a high conductivity such as  $1e+15$  S/m.

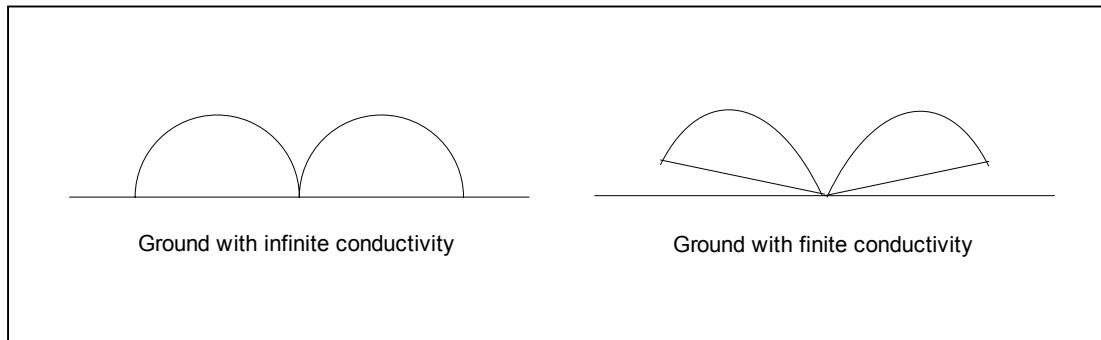


Figure 3.6 Radiation patterns over grounds with finite and infinite conductivity.

### 3.4. HFSS modelling

#### 3.4.1. About HFSS software

HFSS software is a complete solution for drawing passive, 3D structures, simulating designs, and displaying simulation data [22]. The simulation technique used to calculate the full 3D electromagnetic field inside a structure is based on the finite element method. The finite element method divides the problem space into numerous smaller regions (tetrahedrons) and represents the field in each sub-region with a local function [22].

#### 3.4.2. Construction of monopole in HFSS

The construction of structures in HFSS is slightly different from that in IE3D. In HFSS, all structures have mass, that is, each object is a solid. There is a rule that there should not be any overlapping objects. Furthermore, HFSS requires the user to define an air space that contains all objects built. This makes it more difficult to construct the geometry. For example, for a simple monopole, a cylindrical solid

represents the monopole. A rectangular cube enclosing the monopole serves as the air space. It should be noted that this air box is overlapping with the monopole. Hence, the ultimate air space is the resulting structure from the subtraction of the cube and the cylinder.

In HFSS, all surfaces of a structure have to be defined. For the monopole, the surfaces are defined as perfect conductors. The air space has perfectly absorbing boundary conditions at the boundaries of the air box.

### **3.4.3. HFSS simulation settings**

Mesh refinement is enabled for more accurate results. Mesh refinement increases the amount of meshing applied to the structure. The targeted error (global delta error) is set small, while a sufficient number of iterations are set for the simulation results to converge. The simulation will be halted once either the delta error criteria or maximum number of iterations is reached. Therefore, care has to be taken in setting these two parameters such that a balance is reached that gives results with minimum error.

HFSS allows the choice of using either a fast frequency sweep (FFS) or discrete frequency (DF) simulation. In a FFS simulation, a fast and highly accurate method of fitting data points to a rational model is used. A minimum number of frequency samples are considered and the FFS algorithm is applied. More data points are taken when there is a large variation in the sample data. The process stops when FFS finds that the data has converged. For DF simulations, the scattering parameters ( $S$ -parameters) of the structure are computed at discrete frequency points. No

interpolation procedure is performed. Convergence is obtained by comparing data at each discrete frequency point. Hence this method is more accurate. However, DF simulations take longer computational time. In this project, the DF simulation approach is used. Table 3.2 shows the HFSS simulation setup parameters.

Table 3.2 HFSS simulation setup parameters.

MAIN SETUP		
Mesh Setup		
Enable Mesh Refinement	Yes	
Starting Mesh	Initial	
Save Modal Solutions	Dominant	
Save Field Solutions	Last	
Fast Frequency Sweep	No	
Additional Discrete Freq (GHz)	1.9 GHz; 3.0 GHz; 51 points	
REFINEMENT OPTIONS		
Refinement Criteria		
Global delta S-parameter	Yes	Delta error: 0.001
Matrix delta S-parameter	No	
Consecutive Iterations of Delta Error required:	3	
Limit Refinement Passes	Limit # of additional refinement passes to: 12	
Mesh Frequency Override		
Refine at specified freq	Yes	Mesh freq (GHz): 2.45
DISCRETE FREQ		
1.9 GHz; 3.0 GHz; 51 points		
ADVANCED OPTIONS		
Mesh Seeding	(Default)	Used
Max divisions per edge (1-16)	4	4
Max divisions per loop (10-160)	40	40
Nodes per wavelength (0-20)	2	2
Max added nodes (0-300%)	60	60
Aggressive Mesh Refinement	Yes	Yes

#### **3.4.4. Troubleshooting for HFSS modelling**

Error messages may report that the mesher has failed or that an element cannot be defined. These are mainly due to the presence of overlapping 3D objects or undefined boundary conditions. Care should be taken in construction of complex geometries, which may have many overlapping objects and numerous surfaces. If the problem is with the non-convergence of the results obtained, the mesh should be refined, with more nodes per wavelength, or one could simply increase the number of iterations such that they are sufficient to yield converged results.

#### **3.5. Conclusion**

This chapter has described the modelling of a monopole and its array of three elements in commercial software such as IE3D by Zeland Inc. and HFSS by Hewlett-Packard. It was found that both IE3D and HFSS give similar results. Hence, the modelling of the monopole can be done in either software. The pitfalls that were encountered have also been highlighted. The troubleshooting sections discuss the limitations of the software and points out how some simulation results may be invalid. General guidelines given in the users manual do not address these issues explicitly.

## CHAPTER 4

### DECOUPLING OF ARRAY

#### 4.1. Introduction

This chapter describes two designs to decouple a 3-element array. One of the designs decouples the array by modifying the length of each array element. The other design is a generalized design that can be applied to any 3-element array with complex mutual admittances. It also discusses the different analysis techniques that are applied to decouple an array: an eigenmode expansion approach and a network analysis method. Analytical solutions verify both analysis methods. Arrays with three to six elements can be decoupled theoretically. For arrays with more than six elements, more computational resources may be required, which was not available during execution of this project. To illustrate the process of designing a decoupled array, only the 3-element array is considered.

#### 4.2. The need for a decoupled array

For a  $M$ -element array, there exist  $M$  mutually orthogonal eigenmodes. The mode admittance associated with eigenmode  $m$  is given by  $Y_m = G_m + jB_m$ , where  $G_m$  and  $B_m$  are respectively the conductance and susceptance of mode  $m$ . By means of eigenmode representation, the array of three mutually coupled elements can be replaced with a set of three equivalent antennas [8, 9]. In the receive mode, each of the three equivalent antennas can be modelled by means of a current source with source impedance equal to the corresponding mode admittance  $Y_m$  and current source  $i_m$ , as illustrated in Figure 4.1. The receiver channel with input admittance  $Y_{in,rec}$  is

connected to the antenna. A noise voltage and a noise current source, as shown in Figure 4.1, represent the noise characteristics of the receiver channel.

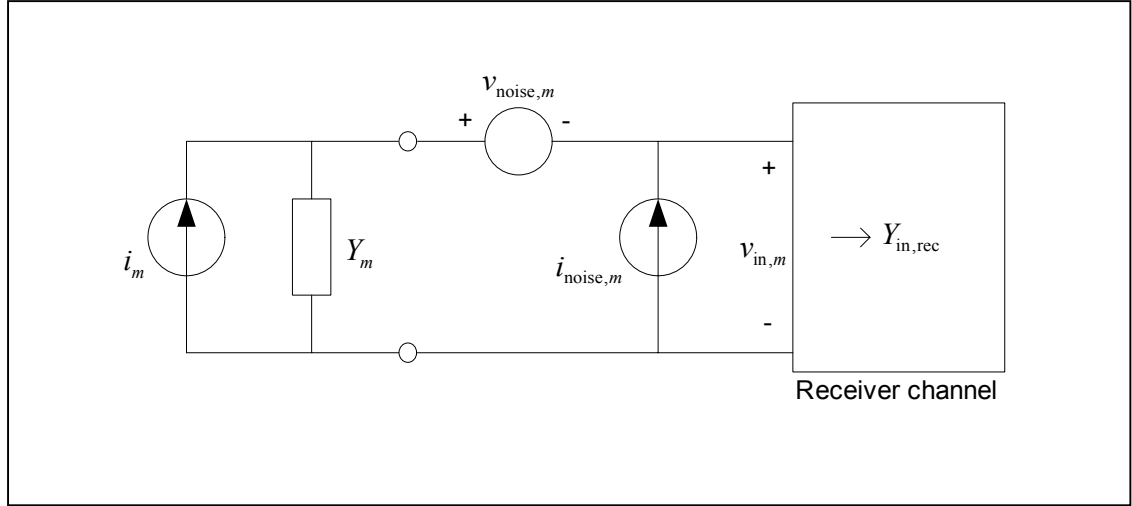


Figure 4.1 Equivalent circuit for  $m$ th eigenmode of array in receive mode.

The array considered has inter-element spacing that is a tenth of a wavelength. This small element spacing results in strong mutual coupling between the array elements. The performance of the array, in terms of power matching and signal-to-noise-ratio (SNR), is affected by the mutual coupling between the array elements.

The power contribution from mode  $m$  is maximized if the condition  $Y_m^* = Y_{\text{in},\text{rec}}$  is met. In an ideal case with no mutual coupling between the array elements, all the mode admittances are equal to each other. Simple two-port matching networks between the antenna ports and receiver channels can transform the mode admittances to meet the condition for maximum power transfer. However, in the presence of mutual coupling, the mode admittances are not identical and simultaneous matching for all modes cannot be achieved via two-port matching networks. If one particular mode is selected for power matching, the other modes will be mismatched. Mismatch

of a mode results in a decrease in transducer power gain for that mode relative to the case of power matching.

The effective receiver noise temperature  $T_{\text{eff}}$  is a function of the source admittance  $Y_m$ , as observed from Figure 4.1. The minimum receiver noise temperature  $T_{\text{eff,min}}$  is achieved when the source admittance equals an optimum value  $Y_{\text{opt}} = G_{\text{opt}} + jB_{\text{opt}}$ .

The effective noise temperature for mode  $m$  can be written as [8, 9]

$$T_{\text{eff},m} = T_{\text{eff,min}} + T_0 R_{\text{eq}} \frac{|Y_m - Y_{\text{opt}}|^2}{G_m}, \quad (4.1)$$

where  $R_{\text{eq}}$  and  $T_0$  are the equivalent noise resistance and the room temperature, respectively.

For an array with incident signal given by  $\mathbf{E}_{\text{inc}}(\Theta, \Phi)$ , the SNR is given by [8, 9]

$$\text{SNR} = \frac{\sum_{m=1}^M |\tilde{w}_m \mathbf{C}(\Theta, \Phi) \cdot \mathbf{E}_{\text{inc}}(\Theta, \Phi)|^2}{T_{\text{eff,min}} \sum_{m=1}^M |\tilde{w}_m|^2 + T_0 R_{\text{eq}} \sum_{m=1}^M |\tilde{w}_m|^2 \frac{|Y_m - Y_{\text{opt}}|^2}{G_m}}, \quad (4.2)$$

where  $\mathbf{C}(\Theta, \Phi)$  is a vector function that defines the mode radiation patterns, and  $\tilde{w}_m$  is a set of effective weights for adjustments to form the desired radiation pattern.

From (4.2), it is clear that the maximum SNR is achieved when all mode admittances are noise-matched:  $Y_m = Y_{\text{opt}}$  for  $m = 1, 2, \dots, M$ . In the presence of mutual coupling between the array elements, noise matching for a selected mode can only be achieved at the cost of noise-mismatch for the remaining modes. In addition, the SNR becomes a function of the effective weights and also a function of the desired radiation pattern.



It has been shown in [8, 9] that signal-to-noise maximization can only be achieved if all mode admittances of the array are identical and matched to the optimum admittance. This necessitates the use of a decoupling network. It has been suggested that by connecting simple reactive elements between the input ports and antenna ports, the mutual coupling between the antenna elements can be completely removed [10]. However, this can only be implemented in cases where the off-diagonal elements of the admittance matrix are all purely imaginary. In the design of a decoupled array, eigenmode and network analyses can be applied.

#### 4.3. Theory of eigenmode analysis

For an array with  $M$ -elements, there exist  $M$  mutually orthogonal radiation patterns (MORP) [8, 9]. Each MORP is associated with a distinct eigenmode. In the eigenmode analysis, for a given admittance matrix  $\mathbf{Y}$ , the eigenvalues and eigenvectors of  $\mathbf{Y}$  are evaluated.

For a three-element array, from equations (2.4) and (2.7),

$$\begin{bmatrix} I_1 \\ I_2 \\ I_3 \end{bmatrix} = \begin{bmatrix} Y_{11} & Y_{12} & Y_{12} \\ Y_{12} & Y_{11} & Y_{12} \\ Y_{12} & Y_{12} & Y_{11} \end{bmatrix} \begin{bmatrix} V_1 \\ V_2 \\ V_3 \end{bmatrix}. \quad (4.3)$$

Equation (4.3) forms a linear matrix system. If  $\mathbf{Y}$  has orthogonal eigenvectors  $\mathbf{x}_A$ ,  $\mathbf{x}_B$  and  $\mathbf{x}_C$ , then  $\mathbf{V}$  can be written as a linear combination of the eigenvectors of  $\mathbf{Y}$ :

$$\mathbf{V} = v_A \mathbf{x}_A + v_B \mathbf{x}_B + v_C \mathbf{x}_C, \quad (4.4)$$

where  $v_A$ ,  $v_B$  and  $v_C$  are constants representing the mode-voltages.

If  $\mathbf{Y}$  has eigenvalues  $Y_A$ ,  $Y_B$  and  $Y_C$ , then

$$\mathbf{I} = \mathbf{Y}\mathbf{V} = v_A Y_A \mathbf{x}_A + v_B Y_B \mathbf{x}_B + v_C Y_C \mathbf{x}_C, \quad (4.5)$$

where the eigenvalues  $Y_A$ ,  $Y_B$  and  $Y_C$  represent the mode-admittances.

Due to symmetry, the admittance matrix of a three-element array is given by

$$\mathbf{Y} = \begin{bmatrix} Y_{11} & Y_{12} & Y_{12} \\ Y_{12} & Y_{11} & Y_{12} \\ Y_{12} & Y_{12} & Y_{11} \end{bmatrix}. \quad (4.6)$$

The eigenvalues (mode-admittances) are:

$$\begin{aligned} Y_A &= Y_{11} + 2Y_{12} \\ Y_B &= Y_C = Y_{11} - Y_{12} \end{aligned} \quad (4.7)$$

The orthonormal and linearly independent eigenvectors are:

$$\mathbf{x}_A = \frac{1}{\sqrt{3}} \begin{bmatrix} 1 \\ 1 \\ 1 \end{bmatrix}, \quad \mathbf{x}_B = \frac{1}{\sqrt{6}} \begin{bmatrix} -1 \\ 2 \\ -1 \end{bmatrix}, \quad \mathbf{x}_C = \frac{1}{\sqrt{2}} \begin{bmatrix} -1 \\ 0 \\ 1 \end{bmatrix}. \quad (4.8)$$

Therefore,

$$\begin{bmatrix} I_1 \\ I_2 \\ I_3 \end{bmatrix} = \frac{v_A Y_A}{\sqrt{3}} \begin{bmatrix} 1 \\ 1 \\ 1 \end{bmatrix} + \frac{v_B Y_B}{\sqrt{6}} \begin{bmatrix} -1 \\ 2 \\ -1 \end{bmatrix} + \frac{v_C Y_C}{\sqrt{2}} \begin{bmatrix} -1 \\ 0 \\ 1 \end{bmatrix}. \quad (4.9)$$

From equation (4.7), it is clear that the mode-admittances of modes A, B and C cannot be simultaneously matched because of the mutual admittance  $Y_{12}$ . If the mutual

coupling is absent or compensated, we would have  $Y_A = Y_B = Y_C = \tilde{Y}_{11}$ , which is the equal to the self-admittance of the antenna element after decoupling. Simultaneously matching of all the modes can then be achieved.

#### 4.4. A design for decoupling an array by modifying element length

As reported in [10], decoupling of an array can only be implemented in cases where the off-diagonal elements of the admittance matrix are all purely imaginary. This can be achieved by modifying the length of the antenna elements [8, 9].

From equation (4.7),

$$Y_{12} = \frac{1}{3}(Y_A - Y_B). \quad (4.10)$$

In general, the mode admittances  $Y_A$  and  $Y_B$  can be written as

$$\begin{aligned} Y_A &= G_A + jB_A \\ Y_B &= G_B + jB_B \end{aligned} \quad (4.11)$$

If mutual admittance  $Y_{12}$  of the array is purely imaginary, then

$$Y_{12} = jB_{12}. \quad (4.12)$$

From the condition given by (4.12), and by substituting (4.11) into (4.10), we obtain

$$G_{12} = \frac{1}{3}(G_A - G_B) = 0. \quad (4.13)$$

Thus

$$G_A = G_B. \quad (4.14)$$

Equation (4.14) gives the condition necessary for the mutual admittance of the array to be purely susceptive. That is, when the conductance of eigenmodes A and B are equal to each other, the array has a purely susceptive mutual admittance to allow the array to be decoupled.

As the mode admittances are frequency-dependent quantities, the mode conductance and susceptance can be plotted against frequency. From the conductance graph, there are points of intersection, which fulfil the condition given by (4.14). At these points, the mutual admittance of the array is purely susceptive. From the normalized frequencies representing these points, new lengths for the array element can be obtained. The resulting array with the modified element length will have a purely imaginary mutual admittance. The array admittance matrix becomes

$$\mathbf{Y} = \begin{bmatrix} Y_{11} & jB_{12} & jB_{12} \\ jB_{12} & Y_{11} & jB_{12} \\ jB_{12} & jB_{12} & Y_{11} \end{bmatrix}. \quad (4.15)$$

The network required to decouple an array with admittance properties given in (4.15) is simply a connection of a lossless element with admittance  $jB_{12}$  between each array element, as shown in Figure 4.2.

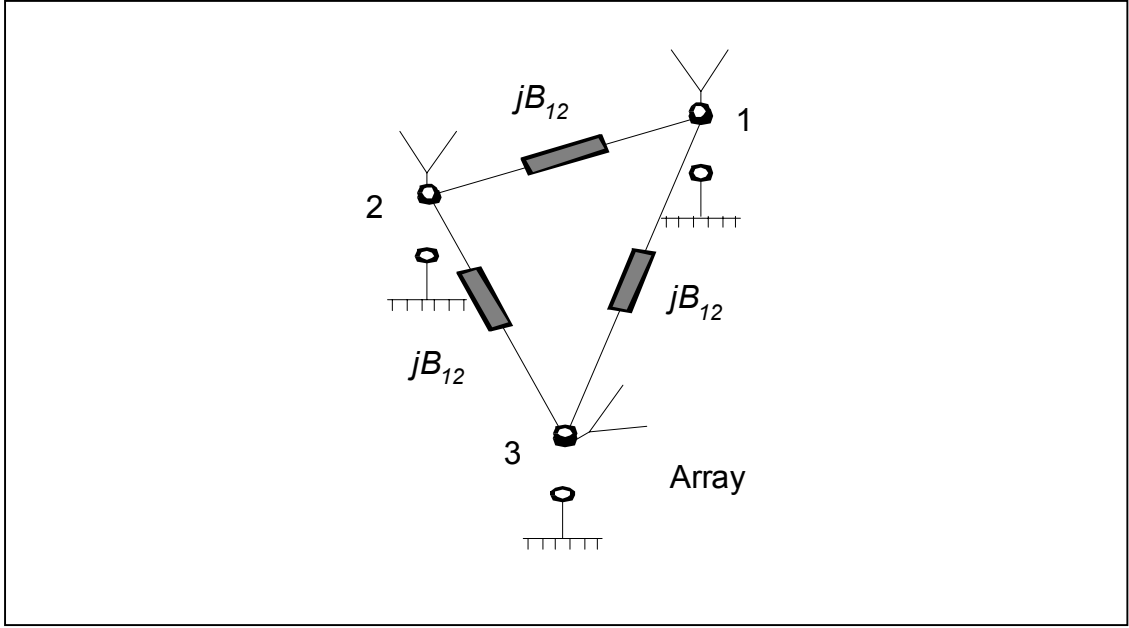


Figure 4.2 Decoupling network for array with modified element length.

The admittance matrix of the decoupling network can be written as

$$\mathbf{Y}_{\text{DN}} = \begin{bmatrix} j2B_{12} & -jB_{12} & -jB_{12} \\ -jB_{12} & j2B_{12} & -jB_{12} \\ -jB_{12} & -jB_{12} & j2B_{12} \end{bmatrix}. \quad (4.16)$$

For the decoupled array, its admittance matrix is given by

$$\tilde{\mathbf{Y}} = \mathbf{Y} + \mathbf{Y}_{\text{DN}} = \mathbf{U} \tilde{Y}_{11}, \quad (4.17)$$

where  $\mathbf{U}$  is the  $3 \times 3$  unity matrix and  $\tilde{Y}_{11} = Y_{11} + j2B_{12} = Y_A$ . This shows that input admittance looking into each array port is  $\tilde{Y}_{11}$ , and simultaneous matching can be achieved at all ports.

In summary, the design procedure to decouple an array by modifying the length of its elements is as follows:

1. Obtain the admittance parameters of the original array over a range of frequencies.
2. Plot the mode admittances over a range of frequencies.
3. Find points of intersection where  $G_A = G_B$ .
4. Obtain the new length of the array element from the chosen intersection point.
5. Obtain the admittance parameters of the array with the new element length.
6. Compute the value of the lossless decoupling element.
7. Obtain the admittance parameters of the decoupled array to verify that decoupling has been achieved, that is,  $\tilde{Y}_{ij} = 0$ .

#### 4.4.1. Example A1

This example serves to illustrate the process of decoupling an array by modifying the length of the array element. The parameters of the array are given in Table 4.1.

Table 4.1 Parameters of the array for example A1.

Operational frequency, $f_0$	2.45 GHz
Wavelength, $\lambda_0$	$c/f_0 = 122.4$ mm
Length of monopole, $l_0$	$\lambda_0 / 4 = 30.6$ mm
Diameter of monopole, $d$	$\lambda_0 / 40 = 3.06$ mm
Array element spacing, $a$	$\lambda_0 / 10 = 12.24$ mm

The array is modelled in IE3D simulations over a range of frequencies. Figures 4.3 to 4.5 show the radiation patterns at the operational frequency for eigenmodes A, B and C respectively. The port excitations are given by the eigenvectors of array.

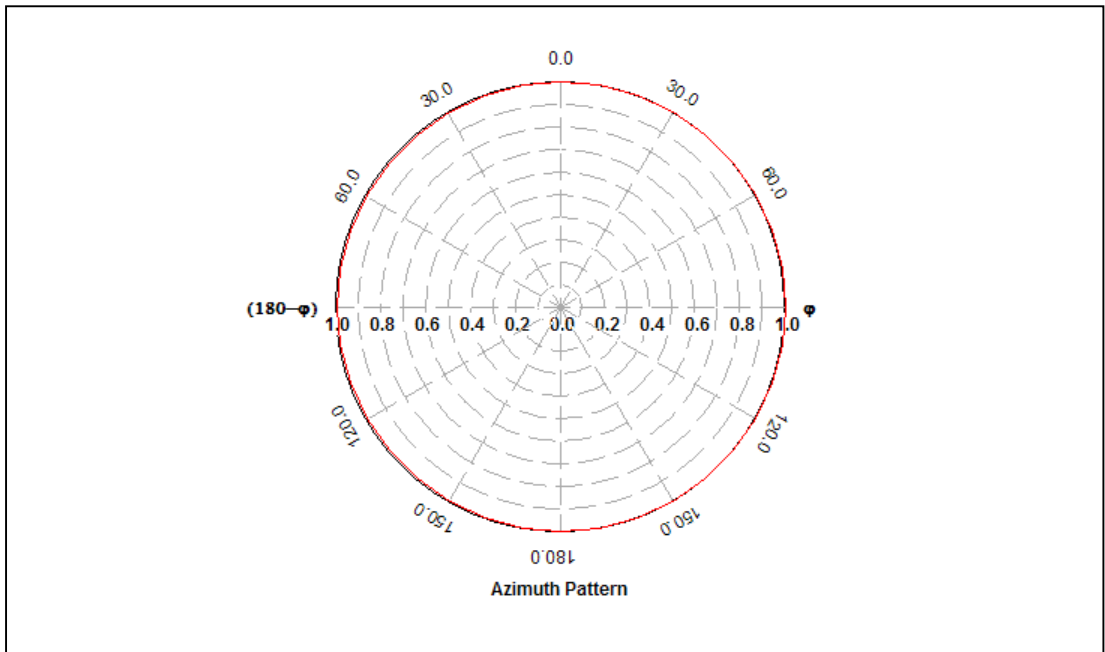


Figure 4.3 Radiation pattern of eigenmode A.

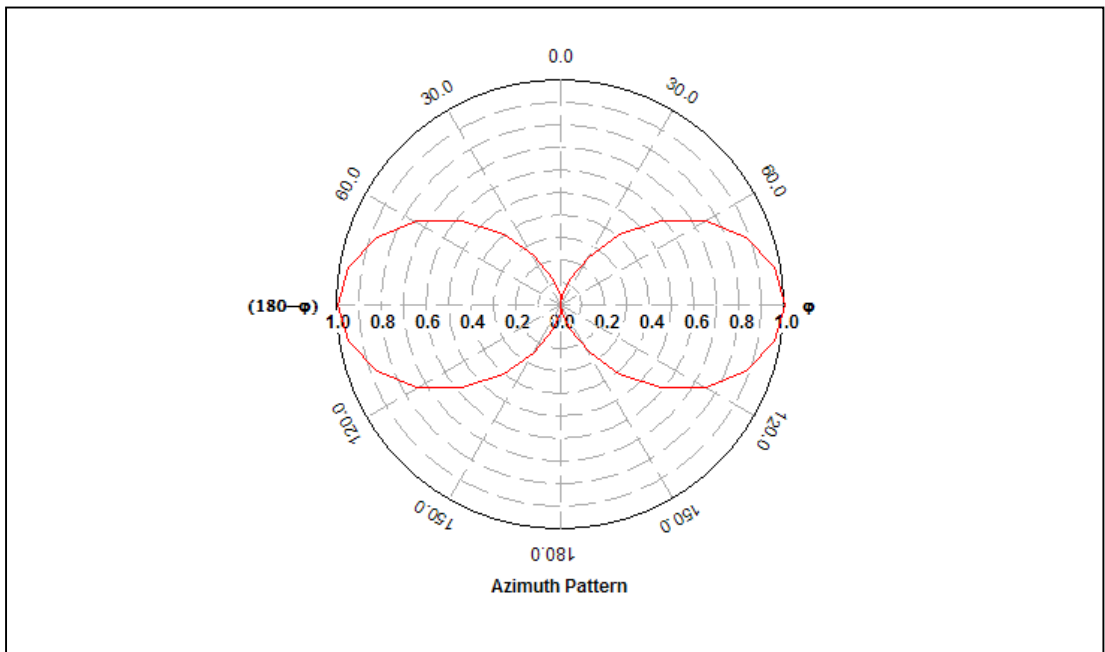


Figure 4.4 Radiation pattern of eigenmode B.

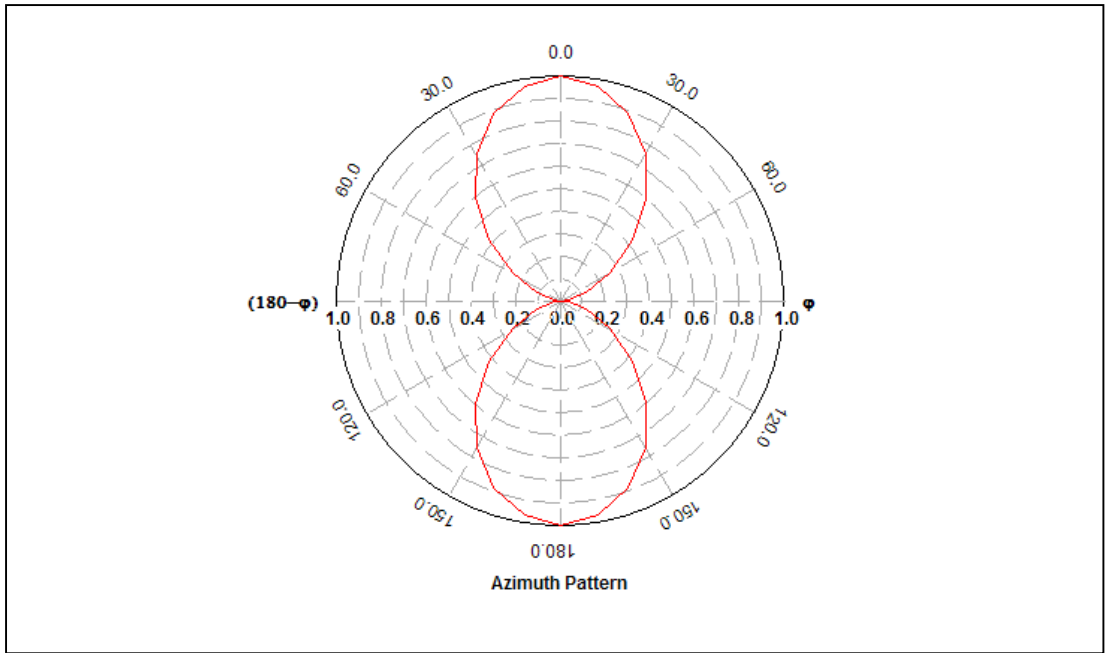


Figure 4.5 Radiation pattern of eigenmode C.

As the mode admittances are frequency-dependent quantities, they can be plotted over a range of frequencies, as shown in Figure 4.6. From the figure, it is observed that there are two points F1 and F2 where  $G_A = G_B$ . Considering point F1, it occurs at the normalized frequency of 0.9994. (See Figure 4.7.) This implies that the new length of the array element is 0.06% shorter than its original length. This gives a new element length of 30.582 mm.



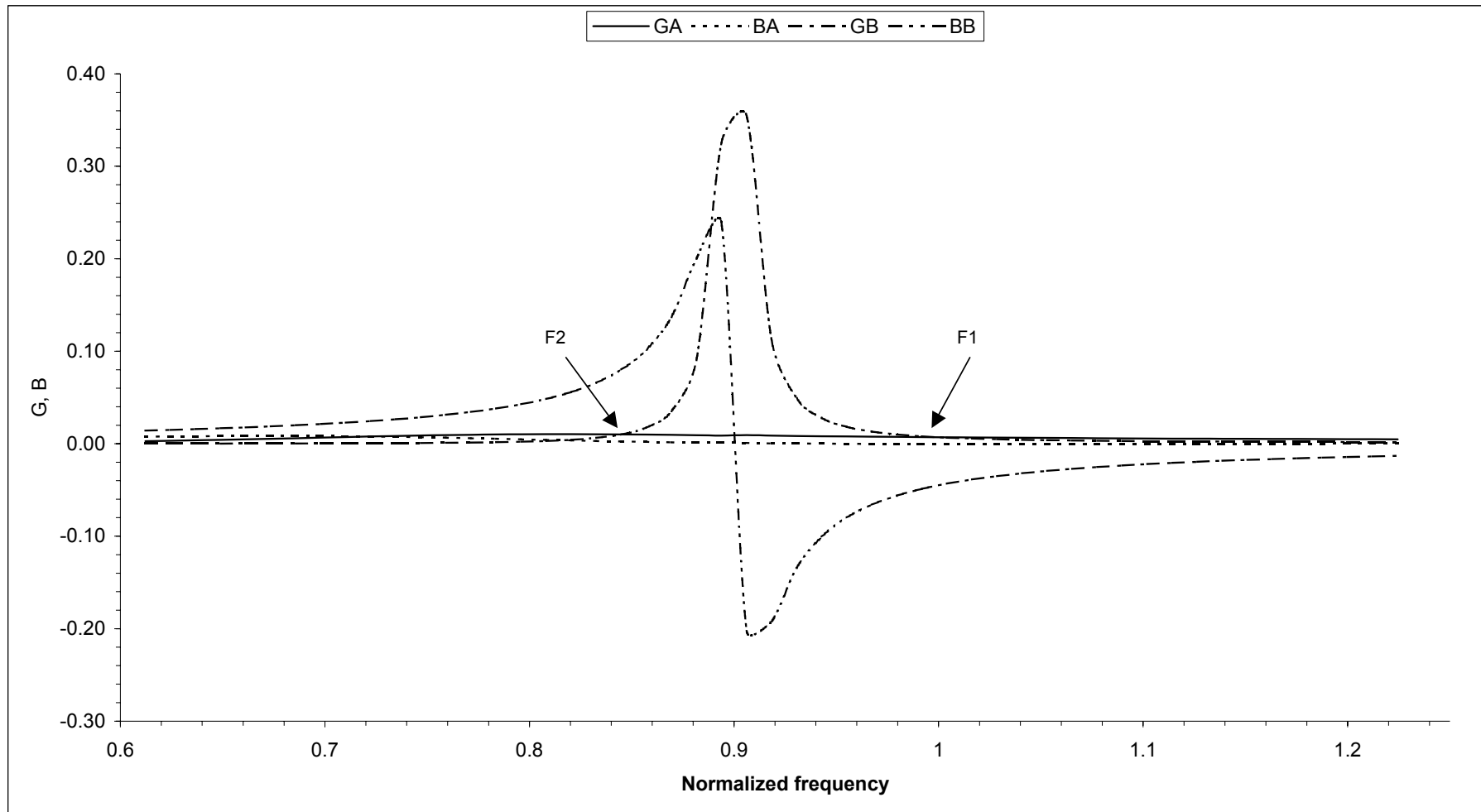


Figure 4.6 Plot of mode admittances over a range of frequencies (Example A1).

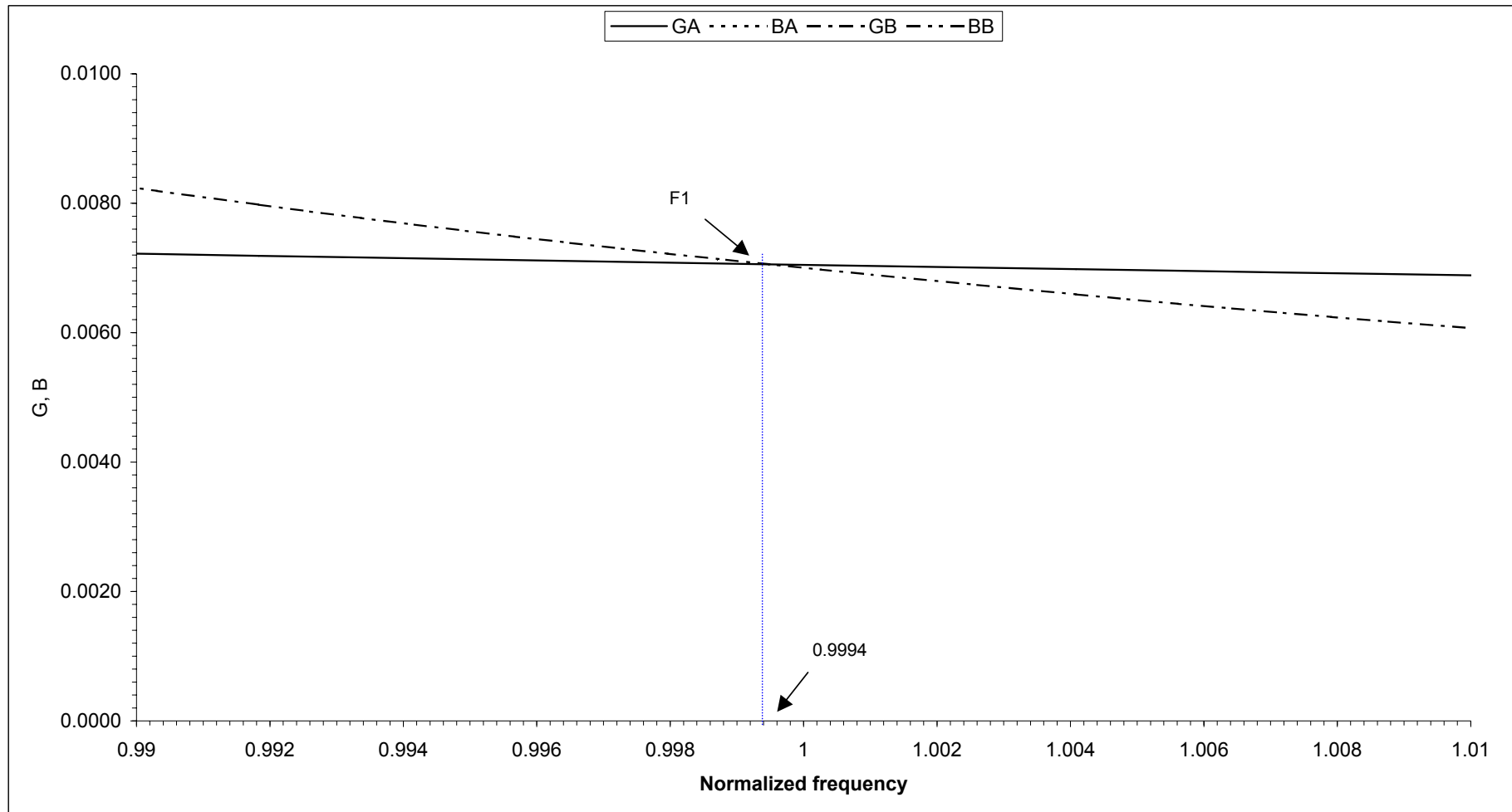


Figure 4.7 Point of intersection, F1 (Example A1).

The array with modified element length is again modelled in IE3D. Its admittance parameters at the operational frequency of 2.45 GHz is given by

$$\begin{aligned} Y_{11} &= 7.06 \times 10^{-3} - j3.02 \times 10^{-2} = 0.031 \angle -76.8^\circ \\ Y_{12} &= -2.12 \times 10^{-6} + j1.50 \times 10^{-2} = 0.015 \angle 90.0^\circ \end{aligned} \quad (4.18)$$

From (4.18), it can be seen that the new array has a mutual admittance that is purely imaginary, that is,  $Y_{12} = jB_{12}$ , where  $B_{12} = 1.50 \times 10^{-2}$ . The decoupling element is therefore a simple capacitor. To solve for the capacitance at 2.45 GHz,

$$C_{12} = \frac{B_{12}}{\omega} = 0.971 \text{ pF}. \quad (4.19)$$

The array with its decoupling network is as shown in Figure 4.8. The self and mutual admittances of the decoupled array is

$$\begin{aligned} \tilde{Y}_{ii} &= 0.00710 \angle -2.5^\circ \\ \tilde{Y}_{ij} &= 0 \end{aligned} \quad (4.20)$$

From (4.20), the array has been decoupled, giving a mutual admittance of zero. The input admittance at each port of the decoupled array is given by  $\tilde{Y}_{ii}$ . This admittance can easily be matched to any desired port impedance. The radiation pattern of the decoupled array has a linear directivity of 9.91 dBi, as shown in Figure 4.9.

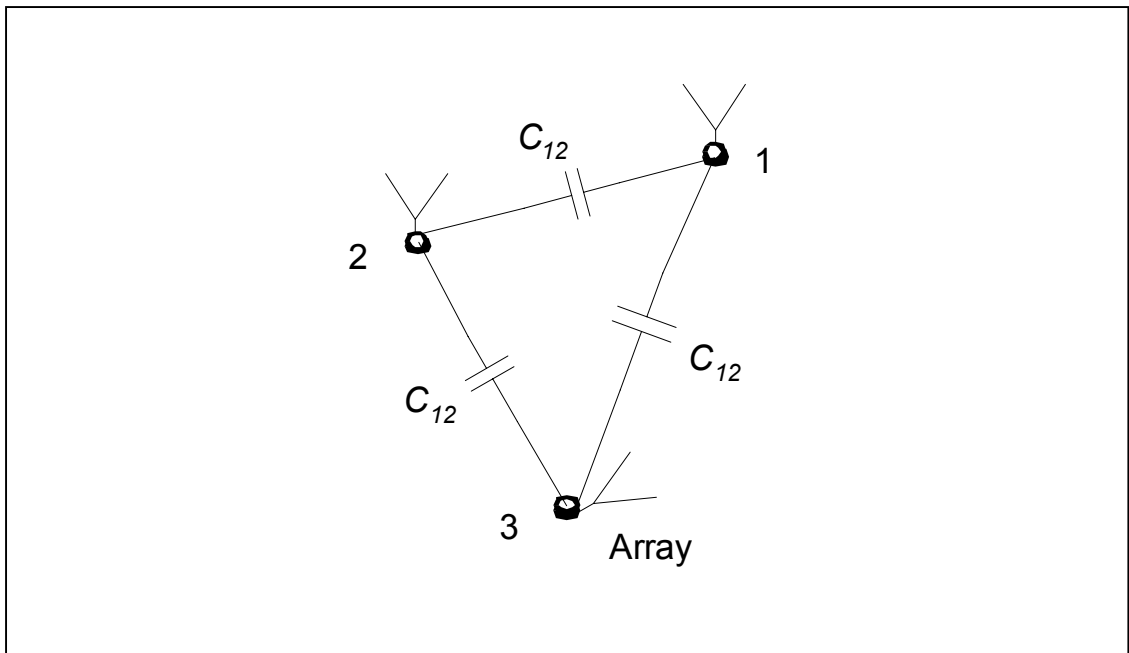


Figure 4.8 An array with its decoupling network.

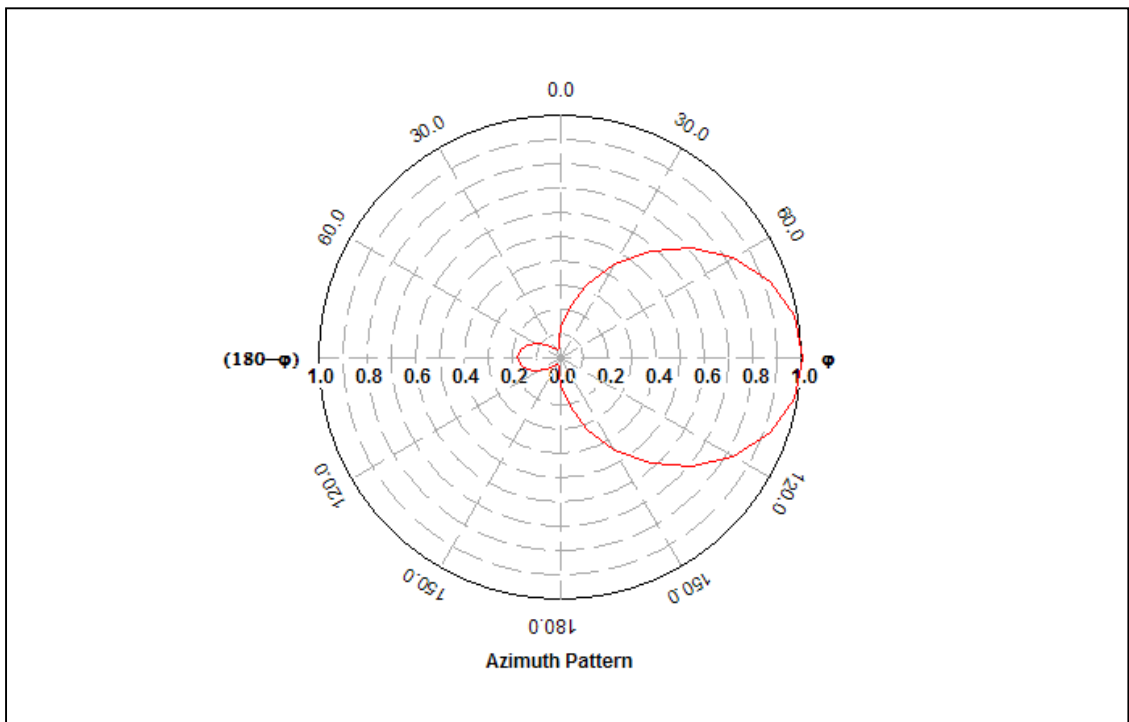


Figure 4.9 Radiation pattern of a decoupled array.

#### 4.4.2. Example A2

In this second example, decoupling of the array requires increasing the length of the array element. Table 4.2 summarizes the parameters of the original array. In this example, the array elements have thicker diameters.

Table 4.2 Parameters of the array for example A2.

Operational frequency, $f_0$	2.45 GHz
Wavelength, $\lambda_0$	$c/f_0 = 122.4$ mm
Length of monopole, $l_0$	$\lambda_0 / 4 = 30.6$ mm
Diameter of monopole, $d$	$\lambda_0 / 20 = 6.12$ mm
Array element spacing, $a$	$\lambda_0 / 10 = 12.24$ mm

Figure 4.10 shows a plot of the mode admittances over a range of frequencies. There are two points of intersection F1 and F2, where the conductance of eigenmodes A and B are equal. A closer look at point F1 (Figure 4.11) reveals a normalized frequency of 1.0324. This implies that the new length of the array element is 3.24% longer than its original length. This gives a new element length of 31.591 mm.

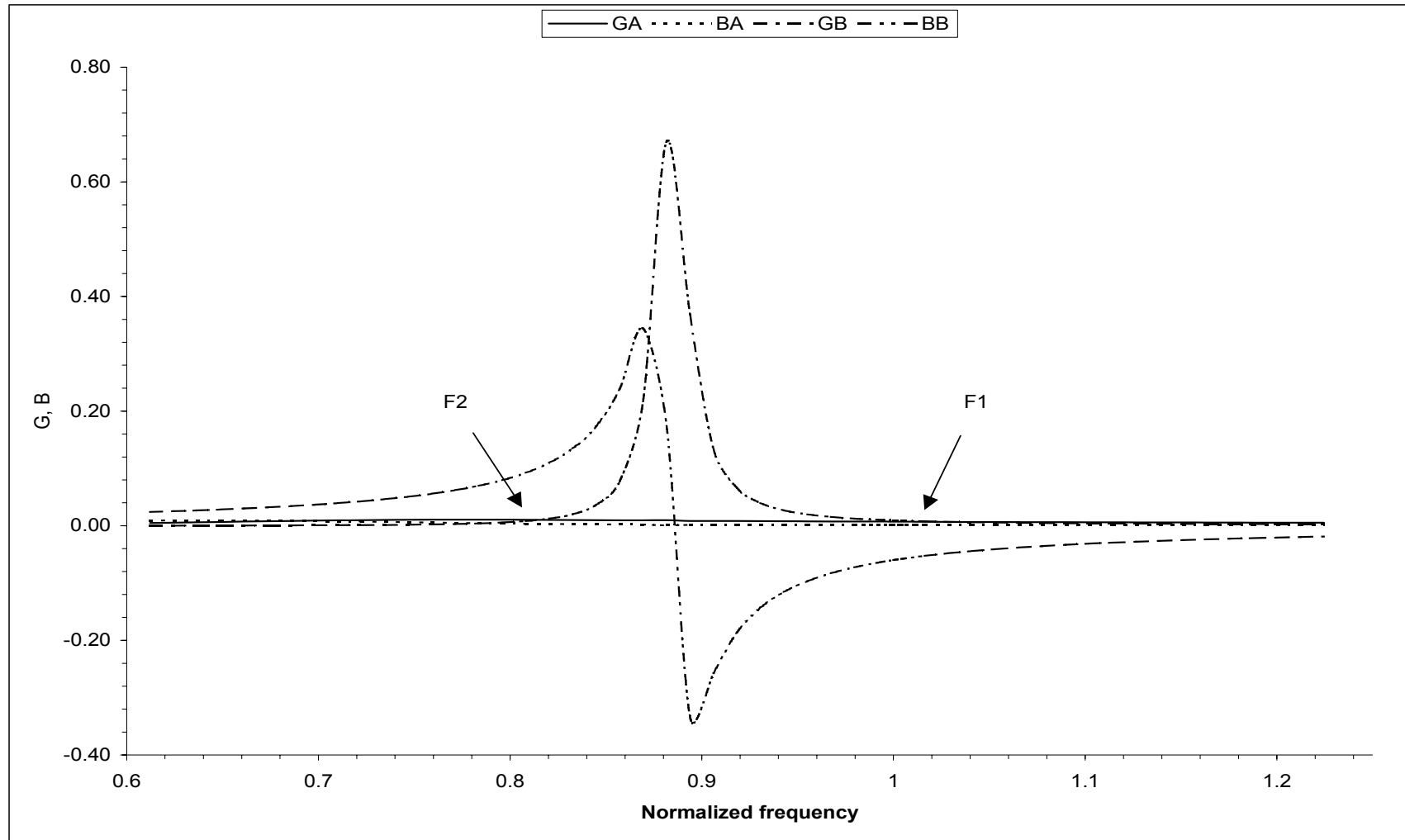


Figure 4.10 Plot of mode admittances over a range of frequencies (Example A2).

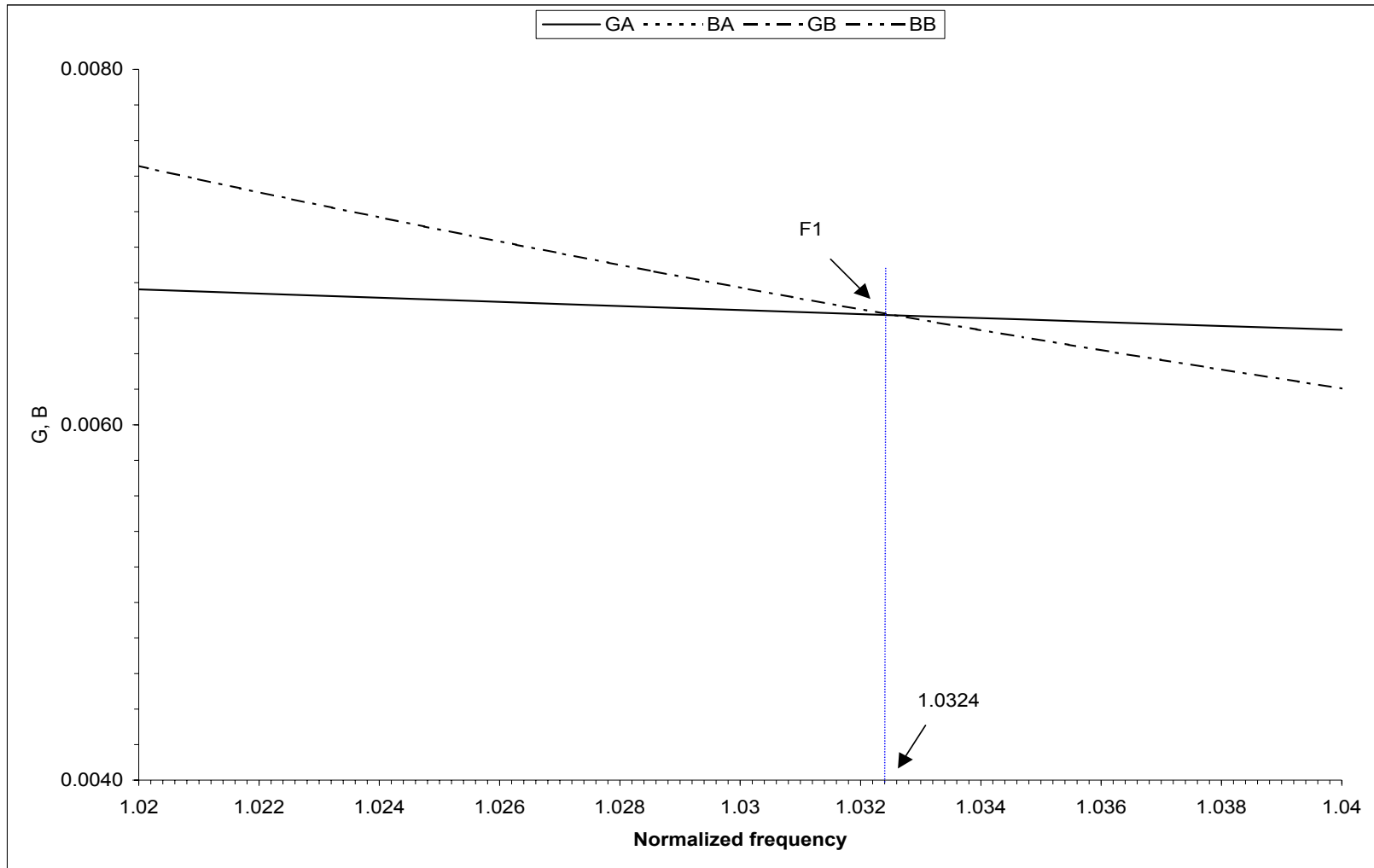


Figure 4.11 Point of intersection, F1 (Example A2).

Simulations of the array with modified element length are run in IE3D. Its admittance parameters at the operational frequency of 2.45 GHz is given by

$$\begin{aligned} Y_{11} &= 6.53 \times 10^{-3} - j3.18 \times 10^{-2} = 0.0325 \angle -78.4^\circ \\ Y_{12} &= 1.13 \times 10^{-5} + j1.63 \times 10^{-2} = 0.0163 \angle 90.0^\circ \end{aligned} \quad (4.21)$$

The decoupling element is again a simple capacitor. To solve for the capacitance at 2.45 GHz,

$$\begin{aligned} B_{12} &= 1.63 \times 10^{-2} \\ C_{12} &= \frac{B_{12}}{\omega} = 1.06 \text{ pF} \end{aligned} \quad (4.22)$$

The self and mutual admittances of the decoupled array is

$$\begin{aligned} \tilde{Y}_{ii} &= 0.00659 \angle 7.8^\circ \\ \tilde{Y}_{ij} &= 0 \end{aligned} \quad (4.23)$$

#### 4.5. A generalized design for the decoupling network of an array

In the previous design method [8, 9], decoupling is done on an array with a susceptible mutual admittance. The length of each array element is modified to give a new array with purely susceptible mutual admittance. This design method is cumbersome because it involves some iteration to obtain the desired element length. Accuracy of the theoretical analysis technique is vital, since any deviations are likely to result in the manufactured array not having purely susceptible mutual admittances.

In the generalized design, decoupling does not necessary have to be carried out on an array with purely susceptible mutual admittance. Instead, an array with any complex



mutual admittance can be analytically decoupled with the help of a lossless network, without having to modify the length of the array elements or their element spacing.

The proposed lossless decoupling network for a 3-element array is as shown in Figure 4.12. The decoupling network consists of a series section with components  $jX_1$  and a parallel section with components  $jB_2$ . Two analysis approaches can be used to compute the components of the decoupling network. The first approach is the eigenmode analysis while the second is a network analysis.

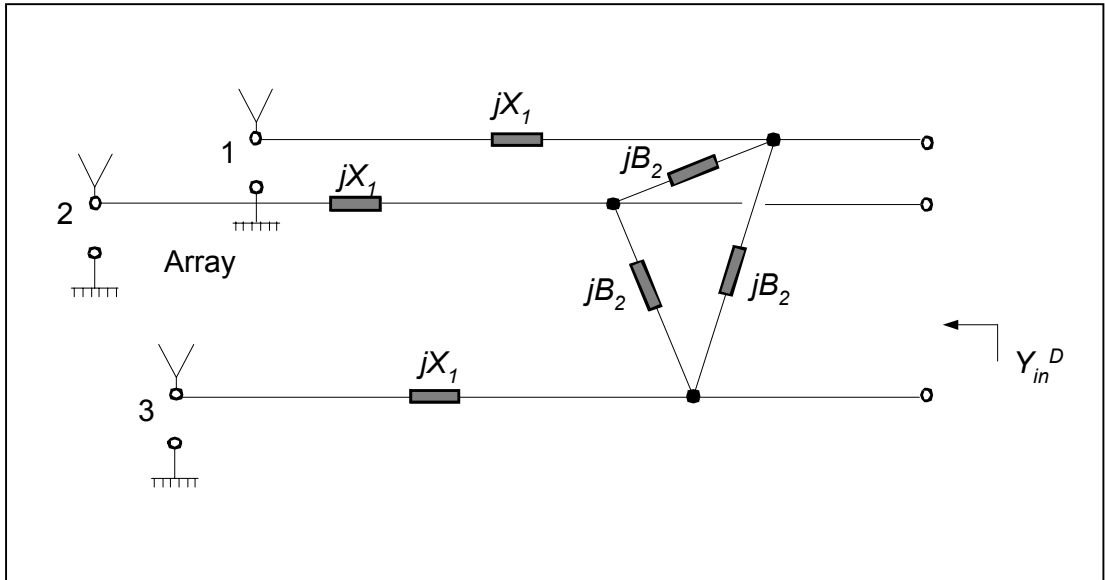


Figure 4.12 A generalized decoupling network for a 3-element array.

#### 4.5.1. Eigenmode analysis

In the eigenmode analysis, the admittance matrix of the array and its eigenvalues are evaluated as described in equations (4.6) and (4.7). The equivalent circuit for the different eigenmodes [9] are shown in Figure 4.13. For each eigenmode, the equivalent circuit consist of a series component and a parallel component. The series component is simply  $jX_1$ . The parallel component can be derived using simple two-

port network theory and equation (4.7). From two-port network theory, the admittance matrix of the parallel section of the decoupling network, as shown in Figure 4.12, can be obtained and is given by

$$\mathbf{Y}_{\text{DNparallel}} = \begin{bmatrix} j2B_2 & -jB_2 & -jB_2 \\ -jB_2 & j2B_2 & -jB_2 \\ -jB_2 & -jB_2 & j2B_2 \end{bmatrix}. \quad (4.24)$$

From (4.7), since  $Y_{11}^{\text{DNparallel}} + 2Y_{12}^{\text{DNparallel}} = 0$ , there is no parallel component in the equivalent circuit for mode A. For mode B or C, the parallel component can be computed as  $Y_{11}^{\text{DNparallel}} - Y_{12}^{\text{DNparallel}} = j3B_2$ .

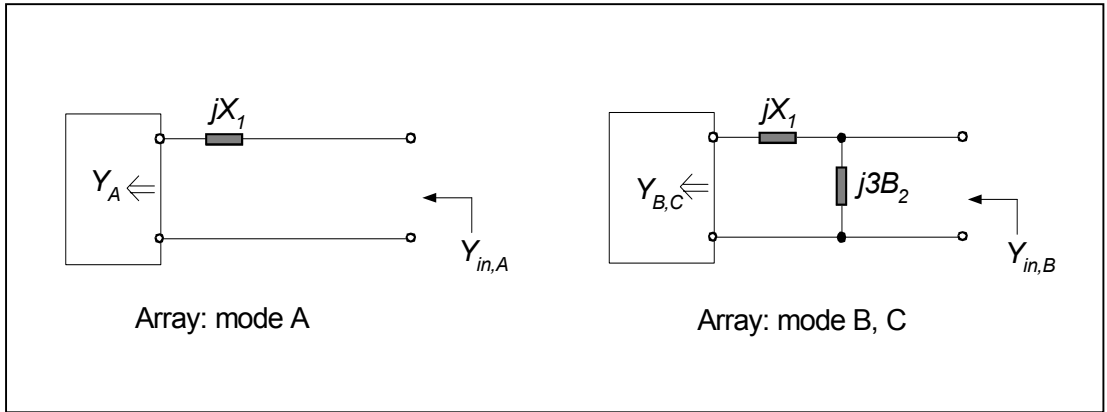


Figure 4.13 Equivalent circuits for different eigenmodes of a 3-element array.

From Figure 4.13, the equivalent modal admittances are

$$Y_{in,A} = \left( \frac{1}{Y_A} + jX_1 \right)^{-1}, \quad (4.25)$$

$$Y_{in,B} = Y_{in,C} = \left( \frac{1}{Y_B} + jX_1 \right)^{-1} + j3B_2. \quad (4.26)$$

In this eigenmode analysis, the decoupling network decouples the ports of the array by matching all the mode admittances. From (4.25) and (4.26),  $X_1$  and  $B_2$  can be obtained by solving the following set of nonlinear simultaneous equations:

$$\begin{aligned} \operatorname{Re}[Y_{in,A}] &= \operatorname{Re}[Y_{in,B}] \\ \operatorname{Im}[Y_{in,A}] &= \operatorname{Im}[Y_{in,B}] \end{aligned} \quad (4.27)$$

Analytical solutions for  $X_1$  and  $B_2$  are obtained in terms of the admittance parameters,  $Y_{11}$  and  $Y_{12}$ , of the array, using *Mathematica* [23]. Appendix A contains the program code based on the eigenmode analysis for decoupling an array with an arbitrary admittance matrix. The program uses the decoupling network as shown in Figure 4.12 and evaluates equation (4.27) to find the solutions. By substituting numerical values for the admittance parameters of the array, the values of  $X_1$  and  $B_2$  can be obtained.

#### 4.5.2. Network analysis

The following impedance and admittance matrices describe the series and parallel sections of the decoupling network (shown in Figure 4.12) respectively:

$$\mathbf{Z}_{\text{DNseries}} = \begin{bmatrix} jX_1 & 0 & 0 \\ 0 & jX_1 & 0 \\ 0 & 0 & jX_1 \end{bmatrix}, \quad (4.28)$$

$$\mathbf{Y}_{\text{DNparallel}} = \begin{bmatrix} j2B_2 & -jB_2 & -jB_2 \\ -jB_2 & j2B_2 & -jB_2 \\ -jB_2 & -jB_2 & j2B_2 \end{bmatrix}. \quad (4.29)$$

The admittance matrix of the decoupled array can be written as:

$$\mathbf{Y}_{\text{in}}^D = \left( \mathbf{Y}_{\text{array}}^{-1} + \mathbf{Z}_{\text{DNseries}} \right)^{-1} + \mathbf{Y}_{\text{DNparallel}} . \quad (4.30)$$

For decoupling to be achieved, the mutual admittance of the decoupled system,  $Y_{12}^D$ , should be zero. Solutions for  $X_1$  and  $B_2$  are obtained by solving the following set of nonlinear simultaneous equations:

$$\begin{aligned} \text{Re}[Y_{12}^D] &= 0 \\ \text{Im}[Y_{12}^D] &= 0 \end{aligned} \quad (4.31)$$

Analytical solutions for  $X_1$  and  $B_2$  are obtained. Appendix B contains the program code based on the network analysis for decoupling an array with an arbitrary admittance matrix. The program uses the decoupling network as shown in Figure 4.12 and evaluates equation (4.31) to find the solutions. By substituting numerical values for the admittance parameters of the array, the values of  $X_1$  and  $B_2$  can be obtained.

It has been verified that solutions thus obtained are consistent with those obtained from the eigenmode analysis. Appendix C contains a program code written in *Mathematica*. The code verifies that both the eigenmode and network analyses give the same decoupling network by subtracting the two different solutions and obtaining a zero output.

#### 4.5.3. Matching network

The decoupled antenna array can easily be matched to any desired impedance, since the impedances looking into each port of the array are now identical. A  $L$ -network topology, consisting of a shunt and series component, is used for the matching network as shown in Figure 4.14.

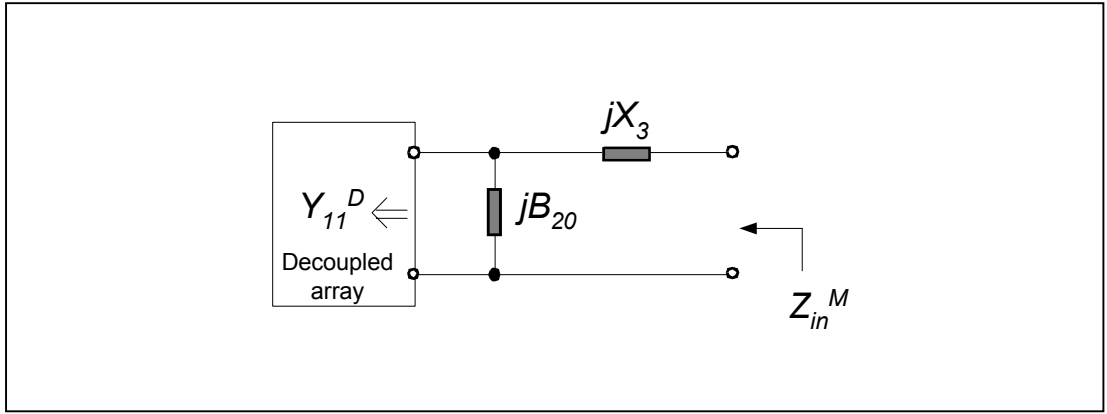


Figure 4.14 A matching network section for a decoupled array.

From Figure 4.14,

$$(Y_{11}^D + jB_{20})^{-1} + jX_3 = Z_{in}^M. \quad (4.32)$$

where  $Y_{11}^D$  is the admittance at each decoupled port and  $Z_{in}^M$  is the impedance at each matched port. If  $Y_{11}^D$  and  $Z_{in}^M$  are known, analytic solutions for  $B_{20}$  and  $X_3$  can be found.

In general, for matching to, for example, a  $50 \, \Omega$  system, the values for the components  $B_{20}$  and  $X_3$  in the matching network can be obtained by solving the following set of simultaneous equations:

$$\begin{aligned} \text{Re}[Z_{in}^M] &= 50 \\ \text{Im}[Z_{in}^M] &= 0 \end{aligned} \quad (4.33)$$

#### 4.5.4. Example B1

This example serves to illustrate the generalized design method for decoupling a 3-element array. Either the eigenmode or network analysis can be applied to solve for the values of the decoupling network. Table 4.3 gives the parameters of the array used in this example. This array is identical to the one used in Example A2.

Table 4.3 Parameters of the array for example B1.

Operational frequency, $f_0$	2.45 GHz
Wavelength, $\lambda_0$	$c/f_0 = 122.4$ mm
Length of monopole, $l_0$	$\lambda_0 / 4 = 30.6$ mm
Diameter of monopole, $d$	$\lambda_0 / 20 = 6.12$ mm
Array element spacing, $a$	$\lambda_0 / 10 = 12.24$ mm

By running simulations in IE3D, the admittance parameters of the array can be obtained. Table 4.4 shows the admittance parameters of the original and decoupled array. Values of the components for the decoupling network are obtained by solving either (4.27) or (4.31). Each decoupling and matching network contains only lossless components such as inductors or capacitors. For an array, there exists two possible decoupling network configurations, and for each decoupling network, there exists two possible matching network configurations. Table 4.5 summarizes the possible decoupling and matching network configurations. Figure 4.15 illustrates the array with its decoupling and matching network.

Table 4.4 Admittance parameters of the array (Example B1).

Original array	Decoupled array
$Y_{11} = 0.0406 \angle -77.8^\circ$	$\tilde{Y}_{11} = 0.00709 \angle 6.8^\circ$
$Y_{12} = 0.0203 \angle 92.2^\circ$	$\tilde{Y}_{12} = 0$

Table 4.5 Decoupling and matching network configurations (Example B1).

Case No.		Decoupling network		Matching network	
		Series	Parallel	Shunt	Series
B1	(a)	$L = 0.164 \text{ nH}$	$C = 1.149 \text{ pF}$	$C = 0.570 \text{ pF}$	$L = 4.41 \text{ nH}$
				$L = 6.29 \text{ nH}$	$C = 0.957 \text{ pF}$
	(b)	$C = 1.788 \text{ pF}$	$L = 4.164 \text{ nH}$	$C = 0.445 \text{ pF}$	$L = 4.85 \text{ nH}$
				$L = 5.58 \text{ nH}$	$C = 0.870 \text{ pF}$

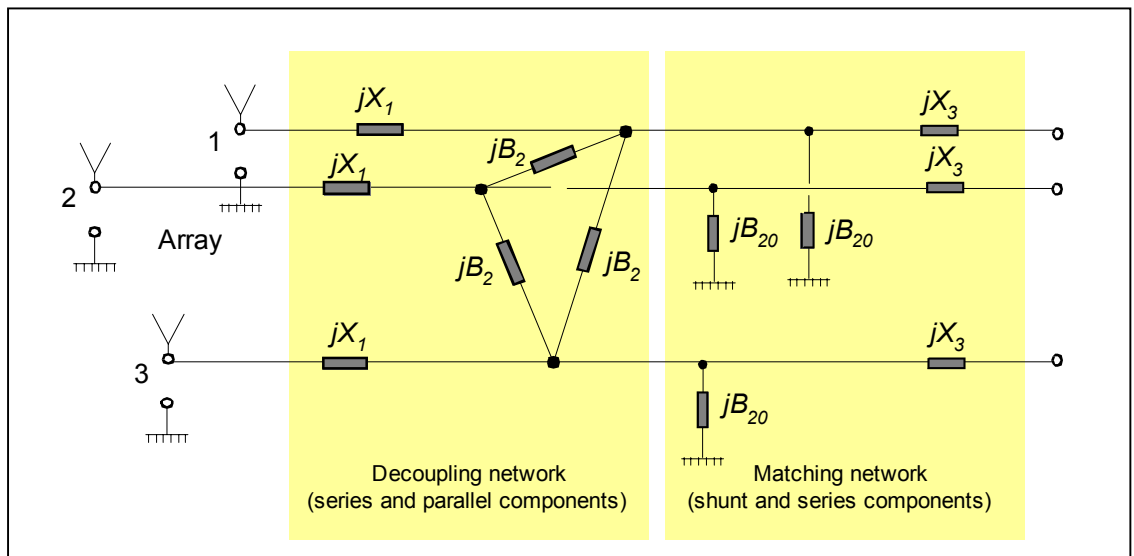


Figure 4.15 A 3-element array with its decoupling and matching network.

#### 4.5.5. Example B2

Table 4.6 gives the parameters of the array used in Example B2. The array has a thinner diameter and a smaller inter-element spacing, as compared to Example B1.

Table 4.6 Parameters of the array for Example B2.

Operational frequency, $f_0$	2.45 GHz
Wavelength, $\lambda_0$	$c/f_0 = 122.4$ mm
Length of monopole, $l_0$	$\lambda_0 / 4 = 30.6$ mm
Diameter of monopole, $d$	$\lambda_0 / 40 = 3.06$ mm
Array element spacing, $a$	$\lambda_0 / 20 = 6.12$ mm

Similarly, Table 4.7 shows the admittance parameters of the original and decoupled array. Table 4.8 summarizes the possible decoupling and matching network configurations. Figure 4.15 gives the topology of the network.

Table 4.7 Admittance parameters of the array (Example B2).

Original array	Decoupled array
$Y_{11} = 0.0821 \angle -84.6^\circ$	$\tilde{Y}_{11} = 0.00628 \angle -7.4^\circ$
$Y_{12} = 0.0401 \angle 91.2^\circ$	$\tilde{Y}_{12} = 0$



Table 4.8 Decoupling and matching network configurations (Example B2).

Case No.		Decoupling network		Matching network	
		Series	Parallel	Shunt	Series
B2	(a)	$C = 3.66 \text{ pF}$	$L = 1.86 \text{ nH}$	$C = 0.657 \text{ pF}$	$L = 4.82 \text{ nH}$
				$L = 7.70 \text{ nH}$	$C = 0.876 \text{ pF}$
	(b)	$L = 0.106 \text{ nH}$	$C = 2.17 \text{ pF}$	$C = 0.694 \text{ pF}$	$L = 4.98 \text{ nH}$
				$L = 8.53 \text{ nH}$	$C = 0.847 \text{ pF}$

#### 4.5.6. Example B3

Table 4.9 gives the parameters of the array used in Example B3. The array has a smaller inter-element spacing, as compared to Example B2.

Table 4.9 Parameters of the array for Example B3.

Operational frequency, $f_0$	2.45 GHz
Wavelength, $\lambda_0$	$c/f_0 = 122.4 \text{ mm}$
Length of monopole, $l_0$	$\lambda_0 / 4 = 30.6 \text{ mm}$
Diameter of monopole, $d$	$\lambda_0 / 40 = 3.06 \text{ mm}$
Array element spacing, $a$	$\lambda_0 / 30 = 4.08 \text{ mm}$

Similarly, Table 4.10 shows the admittance parameters of the original and decoupled array. Table 4.11 summarizes the possible decoupling and matching network configurations. Figure 4.15 gives the topology of the network.

Table 4.10 Admittance parameters of the array (Example B3).

Original array	Decoupled array
$Y_{11} = 0.237 \angle -86.9^\circ$	$\tilde{Y}_{11} = 0.00615 \angle -16.8^\circ$
$Y_{12} = 0.117 \angle 91.7^\circ$	$\tilde{Y}_{12} = 0$

Table 4.11 Decoupling and matching network configurations (Example B3).

Case No.		Decoupling network		Matching network	
		Series	Parallel	Shunt	Series
B3	(a)	$C = 8.64 \text{ pF}$	$L = 0.908 \text{ nH}$	$C = 0.722 \text{ pF}$	$L = 5.00 \text{ nH}$
				$L = 9.08 \text{ nH}$	$C = 0.843 \text{ pF}$
	(b)	$L = 0.128 \text{ nH}$	$C = 4.47 \text{ pF}$	$C = 0.733 \text{ pF}$	$L = 5.15 \text{ nH}$
				$L = 9.59 \text{ nH}$	$C = 0.820 \text{ pF}$

#### 4.6. Analytical solutions for array with more elements

It would be desirable to formulate an analytical concept for the decoupling network. *Mathematica* was used to study the feasibility of obtaining a theoretical model [24, 25]. For a  $M$ -element array ( $M = 3$  to 6), orthogonal eigenvectors and eigenvalues from a generalized admittance matrix with  $Y_{ij}$  as its elements can be obtained. It was found that for  $M = 3, 4$  and 6, simple orthogonal eigenvectors and eigenvalues were obtained. However, for  $M = 5$ , complicated expressions in terms of  $Y_{ij}$  were obtained. Appendices D to G contain the program code for arrays with three to six elements. Solving for arrays with more than six elements was beyond the computational resources available.

Since the eigenvalues and eigenvectors of arrays with more than three elements can be obtained, this implies that these arrays can be decoupled theoretically, through the eigenmode approach. However, it should be noted that configurations of the decoupling network might be different from the generalized network for a 3-element array. The focus of this thesis is on a 3-element array. More work has to be done to investigate the configuration of the decoupling network for arrays with more elements.

#### 4.7. Conclusion

This chapter has described two designs to decouple a 3-element array. One design involves modification to the array element length while the other is a generalized method that can be applied to any array with complex admittance parameters. Two different analysis techniques were also discussed, namely the eigenmode and network analyses. Examples were included to illustrate the use of the two types of analysis.

The chapter also gives a brief discussion on the analytical solutions for arrays with more than three elements. More research has to be done on the configuration of the decoupling network for these arrays.

## **CHAPTER 5**

### **DECOUPLING NETWORK IMPLEMENTATION**

#### **5.1. Introduction**

This chapter describes ways to realize the lumped decoupling elements. It discusses the use of Kuroda's identities to transform the ideal elements into realizable forms in microstrip or stripline. Design considerations on the practical implementation of the decoupling network are also presented. A discussion on the use of interdigital capacitors in the decoupling network is included.

#### **5.2. Realization of lumped elements**

To implement the decoupling and matching networks, the ideal lumped capacitors and inductors have to be converted to realizable forms. One convenient way of realizing the decoupling and matching networks is in microstrip or stripline. The capacitors and inductors are implemented as microstrip or stripline stubs. Kuroda's identities [26 – 29] are applied to transform the lumped components into microstrip or stripline stubs.

##### **5.2.1. Kuroda's identities**

Kuroda's identities form a set of equivalences for impedance inversion [26]. Figure 5.1 shows all the Kuroda's identities. The circuits shown in Figure 5.1 are equivalent with respect to their ABCD matrices. These identities make use of a unit element (U.E.) that has impedance inversion properties. For example, a series inductance followed by a unit element is equivalent to a parallel capacitance preceding a unit element.

In [26] and [27], the unit element is defined as a quarter-wavelength transmission line. However, the unit element in [28] is taken as 1/8 of a wavelength of transmission line. It was verified that both definitions are correct. In fact, the latter [28] is a subset of the former [26, 27]. If 1/8-wavelength unit elements were used, the characteristic impedance of some of the microstrip lines would not be equal to 50  $\Omega$  after application of Kuroda's identities. In contrast, using quarter-wavelength unit elements results in a consistent characteristic impedance of 50  $\Omega$  for all the microstrip lines. Therefore, this definition of a unit element as a quarter-wavelength line was adopted in all investigations.

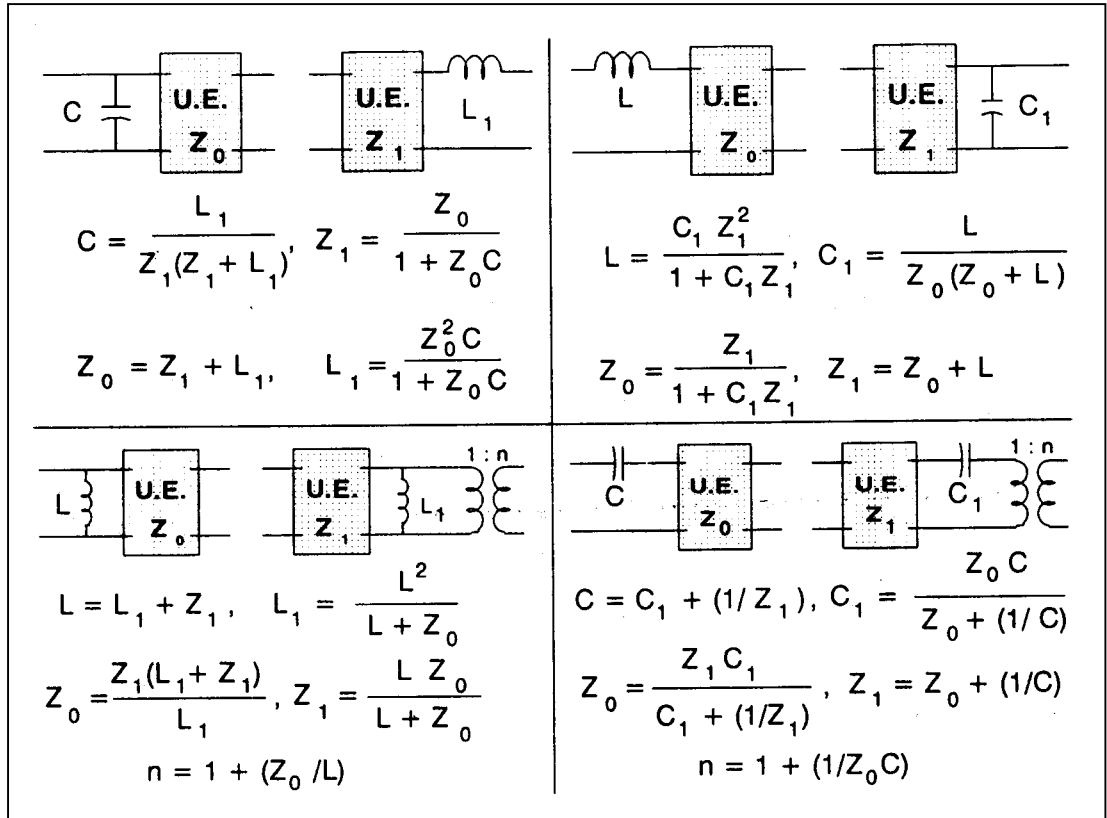


Figure 5.1 Kuroda's identities [26].

### 5.2.2. Realization of series inductors

To realize a series inductor, Kuroda's identity, as shown in Figure 5.2, is applied to transform it to a shunt capacitor. The resulting shunt capacitor can easily be implemented as an open-circuited microstrip stub, with the electrical length  $\theta^{oc}$  of the stub given by

$$\theta^{oc} = \beta l^{oc} = \tan^{-1}(\omega C Z_0). \quad (5.1)$$

Here  $\beta = \frac{2\pi}{\lambda}$  is the phase constant,  $\omega$  is the angular frequency,  $C$  is the capacitance value and  $Z_0$  is the characteristic impedance of the microstrip line.

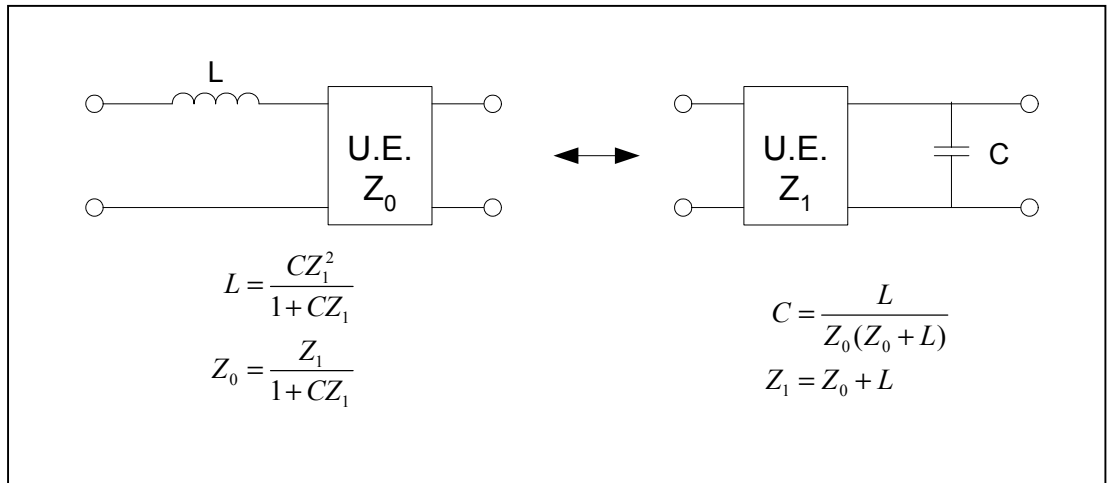


Figure 5.2 Kuroda's identity applied to a series inductor.

To illustrate the process of transformation, Figure 5.3 shows a breakdown of the steps involved in the transformation of a series inductor to a shunt capacitor, using Kuroda's identity. It is well known that insertion of half a wavelength of transmission will not affect the impedance of the network. Hence, a section of half-wavelength transmission line is added to the series inductor. This section of transmission line

provides the unit element required for Kuroda's transformation. The resulting shunt capacitor can easily be realized on microstrip line.

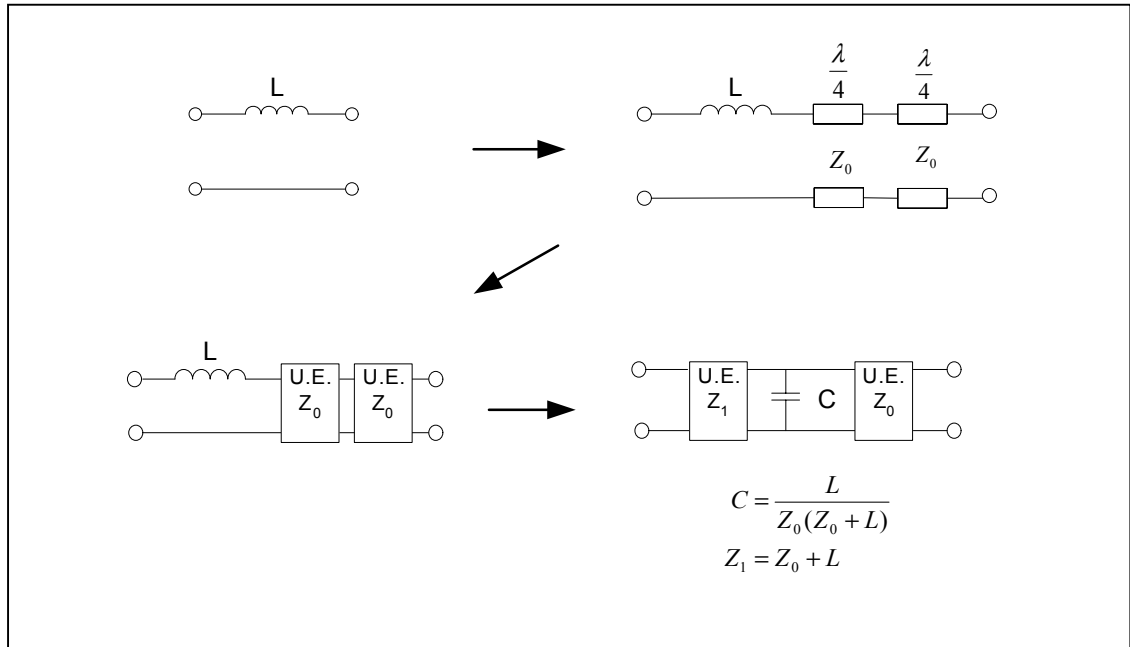


Figure 5.3 Steps involved in the transformation of a series inductor.

### 5.2.3. Realization of series capacitors

From Figure 5.1, it can be observed that the transformation of a series capacitor will result in another series capacitor and a transformer. Hence for a series capacitor, Kuroda's identity cannot be applied directly. Instead, the series capacitor first needs to be transformed to its equivalent (negative) series inductor. Kuroda's identity can then be applied to convert the resulting (negative) series inductor to a shunt capacitor. The shunt capacitor is then realized as a shunt stub. The steps taken to realize a series capacitor are summarized in Figure 5.4.



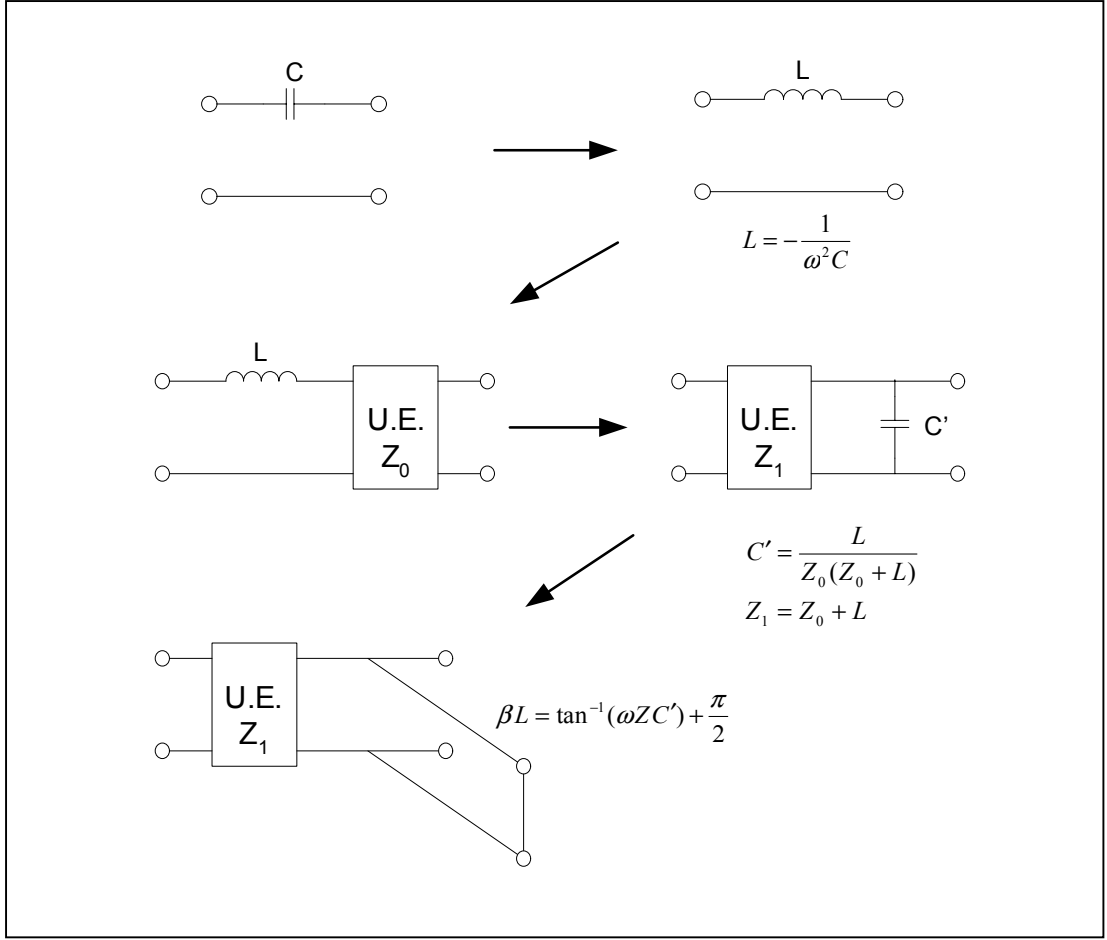


Figure 5.4 Steps to realize a series capacitor.

#### 5.2.4. Realization of shunt inductors and capacitors

A shunt inductor is simply realized as a shunt short-circuited stub to ground. The electrical length of the stub can be computed from

$$\theta^{sc} = \beta l^{sc} = \tan^{-1}\left(\frac{\omega L}{Z_0}\right). \quad (5.2)$$

Shunt capacitors are realized as shunt open-circuited stubs. The electrical length of the stub is given by equation (5.1). In practice, a short-circuited stub is preferred to an open-circuited stub because it is more feasible and realistic to have a short circuit than to have an ideal open-circuit. An open-circuited stub is easily converted to a

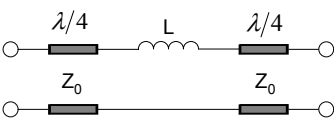
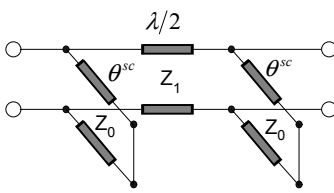
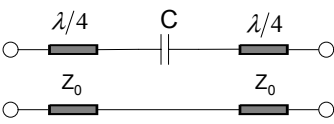
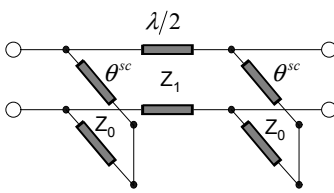
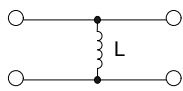
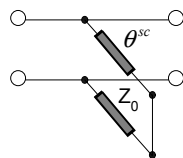
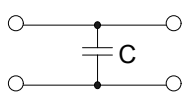
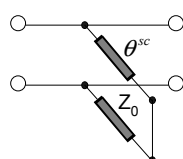
short-circuited stub by adding an additional quarter-wavelength line to the open-circuited stub, so that

$$\theta^{sc} = \theta^{oc} \pm \frac{\pi}{2}. \quad (5.3)$$

### 5.2.5. Summary of realization of ideal components

Table 5.1 summarizes the realization of the ideal capacitors and inductors as microstrip stubs, with the corresponding equations required for the transformations.

Table 5.1 Transformation of ideal components to microstrip stubs.

Initial network	Transformed network	Design equations
		$\theta^{sc} = \tan^{-1} \left( \frac{\omega L}{2Z_0 + L} \right) \pm \frac{\pi}{2}$ $Z_1 = Z_0 + \frac{L}{2}$
		$\theta^{sc} = \tan^{-1} \left( \frac{\omega}{1 - 2Z_0\omega^2 C} \right) \pm \frac{\pi}{2}$ $Z_1 = Z_0 - \frac{1}{2\omega^2 C}$
		$\theta^{sc} = \tan^{-1} \left( \frac{\omega L}{Z_0} \right)$
		$\theta^{sc} = \tan^{-1} (\omega C Z_0) \pm \frac{\pi}{2}$

### 5.3. Preservation of symmetry in decoupling network

The preservation of symmetry is vital for the series components in the parallel section of the decoupling network. Experiments have shown that unless symmetry is preserved, the array would not be decoupled. For an inductor in the parallel section of the decoupling network, symmetry is maintained by representing the inductor as two separate inductors in series, each with inductance value half of that of the original inductor, as shown in Figure 5.5. A capacitor in the parallel section of the decoupling network is first converted to its equivalent (negative) inductance. The resulting equivalent inductor is then implemented with two (negative) series inductors, each with half the original inductance. In addition, for symmetry to hold in the parallel section of the decoupling network, unit elements on each side of the component must add up to multiples of half-wavelengths. These unit elements are features of Kuroda's identities.

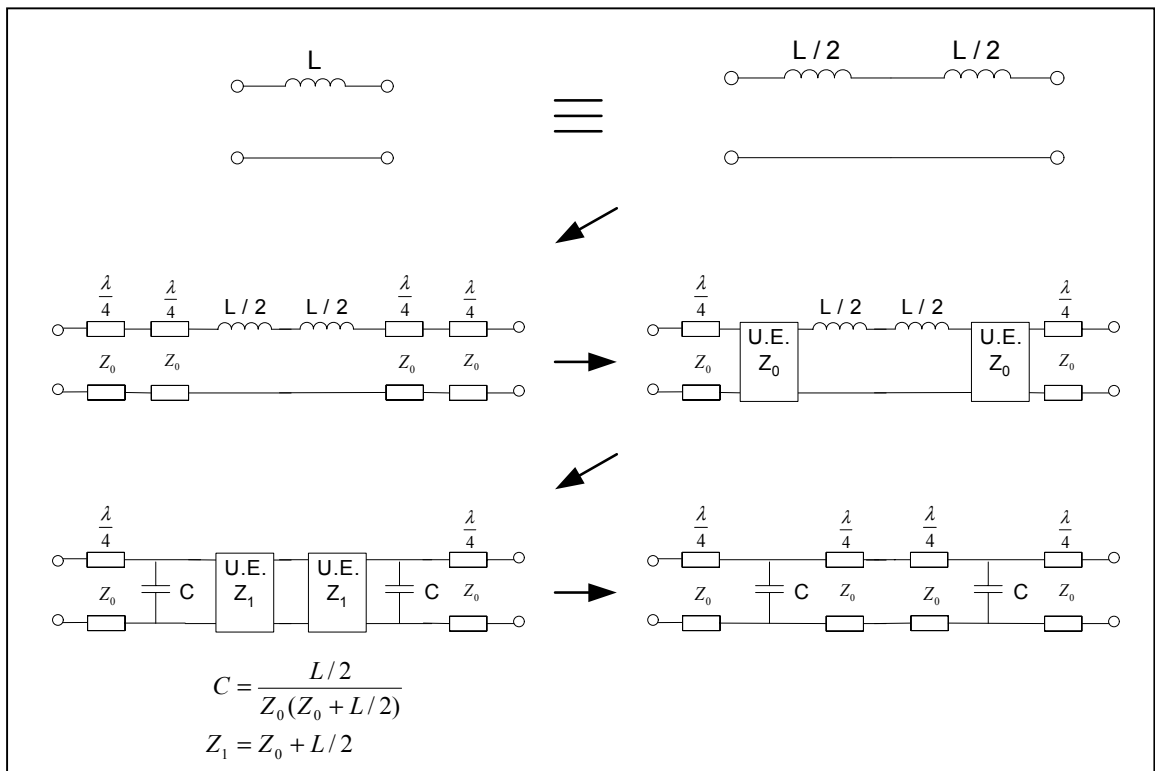


Figure 5.5 Transformation for inductor to maintain symmetry.

#### 5.4. Interdigital capacitors as series capacitors

Besides transforming a series capacitor into its equivalent (negative) inductor, series capacitors may also be realized as interdigital capacitors on microstrip. A typical interdigital capacitor is as shown in Figure 5.6. Figure 5.7 shows the low frequency equivalent circuit for a unit cell of two fingers of the interdigital capacitor, while Figure 5.8 shows the equivalent circuit for the whole interdigital capacitor with  $N$  fingers [30].

From Figure 5.8, the shunt capacitances  $C_T$  and  $C_g$  can be combined as a single shunt capacitance  $C_p$ , where  $C_p = C_T + C_g$ . The single shunt capacitance is equivalent to a length of transmission line,  $\Delta l$  [31]. Figure 5.9 illustrates the implementation of a series capacitor as an interdigital capacitor, taking into consideration the equivalent length of transmission line  $\Delta l$ .

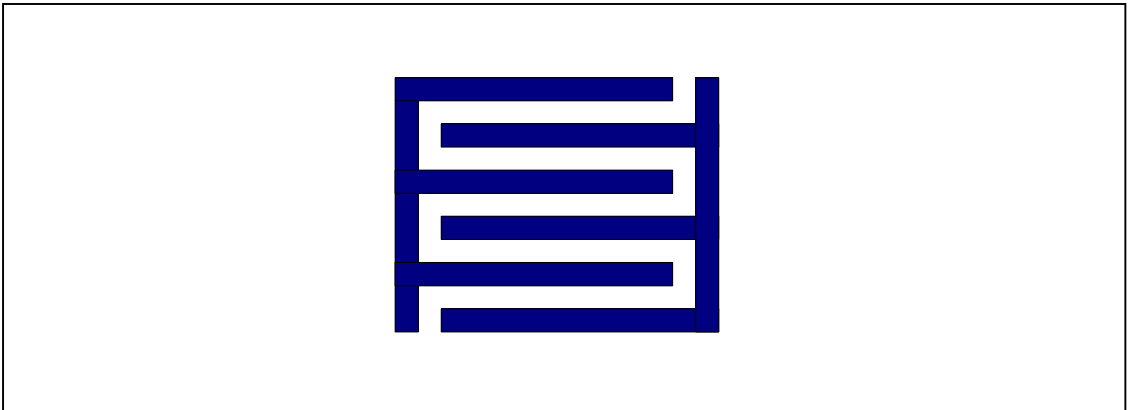


Figure 5.6 A typical interdigital capacitor.

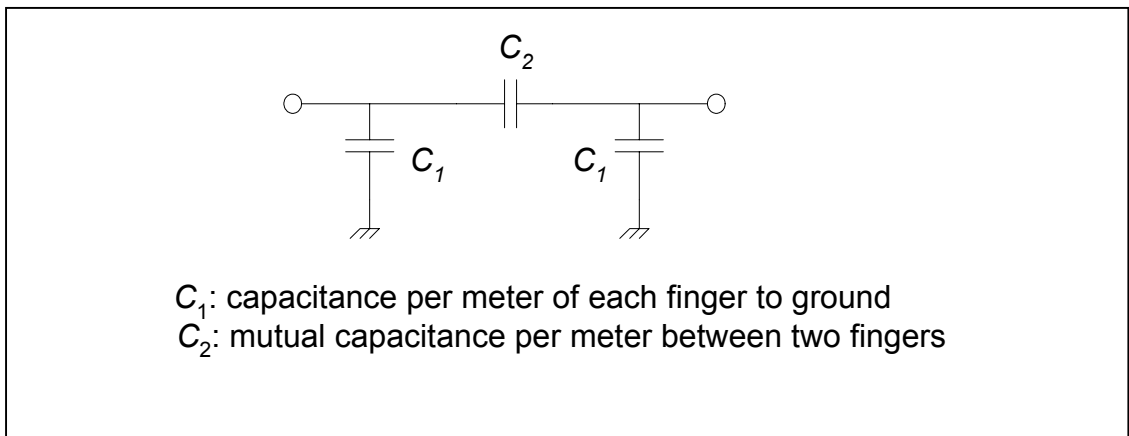


Figure 5.7 An equivalent circuit for a unit cell of two fingers of an interdigital capacitor.

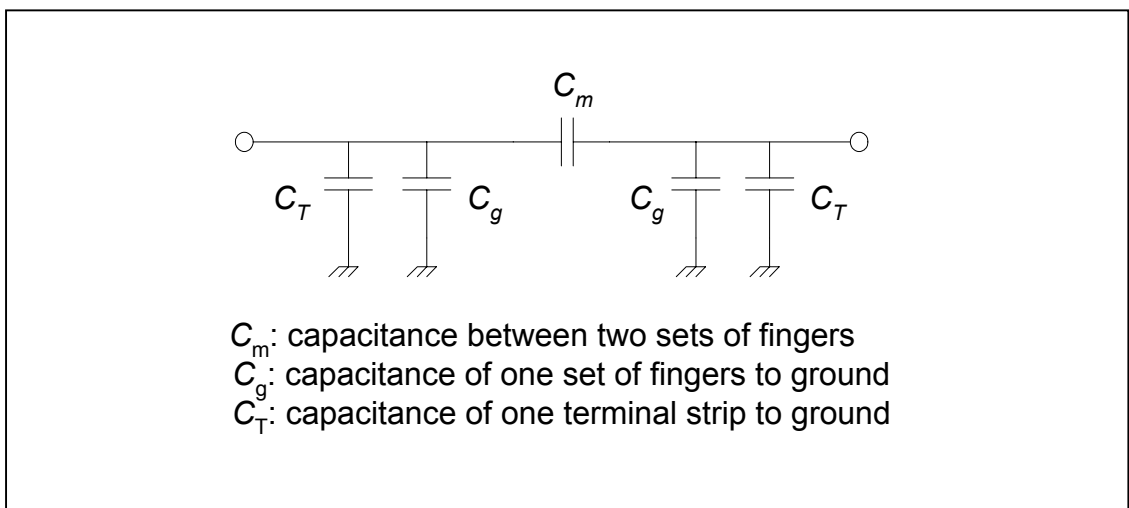


Figure 5.8 An equivalent circuit for the whole interdigital capacitor with  $N$  fingers.

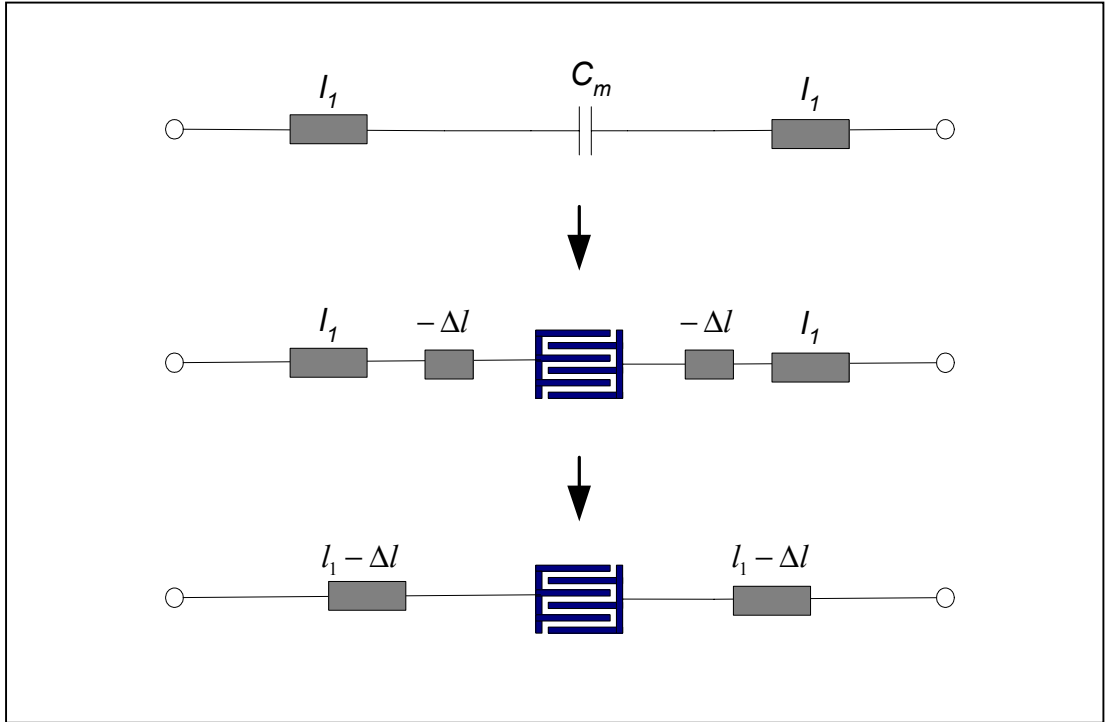


Figure 5.9 Implementation of a series capacitor as an interdigital capacitor.

Design equations for the interdigital capacitor were obtained from [30]. From the design equations, a set of design curves can be generated with the help of *Mathematica*. Appendix H gives the program code needed to generate the design curves. The number of fingers, finger length, width and spacing, and compensation length of the interdigital capacitor can then be obtained from the design curves. Interdigital capacitors have been used in both the decoupling and matching networks and have proved to be as effective as the use of stubs for the capacitors. However, it should be noted that the finger width and spacing are relatively small and may incur fabrication limitations and inaccuracies.

## **5.5. Conclusion**

This chapter discussed ways of realizing ideal lumped capacitors and inductors. The use of Kuroda's identities was illustrated. Design considerations for the decoupling network were also described. Interdigital capacitors were considered as possible candidates for the implementation of series capacitors.

## **CHAPTER 6**

### **EXPERIMENTAL RESULTS**

#### **6.1. Introduction**

This chapter describes the construction of the array and its supporting structure, and the fabrication of the decoupling and matching networks. Both microstrip and stripline designs were manufactured. Measurement results confirm the theory, but a slight shift in frequency is observed.

#### **6.2. Construction of antenna hardware**

##### **6.2.1. Specifications of array element**

In the theoretical modelling of the array, ideal cylindrical monopoles were used. However, these could not be used for practical mounting in the antenna structure. Modifications to the shape of the monopoles had to be done and the resulting new array was analyzed again to obtain its admittance parameters. New decoupling and matching networks were then designed based on the parameters of the array with the new elements.

Figure 6.1 shows a comparison between the ideal monopole and the modified monopoles. Figures 6.1(b) and 6.1(c) show the proposed modified monopoles. The length of the thicker section of the rod was chosen as a quarter of a wavelength. The thinner section of the rod is for support and provides means of connecting the array elements to the decoupling and matching network. The tapered design was at first preferred because it would present a gradual transition from the thinner core to the thicker core of the monopole. However, the design was discarded due to difficulties



associated with the manufacturing of the tapered section. Figure 6.1(c) is the final design of the array element manufactured. Gold-plated brass rods were used to construct the monopole elements for the array. The dimensions of the rod are given in Figure 6.2.

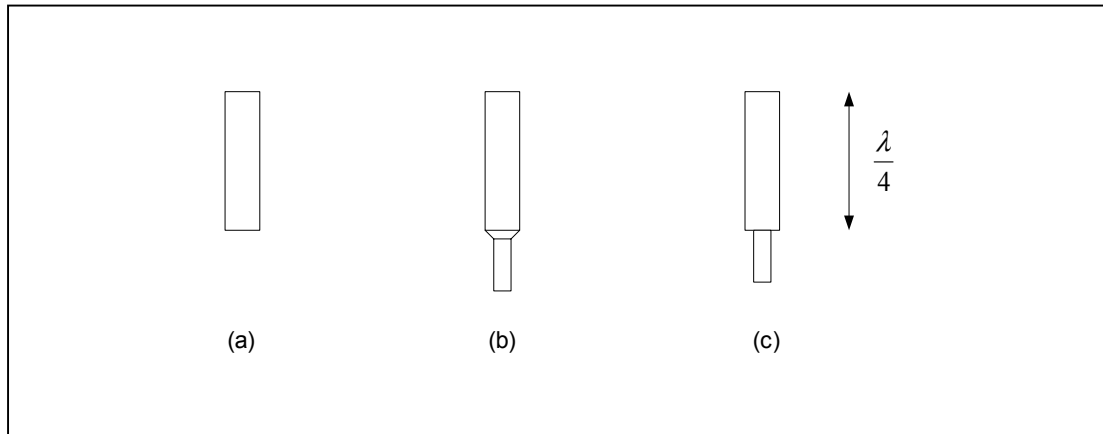


Figure 6.1 Array elements. Monopoles: (a) Ideal. (b) Tapered. (c) Stepped.

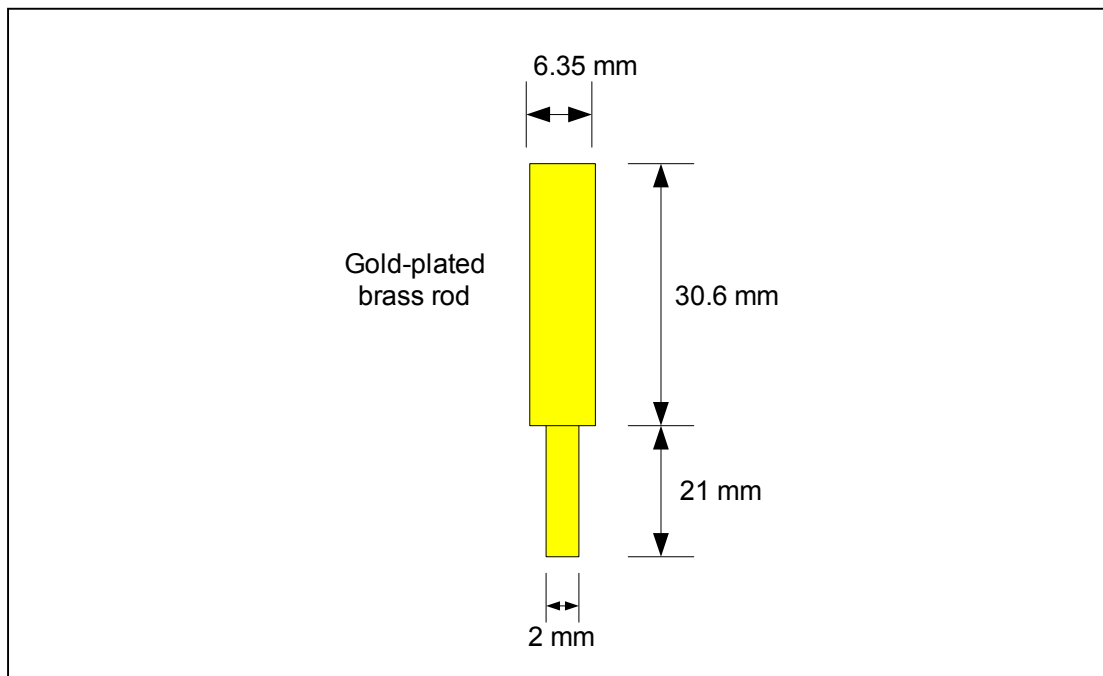


Figure 6.2 Dimensions of the monopole manufactured.

### 6.2.2. Specifications of antenna support structure

The supporting structure for the antenna consisted of a metal ground plate and a hexagonal metal block. The ground plate was mounted on top of the metal block. The microstrip decoupling and matching network was mounted on the other side of the metal block. The array elements were connected to the microstrip network via holes drilled through the metal. These holes were lined with a ring of Teflon to insulate the antenna from the surrounding metal ground. The array elements were then soldered onto the microstrip network. Figure 6.3 shows a cross-section of a monopole and the supporting structure.

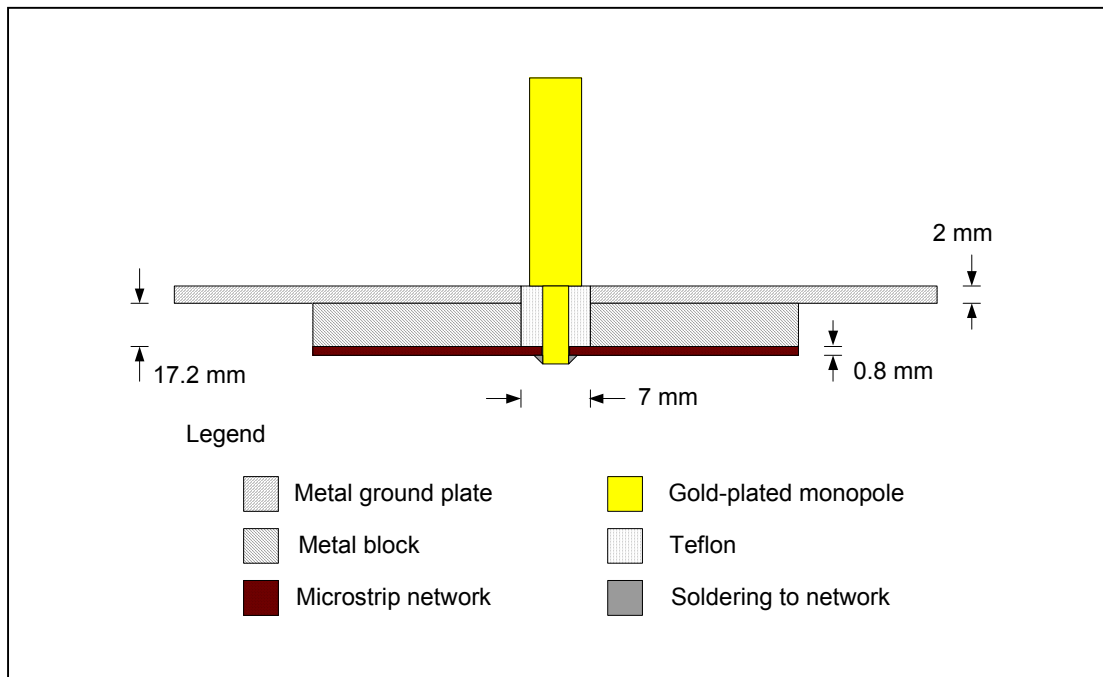


Figure 6.3 A cross-section of a monopole and the supporting structure.

The thin section of the monopole and the ring of Teflon form a coaxial feed. The diameters of the inner and outer conductors were chosen to yield a characteristic impedance of approximately  $50 \Omega$  so as to avoid a mismatch at the feed.

The characteristic impedance  $Z_0$  of a coaxial feed is given by

$$Z_0 = \frac{60}{\sqrt{\epsilon_r}} \ln\left(\frac{b}{a}\right) \quad , \quad (6.1)$$

where  $\epsilon_r$  is the dielectric constant of the insulator,  $a$  and  $b$  are the diameters of the inner and outer conductors respectively. The structure manufactured had dimensions  $a = 2$  mm and  $b = 7$  mm, and uses Teflon with a dielectric constant of  $\epsilon_r = 2.1$ . This gives a characteristic impedance  $Z_0 = 52 \Omega$ . This is very close to  $50 \Omega$  and would not cause mismatch in the network.

### **6.2.3. The complete array**

Figures 6.4 and 6.5 show pictures of the array elements and the supporting structure. The array elements are gold-plated brass rods. The supporting structure is made of aluminium. The circular plate acts as a large ground plane for the array. Detailed dimensions of the structure manufactured are given in Appendix I.

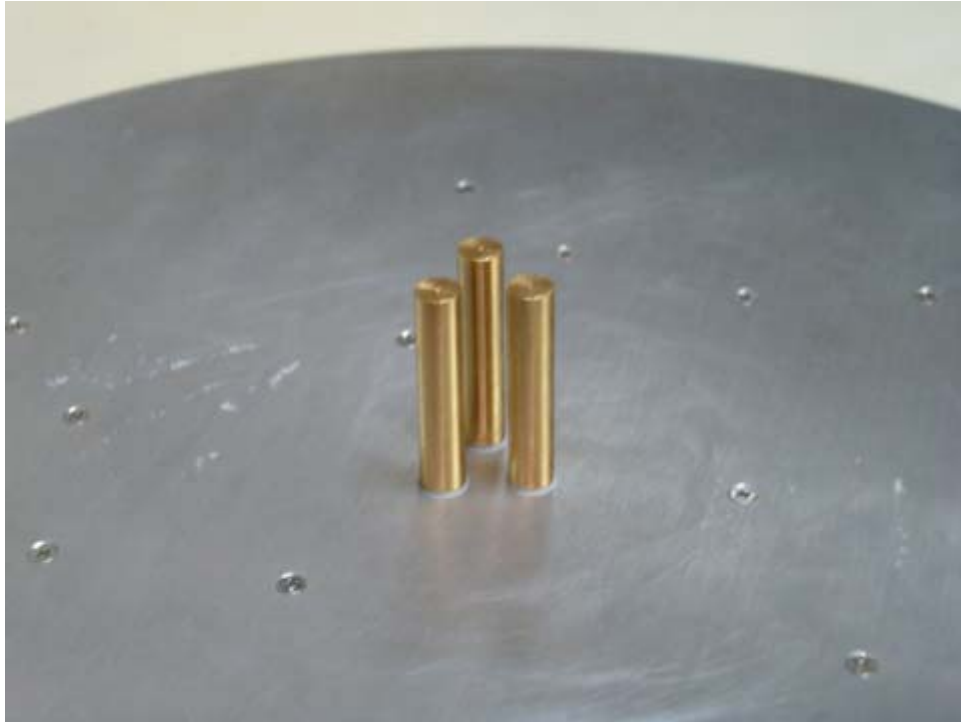


Figure 6.4 Picture showing the elements of the array.

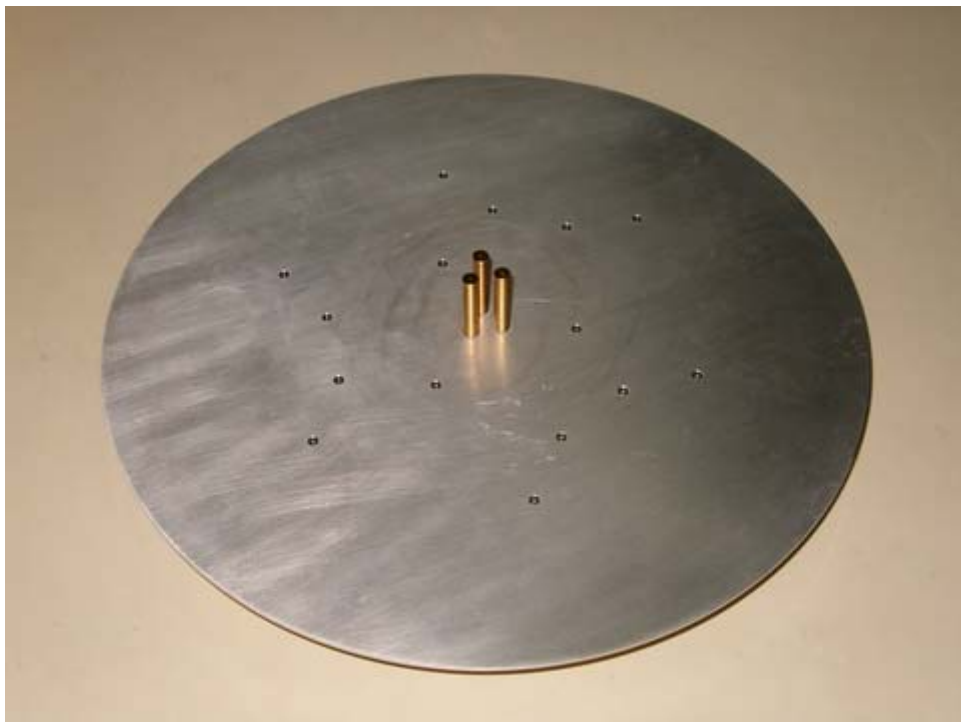


Figure 6.5 (a) Picture showing the top of the supporting structure.



Figure 6.5 (b) Picture showing the bottom of the supporting structure.

#### 6.2.4. Specifications of microstrip network

Rogers (RT/duroid 5880) substrate with dielectric constant of  $\epsilon_r = 2.2$ , a height of 31 mil and loss tangent of 0.0009 was used for the microstrip decoupling and matching networks. In designing the layout of the microstrip network, the lines were meandered to reduce the size of the overall network. Meandering of the lines does not affect the performance of the network as long as the effective length of the curved lines is equivalent to the original length of the straight microstrip lines. The spacing between adjacent lines was kept to at least one line width to limit coupling between them to negligible levels. Figure 6.6 shows the layout of the decoupling and matching network fabricated. Figure 6.6(a) shows the decoupling and matching networks as lumped components, where  $L_1 = 1.9 \text{ nH}$ ,  $L_2 = 7.65 \text{ nH}$ ,  $C_{20} = 0.49 \text{ pF}$  and  $C_3 = 0.578 \text{ pF}$ . With the network parameters of the array obtained from HFSS simulations, the values of the decoupling and matching network components are

obtained as discussed in Chapter 4. By applying the transformation as shown in Figure 5.3,  $L_1$  can be transformed to  $C_1$  with the help of unit elements (U.E.). Similarly, by applying the transformation given in Figure 5.5, the parallel component of the decoupling network can be transformed to  $C_2$ .  $C'_3$  is obtained by using the transformation shown in Figure 5.4. After application of Kuroda's transformation, the network shown in Figure 6.6(b) is obtained. This gives a network that can easily be implemented in microstrip. The microstrip layout is given in Figure 6.6(c). The copper ring traces seen on the layout indicate the locations of the screws used to hold the structure together. The network was mounted on the underside of the metal block in the supporting structure. Figure 6.7 shows a picture of the fabricated circuit.

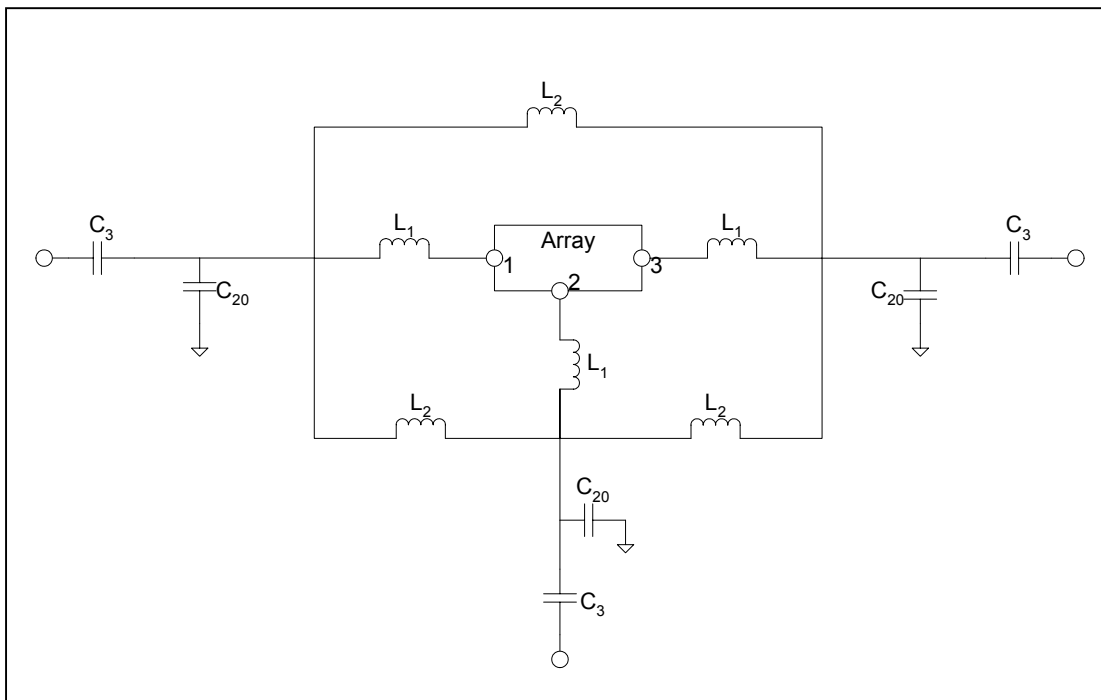


Figure 6.6 (a) Lumped components of the network for microstrip design.

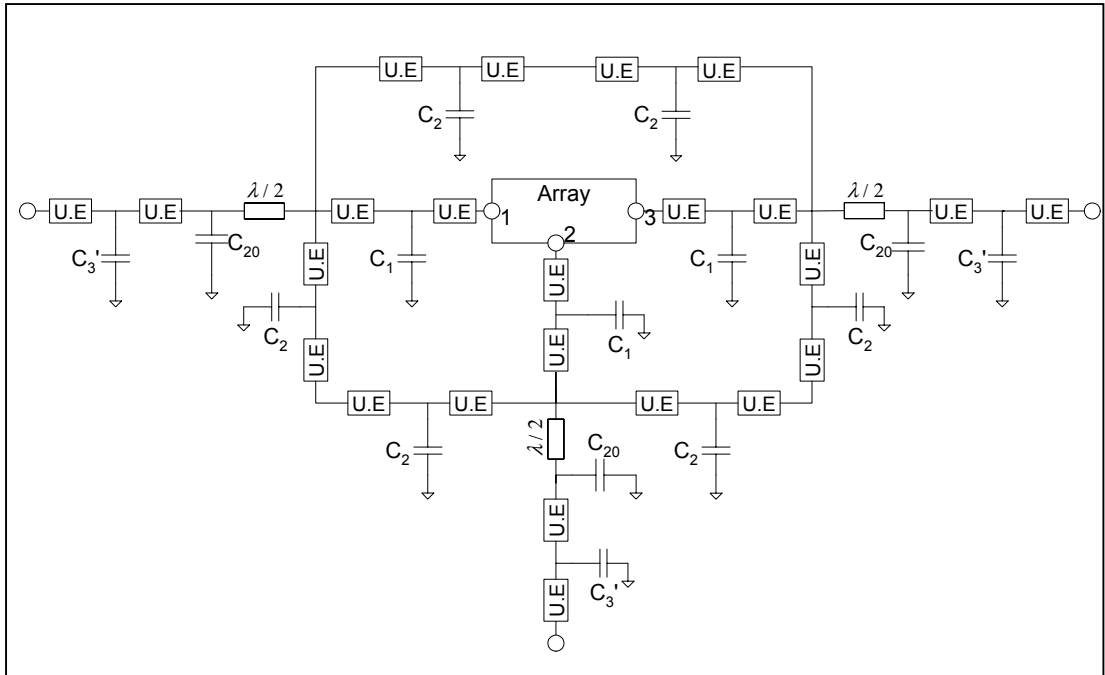


Figure 6.6 (b) Network after Kuroda's transformation for microstrip design.

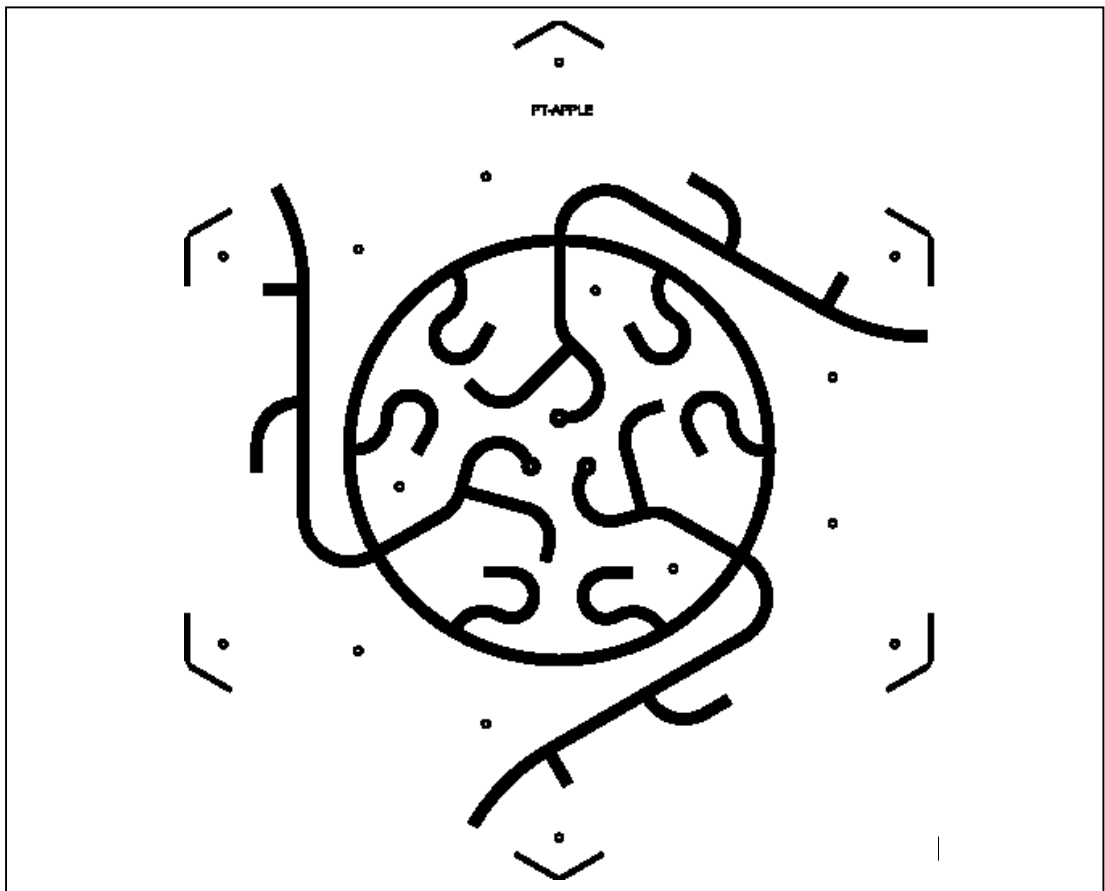


Figure 6.6 (c) Layout of the network for microstrip design.

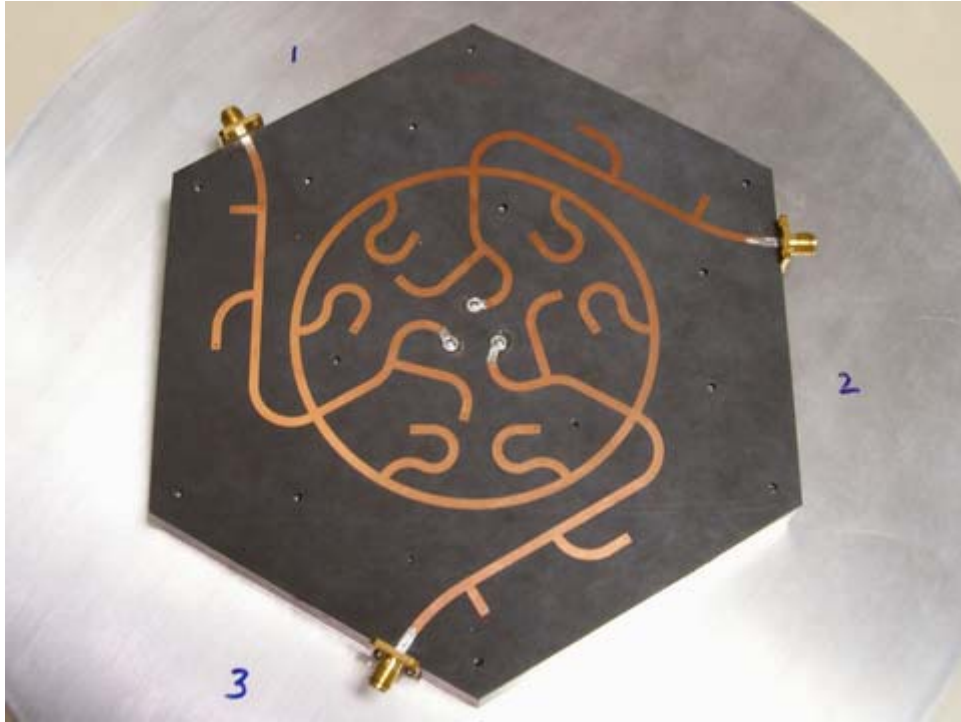


Figure 6.7 Picture showing the fabricated microstrip network.

#### 6.2.5. Specifications of stripline network

The decoupling and matching network was also implemented in stripline. In this case, short-circuited stubs were replaced with open-circuited stubs. This allows the placement of tuning screws at the end of each stub. In the stripline design, two pieces of Rogers (RT/duroid 5880) substrate with dielectric constant of  $\epsilon_r = 2.2$ , a height of 31 mil and loss tangent of 0.0009 were used. Figure 6.8 shows the layout of the network fabricated for the stripline design. Figure 6.9 shows a picture of the fabricated circuit.



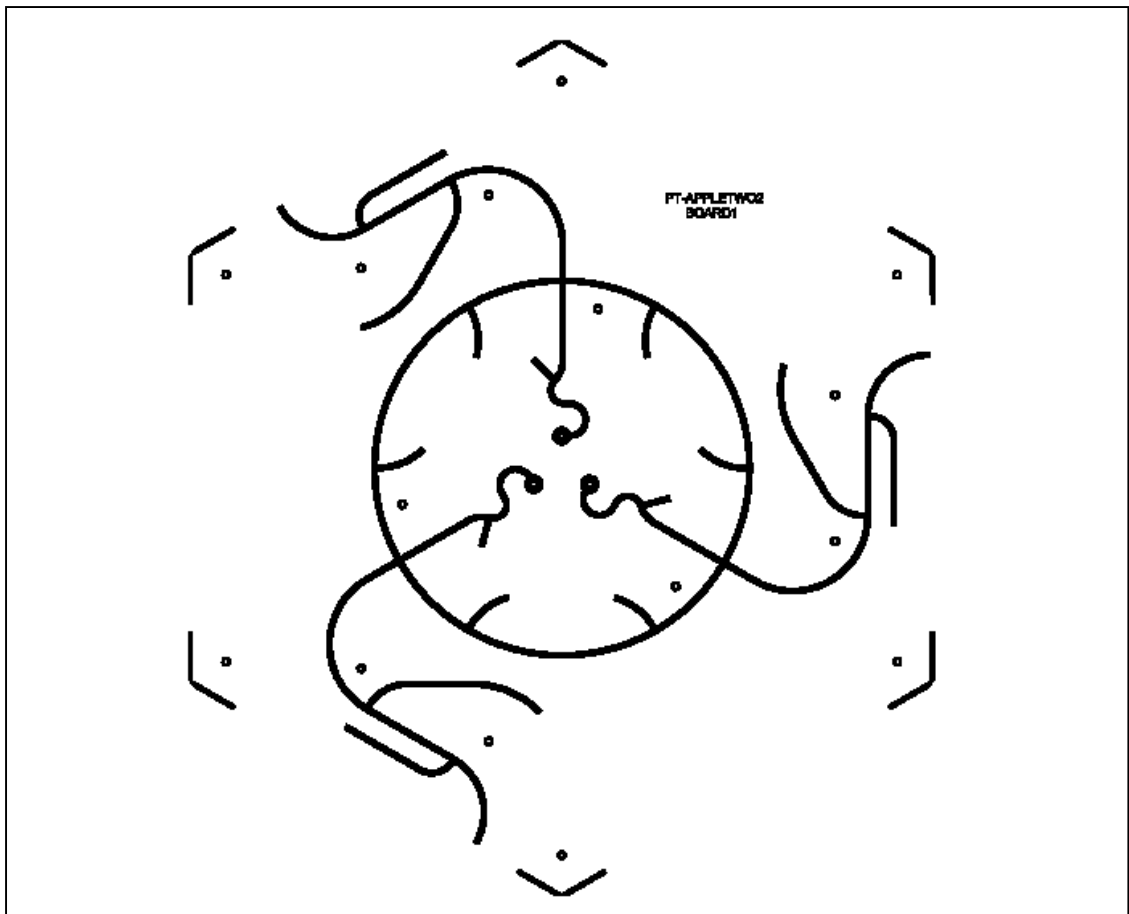


Figure 6.8 Layout of the network for stripline design.

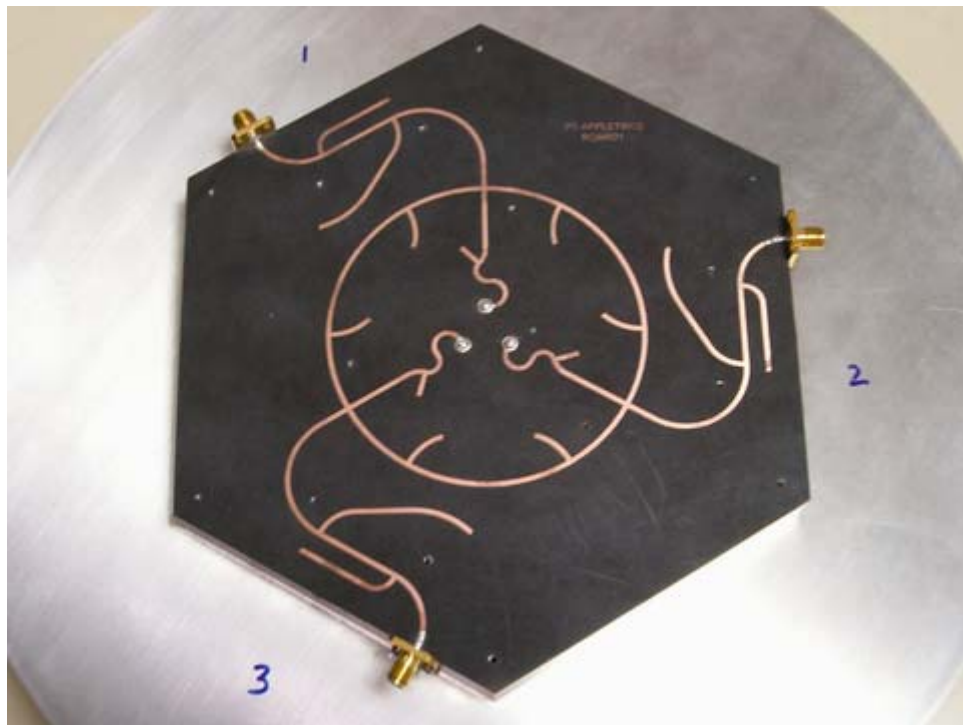


Figure 6.9 Picture showing the fabricated stripline network.

### **6.3. Results**

#### **6.3.1. Verification of array element modelling**

The modelling of the array element was verified. The array was connected to a microstrip network with  $180^\circ$  lines leading from the array elements to the measurement ports. The measured results showed that theoretical modelling of the array element in HFSS software is accurate. Figure 6.10 shows the comparison between the measured and simulation results of the array only.

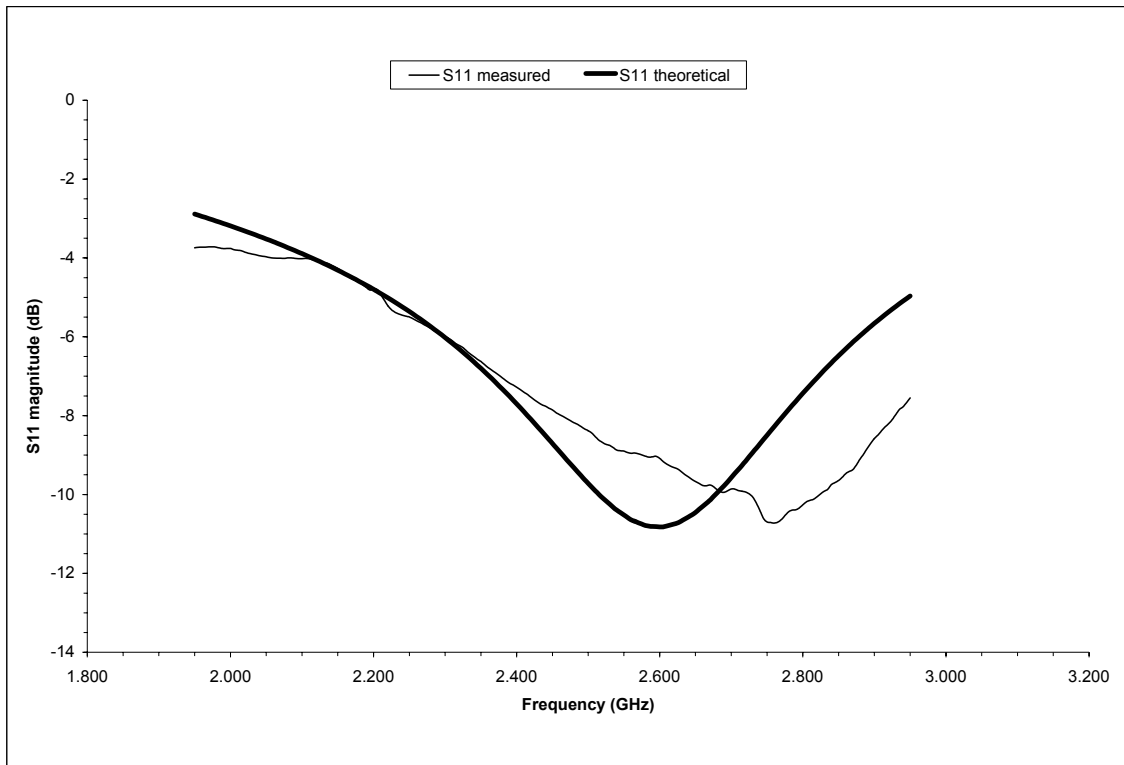


Figure 6.10 (a) Comparison of measured and simulation  $S_{11}$  results of the array.

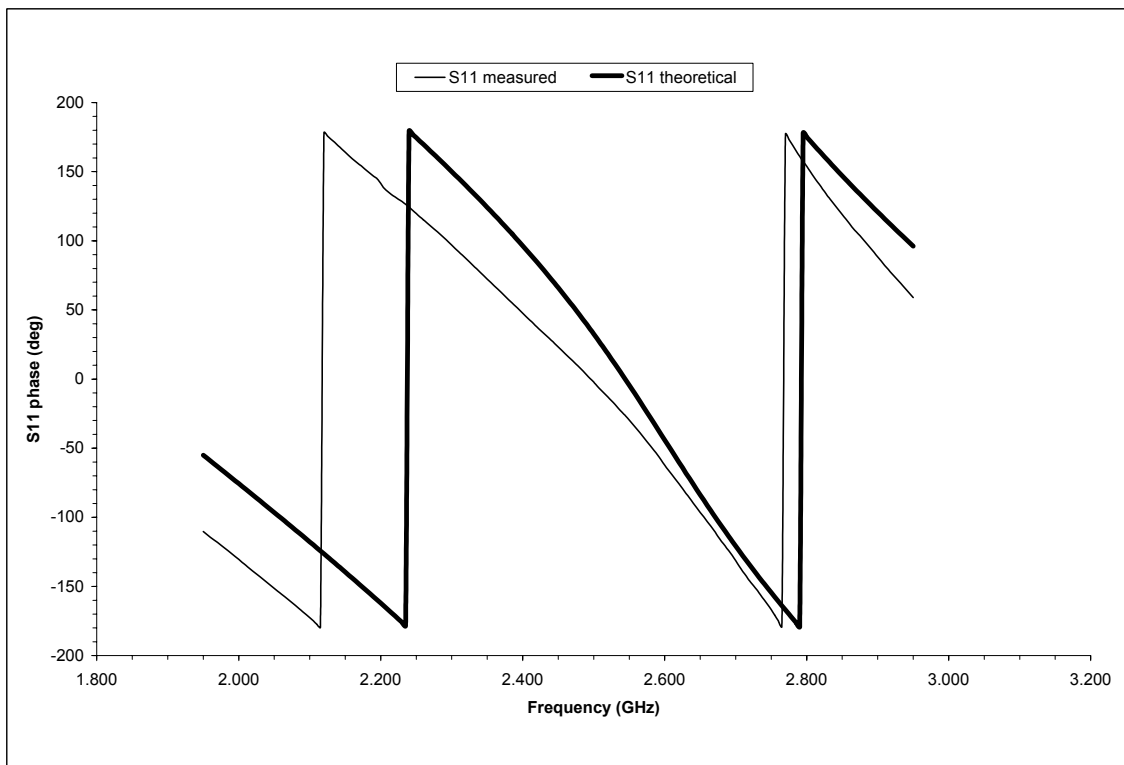


Figure 6.10 (b) Comparison of measured and simulation  $S_{11}$  results of the array.

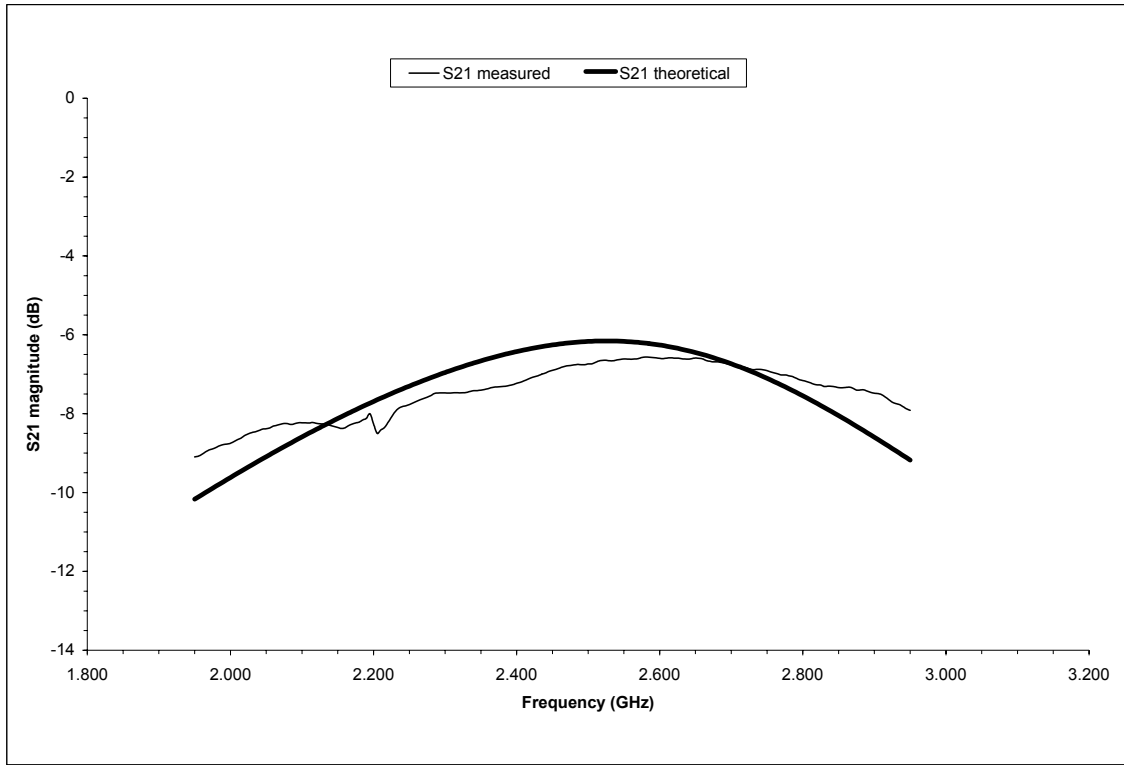


Figure 6.10 (c) Comparison of measured and simulation  $S_{21}$  results of the array.

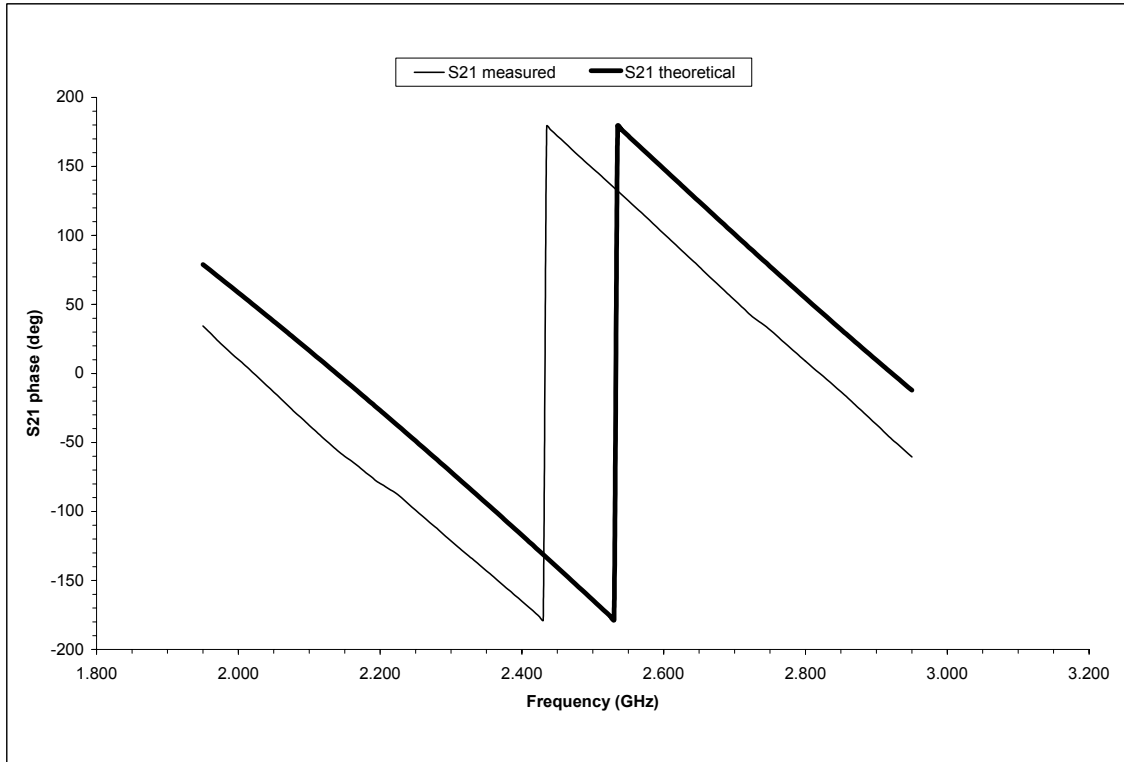


Figure 6.10 (d) Comparison of measured and simulation  $S_{21}$  results of the array.

### 6.3.2. Results of microstrip design

The array with its decoupling and matching network was measured and the results were compared to those obtained from theoretical simulations. Figure 6.11 shows the schematic drawing of the microstrip circuit that was analyzed in the commercial software, Advanced Design System (ADS) [32]. The circuit was optimized to give the required theoretical performance before the layout was generated and fabricated. The measured results in Figure 6.12 confirm the theory, although a slight shift in frequency is observed. The shift in frequency response may be due to inaccuracies in the modelling of the discontinuity at the junction between the feed and the base of the monopole as shown in Figure 6.2, and losses in the microstrip lines were also not accounted for. From the measured results, it is clear that the array has successfully been decoupled, since the array has a low value of  $S_{21}$  (below  $-15$  dB) over the frequency range considered. The array is also matched, having a reflection coefficient of about  $-15$  dB at the minimum of the  $S_{11}$  curve.

Prototype Apple  
(using HFSS array results)

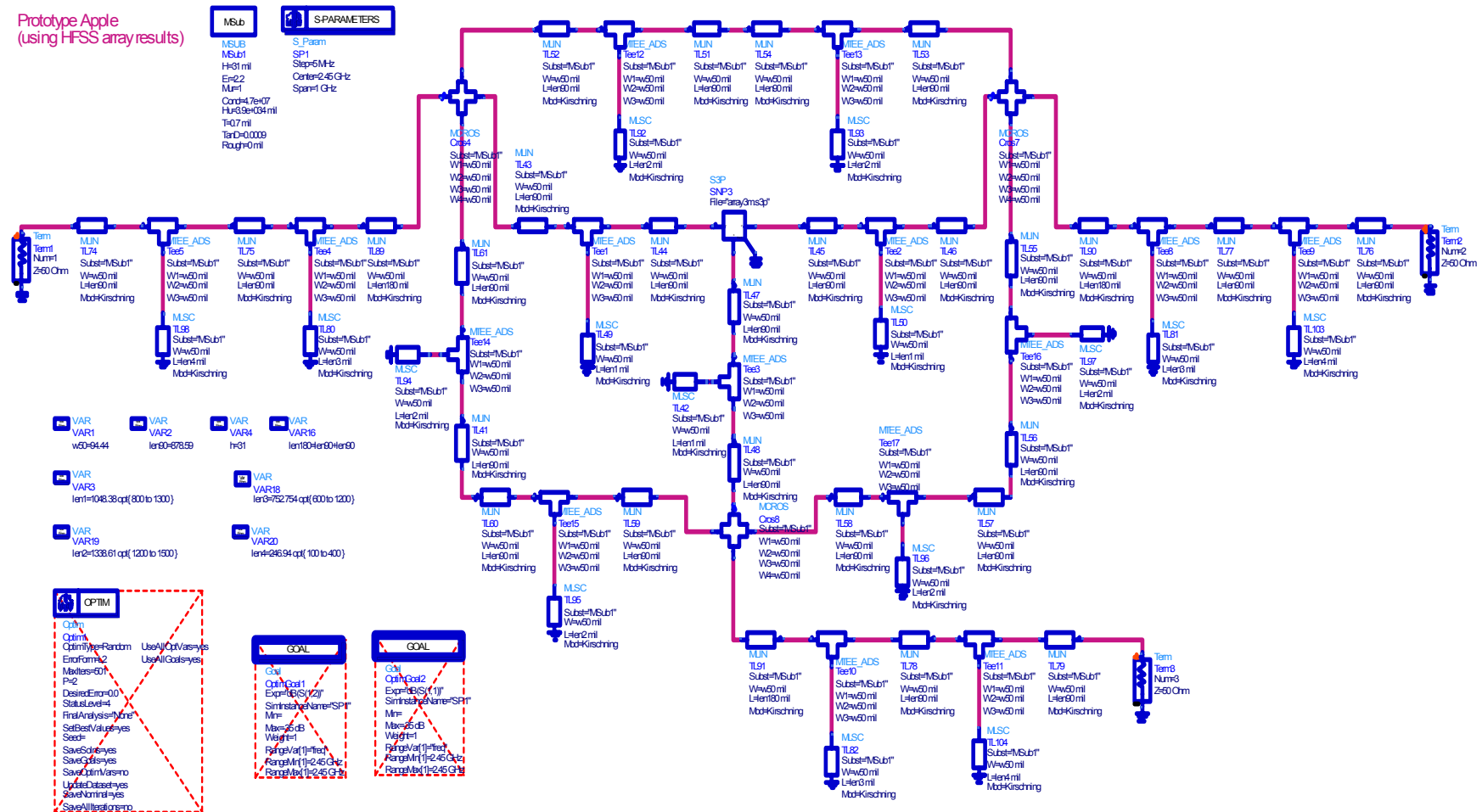


Figure 6.11 Schematic drawing of microstrip circuit in ADS.

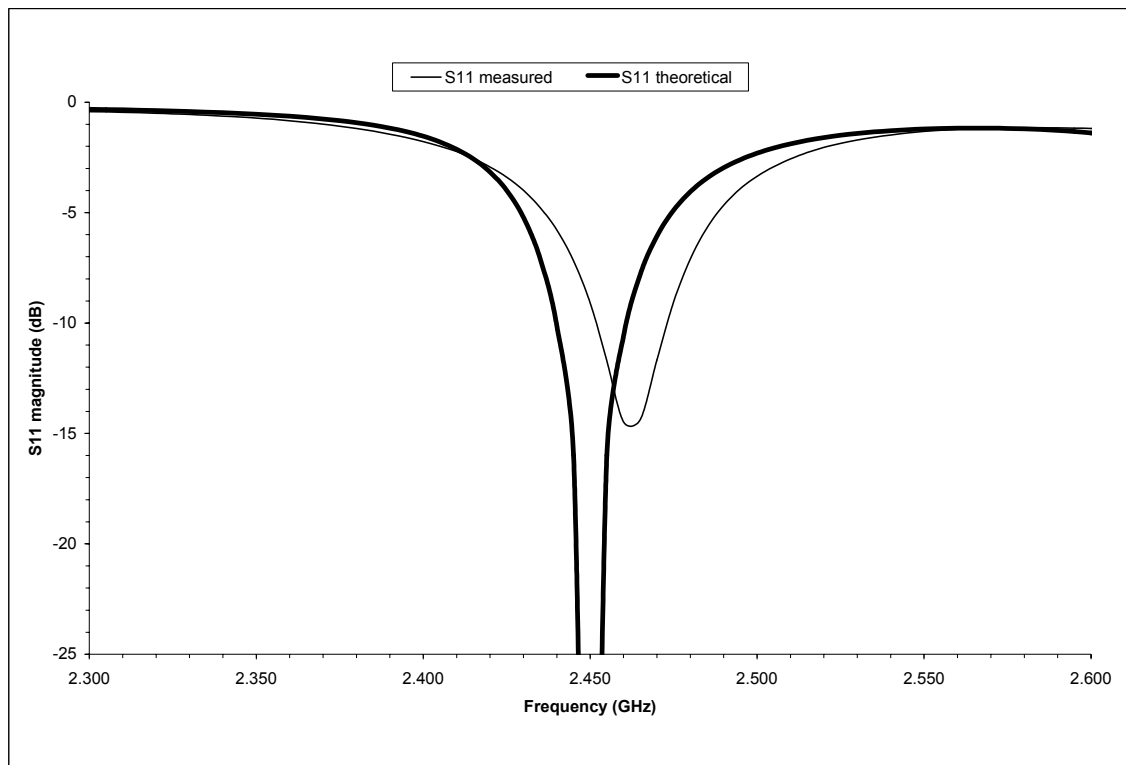


Figure 6.12 (a) Measured and theoretical  $S_{11}$  results for microstrip design.

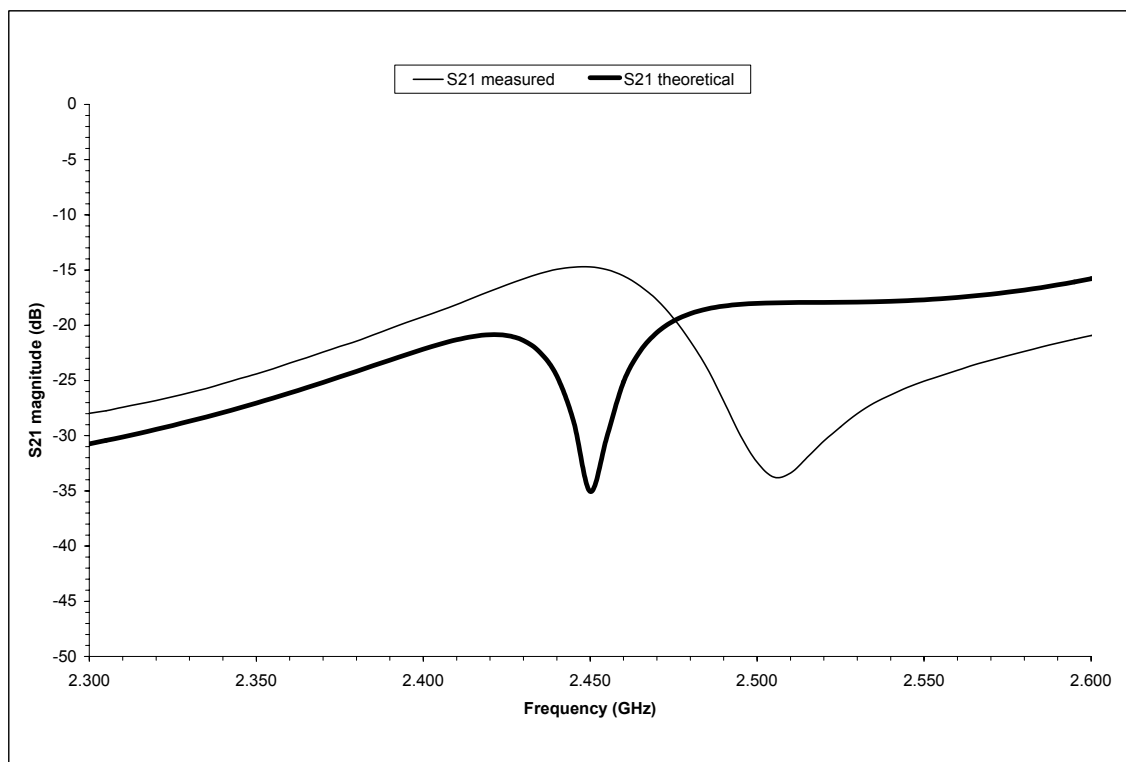


Figure 6.12 (b) Measured and theoretical  $S_{21}$  results for microstrip design.

### 6.3.3. Results of stripline design

Figure 6.13 shows the schematic drawing of the stripline circuit that was analyzed in ADS software. The circuit was optimized to give the required theoretical performance before the layout was generated and fabricated. The measured results in Figure 6.14 confirm the theory, although a slight shift in frequency is observed. This is due to the same reasons as for the microstrip case. Tuning was carried out during the measurement of the array. From the measured results, it is clear that the array has successfully been decoupled, since the array has a low value of  $S_{21}$  (below  $-12$  dB) over the frequency range considered. The array is also matched, having a return loss of about  $-20$  dB at the minimum of the  $S_{11}$  curve.



Prototype AppleTwo  
(using HFSS array results and STRIPLINE design)

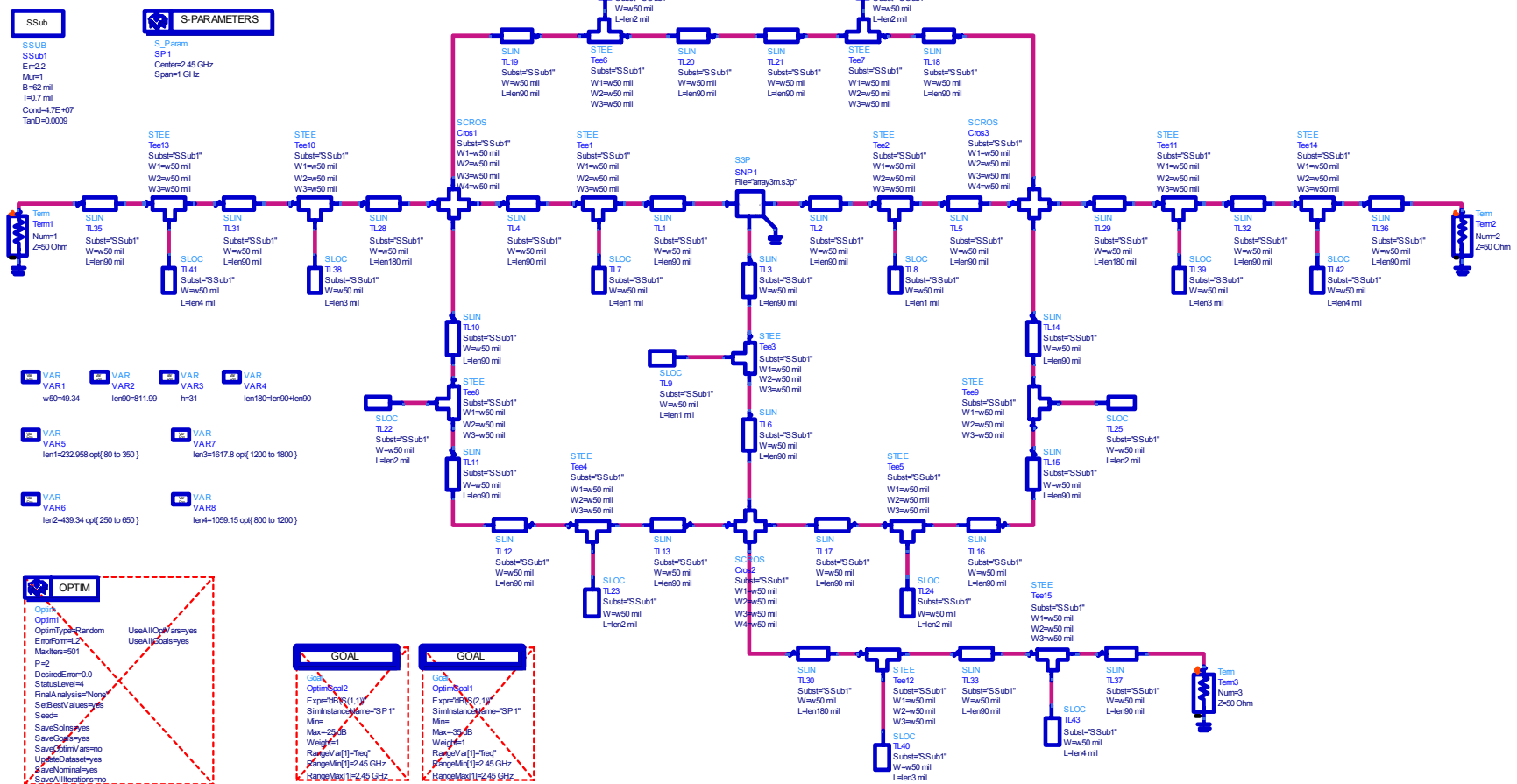


Figure 6.13 Schematic drawing of stripline circuit in ADS.

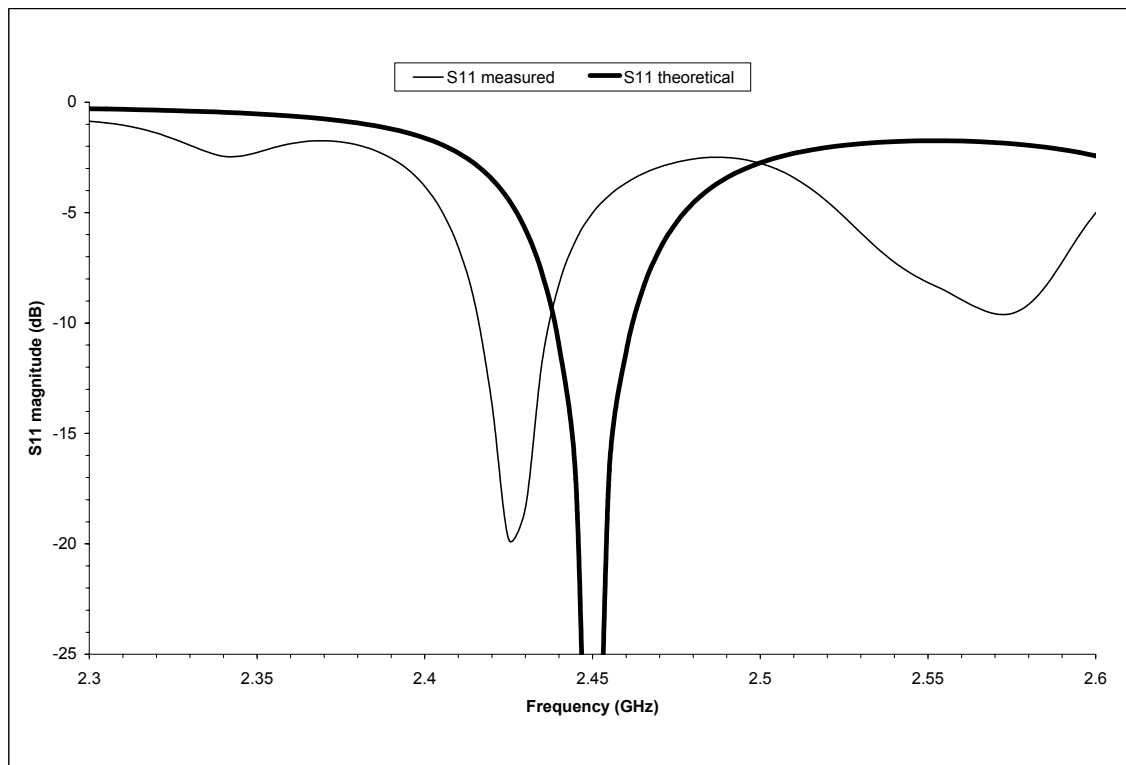


Figure 6.14 (a) Measured and simulation  $S_{11}$  results for stripline design.

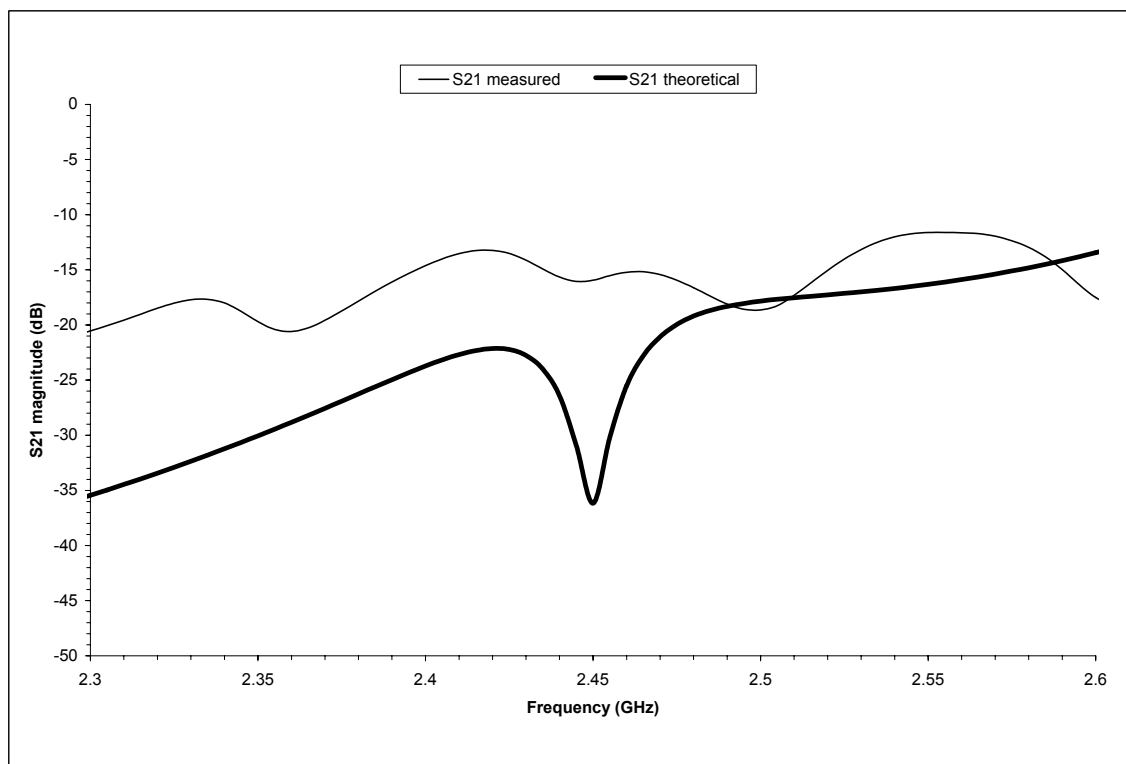


Figure 6.14 (b) Measured and simulation  $S_{21}$  results for stripline design.

#### **6.4. Applications of decoupled array**

The decoupled array has a narrow bandwidth of about 1%. This narrow bandwidth filters away strong out-of-band interfering signals, and reduces mutual interaction with arrays in neighbouring frequencies. Furthermore, several of these antennas with narrow bandwidth can be used to multiplex the whole system bandwidth, performing the function of a frequency multiplexer [33].

Theoretical simulations show that the decoupled array has a superdirective radiation pattern as shown in Figure 4.8. This makes it applicable for direction-finding or beam-forming. It increases the channel capacity and minimizes the power requirements, since the antennas operate only in the required directions, thus saving resources in directions when broadcast is not required. Superdirective arrays can be also be used for adaptive nulling, where disturbances based on their angular distribution of incidence are adaptively rejected [33].

#### **6.5. Conclusion**

This chapter described the construction of the array structure and fabrication of the decoupling and matching network. Measured and theoretical simulation results were compared and presented for both the microstrip and stripline designs. The results showed that decoupling and matching were achieved for the arrays manufactured.

## **CHAPTER 7**

### **CONCLUSION**

This project involved the development of design concepts for compact arrays with considerably reduced element spacing. The reduced element spacing introduce strong mutual coupling between the array elements, which must be accounted for to ensure proper performance of the array. Different ways of achieving decoupling between the array ports were investigated and presented in this thesis. One way of decoupling involves modifying the length of the array elements. This involves physical alterations to the dimensions of the array elements and is not preferred as it is more prone to errors and inaccuracies. In this work, it was shown that an array with arbitrary complex mutual admittance might also be decoupled with the help of a lossless network, without having to modify the length of the antenna elements. This method is preferred, since it provides complete freedom for the design of the radiating elements of the array. Procedures for the design and realization of the decoupling network have been developed and verified with experimental results. Future research can explore the design concepts for arrays with more than three elements, or more significant mutual coupling between the elements. It may be also be interesting to explore the feasibility of wideband decoupling design concepts.

## REFERENCES

- [1] I.J. Gupta and A.A. Ksienski, "Effect of mutual coupling on the performance of adaptive arrays", *IEEE Trans. Antennas and Propagation*, Vol. AP-31, No. 5, September 1983, pp. 785-791.
- [2] E.M. Friel and K.M. Pasala, "Effects of mutual coupling on the performance of STAP antenna arrays", *IEEE Trans. Aerospace and Electronic Systems*, Vol. 36, No. 2, April 2000, pp. 518-527.
- [3] S.R. Rengarajan and A.G. Derneryd, "Application of compound coupling slots in the design of shaped beam antenna patterns", *IEEE Trans. Antennas and Propagation*, Vol. AP-41, No. 1, January 1993, pp. 59-65.
- [4] H. Steyskal and J.S. Herd, "Mutual coupling compensation in small array antennas", *IEEE Trans. Antennas and Propagation*, Vol. AP-38, No. 12, December 1990, pp. 1971-1975.
- [5] P. Darwood, P.N. Fletcher and G.S. Hilton, "Mutual coupling compensation in small planar array antennas", *IEE Proc. Microwave Antennas Propagation*, Vol. 145, No. 1, February 1998, pp. 1-6.
- [6] R. Martin-Cuerdo, D. Segovia-Vargas and M. Sierra-Perez, "Minimization of mutual coupling effects in eigenstructure algorithms based on modal analysis", *IEEE Antennas and Propagation Society International Symposium*, 11 – 16 July, 1999, Vol. 3, pp. 1608-1611.
- [7] R. Borowiec *et. al.*, "Compensation of mutual coupling in small antenna arrays", *IEEE 14<sup>th</sup> International Conf. On Microwaves, Radar and Wireless Communications*, 20 – 22 May, 2002, Vol. 3, pp. 894-897.

- [8] H.J. Chaloupka, X. Wang and J.C. Coetzee, "Superdirective 3-element array for adaptive beamforming", *Microwave and Optical Technology Letters*, March 20, 2003.
- [9] H.J. Chaloupka, X. Wang and J.C. Coetzee, "Performance enhancement of smart antennas with reduced element spacing", *Wireless Communications and Networking, IEEE Conf.*, 16 – 20 March, 2003, Vol. 1, pp. 425 – 430.
- [10] J.B. Anderson and H.H. Rasmussen, "Decoupling and descattering networks for antennas", *IEEE Trans. Antennas and Propagation*, Vol. 24, No. 6, November 1976, pp. 841-846.
- [11] J. Litva and T.K.Y. Lo, *Digital beamforming in wireless communications*, Artech House, London, 1996.
- [12] P.R.P. Hoole, *Smart antennas and signal processing for communications, biomedical and radar systems*, WIT Press, New York, 2001.
- [13] H. Steyskal, "Digital beamforming – an emerging technology", *Military Communications Conference, IEEE Conf.*, 23 – 26 October, 1998, Vol. 2, pp. 399-403.
- [14] S.S. Jeon, *et al.*, "A novel planar array smart antenna system with hybrid analogue-digital beamforming", *MTT-S Digest, IEEE*, Vol. 1, May 2001, pp. 121-124.
- [15] T.W. Nuteson and G.S. Mitchell, "Digital beamforming for smart antennas", *MTT-S Digest, IEEE*, Vol. 1, May 2001, pp. 125-128.
- [16] K. Mori, *et al.*, "DBF array antenna systems at 8.45GHz", *AP-S, IEEE*, Vol. 3, July 2001, pp. 222-225.

- [17] K. Mori, Y. Inoue and H. Arai, "Digital beam forming by using low cost receiver at 2.6GHz", *IEEE 11<sup>th</sup> International Conference on Antennas and Propagation*, 17 – 20 April, 2001, Vol. 1, pp. 24-27.
- [18] T.W. Nuteson, *et al.*, "Digital beamforming and calibration for smart antennas using real-time FPGA processing", *MTT-S Digest, IEEE*, Vol. 1, June 2002, pp. 307-310.
- [19] J.D. Fredrick, *et al.*, "Smart antenna receiver array using a single RF channel and digital beamforming", *MTT-S Digest, IEEE*, Vol. 50, No. 2, December 2002, pp. 3052-3058.
- [20] C.A. Balanis, *Antenna theory: Analysis and design*, 2<sup>nd</sup> ed., Wiley, New York, 1997.
- [21] *IE3D version 9.0 – User manual*, Zeland Software Inc., March 2002.
- [22] *High Frequency Simulation Software (HFSS) version 5.4 – User guide*, Hewlett-Packard, May 1999.
- [23] *Mathematica version 4.0*, Wolfram Research, Inc.
- [24] K.R. Coombes, *et al.*, *The Mathematica primer*, Cambridge University Press, New York, 1998.
- [25] E. Don, *Mathematica*, Schaum's Outlines Series, McGraw-Hill, New York, 2001.
- [26] D.H. Schrader, *Microstrip circuit analysis*, Prentice Hall, New York, 1995.
- [27] J.A.G. Malherbe, *Microwave transmission line filters*, Artech House, London, 1979.
- [28] D.M. Pozar, *Microwave engineering*, 2<sup>nd</sup> ed., Wiley, New York, 1998.
- [29] P.L.D. Abrie, *The design of impedance-matching networks for radio-frequency*, Artech House, London, 1985.

- [30] X.Y. She and Y.L. “Chow, Interdigital microstrip capacitor as a four-port network”, *IEE Proc.*, Vol. 133, Pt. H, No. 3, June 1986, pp. 191-197.
- [31] B.C. Wadell, *Transmission line design handbook*, Artech House, London, 1991.
- [32] *Advanced Design System (ADS)* version 2002, Agilent.
- [33] H.J. Chaloupka, “HTS antennas”, in H. Weinstock and N. Nisenoff (eds.), *Microwave superconductivity*, Kluwer, Dordrecht, 2001.



## **APPENDIX A**

### **PROGRAM CODE FOR EIGENMODE ANALYSIS**

This appendix contains a program code written in *Mathematica* software. This program uses the eigenmode analysis to decouple an array with an arbitrary admittance matrix. From the output of the program, it is shown that any 3-element array with generalized admittances can be analytically decoupled. Although the analytical solutions of the components in the decoupling network run pages long, they are in terms of the array admittance parameters. Numerical values of the admittances of the array can be obtained through IE3D simulations, and hence, numerical quantities can be assigned to the components in the decoupling network.

```

(* ***** *)
(* Program to compute the decoupling network for a 3-element array. *)
(* Unknowns in the decoupling network are x1 and b2. *)
(* Modal analysis used to compute the decoupling network. *)
(* Symbolical approach used. *)
(* Verification of results using network approach is done symbolically. *)
(* NOTE: restart kernel for each notebook evaluation. *)
(* ***** *)

(* symbolic parameters: y11 and y12 *)
y11 = g11 + I * b11;
y12 = g12 + I * b12;
yA = ComplexExpand[y11 + 2 * y12];
yB = ComplexExpand[y11 - y12];

(* expressions for input admittance for modes A and B *)
(* yinA =  $\left(\frac{1}{yA} + I * x1\right)^{-1}$  and yinB =  $\left(\frac{1}{yB} + I * x1\right)^{-1} + I * 3 * b2$  *)

(* Define x1 and b2 to be real variables *)
(* Define g11, b11, g12, b12 to be real variables *)
(* This is NOT globally effective. *)
(* Need to define in every statement. *)
Element[x1, Reals];
Element[b2, Reals];
Element[g11, Reals];
Element[b11, Reals];
Element[g12, Reals];
Element[b12, Reals];

(* Break up computation into intermediate steps *)
denoA1 = ComplexExpand[yA * Conjugate[yA], {x1, b2, g11, b11, g12, b12} ∈ Reals]
a = Together[ComplexExpand[(Conjugate[yA] / denoA1) + I * x1, {x1, b2, g11, b11, g12, b12} ∈ Reals]]
yinA = 1 / a

denoB1 = ComplexExpand[yB * Conjugate[yB], {x1, b2, g11, b11, g12, b12} ∈ Reals]
b = Together[ComplexExpand[(Conjugate[yB] / denoB1) + I * x1, {x1, b2, g11, b11, g12, b12} ∈ Reals]]
c = 1 / b
denoB2 = ComplexExpand[Denominator[c] * Conjugate[Denominator[c]], {x1, b2, g11, b11, g12, b12} ∈ Reals]
yinB = Together[ComplexExpand[yB * Conjugate[Denominator[c]] / denoB2 + I * 3 * b2, {x1, b2, g11, b11, g12, b12} ∈ Reals]]

(* getting real and imaginary parts of yinA *)
denoyinA = ComplexExpand[Denominator[yinA] * Conjugate[Denominator[yinA]], {x1, b2, g11, b11, g12, b12} ∈ Reals]
yinAexpr = ComplexExpand[Numerator[yinA] * Conjugate[Denominator[yinA]] / denoyinA, {x1, b2, g11, b11, g12, b12} ∈ Reals]
yinAreal = Together[ComplexExpand[Re[yinAexpr], {x1, b2, g11, b11, g12, b12} ∈ Reals]]
yinAimg = Together[ComplexExpand[Im[yinAexpr], {x1, b2, g11, b11, g12, b12} ∈ Reals]]

(* getting real and imaginary parts of yinB *)
denoyinB = ComplexExpand[Denominator[yinB] * Conjugate[Denominator[yinB]], {x1, b2, g11, b11, g12, b12} ∈ Reals]
yinBexpr = ComplexExpand[Numerator[yinB] * Conjugate[Denominator[yinB]] / denoyinB, {x1, b2, g11, b11, g12, b12} ∈ Reals]
yinBreal = Together[ComplexExpand[Re[yinBexpr], {x1, b2, g11, b11, g12, b12} ∈ Reals]]
yinBimg = Together[ComplexExpand[Im[yinBexpr], {x1, b2, g11, b11, g12, b12} ∈ Reals]]

(* Solving for unknowns x1 and b2 *)
solnset = Solve[{yinAreal == yinBreal, yinAimg == yinBimg}, {x1, b2}]
soln1x1 = x1 /. solnset[[1]]

$$\frac{-b12 g11 + b11 g12 - \sqrt{g11^2 + g11 g12 - 2 g12^2} \sqrt{b12^2 + g12^2}}{-2 b11 b12 g11 - b12^2 g11 + b11^2 g12 + 2 b12^2 g12 - g11^2 g12 - g11 g12^2 + 2 g12^3}$$

soln1b2 = Together[b2 /. solnset[[1]]]

$$\left( 8 b11^4 b12^5 g11^4 + 16 b11^3 b12^6 g11^4 - 6 b11^2 b12^7 g11^4 - 14 b11 b12^8 g11^4 - 4 b12^9 g11^4 - 8 b11^2 b12^5 g11^6 - 8 b11 b12^6 g11^6 - 2 b12^7 g11^6 - \right.$$


$$8 b11^5 b12^4 g11^3 g12 - 4 b11^4 b12^5 g11^3 g12 + 12 b11^3 b12^6 g11^3 g12 - 22 b11^2 b12^7 g11^3 g12 - 10 b11 b12^8 g11^3 g12 + 12 b12^9 g11^3 g12 +$$


$$32 b11^5 b12^4 g11^5 g12 + 24 b11^4 b12^5 g11^5 g12 - 2 b12^7 g11^5 g12 - 8 b11 b12^4 g11^7 g12 - 4 b12^5 g11^7 g12 + 2 b11^6 b12^3 g11^2 g12^2 - 6 b11^5 b12^4 g11^2 g12^2 -$$


$$24 b11^4 b12^5 g11^2 g12^2 - 28 b11^3 b12^6 g11^2 g12^2 - 12 b11^2 b12^7 g11^2 g12^2 + 60 b11 b12^8 g11^2 g12^2 + 8 b12^9 g11^2 g12^2 - 14 b11^4 b12^3 g11^4 g12^2 +$$


$$52 b11^3 b12^4 g11^4 g12^2 + 6 b11^2 b12^5 g11^4 g12^2 - 40 b11 b12^6 g11^4 g12^2 - 4 b12^7 g11^4 g12^2 - 14 b11^2 b12^3 g11^6 g12^2 - 14 b11 b12^4 g11^6 g12^2 -$$


$$6 b12^5 g11^6 g12^2 - 2 b12^3 g11^5 g12^2 + 2 b11^6 b12^3 g11 g12^3 + 18 b11^5 b12^4 g11 g12^3 + 28 b11^4 b12^5 g11 g12^3 + 16 b11^3 b12^6 g11 g12^3 +$$


```

$$\begin{aligned}
& 24b_{11}^2b_{12}^7g_{11}g_{12}^3 - 40b_{11}b_{12}^3g_{11}g_{12}^3 - 48b_{12}^3g_{11}g_{12}^3 - 4b_{11}^5b_{12}^2g_{11}^3g_{12}^3 - 38b_{11}^4b_{12}^3g_{11}^3g_{12}^3 - 40b_{11}^3b_{12}^4g_{11}^3g_{12}^3 - \\
& 154b_{11}^2b_{12}^5g_{11}^3g_{12}^3 + 56b_{12}^7g_{11}^3g_{12}^3 + 24b_{11}^3b_{12}^2g_{11}^5g_{12}^3 + 78b_{11}^2b_{12}^3g_{11}^5g_{12}^3 + 18b_{11}b_{12}^4g_{11}^5g_{12}^3 + 6b_{12}^5g_{11}^5g_{12}^3 - \\
& 4b_{11}b_{12}^2g_{11}^7g_{12}^3 - 10b_{12}^3g_{11}^7g_{12}^3 - 4b_{11}^6b_{12}^3g_{12}^4 - 4b_{11}^5b_{12}^4g_{12}^4 - 8b_{11}^4b_{12}^5g_{12}^4 - 16b_{11}^3b_{12}^6g_{12}^4 + 16b_{11}^2b_{12}^7g_{12}^4 - \\
& 16b_{11}b_{12}^8g_{12}^4 + 32b_{12}^9g_{12}^4 + 2b_{11}^6b_{12}g_{11}^2g_{12}^4 + 12b_{11}^4b_{12}^2g_{11}^2g_{12}^4 - 12b_{11}^3b_{12}^3g_{11}^2g_{12}^4 + 12b_{11}^2b_{12}^4g_{11}^2g_{12}^4 + \\
& 240b_{11}b_{12}^6g_{11}^2g_{12}^4 + 16b_{12}^7g_{11}^2g_{12}^4 - 22b_{11}^4b_{12}g_{11}^4g_{12}^4 + 16b_{11}^3b_{12}^2g_{11}^4g_{12}^4 - 30b_{11}^2b_{12}^3g_{11}^4g_{12}^4 - 88b_{11}b_{12}^4g_{11}^4g_{12}^4 + \\
& 4b_{12}^5g_{11}^4g_{12}^4 + 22b_{11}^2b_{12}g_{11}^6g_{12}^4 + 8b_{11}b_{12}^2g_{11}^6g_{12}^4 - 2b_{12}^3g_{11}^6g_{12}^4 - 2b_{12}g_{11}^8g_{12}^4 + 2b_{11}^6b_{12}g_{11}g_{12}^5 + 12b_{11}^5b_{12}^2g_{11}g_{12}^5 + \\
& 56b_{11}^4b_{12}^3g_{11}g_{12}^5 + 16b_{11}^3b_{12}^4g_{11}g_{12}^5 + 72b_{11}^2b_{12}^5g_{11}g_{12}^5 - 128b_{11}b_{12}^6g_{11}g_{12}^5 - 192b_{12}^7g_{11}g_{12}^5 + 4b_{11}^5g_{11}^3g_{12}^5 - \\
& 34b_{11}^4b_{12}g_{11}^3g_{12}^5 - 36b_{11}^3b_{12}^2g_{11}^3g_{12}^5 - 242b_{11}^2b_{12}^3g_{11}^3g_{12}^5 - 28b_{11}b_{12}^4g_{11}^3g_{12}^5 + 96b_{12}^5g_{11}^3g_{12}^5 - 8b_{11}^5g_{11}^5g_{12}^5 + \\
& 54b_{11}^4b_{12}g_{11}^5g_{12}^5 + 12b_{11}b_{12}^2g_{11}^5g_{12}^5 + 18b_{12}^3g_{11}^5g_{12}^5 + 4b_{11}g_{11}^7g_{12}^5 - 6b_{12}g_{11}^7g_{12}^5 - 4b_{11}^6b_{12}g_{12}^6 - 8b_{11}^5b_{12}^2g_{12}^6 - \\
& 16b_{11}^4b_{12}^3g_{12}^6 - 48b_{11}^3b_{12}^4g_{12}^6 + 48b_{11}^2b_{12}^5g_{12}^6 - 64b_{11}b_{12}^6g_{12}^6 - 128b_{12}^7g_{12}^6 + 6b_{11}^5g_{11}^3g_{12}^6 + 36b_{11}^4b_{12}g_{11}^3g_{12}^6 + \\
& 60b_{11}^3b_{12}^2g_{11}^3g_{12}^6 + 60b_{11}^2b_{12}^3g_{11}^3g_{12}^6 + 360b_{11}b_{12}^4g_{11}^3g_{12}^6 - 20b_{11}^3g_{11}^4g_{12}^6 - 42b_{11}^2b_{12}g_{11}^4g_{12}^6 - 112b_{11}b_{12}^2g_{11}^4g_{12}^6 + \\
& 4b_{12}^3g_{11}^4g_{12}^6 + 14b_{11}g_{11}^6g_{12}^6 + 2b_{12}g_{11}^6g_{12}^6 - 6b_{11}^5g_{11}g_{12}^7 + 28b_{11}^4b_{12}g_{11}g_{12}^7 - 16b_{11}^3b_{12}^2g_{11}g_{12}^7 + 72b_{11}^2b_{12}^3g_{11}g_{12}^7 - \\
& 144b_{11}b_{12}^4g_{11}g_{12}^7 - 288b_{12}^5g_{11}g_{12}^7 + 16b_{11}^3g_{11}^3g_{12}^7 - 110b_{11}^2b_{12}g_{11}^3g_{12}^7 - 16b_{11}b_{12}^2g_{11}^3g_{12}^7 + 72b_{12}^3g_{11}^3g_{12}^7 - 6b_{11}g_{11}^5g_{12}^7 + \\
& 10b_{12}g_{11}^5g_{12}^7 - 4b_{11}^5g_{12}^8 - 8b_{11}^4b_{12}g_{12}^8 - 48b_{11}^3b_{12}^2g_{12}^8 - 48b_{11}^2b_{12}^3g_{12}^8 - 96b_{11}b_{12}^4g_{12}^8 - 192b_{12}^5g_{12}^8 + 44b_{11}^3g_{11}^2g_{12}^8 - \\
& 36b_{11}^2b_{12}g_{11}^2g_{12}^8 + 240b_{11}b_{12}^2g_{11}^2g_{12}^8 - 16b_{12}^3g_{11}^2g_{12}^8 - 50b_{11}g_{11}^4g_{12}^8 - 16b_{11}^3g_{11}g_{12}^9 - 24b_{11}^2b_{12}g_{11}g_{12}^9 - 64b_{11}b_{12}^2g_{11}g_{12}^9 - \\
& 192b_{12}^3g_{11}g_{12}^9 + 2b_{11}g_{11}^3g_{12}^9 + 20b_{12}g_{11}^3g_{12}^9 - 16b_{11}^3g_{12}^{10} - 16b_{11}^2b_{12}g_{12}^{10} - 64b_{11}b_{12}^2g_{12}^{10} + 128b_{12}^3g_{12}^{10} + 60b_{11}g_{11}^2g_{12}^{10} - \\
& 8b_{12}g_{11}^2g_{12}^{10} - 8b_{11}g_{11}g_{12}^{11} - 48b_{12}g_{11}g_{12}^{11} - 16b_{11}g_{12}^{12} + 32b_{12}g_{12}^{12} - 8b_{11}^4b_{12}^4g_{11}^3\sqrt{g_{11}^2+g_{11}g_{12}-2g_{12}^2}\sqrt{b_{12}^2+g_{12}^2} - \\
& 16b_{11}^3b_{12}^5g_{11}^3\sqrt{g_{11}^2+g_{11}g_{12}-2g_{12}^2}\sqrt{b_{12}^2+g_{12}^2} - 30b_{11}^2b_{12}^6g_{11}^3\sqrt{g_{11}^2+g_{11}g_{12}-2g_{12}^2}\sqrt{b_{12}^2+g_{12}^2} - \\
& 22b_{11}b_{12}^7g_{11}^3\sqrt{g_{11}^2+g_{11}g_{12}-2g_{12}^2}\sqrt{b_{12}^2+g_{12}^2} - 5b_{12}^8g_{11}^3\sqrt{g_{11}^2+g_{11}g_{12}-2g_{12}^2}\sqrt{b_{12}^2+g_{12}^2} - \\
& 8b_{11}^2b_{12}^4g_{11}^5\sqrt{g_{11}^2+g_{11}g_{12}-2g_{12}^2}\sqrt{b_{12}^2+g_{12}^2} - 8b_{11}b_{12}^5g_{11}^5\sqrt{g_{11}^2+g_{11}g_{12}-2g_{12}^2}\sqrt{b_{12}^2+g_{12}^2} - \\
& 2b_{12}^6g_{11}^5\sqrt{g_{11}^2+g_{11}g_{12}-2g_{12}^2}\sqrt{b_{12}^2+g_{12}^2} + 8b_{11}^5b_{12}^3g_{11}^2g_{12}\sqrt{g_{11}^2+g_{11}g_{12}-2g_{12}^2}\sqrt{b_{12}^2+g_{12}^2} + \\
& 8b_{11}^4b_{12}^4g_{11}^2g_{12}\sqrt{g_{11}^2+g_{11}g_{12}-2g_{12}^2}\sqrt{b_{12}^2+g_{12}^2} + 68b_{11}^3b_{12}^5g_{11}^2g_{12}\sqrt{g_{11}^2+g_{11}g_{12}-2g_{12}^2}\sqrt{b_{12}^2+g_{12}^2} + \\
& 73b_{11}^2b_{12}^6g_{11}^2g_{12}\sqrt{g_{11}^2+g_{11}g_{12}-2g_{12}^2}\sqrt{b_{12}^2+g_{12}^2} + 64b_{11}b_{12}^7g_{11}^2g_{12}\sqrt{g_{11}^2+g_{11}g_{12}-2g_{12}^2}\sqrt{b_{12}^2+g_{12}^2} + \\
& 22b_{12}^8g_{11}^2g_{12}\sqrt{g_{11}^2+g_{11}g_{12}-2g_{12}^2}\sqrt{b_{12}^2+g_{12}^2} - 20b_{11}^3b_{12}^4g_{11}^4g_{12}\sqrt{g_{11}^2+g_{11}g_{12}-2g_{12}^2}\sqrt{b_{12}^2+g_{12}^2} - \\
& 20b_{11}b_{12}^5g_{11}^4g_{12}\sqrt{g_{11}^2+g_{11}g_{12}-2g_{12}^2}\sqrt{b_{12}^2+g_{12}^2} - 5b_{12}^6g_{11}^4g_{12}\sqrt{g_{11}^2+g_{11}g_{12}-2g_{12}^2}\sqrt{b_{12}^2+g_{12}^2} - \\
& 8b_{11}b_{12}^3g_{11}^6g_{12}\sqrt{g_{11}^2+g_{11}g_{12}-2g_{12}^2}\sqrt{b_{12}^2+g_{12}^2} - 4b_{12}^4g_{11}^6g_{12}\sqrt{g_{11}^2+g_{11}g_{12}-2g_{12}^2}\sqrt{b_{12}^2+g_{12}^2} - \\
& 2b_{11}^6b_{12}^2g_{11}g_{12}^2\sqrt{g_{11}^2+g_{11}g_{12}-2g_{12}^2}\sqrt{b_{12}^2+g_{12}^2} + 2b_{11}^5b_{12}^3g_{11}g_{12}^2\sqrt{g_{11}^2+g_{11}g_{12}-2g_{12}^2}\sqrt{b_{12}^2+g_{12}^2} - \\
& 43b_{11}^4b_{12}^4g_{11}g_{12}^2\sqrt{g_{11}^2+g_{11}g_{12}-2g_{12}^2}\sqrt{b_{12}^2+g_{12}^2} - 24b_{11}^3b_{12}^5g_{11}g_{12}^2\sqrt{g_{11}^2+g_{11}g_{12}-2g_{12}^2}\sqrt{b_{12}^2+g_{12}^2} - \\
& 92b_{11}^2b_{12}^6g_{11}g_{12}^2\sqrt{g_{11}^2+g_{11}g_{12}-2g_{12}^2}\sqrt{b_{12}^2+g_{12}^2} - 56b_{11}b_{12}^7g_{11}g_{12}^2\sqrt{g_{11}^2+g_{11}g_{12}-2g_{12}^2}\sqrt{b_{12}^2+g_{12}^2} - \\
& 28b_{12}^8g_{11}g_{12}^2\sqrt{g_{11}^2+g_{11}g_{12}-2g_{12}^2}\sqrt{b_{12}^2+g_{12}^2} - 6b_{11}^4b_{12}^2g_{11}^3g_{12}^2\sqrt{g_{11}^2+g_{11}g_{12}-2g_{12}^2}\sqrt{b_{12}^2+g_{12}^2} - \\
& 12b_{11}^3b_{12}^3g_{11}^3g_{12}^2\sqrt{g_{11}^2+g_{11}g_{12}-2g_{12}^2}\sqrt{b_{12}^2+g_{12}^2} + 16b_{11}^2b_{12}^4g_{11}^3g_{12}^2\sqrt{g_{11}^2+g_{11}g_{12}-2g_{12}^2}\sqrt{b_{12}^2+g_{12}^2} + \\
& 22b_{11}b_{12}^5g_{11}^3g_{12}^2\sqrt{g_{11}^2+g_{11}g_{12}-2g_{12}^2}\sqrt{b_{12}^2+g_{12}^2} + 16b_{12}^6g_{11}^3g_{12}^2\sqrt{g_{11}^2+g_{11}g_{12}-2g_{12}^2}\sqrt{b_{12}^2+g_{12}^2} - \\
& 6b_{11}^2b_{12}^2g_{11}^5g_{12}^2\sqrt{g_{11}^2+g_{11}g_{12}-2g_{12}^2}\sqrt{b_{12}^2+g_{12}^2} - 30b_{11}b_{12}^3g_{11}^5g_{12}^2\sqrt{g_{11}^2+g_{11}g_{12}-2g_{12}^2}\sqrt{b_{12}^2+g_{12}^2} - \\
& 9b_{12}^4g_{11}^5g_{12}^2\sqrt{g_{11}^2+g_{11}g_{12}-2g_{12}^2}\sqrt{b_{12}^2+g_{12}^2} - 2b_{12}^2g_{11}^7g_{12}^2\sqrt{g_{11}^2+g_{11}g_{12}-2g_{12}^2}\sqrt{b_{12}^2+g_{12}^2} - \\
& b_{11}^6b_{12}^2g_{12}^3\sqrt{g_{11}^2+g_{11}g_{12}-2g_{12}^2}\sqrt{b_{12}^2+g_{12}^2} + 8b_{11}^5b_{12}^3g_{12}^3\sqrt{g_{11}^2+g_{11}g_{12}-2g_{12}^2}\sqrt{b_{12}^2+g_{12}^2} - \\
& 2b_{11}^4b_{12}^4g_{12}^3\sqrt{g_{11}^2+g_{11}g_{12}-2g_{12}^2}\sqrt{b_{12}^2+g_{12}^2} + 32b_{11}^3b_{12}^5g_{12}^3\sqrt{g_{11}^2+g_{11}g_{12}-2g_{12}^2}\sqrt{b_{12}^2+g_{12}^2} + \\
& 4b_{11}^2b_{12}^6g_{12}^3\sqrt{g_{11}^2+g_{11}g_{12}-2g_{12}^2}\sqrt{b_{12}^2+g_{12}^2} + 32b_{11}b_{12}^7g_{12}^3\sqrt{g_{11}^2+g_{11}g_{12}-2g_{12}^2}\sqrt{b_{12}^2+g_{12}^2} + \\
& 8b_{12}^8g_{12}^3\sqrt{g_{11}^2+g_{11}g_{12}-2g_{12}^2}\sqrt{b_{12}^2+g_{12}^2} + 8b_{11}^5b_{12}g_{11}^2g_{12}^3\sqrt{g_{11}^2+g_{11}g_{12}-2g_{12}^2}\sqrt{b_{12}^2+g_{12}^2} + \\
& 11b_{11}^4b_{12}^2g_{11}^2g_{12}^3\sqrt{g_{11}^2+g_{11}g_{12}-2g_{12}^2}\sqrt{b_{12}^2+g_{12}^2} + 56b_{11}^3b_{12}^3g_{11}^2g_{12}^3\sqrt{g_{11}^2+g_{11}g_{12}-2g_{12}^2}\sqrt{b_{12}^2+g_{12}^2} + \\
& 135b_{11}^2b_{12}^4g_{11}^2g_{12}^3\sqrt{g_{11}^2+g_{11}g_{12}-2g_{12}^2}\sqrt{b_{12}^2+g_{12}^2} + 96b_{11}b_{12}^5g_{11}^2g_{12}^3\sqrt{g_{11}^2+g_{11}g_{12}-2g_{12}^2}\sqrt{b_{12}^2+g_{12}^2} + \\
& 36b_{12}^6g_{11}^2g_{12}^3\sqrt{g_{11}^2+g_{11}g_{12}-2g_{12}^2}\sqrt{b_{12}^2+g_{12}^2} - 15b_{11}^2b_{12}^2g_{11}^4g_{12}^3\sqrt{g_{11}^2+g_{11}g_{12}-2g_{12}^2}\sqrt{b_{12}^2+g_{12}^2} + \\
& 15b_{12}^4g_{11}^4g_{12}^3\sqrt{g_{11}^2+g_{11}g_{12}-2g_{12}^2}\sqrt{b_{12}^2+g_{12}^2} - 8b_{11}b_{12}g_{11}^6g_{12}^3\sqrt{g_{11}^2+g_{11}g_{12}-2g_{12}^2}\sqrt{b_{12}^2+g_{12}^2} - \\
& 11b_{12}^2g_{11}^6g_{12}^3\sqrt{g_{11}^2+g_{11}g_{12}-2g_{12}^2}\sqrt{b_{12}^2+g_{12}^2} - 2b_{11}^6g_{11}g_{12}^4\sqrt{g_{11}^2+g_{11}g_{12}-2g_{12}^2}\sqrt{b_{12}^2+g_{12}^2} + \\
& 2b_{11}^5b_{12}g_{11}g_{12}^4\sqrt{g_{11}^2+g_{11}g_{12}-2g_{12}^2}\sqrt{b_{12}^2+g_{12}^2} - 46b_{11}^4b_{12}^2g_{11}g_{12}^4\sqrt{g_{11}^2+g_{11}g_{12}-2g_{12}^2}\sqrt{b_{12}^2+g_{12}^2} - \\
& 48b_{11}^3b_{12}^3g_{11}g_{12}^4\sqrt{g_{11}^2+g_{11}g_{12}-2g_{12}^2}\sqrt{b_{12}^2+g_{12}^2} - 180b_{11}^2b_{12}^4g_{11}g_{12}^4\sqrt{g_{11}^2+g_{11}g_{12}-2g_{12}^2}\sqrt{b_{12}^2+g_{12}^2} - \\
& 168b_{11}b_{12}^5g_{11}g_{12}^4\sqrt{g_{11}^2+g_{11}g_{12}-2g_{12}^2}\sqrt{b_{12}^2+g_{12}^2} - 80b_{12}^6g_{11}g_{12}^4\sqrt{g_{11}^2+g_{11}g_{12}-2g_{12}^2}\sqrt{b_{12}^2+g_{12}^2} + \\
& 2b_{11}^4g_{11}^3g_{12}^4\sqrt{g_{11}^2+g_{11}g_{12}-2g_{12}^2}\sqrt{b_{12}^2+g_{12}^2} + 4b_{11}^3b_{12}g_{11}^3g_{12}^4\sqrt{g_{11}^2+g_{11}g_{12}-2g_{12}^2}\sqrt{b_{12}^2+g_{12}^2} + \\
& 42b_{11}^2b_{12}^2g_{11}^3g_{12}^4\sqrt{g_{11}^2+g_{11}g_{12}-2g_{12}^2}\sqrt{b_{12}^2+g_{12}^2} - 110b_{11}b_{12}^3g_{11}^3g_{12}^4\sqrt{g_{11}^2+g_{11}g_{12}-2g_{12}^2}\sqrt{b_{12}^2+g_{12}^2} + \\
& 46b_{12}^4g_{11}^3g_{12}^4\sqrt{g_{11}^2+g_{11}g_{12}-2g_{12}^2}\sqrt{b_{12}^2+g_{12}^2} + 2b_{11}^2g_{11}^5g_{12}^4\sqrt{g_{11}^2+g_{11}g_{12}-2g_{12}^2}\sqrt{b_{12}^2+g_{12}^2} - \\
& 22b_{11}b_{12}g_{11}^5g_{12}^4\sqrt{g_{11}^2+g_{11}g_{12}-2g_{12}^2}\sqrt{b_{12}^2+g_{12}^2} - 4b_{12}^2g_{11}^5g_{12}^4\sqrt{g_{11}^2+g_{11}g_{12}-2g_{12}^2}\sqrt{b_{12}^2+g_{12}^2} - \\
& 2g_{11}^7g_{12}^4\sqrt{g_{11}^2+g_{11}g_{12}-2g_{12}^2}\sqrt{b_{12}^2+g_{12}^2} - b_{11}^6g_{12}^5\sqrt{g_{11}^2+g_{11}g_{12}-2g_{12}^2}\sqrt{b_{12}^2+g_{12}^2} + \\
& 8b_{11}^5b_{12}g_{12}^5\sqrt{g_{11}^2+g_{11}g_{12}-2g_{12}^2}\sqrt{b_{12}^2+g_{12}^2} - 4b_{11}^4b_{12}^2g_{12}^5\sqrt{g_{11}^2+g_{11}g_{12}-2g_{12}^2}\sqrt{b_{12}^2+g_{12}^2} +
\end{aligned}$$

$$\begin{aligned}
& 64 b_{11}^3 b_{12}^3 g_{12}^5 \sqrt{g_{11}^2 + g_{11} g_{12} - 2 g_{12}^2} \sqrt{b_{12}^2 + g_{12}^2} + 12 b_{11}^2 b_{12}^4 g_{12}^5 \sqrt{g_{11}^2 + g_{11} g_{12} - 2 g_{12}^2} \sqrt{b_{12}^2 + g_{12}^2} + \\
& 96 b_{11} b_{12}^5 g_{12}^5 \sqrt{g_{11}^2 + g_{11} g_{12} - 2 g_{12}^2} \sqrt{b_{12}^2 + g_{12}^2} + 32 b_{12}^6 g_{12}^5 \sqrt{g_{11}^2 + g_{11} g_{12} - 2 g_{12}^2} \sqrt{b_{12}^2 + g_{12}^2} + \\
& 3 b_{11}^4 g_{11}^2 g_{12}^5 \sqrt{g_{11}^2 + g_{11} g_{12} - 2 g_{12}^2} \sqrt{b_{12}^2 + g_{12}^2} - 12 b_{11}^3 b_{12} g_{11}^2 g_{12}^5 \sqrt{g_{11}^2 + g_{11} g_{12} - 2 g_{12}^2} \sqrt{b_{12}^2 + g_{12}^2} + \\
& 51 b_{11}^2 b_{12}^2 g_{11}^2 g_{12}^5 \sqrt{g_{11}^2 + g_{11} g_{12} - 2 g_{12}^2} \sqrt{b_{12}^2 + g_{12}^2} - 24 b_{12}^4 g_{11}^2 g_{12}^5 \sqrt{g_{11}^2 + g_{11} g_{12} - 2 g_{12}^2} \sqrt{b_{12}^2 + g_{12}^2} + \\
& 5 b_{11}^2 g_{11}^4 g_{12}^5 \sqrt{g_{11}^2 + g_{11} g_{12} - 2 g_{12}^2} \sqrt{b_{12}^2 + g_{12}^2} + 20 b_{11} b_{12} g_{11}^4 g_{12}^5 \sqrt{g_{11}^2 + g_{11} g_{12} - 2 g_{12}^2} \sqrt{b_{12}^2 + g_{12}^2} + \\
& 45 b_{12}^2 g_{11}^4 g_{12}^5 \sqrt{g_{11}^2 + g_{11} g_{12} - 2 g_{12}^2} \sqrt{b_{12}^2 + g_{12}^2} - 7 g_{11}^6 g_{12}^5 \sqrt{g_{11}^2 + g_{11} g_{12} - 2 g_{12}^2} \sqrt{b_{12}^2 + g_{12}^2} - \\
& 3 b_{11}^4 g_{11} g_{12}^6 \sqrt{g_{11}^2 + g_{11} g_{12} - 2 g_{12}^2} \sqrt{b_{12}^2 + g_{12}^2} - 24 b_{11}^3 b_{12} g_{11} g_{12}^6 \sqrt{g_{11}^2 + g_{11} g_{12} - 2 g_{12}^2} \sqrt{b_{12}^2 + g_{12}^2} - \\
& 84 b_{11}^2 b_{12}^2 g_{11} g_{12}^6 \sqrt{g_{11}^2 + g_{11} g_{12} - 2 g_{12}^2} \sqrt{b_{12}^2 + g_{12}^2} - 168 b_{11} b_{12}^3 g_{11} g_{12}^6 \sqrt{g_{11}^2 + g_{11} g_{12} - 2 g_{12}^2} \sqrt{b_{12}^2 + g_{12}^2} - \\
& 72 b_{12}^4 g_{11} g_{12}^6 \sqrt{g_{11}^2 + g_{11} g_{12} - 2 g_{12}^2} \sqrt{b_{12}^2 + g_{12}^2} - 4 b_{11}^2 g_{11}^3 g_{12}^6 \sqrt{g_{11}^2 + g_{11} g_{12} - 2 g_{12}^2} \sqrt{b_{12}^2 + g_{12}^2} + \\
& 66 b_{11} b_{12} g_{11}^3 g_{12}^6 \sqrt{g_{11}^2 + g_{11} g_{12} - 2 g_{12}^2} \sqrt{b_{12}^2 + g_{12}^2} + 24 b_{12}^2 g_{11}^3 g_{12}^6 \sqrt{g_{11}^2 + g_{11} g_{12} - 2 g_{12}^2} \sqrt{b_{12}^2 + g_{12}^2} + \\
& 3 g_{11}^5 g_{12}^6 \sqrt{g_{11}^2 + g_{11} g_{12} - 2 g_{12}^2} \sqrt{b_{12}^2 + g_{12}^2} - 2 b_{11}^4 g_{12}^7 \sqrt{g_{11}^2 + g_{11} g_{12} - 2 g_{12}^2} \sqrt{b_{12}^2 + g_{12}^2} + \\
& 32 b_{11}^3 b_{12} g_{12}^7 \sqrt{g_{11}^2 + g_{11} g_{12} - 2 g_{12}^2} \sqrt{b_{12}^2 + g_{12}^2} + 12 b_{11}^2 b_{12}^2 g_{12}^7 \sqrt{g_{11}^2 + g_{11} g_{12} - 2 g_{12}^2} \sqrt{b_{12}^2 + g_{12}^2} + \\
& 96 b_{11} b_{12}^3 g_{12}^7 \sqrt{g_{11}^2 + g_{11} g_{12} - 2 g_{12}^2} \sqrt{b_{12}^2 + g_{12}^2} + 48 b_{12}^4 g_{12}^7 \sqrt{g_{11}^2 + g_{11} g_{12} - 2 g_{12}^2} \sqrt{b_{12}^2 + g_{12}^2} - \\
& 11 b_{11}^2 g_{11}^2 g_{12}^7 \sqrt{g_{11}^2 + g_{11} g_{12} - 2 g_{12}^2} \sqrt{b_{12}^2 + g_{12}^2} - 32 b_{11} b_{12} g_{11}^2 g_{12}^7 \sqrt{g_{11}^2 + g_{11} g_{12} - 2 g_{12}^2} \sqrt{b_{12}^2 + g_{12}^2} - \\
& 68 b_{12}^2 g_{11}^2 g_{12}^7 \sqrt{g_{11}^2 + g_{11} g_{12} - 2 g_{12}^2} \sqrt{b_{12}^2 + g_{12}^2} + 25 g_{11}^4 g_{12}^7 \sqrt{g_{11}^2 + g_{11} g_{12} - 2 g_{12}^2} \sqrt{b_{12}^2 + g_{12}^2} + \\
& 4 b_{11}^2 g_{11} g_{12}^8 \sqrt{g_{11}^2 + g_{11} g_{12} - 2 g_{12}^2} \sqrt{b_{12}^2 + g_{12}^2} - 56 b_{11} b_{12} g_{11} g_{12}^8 \sqrt{g_{11}^2 + g_{11} g_{12} - 2 g_{12}^2} \sqrt{b_{12}^2 + g_{12}^2} - \\
& 16 b_{12}^2 g_{11} g_{12}^8 \sqrt{g_{11}^2 + g_{11} g_{12} - 2 g_{12}^2} \sqrt{b_{12}^2 + g_{12}^2} - g_{11}^3 g_{12}^8 \sqrt{g_{11}^2 + g_{11} g_{12} - 2 g_{12}^2} \sqrt{b_{12}^2 + g_{12}^2} + \\
& 4 b_{11}^2 g_{12}^8 \sqrt{g_{11}^2 + g_{11} g_{12} - 2 g_{12}^2} \sqrt{b_{12}^2 + g_{12}^2} + 32 b_{11} b_{12} g_{12}^8 \sqrt{g_{11}^2 + g_{11} g_{12} - 2 g_{12}^2} \sqrt{b_{12}^2 + g_{12}^2} + \\
& 32 b_{12}^2 g_{12}^8 \sqrt{g_{11}^2 + g_{11} g_{12} - 2 g_{12}^2} \sqrt{b_{12}^2 + g_{12}^2} - 30 g_{11}^2 g_{12}^9 \sqrt{g_{11}^2 + g_{11} g_{12} - 2 g_{12}^2} \sqrt{b_{12}^2 + g_{12}^2} + \\
& 4 g_{11} g_{12}^{10} \sqrt{g_{11}^2 + g_{11} g_{12} - 2 g_{12}^2} \sqrt{b_{12}^2 + g_{12}^2} + 8 g_{12}^{11} \sqrt{g_{11}^2 + g_{11} g_{12} - 2 g_{12}^2} \sqrt{b_{12}^2 + g_{12}^2} \Big) / \\
& \left( (g_{11} - g_{12}) (g_{11} + 2 g_{12}) \left( -2 b_{11}^2 b_{12}^2 g_{11} - 2 b_{11} b_{12}^3 g_{11} - 5 b_{12}^4 g_{11} - 2 b_{12}^2 g_{11}^3 - b_{11}^3 b_{12}^2 g_{12} - 8 b_{11} b_{12}^3 g_{12} + 2 b_{12}^4 g_{12} - \right. \right. \\
& \quad 3 b_{12}^2 g_{11}^2 g_{12} - 2 b_{11}^2 g_{11} g_{12}^2 - 2 b_{11} b_{12} g_{11} g_{12}^2 - 2 b_{12}^2 g_{11} g_{12}^2 - 2 g_{11}^3 g_{12}^2 - b_{11}^2 g_{12}^3 + 8 b_{11} b_{12} g_{12}^3 + 4 b_{12}^2 g_{12}^3 - \\
& \quad 3 g_{11}^2 g_{12}^3 - 3 g_{11} g_{12}^4 + 2 g_{12}^5 - 2 b_{11}^2 b_{12} \sqrt{g_{11}^2 + g_{11} g_{12} - 2 g_{12}^2} \sqrt{b_{12}^2 + g_{12}^2} + 2 b_{11} b_{12}^2 \sqrt{g_{11}^2 + g_{11} g_{12} - 2 g_{12}^2} \sqrt{b_{12}^2 + g_{12}^2} - \\
& \quad \left. 4 b_{12}^2 \sqrt{g_{11}^2 + g_{11} g_{12} - 2 g_{12}^2} \sqrt{b_{12}^2 + g_{12}^2} - 2 b_{12} g_{11}^2 \sqrt{g_{11}^2 + g_{11} g_{12} - 2 g_{12}^2} \sqrt{b_{12}^2 + g_{12}^2} + 4 b_{11} g_{11} g_{12} \sqrt{g_{11}^2 + g_{11} g_{12} - 2 g_{12}^2} \right. \\
& \quad \left. \sqrt{b_{12}^2 + g_{12}^2} + 2 b_{11} g_{12}^2 \sqrt{g_{11}^2 + g_{11} g_{12} - 2 g_{12}^2} \sqrt{b_{12}^2 + g_{12}^2} - 4 b_{12} g_{12}^2 \sqrt{g_{11}^2 + g_{11} g_{12} - 2 g_{12}^2} \sqrt{b_{12}^2 + g_{12}^2} \right)^2 \Big) \\
\end{aligned}$$

soln2x1 = x1 /. solnset[[2]]

$$\frac{-b_{12} g_{11} - b_{11} g_{12} - \sqrt{g_{11}^2 + g_{11} g_{12} - 2 g_{12}^2} \sqrt{b_{12}^2 + g_{12}^2}}{-2 b_{11} b_{12} g_{11} - b_{12}^2 g_{11} + b_{11}^2 g_{12} + 2 b_{12}^2 g_{12} - g_{11}^2 g_{12} - g_{11} g_{12}^2 + 2 g_{12}^3}$$

soln2b2 = Together[b2 /. solnset[[2]]]

$$\begin{aligned}
& \left( 8 b_{11}^4 b_{12}^5 g_{11}^4 + 16 b_{11}^3 b_{12}^6 g_{11}^4 - 6 b_{11}^2 b_{12}^7 g_{11}^4 - 14 b_{11} b_{12}^8 g_{11}^4 - 4 b_{12}^9 g_{11}^4 - 8 b_{11}^2 b_{12}^5 g_{11}^6 - 8 b_{11} b_{12}^6 g_{11}^6 - 2 b_{12}^7 g_{11}^6 - \right. \\
& \quad 8 b_{11}^5 b_{12}^4 g_{11}^3 g_{12} - 4 b_{11}^4 b_{12}^5 g_{11}^3 g_{12} + 12 b_{11}^3 b_{12}^6 g_{11}^3 g_{12} - 22 b_{11}^2 b_{12}^7 g_{11}^3 g_{12} + 10 b_{11} b_{12}^8 g_{11}^3 g_{12} + 12 b_{12}^9 g_{11}^3 g_{12} + \\
& \quad 32 b_{11}^2 b_{12}^4 g_{11}^5 g_{12} + 24 b_{11}^3 b_{12}^5 g_{11}^5 g_{12} - 2 b_{12}^2 g_{11}^5 g_{12} - 8 b_{11} b_{12}^2 g_{11}^5 g_{12} - 4 b_{12}^3 g_{11}^5 g_{12} + 2 b_{11}^2 b_{12}^3 g_{11}^5 g_{12}^2 - 6 b_{11}^3 b_{12}^4 g_{11}^5 g_{12}^2 - \\
& \quad 24 b_{11}^4 b_{12}^5 g_{11}^5 g_{12}^2 - 28 b_{11}^5 b_{12}^6 g_{11}^5 g_{12}^2 - 12 b_{11}^2 b_{12}^7 g_{11}^5 g_{12}^2 + 60 b_{11} b_{12}^8 g_{11}^5 g_{12}^2 + 8 b_{12}^9 g_{11}^5 g_{12}^2 - 14 b_{11}^4 b_{12}^3 g_{11}^4 g_{12}^2 + \\
& \quad 52 b_{11}^3 b_{12}^4 g_{11}^4 g_{12}^2 + 6 b_{11}^2 b_{12}^5 g_{11}^4 g_{12}^2 - 40 b_{11} b_{12}^6 g_{11}^4 g_{12}^2 - 4 b_{12}^7 g_{11}^4 g_{12}^2 - 14 b_{11}^2 b_{12}^7 g_{11}^4 g_{12}^2 - 14 b_{11} b_{12}^8 g_{11}^4 g_{12}^2 - \\
& \quad 6 b_{12}^9 g_{11}^4 g_{12}^2 - 2 b_{12}^3 g_{11}^5 g_{12}^2 + 2 b_{11}^6 b_{12}^3 g_{11} g_{12}^3 + 18 b_{11}^5 b_{12}^4 g_{11} g_{12}^3 + 28 b_{11}^4 b_{12}^5 g_{11} g_{12}^3 + 16 b_{11}^3 b_{12}^6 g_{11} g_{12}^3 + \\
& \quad 24 b_{11}^2 b_{12}^7 g_{11} g_{12}^3 - 40 b_{11} b_{12}^8 g_{11} g_{12}^3 - 48 b_{12}^9 g_{11} g_{12}^3 - 4 b_{11}^5 b_{12}^2 g_{11}^3 g_{12}^3 - 38 b_{11}^4 b_{12}^3 g_{11}^3 g_{12}^3 - 40 b_{11}^3 b_{12}^4 g_{11}^3 g_{12}^3 - \\
& \quad 154 b_{11}^2 b_{12}^5 g_{11}^3 g_{12}^3 + 56 b_{12}^6 g_{11}^3 g_{12}^3 + 24 b_{11}^3 b_{12}^2 g_{11}^5 g_{12}^3 + 78 b_{11}^2 b_{12}^3 g_{11}^5 g_{12}^3 + 18 b_{11} b_{12}^4 g_{11}^5 g_{12}^3 + 6 b_{12}^5 g_{11}^5 g_{12}^3 - \\
& \quad 4 b_{11} b_{12}^2 g_{11}^7 g_{12}^3 - 10 b_{12}^3 g_{11}^7 g_{12}^3 - 4 b_{11}^6 b_{12}^3 g_{12}^4 - 4 b_{11}^5 b_{12}^4 g_{12}^4 - 8 b_{11}^4 b_{12}^5 g_{12}^4 - 16 b_{11}^3 b_{12}^6 g_{12}^4 + 16 b_{11}^2 b_{12}^7 g_{12}^4 - \\
& \quad 16 b_{11} b_{12}^8 g_{12}^4 + 32 b_{12}^9 g_{12}^4 + 2 b_{11}^6 b_{12} g_{11}^2 g_{12}^4 + 12 b_{11}^5 b_{12}^2 g_{11}^2 g_{12}^4 - 12 b_{11}^4 b_{12}^3 g_{11}^2 g_{12}^4 - 12 b_{11}^3 b_{12}^4 g_{11}^2 g_{12}^4 + \\
& \quad 240 b_{11} b_{12}^6 g_{11}^2 g_{12}^4 + 16 b_{12}^7 g_{11}^2 g_{12}^4 - 22 b_{11}^4 b_{12} g_{11}^4 g_{12}^4 + 16 b_{11}^3 b_{12}^2 g_{11}^4 g_{12}^4 - 30 b_{11}^2 b_{12}^3 g_{11}^4 g_{12}^4 - 88 b_{11} b_{12}^4 g_{11}^4 g_{12}^4 + \\
& \quad 4 b_{12}^5 g_{11}^4 g_{12}^4 + 22 b_{11}^2 b_{12} g_{11}^6 g_{12}^4 + 8 b_{11} b_{12}^2 g_{11}^6 g_{12}^4 - 2 b_{12}^3 g_{11}^6 g_{12}^4 - 2 b_{12} g_{11}^5 g_{12}^4 + 2 b_{11}^6 b_{12} g_{11} g_{12}^5 - 12 b_{11}^5 b_{12}^2 g_{11} g_{12}^5 + \\
& \quad 56 b_{11}^4 b_{12}^3 g_{11} g_{12}^5 + 16 b_{11}^3 b_{12}^4 g_{11} g_{12}^5 + 72 b_{11}^2 b_{12}^5 g_{11} g_{12}^5 - 128 b_{11} b_{12}^6 g_{11} g_{12}^5 - 192 b_{12}^7 g_{11} g_{12}^5 + 4 b_{11}^5 g_{11}^3 g_{12}^5 - \\
& \quad 34 b_{11}^4 b_{12} g_{11}^3 g_{12}^5 - 36 b_{11}^3 b_{12}^2 g_{11}^3 g_{12}^5 - 242 b_{11}^2 b_{12}^3 g_{11}^3 g_{12}^5 - 28 b_{11} b_{12}^4 g_{11}^3 g_{12}^5 + 96 b_{12}^5 g_{11}^3 g_{12}^5 - 8 b_{11}^3 g_{11}^5 g_{12}^5 + \\
& \quad 54 b_{11}^2 b_{12} g_{11}^5 g_{12}^5 + 12 b_{11} b_{12}^2 g_{11}^5 g_{12}^5 + 18 b_{12}^3 g_{11}^5 g_{12}^5 + 4 b_{11}^4 g_{11}^7 g_{12}^5 - 6 b_{12} g_{11}^7 g_{12}^5 - 4 b_{11}^6 b_{12} g_{12}^6 - 8 b_{11}^5 b_{12}^2 g_{12}^6 - \\
& \quad 16 b_{11}^4 b_{12}^3 g_{12}^6 - 48 b_{11}^3 b_{12}^4 g_{12}^6 + 48 b_{11}^2 b_{12}^5 g_{12}^6 - 64 b_{11} b_{12}^6 g_{12}^6 + 128 b_{12}^7 g_{12}^6 + 6 b_{11}^5 g_{11}^3 g_{12}^6 + 36 b_{11}^4 b_{12} g_{11}^3 g_{12}^6 + \\
& \quad 60 b_{11}^3 b_{12}^2 g_{11}^3 g_{12}^6 + 60 b_{11}^2 b_{12}^3 g_{11}^3 g_{12}^6 + 360 b_{11} b_{12}^4 g_{11}^3 g_{12}^6 - 20 b_{11}^4 g_{11}^4 g_{12}^6 - 42 b_{11}^3 b_{12} g_{11}^4 g_{12}^6 - 112 b_{11}^2 b_{12}^2 g_{11}^4 g_{12}^6 + \\
& \quad 4 b_{12}^3 g_{11}^4 g_{12}^6 + 14 b_{11} g_{11}^6 g_{12}^6 + 2 b_{12} g_{11}^6 g_{12}^6 - 6 b_{11}^5 g_{11} g_{12}^7 + 28 b_{11}^4 b_{12} g_{11} g_{12}^7 - 16 b_{11}^3 b_{12}^2 g_{11} g_{12}^7 + 72 b_{11}^2 b_{12}^3 g_{11} g_{12}^7 - \\
& \quad 144 b_{11} b_{12}^4 g_{11} g_{12}^7 - 288 b_{12}^5 g_{11} g_{12}^7 + 16 b_{11}^3 g_{11}^3 g_{12}^7 - 110 b_{11}^2 b_{12} g_{11}^3 g_{12}^7 - 16 b_{11} b_{12}^2 g_{11}^3 g_{12}^7 + 72 b_{12}^3 g_{11}^3 g_{12}^7 - 6 b_{11} g_{11}^5 g_{12}^7 + \\
& \quad 10 b_{12} g_{11}^5 g_{12}^7 - 4 b_{11}^5 g_{12}^8 - 8 b_{11}^4 b_{12} g_{12}^8 - 48 b_{11}^3 b_{12}^2 g_{12}^8 + 48 b_{11}^2 b_{12}^3 g_{12}^8 - 96 b_{11} b_{12}^4 g_{12}^8 - 192 b_{12}^5 g_{12}^8 + 44 b_{11}^3 g_{11}^2 g_{12}^8 - \\
& \quad 36 b_{11}^2 b_{12} g_{11}^2 g_{12}^8 + 240 b_{11} b_{12}^2 g_{11}^2 g_{12}^8 - 16 b_{12}^3 g_{11}^2 g_{12}^8 - 50 b_{11} g_{11}^4 g_{12}^8 - 16 b_{11}^3 g_{11} g_{12}^8 + 24 b_{11}^2 b_{12} g_{11} g_{12}^8 - 64 b_{11} b_{12}^2 g_{11} g_{12}^8 - \\
& \quad 192 b_{12}^3 g_{11} g_{12}^8 + 2 b_{11} g_{11}^3 g_{12}^8 + 20 b_{12} g_{11}^3 g_{12}^8 - 16 b_{11}^2 g_{12}^{10} - 16 b_{11}^2 b_{12} g_{12}^{10} - 64 b_{11} b_{12}^2 g_{12}^{10} + 128 b_{12}^3 g_{12}^{10} + 60 b_{11} g_{11}^2 g_{12}^{10} - \\
& \quad 8 b_{12} g_{11}^2 g_{12}^{10} - 8 b_{11} g_{11} g_{12}^{11} - 48 b_{12} g_{11} g_{12}^{11} - 16 b_{11} g_{12}^{12} + 32 b_{12} g_{12}^{12} + 8 b_{11}^4 b_{12}^4 g_{11}^4 \sqrt{g_{11}^2 + g_{11} g_{12} - 2 g_{12}^2} \sqrt{b_{12}^2 + g_{12}^2} + \\
& \quad 16 b_{11}^3 b_{12}^5 g_{11}^3 \sqrt{g_{11}^2 + g_{11} g_{12} - 2 g_{12}^2} \sqrt{b_{12}^2 + g_{12}^2} + 30 b_{11}^2 b_{12}^6 g_{11}^2 \sqrt{g_{11}^2 + g_{11} g_{12} - 2 g_{12}^2} \sqrt{b_{12}^2 + g_{12}^2} +
\end{aligned}$$

97

$$\begin{aligned}
& 68 b_{12}^2 g_{11}^2 g_{12}^7 \sqrt{g_{11}^2 + g_{11} g_{12} - 2 g_{12}^2} \sqrt{b_{12}^2 + g_{12}^2} - 25 g_{11}^4 g_{12}^7 \sqrt{g_{11}^2 + g_{11} g_{12} - 2 g_{12}^2} \sqrt{b_{12}^2 + g_{12}^2} - \\
& 4 b_{11}^2 g_{11} g_{12}^8 \sqrt{g_{11}^2 + g_{11} g_{12} - 2 g_{12}^2} \sqrt{b_{12}^2 + g_{12}^2} + 56 b_{11} b_{12} g_{11} g_{12}^8 \sqrt{g_{11}^2 + g_{11} g_{12} - 2 g_{12}^2} \sqrt{b_{12}^2 + g_{12}^2} + \\
& 16 b_{12}^2 g_{11} g_{12}^8 \sqrt{g_{11}^2 + g_{11} g_{12} - 2 g_{12}^2} \sqrt{b_{12}^2 + g_{12}^2} + g_{11}^8 g_{12}^8 \sqrt{g_{11}^2 + g_{11} g_{12} - 2 g_{12}^2} \sqrt{b_{12}^2 + g_{12}^2} - \\
& 4 b_{11}^2 g_{12}^9 \sqrt{g_{11}^2 + g_{11} g_{12} - 2 g_{12}^2} \sqrt{b_{12}^2 + g_{12}^2} - 32 b_{11} b_{12} g_{12}^9 \sqrt{g_{11}^2 + g_{11} g_{12} - 2 g_{12}^2} \sqrt{b_{12}^2 + g_{12}^2} - \\
& 32 b_{12}^2 g_{12}^9 \sqrt{g_{11}^2 + g_{11} g_{12} - 2 g_{12}^2} \sqrt{b_{12}^2 + g_{12}^2} + 30 g_{11}^2 g_{12}^9 \sqrt{g_{11}^2 + g_{11} g_{12} - 2 g_{12}^2} \sqrt{b_{12}^2 + g_{12}^2} - \\
& 4 g_{11} g_{12}^{10} \sqrt{g_{11}^2 + g_{11} g_{12} - 2 g_{12}^2} \sqrt{b_{12}^2 + g_{12}^2} - 8 g_{12}^{11} \sqrt{g_{11}^2 + g_{11} g_{12} - 2 g_{12}^2} \sqrt{b_{12}^2 + g_{12}^2} \Big) / \\
& \Big( (g_{11} - g_{12}) (g_{11} + 2 g_{12}) \Big( 2 b_{11}^2 b_{12}^2 g_{11} + 2 b_{11} b_{12}^3 g_{11} + 5 b_{12}^4 g_{11} + 2 b_{12}^2 g_{11}^3 + b_{11}^2 b_{12}^2 g_{12} - 8 b_{11} b_{12}^3 g_{12} - 2 b_{12}^4 g_{12} + \\
& 3 b_{12}^2 g_{11}^2 g_{12} - 2 b_{11}^2 g_{11} g_{12}^2 + 2 b_{11} b_{12} g_{11} g_{12}^2 + 2 b_{12}^2 g_{11} g_{12}^2 + 2 g_{11}^3 g_{12}^2 + b_{11}^2 g_{12}^3 - 8 b_{11} b_{12} g_{12}^3 - 4 b_{12}^2 g_{12}^3 + \\
& 3 g_{11}^2 g_{12}^3 - 3 g_{11} g_{12}^4 - 2 g_{12}^5 - 2 b_{11}^2 b_{12} \sqrt{g_{11}^2 + g_{11} g_{12} - 2 g_{12}^2} \sqrt{b_{12}^2 + g_{12}^2} + 2 b_{11} b_{12}^2 \sqrt{g_{11}^2 + g_{11} g_{12} - 2 g_{12}^2} \sqrt{b_{12}^2 + g_{12}^2} - \\
& 4 b_{12}^3 \sqrt{g_{11}^2 + g_{11} g_{12} - 2 g_{12}^2} \sqrt{b_{12}^2 + g_{12}^2} - 2 b_{12} g_{11}^2 \sqrt{g_{11}^2 + g_{11} g_{12} - 2 g_{12}^2} \sqrt{b_{12}^2 + g_{12}^2} + 4 b_{11} g_{11} g_{12} \sqrt{g_{11}^2 + g_{11} g_{12} - 2 g_{12}^2} \sqrt{b_{12}^2 + g_{12}^2} - \\
& \sqrt{b_{12}^2 + g_{12}^2} + 2 b_{11} g_{12}^2 \sqrt{g_{11}^2 + g_{11} g_{12} - 2 g_{12}^2} \sqrt{b_{12}^2 + g_{12}^2} - 4 b_{12} g_{12}^2 \sqrt{g_{11}^2 + g_{11} g_{12} - 2 g_{12}^2} \sqrt{b_{12}^2 + g_{12}^2} \Big)^2 \Big)
\end{aligned}$$

## **APPENDIX B**

### **PROGRAM CODE FOR NETWORK ANALYSIS**

This appendix presents the program code written in *Mathematica* software. The code uses the network analysis to decouple an array with a generalized admittance matrix. Analytically solutions were obtained for the decoupling network. These analytical solutions are in terms of the array admittance parameters. Numerical values can easily be obtained once the array admittances are known.



```

(* Program to compute the decoupling network using *)
(* network approach, instead of modal approach. *)
(* For a 3-element array. *)
(* DN has 2 elements: X1 and B2. *)

y11 = g11 + I * b11;
y12 = g12 + I * b12;

yarray =  $\begin{pmatrix} y11 & y12 & y12 \\ y12 & y11 & y12 \\ y12 & y12 & y11 \end{pmatrix}$ ;

zseries =  $\begin{pmatrix} I * x1 & 0 & 0 \\ 0 & I * x1 & 0 \\ 0 & 0 & I * x1 \end{pmatrix}$ ;

yparallel =  $\begin{pmatrix} I * 2 * b2 & -I * b2 & -I * b2 \\ -I * b2 & I * 2 * b2 & -I * b2 \\ -I * b2 & -I * b2 & I * 2 * b2 \end{pmatrix}$ ;

yin = Inverse[Inverse[yarray] + zseries] + yparallel

(* ***** The decoupled y-parameters ***** *)

y11d = yin[[1, 1]] // Together
General::spell1: Possible spelling error: new symbol name "y11d" is similar to existing symbol "y11".

$$\frac{(i b11 - 2 i b2 + g11 - i b11^2 x1 - i b11 b12 x1 + 2 i b12^2 x1 - 4 i b11 b2 x1 - 2 i b12 b2 x1 - 2 b11 g11 x1 - b12 g11 x1 - 4 b2 g11 x1 + i g11^2 x1 - b11 g12 x1 + 4 b12 g12 x1 - 2 b2 g12 x1 + i g11 g12 x1 - 2 i g12^2 x1 + 2 i b11^2 b2 x1^2 + 2 i b11 b12 b2 x1^2 - 4 i b12^2 b2 x1^2 + 4 b11 b2 g11 x1^2 - 2 b12 b2 g11 x1^2 - 2 i b2 g11^2 x1^2 + 2 b11 b2 g12 x1^2 - 8 b12 b2 g12 x1^2 - 2 i b2 g11 g12 x1^2 + 4 i b2 g12^2 x1^2) / ((-1 + b11 x1 - b12 x1 - i g11 x1 + i g12 x1) (-1 + b11 x1 + 2 b12 x1 - i g11 x1 - 2 i g12 x1))$$


y12d = yin[[1, 2]] // Together
General::spell1: Possible spelling error: new symbol name "y12d" is similar to existing symbol "y12".

$$\frac{(i b12 - i b2 - g12 + 2 i b11 b2 x1 + i b12 b2 x1 + 2 b2 g11 x1 - b2 g12 x1 - i b11^2 b2 x1^2 - i b11 b12 b2 x1^2 + 2 i b12^2 b2 x1^2 - 2 b11 b2 g11 x1^2 - b12 b2 g11 x1^2 + i b2 g11^2 x1^2 - b11 b2 g12 x1^2 + 4 b12 b2 g12 x1^2 + i b2 g11 g12 x1^2 - 2 i b2 g12^2 x1^2) / ((-1 + b11 x1 - b12 x1 - i g11 x1 + i g12 x1) (-1 + b11 x1 + 2 b12 x1 - i g11 x1 - 2 i g12 x1))$$


y13d = yin[[1, 3]] // Together
y21d = yin[[2, 1]] // Together
y22d = yin[[2, 2]] // Together
y23d = yin[[2, 3]] // Together
y31d = yin[[3, 1]] // Together
y32d = yin[[3, 2]] // Together
y33d = yin[[3, 3]] // Together
TrueQ[y11d == y22d == y33d]
True
TrueQ[y12d == y21d == y13d == y31d == y23d == y32d]
True
denoy12d = ComplexExpand[Denominator[y12d] * Conjugate[Denominator[y12d]], {x1, b2, g11, b11, g12, b12} ∈ Reals]
numery12d = ComplexExpand[Numerator[y12d] * Conjugate[Denominator[y12d]], {x1, b2, g11, b11, g12, b12} ∈ Reals]
y12dexpr = ComplexExpand[numery12d/denoy12d, {x1, b2, g11, b11, g12, b12} ∈ Reals]
y12dreal = ComplexExpand[Re[y12dexpr], {x1, b2, g11, b11, g12, b12} ∈ Reals]
y12dimg = ComplexExpand[Im[y12dexpr], {x1, b2, g11, b11, g12, b12} ∈ Reals]
solnset = Solve[{y12dreal == 0, y12dimg == 0}, {x1, b2}]
soln1x1 = x1 /. solnset[[1]]

$$\frac{-b12 g11 + b11 g12 - \sqrt{g11^2 + g11 g12 - 2 g12^2} \sqrt{b12^2 + g12^2}}{-2 b11 b12 g11 - b12^2 g11 + b11^2 g12 + 2 b12^2 g12 - g11^2 g12 - g11 g12^2 + 2 g12^3}$$

soln1b2 = Together[b2 /. solnset[[1]]]

$$-\left( (2 b11 b12 g11 + b12^2 g11 - b11^2 g12 - 2 b12^2 g12 + g11^2 g12 + g11 g12^2 - 2 g12^3)^2 \right)$$


```



$$\begin{aligned}
& \left( -2 b_{11}^2 b_{12} g_{11}^2 - 2 b_{11} b_{12}^2 g_{11}^2 + 4 b_{12}^3 g_{11}^2 + 2 b_{12} g_{11}^4 - 2 b_{11}^2 b_{12} g_{11} g_{12} - 2 b_{11} b_{12}^2 g_{11} g_{12} + 4 b_{12}^3 g_{11} g_{12} - 4 b_{11} g_{11}^3 g_{12} + \right. \\
& 2 b_{12} g_{11}^3 g_{12} + 4 b_{11}^2 b_{12} g_{12}^2 + 4 b_{11} b_{12}^2 g_{12}^2 - 8 b_{12}^3 g_{12}^2 - 6 b_{11} g_{11}^2 g_{12}^2 + 6 b_{11} g_{11} g_{12}^3 + 4 b_{12} g_{11} g_{12}^3 + 4 b_{11} g_{12}^4 - \\
& 8 b_{12} g_{12}^4 + 2 b_{11}^2 g_{11} \sqrt{g_{11}^2 + g_{11} g_{12} - 2 g_{12}^2} \sqrt{b_{12}^2 + g_{12}^2} + 2 b_{11} b_{12} g_{11} \sqrt{g_{11}^2 + g_{11} g_{12} - 2 g_{12}^2} \sqrt{b_{12}^2 + g_{12}^2} + \\
& 5 b_{12}^2 g_{11} \sqrt{g_{11}^2 + g_{11} g_{12} - 2 g_{12}^2} \sqrt{b_{12}^2 + g_{12}^2} + 2 g_{11}^3 \sqrt{g_{11}^2 + g_{11} g_{12} - 2 g_{12}^2} \sqrt{b_{12}^2 + g_{12}^2} + \\
& b_{11}^2 g_{12} \sqrt{g_{11}^2 + g_{11} g_{12} - 2 g_{12}^2} \sqrt{b_{12}^2 + g_{12}^2} - 8 b_{11} b_{12} g_{12} \sqrt{g_{11}^2 + g_{11} g_{12} - 2 g_{12}^2} \sqrt{b_{12}^2 + g_{12}^2} - \\
& 2 b_{12}^2 g_{12} \sqrt{g_{11}^2 + g_{11} g_{12} - 2 g_{12}^2} \sqrt{b_{12}^2 + g_{12}^2} + 3 g_{11}^2 g_{12} \sqrt{g_{11}^2 + g_{11} g_{12} - 2 g_{12}^2} \sqrt{b_{12}^2 + g_{12}^2} - \\
& \left. 3 g_{11} g_{12}^2 \sqrt{g_{11}^2 + g_{11} g_{12} - 2 g_{12}^2} \sqrt{b_{12}^2 + g_{12}^2} - 2 g_{12}^3 \sqrt{g_{11}^2 + g_{11} g_{12} - 2 g_{12}^2} \sqrt{b_{12}^2 + g_{12}^2} \right) \Bigg) / \\
& \left( 8 b_{11}^4 b_{12}^2 g_{11}^4 + 16 b_{11}^3 b_{12}^3 g_{11}^4 + 12 b_{11}^2 b_{12}^4 g_{11}^4 + 4 b_{11} b_{12}^5 g_{11}^4 + 41 b_{12}^6 g_{11}^4 + 36 b_{12}^4 g_{11}^6 + 8 b_{12}^2 g_{11}^8 + \right. \\
& 16 b_{11}^4 b_{12}^2 g_{11}^3 g_{12} - 4 b_{11}^3 b_{12}^3 g_{11}^3 g_{12} - 30 b_{11}^2 b_{12}^4 g_{11}^3 g_{12} - 100 b_{11} b_{12}^5 g_{11}^3 g_{12} + 37 b_{12}^6 g_{11}^3 g_{12} + \\
& 16 b_{11}^3 b_{12}^3 g_{11}^5 g_{12} + 24 b_{11}^4 b_{12}^2 g_{11}^5 g_{12} - 60 b_{11} b_{12}^5 g_{11}^5 g_{12} + 74 b_{12}^6 g_{11}^5 g_{12} - 16 b_{11} b_{12} g_{11}^7 g_{12} + 24 b_{12}^2 g_{11}^7 g_{12} - \\
& 15 b_{11}^4 b_{12}^2 g_{11}^2 g_{12}^2 - 84 b_{11}^3 b_{12}^3 g_{11}^2 g_{12}^2 + 18 b_{11}^2 b_{12}^4 g_{11}^2 g_{12}^2 - 48 b_{11} b_{12}^5 g_{11}^2 g_{12}^2 - 114 b_{12}^6 g_{11}^2 g_{12}^2 + \\
& 4 b_{11}^4 g_{11}^4 g_{12}^2 + 48 b_{11}^3 b_{12} g_{11}^4 g_{12}^2 + 66 b_{11}^2 b_{12}^2 g_{11}^4 g_{12}^2 - 148 b_{11} b_{12}^3 g_{11}^4 g_{12}^2 - 51 b_{12}^4 g_{11}^4 g_{12}^2 + \\
& 24 b_{11}^2 g_{11}^6 g_{12}^2 - 32 b_{11} b_{12} g_{11}^6 g_{12}^2 + 25 b_{12}^2 g_{11}^6 g_{12}^2 + 4 g_{11}^8 g_{12}^2 - 23 b_{11}^4 b_{12}^2 g_{11} g_{12}^3 + 8 b_{11}^3 b_{12}^3 g_{11} g_{12}^3 + \\
& 168 b_{11}^2 b_{12}^4 g_{11} g_{12}^3 + 272 b_{11} b_{12}^5 g_{11} g_{12}^3 - 20 b_{12}^6 g_{11} g_{12}^3 + 8 b_{11}^4 g_{11}^3 g_{12}^3 - 52 b_{11}^3 b_{12} g_{11}^3 g_{12}^3 - \\
& 90 b_{11}^2 b_{12}^2 g_{11}^3 g_{12}^3 + 16 b_{11} b_{12}^3 g_{11}^3 g_{12}^3 - 89 b_{12}^4 g_{11}^3 g_{12}^3 + 72 b_{11}^2 g_{11}^5 g_{12}^3 - 12 b_{11} b_{12} g_{11}^5 g_{12}^3 + 5 b_{12}^2 g_{11}^5 g_{12}^3 + \\
& 16 g_{11}^7 g_{12}^3 + 14 b_{11}^4 b_{12}^2 g_{12}^4 + 64 b_{11}^3 b_{12}^3 g_{12}^4 - 168 b_{11}^2 b_{12}^4 g_{12}^4 - 128 b_{11} b_{12}^5 g_{12}^4 + 56 b_{12}^6 g_{12}^4 - 3 b_{11}^4 g_{11}^4 g_{12}^4 - \\
& 148 b_{11}^3 b_{12} g_{11}^4 g_{12}^4 - 96 b_{11}^2 b_{12}^2 g_{11}^4 g_{12}^4 + 288 b_{11} b_{12}^3 g_{11}^4 g_{12}^4 - 14 b_{12}^4 g_{11}^4 g_{12}^4 - 18 b_{11}^2 g_{11}^4 g_{12}^4 - \\
& 88 b_{11} b_{12} g_{11}^4 g_{12}^4 - 99 b_{12}^2 g_{11}^4 g_{12}^4 + g_{11}^6 g_{12}^4 - 7 b_{11}^4 g_{11} g_{12}^5 + 72 b_{11}^3 b_{12} g_{11} g_{12}^5 + 240 b_{11}^2 b_{12}^2 g_{11} g_{12}^5 + \\
& 160 b_{11} b_{12}^3 g_{11} g_{12}^5 - 60 b_{12}^4 g_{11} g_{12}^5 - 156 b_{11}^2 g_{11}^3 g_{12}^5 + 52 b_{11} b_{12} g_{11}^3 g_{12}^5 - 65 b_{12}^2 g_{11}^3 g_{12}^5 - 53 g_{11}^5 g_{12}^5 - \\
& 26 g_{11}^4 g_{12}^5 + 64 b_{11}^3 b_{12} g_{12}^6 - 144 b_{11}^2 b_{12}^2 g_{12}^6 - 256 b_{11} b_{12}^3 g_{12}^6 + 104 b_{12}^4 g_{12}^6 - 18 b_{11}^2 g_{11}^2 g_{12}^6 - 336 b_{11} b_{12} g_{11}^2 g_{12}^6 + \\
& 122 b_{12}^2 g_{11}^2 g_{12}^6 - 23 g_{11}^4 g_{12}^6 + 72 b_{11}^2 g_{11} g_{12}^7 - 112 b_{11} b_{12} g_{11} g_{12}^7 - 60 b_{12}^2 g_{11} g_{12}^7 + 61 g_{11}^3 g_{12}^7 - 24 b_{11}^2 g_{12}^8 - \\
& 128 b_{11} b_{12} g_{12}^8 + 40 b_{12}^2 g_{12}^8 + 22 g_{11}^2 g_{12}^8 - 20 g_{11} g_{12}^9 - 8 g_{12}^{10} - 8 b_{11}^4 b_{12} g_{11}^3 \sqrt{g_{11}^2 + g_{11} g_{12} - 2 g_{12}^2} \sqrt{b_{12}^2 + g_{12}^2} - \\
& 16 b_{11}^3 b_{12}^2 g_{11}^3 \sqrt{g_{11}^2 + g_{11} g_{12} - 2 g_{12}^2} \sqrt{b_{12}^2 + g_{12}^2} - 12 b_{11}^2 b_{12}^3 g_{11}^3 \sqrt{g_{11}^2 + g_{11} g_{12} - 2 g_{12}^2} \sqrt{b_{12}^2 + g_{12}^2} - \\
& 4 b_{11} b_{12}^4 g_{11}^3 \sqrt{g_{11}^2 + g_{11} g_{12} - 2 g_{12}^2} \sqrt{b_{12}^2 + g_{12}^2} + 40 b_{12}^5 g_{11}^3 \sqrt{g_{11}^2 + g_{11} g_{12} - 2 g_{12}^2} \sqrt{b_{12}^2 + g_{12}^2} + \\
& 36 b_{12}^3 g_{11}^5 \sqrt{g_{11}^2 + g_{11} g_{12} - 2 g_{12}^2} \sqrt{b_{12}^2 + g_{12}^2} + 8 b_{12} g_{11}^7 \sqrt{g_{11}^2 + g_{11} g_{12} - 2 g_{12}^2} \sqrt{b_{12}^2 + g_{12}^2} - \\
& 12 b_{11}^4 b_{12} g_{11}^2 g_{12} \sqrt{g_{11}^2 + g_{11} g_{12} - 2 g_{12}^2} \sqrt{b_{12}^2 + g_{12}^2} + 12 b_{11}^3 b_{12}^2 g_{11}^2 g_{12} \sqrt{g_{11}^2 + g_{11} g_{12} - 2 g_{12}^2} \sqrt{b_{12}^2 + g_{12}^2} + \\
& 36 b_{11}^2 b_{12}^3 g_{11}^2 g_{12} \sqrt{g_{11}^2 + g_{11} g_{12} - 2 g_{12}^2} \sqrt{b_{12}^2 + g_{12}^2} - 60 b_{11} b_{12}^4 g_{11}^2 g_{12} \sqrt{g_{11}^2 + g_{11} g_{12} - 2 g_{12}^2} \sqrt{b_{12}^2 + g_{12}^2} + \\
& 24 b_{12}^5 g_{11}^2 g_{12} \sqrt{g_{11}^2 + g_{11} g_{12} - 2 g_{12}^2} \sqrt{b_{12}^2 + g_{12}^2} - 16 b_{11}^3 g_{11}^4 g_{12} \sqrt{g_{11}^2 + g_{11} g_{12} - 2 g_{12}^2} \sqrt{b_{12}^2 + g_{12}^2} - \\
& 24 b_{11}^2 b_{12} g_{11}^4 g_{12} \sqrt{g_{11}^2 + g_{11} g_{12} - 2 g_{12}^2} \sqrt{b_{12}^2 + g_{12}^2} - 84 b_{11} b_{12}^2 g_{11}^4 g_{12} \sqrt{g_{11}^2 + g_{11} g_{12} - 2 g_{12}^2} \sqrt{b_{12}^2 + g_{12}^2} + \\
& 52 b_{12}^3 g_{11}^4 g_{12} \sqrt{g_{11}^2 + g_{11} g_{12} - 2 g_{12}^2} \sqrt{b_{12}^2 + g_{12}^2} - 16 b_{11} g_{11}^6 g_{12} \sqrt{g_{11}^2 + g_{11} g_{12} - 2 g_{12}^2} \sqrt{b_{12}^2 + g_{12}^2} + \\
& 20 b_{12} g_{11}^6 g_{12} \sqrt{g_{11}^2 + g_{11} g_{12} - 2 g_{12}^2} \sqrt{b_{12}^2 + g_{12}^2} + 12 b_{11}^4 b_{12} g_{11} g_{12}^2 \sqrt{g_{11}^2 + g_{11} g_{12} - 2 g_{12}^2} \sqrt{b_{12}^2 + g_{12}^2} + \\
& 60 b_{11}^3 b_{12}^2 g_{11} g_{12}^2 \sqrt{g_{11}^2 + g_{11} g_{12} - 2 g_{12}^2} \sqrt{b_{12}^2 + g_{12}^2} + 72 b_{11}^2 b_{12}^3 g_{11} g_{12}^2 \sqrt{g_{11}^2 + g_{11} g_{12} - 2 g_{12}^2} \sqrt{b_{12}^2 + g_{12}^2} - \\
& 48 b_{11} b_{12}^4 g_{11} g_{12}^2 \sqrt{g_{11}^2 + g_{11} g_{12} - 2 g_{12}^2} \sqrt{b_{12}^2 + g_{12}^2} - 96 b_{12}^5 g_{11} g_{12}^2 \sqrt{g_{11}^2 + g_{11} g_{12} - 2 g_{12}^2} \sqrt{b_{12}^2 + g_{12}^2} - \\
& 32 b_{11}^3 g_{11}^3 g_{12}^2 \sqrt{g_{11}^2 + g_{11} g_{12} - 2 g_{12}^2} \sqrt{b_{12}^2 + g_{12}^2} + 60 b_{11}^2 b_{12} g_{11}^3 g_{12}^2 \sqrt{g_{11}^2 + g_{11} g_{12} - 2 g_{12}^2} \sqrt{b_{12}^2 + g_{12}^2} - \\
& 60 b_{11} b_{12}^2 g_{11}^3 g_{12}^2 \sqrt{g_{11}^2 + g_{11} g_{12} - 2 g_{12}^2} \sqrt{b_{12}^2 + g_{12}^2} - 40 b_{12}^3 g_{11}^3 g_{12}^2 \sqrt{g_{11}^2 + g_{11} g_{12} - 2 g_{12}^2} \sqrt{b_{12}^2 + g_{12}^2} - \\
& 48 b_{11} g_{11}^5 g_{12}^2 \sqrt{g_{11}^2 + g_{11} g_{12} - 2 g_{12}^2} \sqrt{b_{12}^2 + g_{12}^2} + 8 b_{11}^4 b_{12} g_{12}^3 \sqrt{g_{11}^2 + g_{11} g_{12} - 2 g_{12}^2} \sqrt{b_{12}^2 + g_{12}^2} - \\
& 56 b_{11}^3 b_{12}^2 g_{12}^3 \sqrt{g_{11}^2 + g_{11} g_{12} - 2 g_{12}^2} \sqrt{b_{12}^2 + g_{12}^2} - 96 b_{11}^2 b_{12}^3 g_{12}^3 \sqrt{g_{11}^2 + g_{11} g_{12} - 2 g_{12}^2} \sqrt{b_{12}^2 + g_{12}^2} + \\
& 112 b_{11} b_{12}^4 g_{12}^3 \sqrt{g_{11}^2 + g_{11} g_{12} - 2 g_{12}^2} \sqrt{b_{12}^2 + g_{12}^2} + 32 b_{12}^5 g_{12}^3 \sqrt{g_{11}^2 + g_{11} g_{12} - 2 g_{12}^2} \sqrt{b_{12}^2 + g_{12}^2} + \\
& 12 b_{11}^3 g_{11}^2 g_{12}^3 \sqrt{g_{11}^2 + g_{11} g_{12} - 2 g_{12}^2} \sqrt{b_{12}^2 + g_{12}^2} + 180 b_{11}^2 b_{12} g_{11}^2 g_{12}^3 \sqrt{g_{11}^2 + g_{11} g_{12} - 2 g_{12}^2} \sqrt{b_{12}^2 + g_{12}^2} + \\
& 144 b_{11} b_{12}^2 g_{11}^2 g_{12}^3 \sqrt{g_{11}^2 + g_{11} g_{12} - 2 g_{12}^2} \sqrt{b_{12}^2 + g_{12}^2} - 48 b_{12}^3 g_{11}^2 g_{12}^3 \sqrt{g_{11}^2 + g_{11} g_{12} - 2 g_{12}^2} \sqrt{b_{12}^2 + g_{12}^2} + \\
& 12 b_{11} g_{11}^4 g_{12}^3 \sqrt{g_{11}^2 + g_{11} g_{12} - 2 g_{12}^2} \sqrt{b_{12}^2 + g_{12}^2} - 4 b_{12} g_{11}^4 g_{12}^3 \sqrt{g_{11}^2 + g_{11} g_{12} - 2 g_{12}^2} \sqrt{b_{12}^2 + g_{12}^2} + \\
& 28 b_{11}^3 g_{11} g_{12}^4 \sqrt{g_{11}^2 + g_{11} g_{12} - 2 g_{12}^2} \sqrt{b_{12}^2 + g_{12}^2} - 120 b_{11}^2 b_{12} g_{11} g_{12}^4 \sqrt{g_{11}^2 + g_{11} g_{12} - 2 g_{12}^2} \sqrt{b_{12}^2 + g_{12}^2} - \\
& 96 b_{11} b_{12}^2 g_{11} g_{12}^4 \sqrt{g_{11}^2 + g_{11} g_{12} - 2 g_{12}^2} \sqrt{b_{12}^2 + g_{12}^2} - 64 b_{12}^3 g_{11} g_{12}^4 \sqrt{g_{11}^2 + g_{11} g_{12} - 2 g_{12}^2} \sqrt{b_{12}^2 + g_{12}^2} + \\
& 104 b_{11} g_{11}^3 g_{12}^4 \sqrt{g_{11}^2 + g_{11} g_{12} - 2 g_{12}^2} \sqrt{b_{12}^2 + g_{12}^2} - 16 b_{12} g_{11}^3 g_{12}^4 \sqrt{g_{11}^2 + g_{11} g_{12} - 2 g_{12}^2} \sqrt{b_{12}^2 + g_{12}^2} + \\
& 8 b_{11}^3 g_{12}^5 \sqrt{g_{11}^2 + g_{11} g_{12} - 2 g_{12}^2} \sqrt{b_{12}^2 + g_{12}^2} - 96 b_{11}^2 b_{12} g_{12}^5 \sqrt{g_{11}^2 + g_{11} g_{12} - 2 g_{12}^2} \sqrt{b_{12}^2 + g_{12}^2} + \\
& 96 b_{11} b_{12}^2 g_{12}^5 \sqrt{g_{11}^2 + g_{11} g_{12} - 2 g_{12}^2} \sqrt{b_{12}^2 + g_{12}^2} + 64 b_{12}^3 g_{12}^5 \sqrt{g_{11}^2 + g_{11} g_{12} - 2 g_{12}^2} \sqrt{b_{12}^2 + g_{12}^2} + \\
& 12 b_{11} g_{11}^2 g_{12}^5 \sqrt{g_{11}^2 + g_{11} g_{12} - 2 g_{12}^2} \sqrt{b_{12}^2 + g_{12}^2} - 72 b_{12} g_{11}^2 g_{12}^5 \sqrt{g_{11}^2 + g_{11} g_{12} - 2 g_{12}^2} \sqrt{b_{12}^2 + g_{12}^2} - \\
& 48 b_{11} g_{11} g_{12}^6 \sqrt{g_{11}^2 + g_{11} g_{12} - 2 g_{12}^2} \sqrt{b_{12}^2 + g_{12}^2} + 32 b_{12} g_{11} g_{12}^6 \sqrt{g_{11}^2 + g_{11} g_{12} - 2 g_{12}^2} \sqrt{b_{12}^2 + g_{12}^2} - \\
& 16 b_{11} g_{12}^7 \sqrt{g_{11}^2 + g_{11} g_{12} - 2 g_{12}^2} \sqrt{b_{12}^2 + g_{12}^2} + 32 b_{12} g_{12}^7 \sqrt{g_{11}^2 + g_{11} g_{12} - 2 g_{12}^2} \sqrt{b_{12}^2 + g_{12}^2} \Bigg)
\end{aligned}$$

`soln2x1 = x1 /. solnset[2]`

$$\frac{-b12 g11 + b11 g12 - \sqrt{g11^2 + g11 g12 - 2 g12^2} \sqrt{b12^2 + g12^2}}{-2 b11 b12 g11 - b12^2 g11 + b11^2 g12 + 2 b12^2 g12 - g11^2 g12 - g11 g12^2 + 2 g12^3}$$

soln2b2 = Together[b2 /. solnset[[2]]]

$$\begin{aligned} & - \left( (2 b11 b12 g11 + b12^2 g11 - b11^2 g12 - 2 b12^2 g12 + g11^2 g12 + g11 g12^2 - 2 g12^3)^2 \right. \\ & \quad \left( -2 b11^3 b12 g11^2 - 2 b11 b12^2 g11^2 + 4 b12^3 g11^2 + 2 b12 g11^4 - 2 b11^3 b12 g11 g12 - 2 b11 b12^2 g11 g12 + 4 b12^3 g11 g12 - 4 b11 g11^3 g12 + \right. \\ & \quad 2 b12 g11^3 g12 + 4 b11^2 b12 g12^2 + 4 b11 b12^2 g12^2 - 8 b12^3 g12^2 - 6 b11 g11^2 g12^2 + 6 b11 g11 g12^3 + 4 b12 g11 g12^3 + 4 b11 g12^4 - \\ & \quad 8 b12 g12^4 - 2 b11^2 g11 \sqrt{g11^2 + g11 g12 - 2 g12^2} \sqrt{b12^2 + g12^2} - 2 b11 b12 g11 \sqrt{g11^2 + g11 g12 - 2 g12^2} \sqrt{b12^2 + g12^2} - \\ & \quad 5 b12^2 g11 \sqrt{g11^2 + g11 g12 - 2 g12^2} \sqrt{b12^2 + g12^2} - 2 g11^3 \sqrt{g11^2 + g11 g12 - 2 g12^2} \sqrt{b12^2 + g12^2} - \\ & \quad b11^2 g12 \sqrt{g11^2 + g11 g12 - 2 g12^2} \sqrt{b12^2 + g12^2} + 8 b11 b12 g12 \sqrt{g11^2 + g11 g12 - 2 g12^2} \sqrt{b12^2 + g12^2} + \\ & \quad 2 b12^2 g12 \sqrt{g11^2 + g11 g12 - 2 g12^2} \sqrt{b12^2 + g12^2} - 3 g11^2 g12 \sqrt{g11^2 + g11 g12 - 2 g12^2} \sqrt{b12^2 + g12^2} + \\ & \quad \left. 3 g11 g12^2 \sqrt{g11^2 + g11 g12 - 2 g12^2} \sqrt{b12^2 + g12^2} + 2 g12^3 \sqrt{g11^2 + g11 g12 - 2 g12^2} \sqrt{b12^2 + g12^2} \right) \Big) / \\ & \quad \left( 8 b11^4 b12^2 g11^4 + 16 b11^3 b12^3 g11^4 + 12 b11^2 b12^4 g11^4 + 4 b11 b12^5 g11^4 + 41 b12^6 g11^4 + 36 b12^4 g11^5 + 8 b12^2 g11^6 + \right. \\ & \quad 16 b11^4 b12^2 g11^3 g12 - 4 b11^3 b12^3 g11^3 g12 - 30 b11^2 b12^4 g11^3 g12 - 100 b11 b12^5 g11^3 g12 + 37 b12^6 g11^3 g12 + \\ & \quad 16 b11^3 b12 g11^5 g12 + 24 b11^2 b12^2 g11^5 g12 - 60 b11 b12^3 g11^5 g12 + 74 b12^4 g11^5 g12 - 16 b11 b12 g11^7 g12 + 24 b12^2 g11^7 g12 - \\ & \quad 15 b11^4 b12^2 g11^2 g12^2 - 84 b11^3 b12^3 g11^2 g12^2 - 18 b11^2 b12^4 g11^2 g12^2 - 48 b11 b12^5 g11^2 g12^2 - 114 b12^6 g11^2 g12^2 + \\ & \quad 4 b11^4 g11^4 g12^2 + 48 b11^3 b12 g11^4 g12^2 + 66 b11^2 b12^2 g11^4 g12^2 - 148 b11 b12^3 g11^4 g12^2 - 51 b12^4 g11^4 g12^2 + \\ & \quad 24 b11^2 g11^6 g12^2 - 32 b11 b12 g11^6 g12^2 + 25 b12^2 g11^6 g12^2 + 4 g11^5 g12^2 - 23 b11^4 b12^2 g11 g12^3 + 8 b11^3 b12^3 g11 g12^3 + \\ & \quad 168 b11^2 b12^4 g11 g12^3 + 272 b11 b12^5 g11 g12^3 - 20 b12^6 g11 g12^3 + 8 b11^4 g11^3 g12^3 - 52 b11^3 b12 g11^3 g12^3 - \\ & \quad 90 b11^2 b12^2 g11^3 g12^3 + 16 b11 b12^3 g11^3 g12^3 - 89 b12^4 g11^3 g12^3 + 72 b11^2 g11^5 g12^3 - 12 b11 b12 g11^5 g12^3 - 5 b12^2 g11^5 g12^3 + \\ & \quad 16 g11^7 g12^3 + 14 b11^4 b12^2 g12^4 + 64 b11^3 b12^3 g12^4 - 168 b11^2 b12^4 g12^4 - 128 b11 b12^5 g12^4 + 56 b12^6 g12^4 - 3 b11^4 g11^2 g12^4 - \\ & \quad 148 b11^3 b12 g11^2 g12^4 - 96 b11^2 b12^2 g11^2 g12^4 + 288 b11 b12^3 g11^2 g12^4 - 14 b12^4 g11^2 g12^4 - 18 b11^2 g11^4 g12^4 - \\ & \quad 88 b11 b12 g11^4 g12^4 - 99 b12^2 g11^4 g12^4 + g11^6 g12^4 - 7 b11^4 g11 g12^5 + 72 b11^3 b12 g11 g12^5 + 240 b11^2 b12^2 g11 g12^5 + \\ & \quad 160 b11 b12^3 g11 g12^5 - 60 b12^4 g11 g12^5 - 156 b11^2 g11^3 g12^5 + 52 b11 b12 g11^3 g12^5 - 65 b12^2 g11^3 g12^5 - 53 g11^5 g12^5 - \\ & \quad 2 b11^4 g12^6 + 64 b11^3 b12 g12^6 - 144 b11^2 b12^2 g12^6 - 256 b11 b12^3 g12^6 + 104 b12^4 g12^6 - 18 b11^2 g11^2 g12^6 - 336 b11 b12 g11^2 g12^6 + \\ & \quad 122 b12^2 g11^2 g12^6 - 23 g11^4 g12^6 + 72 b11^2 g11 g12^7 - 112 b11 b12 g11 g12^7 - 60 b12^2 g11 g12^7 + 61 g11^3 g12^7 - 24 b11^2 g12^8 - \\ & \quad 128 b11 b12 g12^8 + 40 b12^2 g12^8 + 22 g11^2 g12^8 - 20 g11 g12^9 - 8 g12^{10} + 8 b11^4 b12 g11^3 \sqrt{g11^2 + g11 g12 - 2 g12^2} \sqrt{b12^2 + g12^2} + \\ & \quad 16 b11^3 b12^2 g11^3 \sqrt{g11^2 + g11 g12 - 2 g12^2} \sqrt{b12^2 + g12^2} + 12 b11^2 b12^3 g11^3 \sqrt{g11^2 + g11 g12 - 2 g12^2} \sqrt{b12^2 + g12^2} + \\ & \quad 4 b11 b12^4 g11^3 \sqrt{g11^2 + g11 g12 - 2 g12^2} \sqrt{b12^2 + g12^2} - 40 b12^5 g11^3 \sqrt{g11^2 + g11 g12 - 2 g12^2} \sqrt{b12^2 + g12^2} - \\ & \quad 36 b12^3 g11^5 \sqrt{g11^2 + g11 g12 - 2 g12^2} \sqrt{b12^2 + g12^2} - 8 b12 g11^7 \sqrt{g11^2 + g11 g12 - 2 g12^2} \sqrt{b12^2 + g12^2} + \\ & \quad 12 b11^4 b12 g11^2 g12 \sqrt{g11^2 + g11 g12 - 2 g12^2} \sqrt{b12^2 + g12^2} - 12 b11^3 b12^2 g11^2 g12 \sqrt{g11^2 + g11 g12 - 2 g12^2} \sqrt{b12^2 + g12^2} - \\ & \quad 36 b11^2 b12^3 g11^2 g12 \sqrt{g11^2 + g11 g12 - 2 g12^2} \sqrt{b12^2 + g12^2} + 60 b11 b12^4 g11^2 g12 \sqrt{g11^2 + g11 g12 - 2 g12^2} \sqrt{b12^2 + g12^2} - \\ & \quad 24 b12^5 g11^2 g12 \sqrt{g11^2 + g11 g12 - 2 g12^2} \sqrt{b12^2 + g12^2} + 16 b11^3 g11^4 g12 \sqrt{g11^2 + g11 g12 - 2 g12^2} \sqrt{b12^2 + g12^2} + \\ & \quad 24 b11^2 b12 g11^4 g12 \sqrt{g11^2 + g11 g12 - 2 g12^2} \sqrt{b12^2 + g12^2} + 84 b11 b12^2 g11^4 g12 \sqrt{g11^2 + g11 g12 - 2 g12^2} \sqrt{b12^2 + g12^2} - \\ & \quad 52 b12^3 g11^4 g12 \sqrt{g11^2 + g11 g12 - 2 g12^2} \sqrt{b12^2 + g12^2} + 16 b11 g11^6 g12 \sqrt{g11^2 + g11 g12 - 2 g12^2} \sqrt{b12^2 + g12^2} - \\ & \quad 20 b12 g11^6 g12 \sqrt{g11^2 + g11 g12 - 2 g12^2} \sqrt{b12^2 + g12^2} - 12 b11^4 b12 g11 g12^2 \sqrt{g11^2 + g11 g12 - 2 g12^2} \sqrt{b12^2 + g12^2} - \\ & \quad 60 b11^3 b12^2 g11 g12^2 \sqrt{g11^2 + g11 g12 - 2 g12^2} \sqrt{b12^2 + g12^2} - 72 b11^2 b12^3 g11 g12^2 \sqrt{g11^2 + g11 g12 - 2 g12^2} \sqrt{b12^2 + g12^2} + \\ & \quad 48 b11 b12^4 g11 g12^2 \sqrt{g11^2 + g11 g12 - 2 g12^2} \sqrt{b12^2 + g12^2} + 96 b12^5 g11 g12^2 \sqrt{g11^2 + g11 g12 - 2 g12^2} \sqrt{b12^2 + g12^2} + \\ & \quad 32 b11^3 g11^3 g12^2 \sqrt{g11^2 + g11 g12 - 2 g12^2} \sqrt{b12^2 + g12^2} - 60 b11^2 b12 g11^3 g12^2 \sqrt{g11^2 + g11 g12 - 2 g12^2} \sqrt{b12^2 + g12^2} + \\ & \quad 60 b11 b12^2 g11^3 g12^2 \sqrt{g11^2 + g11 g12 - 2 g12^2} \sqrt{b12^2 + g12^2} + 40 b12^3 g11^3 g12^2 \sqrt{g11^2 + g11 g12 - 2 g12^2} \sqrt{b12^2 + g12^2} - \\ & \quad 48 b11 g11^5 g12^2 \sqrt{g11^2 + g11 g12 - 2 g12^2} \sqrt{b12^2 + g12^2} - 8 b11^4 b12 g12^3 \sqrt{g11^2 + g11 g12 - 2 g12^2} \sqrt{b12^2 + g12^2} + \\ & \quad 56 b11^3 b12^2 g12^3 \sqrt{g11^2 + g11 g12 - 2 g12^2} \sqrt{b12^2 + g12^2} + 96 b11^2 b12^3 g12^3 \sqrt{g11^2 + g11 g12 - 2 g12^2} \sqrt{b12^2 + g12^2} - \\ & \quad 112 b11 b12^4 g12^3 \sqrt{g11^2 + g11 g12 - 2 g12^2} \sqrt{b12^2 + g12^2} - 32 b12^5 g12^3 \sqrt{g11^2 + g11 g12 - 2 g12^2} \sqrt{b12^2 + g12^2} - \\ & \quad 12 b11^3 g11^2 g12^3 \sqrt{g11^2 + g11 g12 - 2 g12^2} \sqrt{b12^2 + g12^2} - 180 b11^2 b12 g11^2 g12^3 \sqrt{g11^2 + g11 g12 - 2 g12^2} \sqrt{b12^2 + g12^2} - \\ & \quad 144 b11 b12^2 g11^2 g12^3 \sqrt{g11^2 + g11 g12 - 2 g12^2} \sqrt{b12^2 + g12^2} + 48 b12^3 g11^2 g12^3 \sqrt{g11^2 + g11 g12 - 2 g12^2} \sqrt{b12^2 + g12^2} - \\ & \quad 12 b11 g11^4 g12^3 \sqrt{g11^2 + g11 g12 - 2 g12^2} \sqrt{b12^2 + g12^2} + 4 b12 g11^4 g12^3 \sqrt{g11^2 + g11 g12 - 2 g12^2} \sqrt{b12^2 + g12^2} - \\ & \quad 28 b11^3 g11 g12^4 \sqrt{g11^2 + g11 g12 - 2 g12^2} \sqrt{b12^2 + g12^2} + 120 b11^2 b12 g11 g12^4 \sqrt{g11^2 + g11 g12 - 2 g12^2} \sqrt{b12^2 + g12^2} + \\ & \quad 96 b11 b12^2 g11 g12^4 \sqrt{g11^2 + g11 g12 - 2 g12^2} \sqrt{b12^2 + g12^2} + 64 b12^3 g11 g12^4 \sqrt{g11^2 + g11 g12 - 2 g12^2} \sqrt{b12^2 + g12^2} - \\ & \quad 104 b11 g11^3 g12^4 \sqrt{g11^2 + g11 g12 - 2 g12^2} \sqrt{b12^2 + g12^2} + 16 b12 g11^3 g12^4 \sqrt{g11^2 + g11 g12 - 2 g12^2} \sqrt{b12^2 + g12^2} - \\ & \quad 8 b11^3 g12^5 \sqrt{g11^2 + g11 g12 - 2 g12^2} \sqrt{b12^2 + g12^2} + 96 b11^2 b12 g12^5 \sqrt{g11^2 + g11 g12 - 2 g12^2} \sqrt{b12^2 + g12^2} - \\ & \quad 96 b11 b12^2 g12^5 \sqrt{g11^2 + g11 g12 - 2 g12^2} \sqrt{b12^2 + g12^2} - 64 b12^3 g12^5 \sqrt{g11^2 + g11 g12 - 2 g12^2} \sqrt{b12^2 + g12^2} - \\ & \quad 12 b11 g11^2 g12^5 \sqrt{g11^2 + g11 g12 - 2 g12^2} \sqrt{b12^2 + g12^2} + 72 b12 g11^2 g12^5 \sqrt{g11^2 + g11 g12 - 2 g12^2} \sqrt{b12^2 + g12^2} + \\ & \quad 48 b11 g11 g12^6 \sqrt{g11^2 + g11 g12 - 2 g12^2} \sqrt{b12^2 + g12^2} - 32 b12 g11 g12^6 \sqrt{g11^2 + g11 g12 - 2 g12^2} \sqrt{b12^2 + g12^2} + \\ & \quad \left. 16 b11 g12^7 \sqrt{g11^2 + g11 g12 - 2 g12^2} \sqrt{b12^2 + g12^2} - 32 b12 g12^7 \sqrt{g11^2 + g11 g12 - 2 g12^2} \sqrt{b12^2 + g12^2} \right) \end{aligned}$$

## **APPENDIX C**

### **PROGRAM CODE FOR VERIFYING EIGENMODE AND NETWORK ANALYSES**

This appendix contains a program code written in *Mathematica* software. The code verifies that both the eigenmode and network analyses give the same decoupling network solutions. Program codes in Appendices A and B need to be executed first before the program in this appendix can be run. From the output of this program, it is clear that both the eigenmode and network analyses give the same decoupling solution because a subtraction of the two different solutions gives a zero output.

```

(*) Comparison between x1 and b2 from network and *)
(*) modal analysis. *)
(*) RESULTS: Both methods give the same x1 and b2. *)
(*) See end of this file for the verification. *)

(*) aa: x1 soln1 network *)
(*) bb: x1 soln1 modal *)
(*) cc: b2 soln1 network *)
(*) dd: b2 soln1 modal *)
(*) ee: x1 soln2 network *)
(*) ff: x1 soln2 modal *)
(*) gg: b2 soln2 network *)
(*) hh: b2 soln2 modal *)

(*) comparing x1 of soln1 from netwk and modal *)
(*) aa -- network, bb -- modal *)

aa = 
$$\left( -b_{12} g_{11} + b_{11} g_{12} - \sqrt{g_{11}^2 + g_{11} g_{12} - 2 g_{12}^2} \sqrt{b_{12}^2 + g_{12}^2} \right) / \left( -2 b_{11} b_{12} g_{11} - b_{12}^2 g_{11} + b_{11}^2 g_{12} + 2 b_{12}^2 g_{12} - g_{11}^2 g_{12} - g_{11} g_{12}^2 + 2 g_{12}^3 \right);$$

bb = 
$$\left( -b_{12} g_{11} + b_{11} g_{12} - \sqrt{g_{11}^2 + g_{11} g_{12} - 2 g_{12}^2} \sqrt{b_{12}^2 + g_{12}^2} \right) / \left( -2 b_{11} b_{12} g_{11} - b_{12}^2 g_{11} + b_{11}^2 g_{12} + 2 b_{12}^2 g_{12} - g_{11}^2 g_{12} - g_{11} g_{12}^2 + 2 g_{12}^3 \right);$$


(*) comparing b2 of soln1 from netwk and modal *)
(*) cc -- network, dd -- modal *)

cc =
- 
$$\left( (2 b_{11} b_{12} g_{11} + b_{12}^2 g_{11} - b_{11}^2 g_{12} - 2 b_{12}^2 g_{12} + g_{11}^2 g_{12} + g_{11} g_{12}^2 - 2 g_{12}^3)^2 \right.$$


$$\left( -2 b_{11}^2 b_{12} g_{11}^2 - 2 b_{11} b_{12}^2 g_{11}^2 + 4 b_{12}^3 g_{11}^2 + 2 b_{12} g_{11}^4 - 2 b_{11}^2 b_{12} g_{11} g_{12} - 2 b_{11} b_{12}^2 g_{11} g_{12} + 4 b_{12}^3 g_{11} g_{12} - \right.$$


$$4 b_{11} g_{11}^3 g_{12} + 2 b_{12} g_{11}^3 g_{12} + 4 b_{11}^2 b_{12} g_{12}^2 + 4 b_{11} b_{12}^2 g_{12}^2 - 8 b_{12}^3 g_{12}^2 - 6 b_{11} g_{11}^2 g_{12}^2 + 6 b_{11} g_{11} g_{12}^3 + 4 b_{12} g_{11} g_{12}^3 +$$


$$4 b_{11} g_{12}^4 - 8 b_{12} g_{12}^4 + 2 b_{11}^2 g_{11} \sqrt{g_{11}^2 + g_{11} g_{12} - 2 g_{12}^2} \sqrt{b_{12}^2 + g_{12}^2} + 2 b_{11} b_{12} g_{11} \sqrt{g_{11}^2 + g_{11} g_{12} - 2 g_{12}^2} \sqrt{b_{12}^2 + g_{12}^2} +$$


$$5 b_{12}^2 g_{11} \sqrt{g_{11}^2 + g_{11} g_{12} - 2 g_{12}^2} \sqrt{b_{12}^2 + g_{12}^2} + 2 g_{11}^3 \sqrt{g_{11}^2 + g_{11} g_{12} - 2 g_{12}^2} \sqrt{b_{12}^2 + g_{12}^2} +$$


$$b_{11}^2 g_{12} \sqrt{g_{11}^2 + g_{11} g_{12} - 2 g_{12}^2} \sqrt{b_{12}^2 + g_{12}^2} - 8 b_{11} b_{12} g_{12} \sqrt{g_{11}^2 + g_{11} g_{12} - 2 g_{12}^2} \sqrt{b_{12}^2 + g_{12}^2} -$$


$$2 b_{12}^2 g_{12} \sqrt{g_{11}^2 + g_{11} g_{12} - 2 g_{12}^2} \sqrt{b_{12}^2 + g_{12}^2} + 3 g_{11}^2 g_{12} \sqrt{g_{11}^2 + g_{11} g_{12} - 2 g_{12}^2} \sqrt{b_{12}^2 + g_{12}^2} -$$


$$\left. \left. 3 g_{11} g_{12}^2 \sqrt{g_{11}^2 + g_{11} g_{12} - 2 g_{12}^2} \sqrt{b_{12}^2 + g_{12}^2} - 2 g_{12}^3 \sqrt{g_{11}^2 + g_{11} g_{12} - 2 g_{12}^2} \sqrt{b_{12}^2 + g_{12}^2} \right) \right) /$$


$$\left( 8 b_{11}^4 b_{12}^2 g_{11}^4 + 16 b_{11}^3 b_{12}^3 g_{11}^4 + 12 b_{11}^2 b_{12}^4 g_{11}^4 + 4 b_{11} b_{12}^5 g_{11}^4 + 41 b_{12}^6 g_{11}^4 + 36 b_{12}^4 g_{11}^6 + 8 b_{12}^2 g_{11}^8 + \right.$$


$$16 b_{11}^4 b_{12}^2 g_{11}^3 g_{12} - 4 b_{11}^3 b_{12}^3 g_{11}^3 g_{12} - 30 b_{11}^2 b_{12}^4 g_{11}^3 g_{12} - 100 b_{11} b_{12}^5 g_{11}^3 g_{12} + 37 b_{12}^6 g_{11}^3 g_{12} + 16 b_{11}^3 b_{12} g_{11}^5 g_{12} +$$


$$24 b_{11}^2 b_{12}^2 g_{11}^5 g_{12} - 60 b_{11} b_{12}^3 g_{11}^5 g_{12} + 74 b_{12}^4 g_{11}^5 g_{12} - 16 b_{11} b_{12} g_{11}^7 g_{12} + 24 b_{12}^2 g_{11}^7 g_{12} - 15 b_{11}^4 b_{12}^2 g_{11}^2 g_{12}^2 -$$


$$84 b_{11}^3 b_{12}^3 g_{11}^2 g_{12}^2 + 18 b_{11}^2 b_{12}^4 g_{11}^2 g_{12}^2 - 48 b_{11} b_{12}^5 g_{11}^2 g_{12}^2 - 114 b_{12}^6 g_{11}^2 g_{12}^2 + 4 b_{11}^4 g_{11}^4 g_{12}^2 + 48 b_{11}^3 b_{12} g_{11}^4 g_{12}^2 +$$


$$66 b_{11}^2 b_{12}^2 g_{11}^4 g_{12}^2 - 148 b_{11} b_{12}^3 g_{11}^4 g_{12}^2 - 51 b_{12}^4 g_{11}^4 g_{12}^2 + 24 b_{11}^2 g_{11}^6 g_{12}^2 - 32 b_{11} b_{12} g_{11}^6 g_{12}^2 + 25 b_{12}^2 g_{11}^6 g_{12}^2 +$$


$$4 g_{11}^6 g_{12}^2 - 23 b_{11}^4 b_{12}^2 g_{11} g_{12}^3 + 8 b_{11}^3 b_{12}^3 g_{11} g_{12}^3 + 168 b_{11}^2 b_{12}^4 g_{11} g_{12}^3 + 272 b_{11} b_{12}^5 g_{11} g_{12}^3 - 20 b_{12}^6 g_{11} g_{12}^3 +$$


$$8 b_{11}^4 g_{11}^3 g_{12}^3 - 52 b_{11}^3 b_{12} g_{11}^3 g_{12}^3 - 90 b_{11}^2 b_{12}^2 g_{11}^3 g_{12}^3 + 16 b_{11} b_{12}^3 g_{11}^3 g_{12}^3 - 89 b_{12}^4 g_{11}^3 g_{12}^3 + 72 b_{11}^2 g_{11}^5 g_{12}^3 -$$


$$12 b_{11} b_{12} g_{11}^5 g_{12}^3 + 5 b_{12}^2 g_{11}^5 g_{12}^3 + 16 g_{11}^7 g_{12}^3 + 14 b_{11}^4 b_{12}^2 g_{12}^4 + 64 b_{11}^3 b_{12}^3 g_{12}^4 - 168 b_{11}^2 b_{12}^4 g_{12}^4 - 128 b_{11} b_{12}^5 g_{12}^4 +$$


$$56 b_{12}^6 g_{12}^4 - 3 b_{11}^4 g_{11}^2 g_{12}^4 - 148 b_{11}^3 b_{12} g_{11}^2 g_{12}^4 - 96 b_{11}^2 b_{12}^2 g_{11}^2 g_{12}^4 + 288 b_{11} b_{12}^3 g_{11}^2 g_{12}^4 - 14 b_{12}^4 g_{11}^2 g_{12}^4 -$$


$$18 b_{11}^2 g_{11}^4 g_{12}^4 - 88 b_{11} b_{12} g_{11}^4 g_{12}^4 - 99 b_{12}^2 g_{11}^4 g_{12}^4 + g_{11}^6 g_{12}^4 - 7 b_{11}^4 g_{11} g_{12}^5 + 72 b_{11}^3 b_{12} g_{11} g_{12}^5 + 240 b_{11}^2 b_{12}^2 g_{11} g_{12}^5 +$$


$$160 b_{11} b_{12}^3 g_{11} g_{12}^5 - 60 b_{12}^4 g_{11} g_{12}^5 - 156 b_{11}^2 g_{11}^3 g_{12}^5 + 52 b_{11} b_{12} g_{11}^3 g_{12}^5 - 65 b_{12}^2 g_{11}^3 g_{12}^5 - 53 g_{11}^5 g_{12}^5 - 2 b_{11}^4 g_{12}^6 +$$


$$64 b_{11}^3 b_{12} g_{12}^6 - 144 b_{11}^2 b_{12}^2 g_{12}^6 - 256 b_{11} b_{12}^3 g_{12}^6 + 104 b_{12}^4 g_{12}^6 - 18 b_{11}^2 g_{11}^2 g_{12}^6 + 336 b_{11} b_{12} g_{11}^2 g_{12}^6 +$$


$$122 b_{12}^2 g_{11}^2 g_{12}^6 - 23 g_{11}^4 g_{12}^6 + 72 b_{11}^2 g_{11} g_{12}^7 - 112 b_{11} b_{12} g_{11} g_{12}^7 - 60 b_{12}^2 g_{11} g_{12}^7 + 61 g_{11}^3 g_{12}^7 + 24 b_{11}^2 g_{12}^8 -$$


$$128 b_{11} b_{12} g_{12}^8 + 40 b_{12}^2 g_{12}^8 + 22 g_{11}^2 g_{12}^8 - 20 g_{11} g_{12}^9 - 8 g_{12}^{10} - 8 b_{11}^4 b_{12} g_{11}^3 \sqrt{g_{11}^2 + g_{11} g_{12} - 2 g_{12}^2} \sqrt{b_{12}^2 + g_{12}^2} -$$


$$16 b_{11}^3 b_{12}^2 g_{11}^3 \sqrt{g_{11}^2 + g_{11} g_{12} - 2 g_{12}^2} \sqrt{b_{12}^2 + g_{12}^2} - 12 b_{11}^2 b_{12}^3 g_{11}^3 \sqrt{g_{11}^2 + g_{11} g_{12} - 2 g_{12}^2} \sqrt{b_{12}^2 + g_{12}^2} -$$


$$4 b_{11} b_{12}^4 g_{11}^3 \sqrt{g_{11}^2 + g_{11} g_{12} - 2 g_{12}^2} \sqrt{b_{12}^2 + g_{12}^2} + 40 b_{12}^5 g_{11}^3 \sqrt{g_{11}^2 + g_{11} g_{12} - 2 g_{12}^2} \sqrt{b_{12}^2 + g_{12}^2} +$$


$$36 b_{12}^3 g_{11}^5 \sqrt{g_{11}^2 + g_{11} g_{12} - 2 g_{12}^2} \sqrt{b_{12}^2 + g_{12}^2} + 8 b_{12} g_{11}^7 \sqrt{g_{11}^2 + g_{11} g_{12} - 2 g_{12}^2} \sqrt{b_{12}^2 + g_{12}^2} -$$


$$12 b_{11}^4 b_{12} g_{11}^2 g_{12} \sqrt{g_{11}^2 + g_{11} g_{12} - 2 g_{12}^2} \sqrt{b_{12}^2 + g_{12}^2} + 12 b_{11}^3 b_{12}^2 g_{11}^2 g_{12} \sqrt{g_{11}^2 + g_{11} g_{12} - 2 g_{12}^2} \sqrt{b_{12}^2 + g_{12}^2} +$$


$$36 b_{11}^2 b_{12}^3 g_{11}^2 g_{12} \sqrt{g_{11}^2 + g_{11} g_{12} - 2 g_{12}^2} \sqrt{b_{12}^2 + g_{12}^2} - 60 b_{11} b_{12}^4 g_{11}^2 g_{12} \sqrt{g_{11}^2 + g_{11} g_{12} - 2 g_{12}^2} \sqrt{b_{12}^2 + g_{12}^2} +$$


$$24 b_{12}^5 g_{11}^2 g_{12} \sqrt{g_{11}^2 + g_{11} g_{12} - 2 g_{12}^2} \sqrt{b_{12}^2 + g_{12}^2} - 16 b_{11}^3 g_{11}^4 g_{12} \sqrt{g_{11}^2 + g_{11} g_{12} - 2 g_{12}^2} \sqrt{b_{12}^2 + g_{12}^2} -$$


$$24 b_{11}^2 b_{12} g_{11}^4 g_{12} \sqrt{g_{11}^2 + g_{11} g_{12} - 2 g_{12}^2} \sqrt{b_{12}^2 + g_{12}^2} - 84 b_{11} b_{12}^2 g_{11}^4 g_{12} \sqrt{g_{11}^2 + g_{11} g_{12} - 2 g_{12}^2} \sqrt{b_{12}^2 + g_{12}^2} +$$


$$52 b_{12}^3 g_{11}^4 g_{12} \sqrt{g_{11}^2 + g_{11} g_{12} - 2 g_{12}^2} \sqrt{b_{12}^2 + g_{12}^2} - 16 b_{11} g_{11}^6 g_{12} \sqrt{g_{11}^2 + g_{11} g_{12} - 2 g_{12}^2} \sqrt{b_{12}^2 + g_{12}^2} +$$


$$20 b_{12} g_{11}^6 g_{12} \sqrt{g_{11}^2 + g_{11} g_{12} - 2 g_{12}^2} \sqrt{b_{12}^2 + g_{12}^2} + 12 b_{11}^4 b_{12} g_{11} g_{12}^2 \sqrt{g_{11}^2 + g_{11} g_{12} - 2 g_{12}^2} \sqrt{b_{12}^2 + g_{12}^2} +$$


$$60 b_{11}^3 b_{12}^2 g_{11} g_{12}^2 \sqrt{g_{11}^2 + g_{11} g_{12} - 2 g_{12}^2} \sqrt{b_{12}^2 + g_{12}^2} + 72 b_{11}^2 b_{12}^3 g_{11} g_{12}^2 \sqrt{g_{11}^2 + g_{11} g_{12} - 2 g_{12}^2} \sqrt{b_{12}^2 + g_{12}^2} -$$


$$48 b_{11} b_{12}^4 g_{11} g_{12}^2 \sqrt{g_{11}^2 + g_{11} g_{12} - 2 g_{12}^2} \sqrt{b_{12}^2 + g_{12}^2} - 96 b_{12}^5 g_{11} g_{12}^2 \sqrt{g_{11}^2 + g_{11} g_{12} - 2 g_{12}^2} \sqrt{b_{12}^2 + g_{12}^2} -$$


$$32 b_{11}^3 g_{11}^3 g_{12}^2 \sqrt{g_{11}^2 + g_{11} g_{12} - 2 g_{12}^2} \sqrt{b_{12}^2 + g_{12}^2} + 60 b_{11}^2 b_{12} g_{11}^3 g_{12}^2 \sqrt{g_{11}^2 + g_{11} g_{12} - 2 g_{12}^2} \sqrt{b_{12}^2 + g_{12}^2} -$$


$$60 b_{11} b_{12}^2 g_{11}^3 g_{12}^2 \sqrt{g_{11}^2 + g_{11} g_{12} - 2 g_{12}^2} \sqrt{b_{12}^2 + g_{12}^2} - 40 b_{12}^3 g_{11}^3 g_{12}^2 \sqrt{g_{11}^2 + g_{11} g_{12} - 2 g_{12}^2} \sqrt{b_{12}^2 + g_{12}^2} -$$


```





$$\begin{aligned}
& 2 b12^2 g11^7 g12^2 \sqrt{g11^2 + g11 g12 - 2 g12^2} \sqrt{b12^2 + g12^2} - b11^6 b12^2 g12^3 \sqrt{g11^2 + g11 g12 - 2 g12^2} \sqrt{b12^2 + g12^2} + \\
& 8 b11^5 b12^3 g12^3 \sqrt{g11^2 + g11 g12 - 2 g12^2} \sqrt{b12^2 + g12^2} - 2 b11^4 b12^4 g12^3 \sqrt{g11^2 + g11 g12 - 2 g12^2} \sqrt{b12^2 + g12^2} + \\
& 32 b11^3 b12^5 g12^3 \sqrt{g11^2 + g11 g12 - 2 g12^2} \sqrt{b12^2 + g12^2} + 4 b11^2 b12^6 g12^3 \sqrt{g11^2 + g11 g12 - 2 g12^2} \sqrt{b12^2 + g12^2} + \\
& 32 b11 b12^7 g12^3 \sqrt{g11^2 + g11 g12 - 2 g12^2} \sqrt{b12^2 + g12^2} + 8 b12^8 g12^3 \sqrt{g11^2 + g11 g12 - 2 g12^2} \sqrt{b12^2 + g12^2} + \\
& 8 b11^5 b12 g11^2 g12^3 \sqrt{g11^2 + g11 g12 - 2 g12^2} \sqrt{b12^2 + g12^2} + 11 b11^4 b12^2 g11^2 g12^3 \sqrt{g11^2 + g11 g12 - 2 g12^2} \sqrt{b12^2 + g12^2} + \\
& 56 b11^3 b12^3 g11^2 g12^3 \sqrt{g11^2 + g11 g12 - 2 g12^2} \sqrt{b12^2 + g12^2} + 135 b11^2 b12^4 g11^2 g12^3 \sqrt{g11^2 + g11 g12 - 2 g12^2} \sqrt{b12^2 + g12^2} + \\
& 96 b11 b12^5 g11^2 g12^3 \sqrt{g11^2 + g11 g12 - 2 g12^2} \sqrt{b12^2 + g12^2} + 36 b12^6 g11^2 g12^3 \sqrt{g11^2 + g11 g12 - 2 g12^2} \sqrt{b12^2 + g12^2} - \\
& 15 b11^2 b12^2 g11^4 g12^3 \sqrt{g11^2 + g11 g12 - 2 g12^2} \sqrt{b12^2 + g12^2} + 15 b12^4 g11^4 g12^3 \sqrt{g11^2 + g11 g12 - 2 g12^2} \sqrt{b12^2 + g12^2} - \\
& 8 b11 b12 g11^6 g12^3 \sqrt{g11^2 + g11 g12 - 2 g12^2} \sqrt{b12^2 + g12^2} - 11 b12^2 g11^6 g12^3 \sqrt{g11^2 + g11 g12 - 2 g12^2} \sqrt{b12^2 + g12^2} - \\
& 2 b11^6 g11 g12^4 \sqrt{g11^2 + g11 g12 - 2 g12^2} \sqrt{b12^2 + g12^2} + 2 b11^5 b12 g11 g12^4 \sqrt{g11^2 + g11 g12 - 2 g12^2} \sqrt{b12^2 + g12^2} - \\
& 46 b11^4 b12^2 g11 g12^4 \sqrt{g11^2 + g11 g12 - 2 g12^2} \sqrt{b12^2 + g12^2} - 48 b11^3 b12^3 g11 g12^4 \sqrt{g11^2 + g11 g12 - 2 g12^2} \sqrt{b12^2 + g12^2} - \\
& 180 b11^2 b12^4 g11 g12^4 \sqrt{g11^2 + g11 g12 - 2 g12^2} \sqrt{b12^2 + g12^2} - 168 b11 b12^5 g11 g12^4 \sqrt{g11^2 + g11 g12 - 2 g12^2} \sqrt{b12^2 + g12^2} - \\
& 80 b12^6 g11 g12^4 \sqrt{g11^2 + g11 g12 - 2 g12^2} \sqrt{b12^2 + g12^2} + 2 b11^4 g11^3 g12^4 \sqrt{g11^2 + g11 g12 - 2 g12^2} \sqrt{b12^2 + g12^2} + \\
& 4 b11^3 b12 g11^3 g12^4 \sqrt{g11^2 + g11 g12 - 2 g12^2} \sqrt{b12^2 + g12^2} + 42 b11^2 b12^2 g11^3 g12^4 \sqrt{g11^2 + g11 g12 - 2 g12^2} \sqrt{b12^2 + g12^2} + \\
& 110 b11 b12^3 g11^3 g12^4 \sqrt{g11^2 + g11 g12 - 2 g12^2} \sqrt{b12^2 + g12^2} + 46 b12^4 g11^3 g12^4 \sqrt{g11^2 + g11 g12 - 2 g12^2} \sqrt{b12^2 + g12^2} + \\
& 2 b11^2 g11^5 g12^4 \sqrt{g11^2 + g11 g12 - 2 g12^2} \sqrt{b12^2 + g12^2} - 22 b11 b12 g11^5 g12^4 \sqrt{g11^2 + g11 g12 - 2 g12^2} \sqrt{b12^2 + g12^2} - \\
& 4 b12^2 g11^5 g12^4 \sqrt{g11^2 + g11 g12 - 2 g12^2} \sqrt{b12^2 + g12^2} - 2 g11^7 g12^4 \sqrt{g11^2 + g11 g12 - 2 g12^2} \sqrt{b12^2 + g12^2} - \\
& b11^6 g12^5 \sqrt{g11^2 + g11 g12 - 2 g12^2} \sqrt{b12^2 + g12^2} + 8 b11^5 b12 g12^5 \sqrt{g11^2 + g11 g12 - 2 g12^2} \sqrt{b12^2 + g12^2} - \\
& 4 b11^4 b12^2 g12^5 \sqrt{g11^2 + g11 g12 - 2 g12^2} \sqrt{b12^2 + g12^2} + 64 b11^3 b12^3 g12^5 \sqrt{g11^2 + g11 g12 - 2 g12^2} \sqrt{b12^2 + g12^2} + \\
& 12 b11^2 b12^4 g12^5 \sqrt{g11^2 + g11 g12 - 2 g12^2} \sqrt{b12^2 + g12^2} + 96 b11 b12^5 g12^5 \sqrt{g11^2 + g11 g12 - 2 g12^2} \sqrt{b12^2 + g12^2} + \\
& 32 b12^6 g12^5 \sqrt{g11^2 + g11 g12 - 2 g12^2} \sqrt{b12^2 + g12^2} + 3 b11^4 g11^2 g12^5 \sqrt{g11^2 + g11 g12 - 2 g12^2} \sqrt{b12^2 + g12^2} - \\
& 12 b11^3 b12 g11^2 g12^5 \sqrt{g11^2 + g11 g12 - 2 g12^2} \sqrt{b12^2 + g12^2} + 51 b11^2 b12^2 g11^2 g12^5 \sqrt{g11^2 + g11 g12 - 2 g12^2} \sqrt{b12^2 + g12^2} - \\
& 24 b12^4 g11^2 g12^5 \sqrt{g11^2 + g11 g12 - 2 g12^2} \sqrt{b12^2 + g12^2} + 5 b11^2 g11^4 g12^5 \sqrt{g11^2 + g11 g12 - 2 g12^2} \sqrt{b12^2 + g12^2} + \\
& 20 b11 b12 g11^4 g12^5 \sqrt{g11^2 + g11 g12 - 2 g12^2} \sqrt{b12^2 + g12^2} + 45 b12^2 g11^4 g12^5 \sqrt{g11^2 + g11 g12 - 2 g12^2} \sqrt{b12^2 + g12^2} - \\
& 7 g11^6 g12^5 \sqrt{g11^2 + g11 g12 - 2 g12^2} \sqrt{b12^2 + g12^2} - 3 b11^4 g11 g12^6 \sqrt{g11^2 + g11 g12 - 2 g12^2} \sqrt{b12^2 + g12^2} - \\
& 24 b11^3 b12 g11 g12^6 \sqrt{g11^2 + g11 g12 - 2 g12^2} \sqrt{b12^2 + g12^2} - 84 b11^2 b12^2 g11 g12^6 \sqrt{g11^2 + g11 g12 - 2 g12^2} \sqrt{b12^2 + g12^2} - \\
& 168 b11 b12^3 g11 g12^6 \sqrt{g11^2 + g11 g12 - 2 g12^2} \sqrt{b12^2 + g12^2} - 72 b12^4 g11 g12^6 \sqrt{g11^2 + g11 g12 - 2 g12^2} \sqrt{b12^2 + g12^2} - \\
& 4 b11^2 g11^3 g12^6 \sqrt{g11^2 + g11 g12 - 2 g12^2} \sqrt{b12^2 + g12^2} + 66 b11 b12 g11^3 g12^6 \sqrt{g11^2 + g11 g12 - 2 g12^2} \sqrt{b12^2 + g12^2} + \\
& 24 b12^2 g11^3 g12^6 \sqrt{g11^2 + g11 g12 - 2 g12^2} \sqrt{b12^2 + g12^2} + 3 g11^5 g12^6 \sqrt{g11^2 + g11 g12 - 2 g12^2} \sqrt{b12^2 + g12^2} - \\
& 2 b11^4 g12^7 \sqrt{g11^2 + g11 g12 - 2 g12^2} \sqrt{b12^2 + g12^2} + 32 b11^3 b12 g12^7 \sqrt{g11^2 + g11 g12 - 2 g12^2} \sqrt{b12^2 + g12^2} + \\
& 12 b11^2 b12^2 g12^7 \sqrt{g11^2 + g11 g12 - 2 g12^2} \sqrt{b12^2 + g12^2} + 96 b11 b12^3 g12^7 \sqrt{g11^2 + g11 g12 - 2 g12^2} \sqrt{b12^2 + g12^2} + \\
& 48 b12^4 g12^7 \sqrt{g11^2 + g11 g12 - 2 g12^2} \sqrt{b12^2 + g12^2} - 11 b11^2 g11^2 g12^7 \sqrt{g11^2 + g11 g12 - 2 g12^2} \sqrt{b12^2 + g12^2} - \\
& 32 b11 b12 g11^2 g12^7 \sqrt{g11^2 + g11 g12 - 2 g12^2} \sqrt{b12^2 + g12^2} - 68 b12^2 g11^2 g12^7 \sqrt{g11^2 + g11 g12 - 2 g12^2} \sqrt{b12^2 + g12^2} + \\
& 25 g11^4 g12^7 \sqrt{g11^2 + g11 g12 - 2 g12^2} \sqrt{b12^2 + g12^2} + 4 b11^2 g11 g12^8 \sqrt{g11^2 + g11 g12 - 2 g12^2} \sqrt{b12^2 + g12^2} - \\
& 56 b11 b12 g11 g12^8 \sqrt{g11^2 + g11 g12 - 2 g12^2} \sqrt{b12^2 + g12^2} - 16 b12^2 g11 g12^8 \sqrt{g11^2 + g11 g12 - 2 g12^2} \sqrt{b12^2 + g12^2} - \\
& g11^3 g12^8 \sqrt{g11^2 + g11 g12 - 2 g12^2} \sqrt{b12^2 + g12^2} + 4 b11^2 g12^8 \sqrt{g11^2 + g11 g12 - 2 g12^2} \sqrt{b12^2 + g12^2} + \\
& 32 b11 b12 g12^8 \sqrt{g11^2 + g11 g12 - 2 g12^2} \sqrt{b12^2 + g12^2} + 32 b12^2 g12^8 \sqrt{g11^2 + g11 g12 - 2 g12^2} \sqrt{b12^2 + g12^2} - \\
& 30 g11^2 g12^9 \sqrt{g11^2 + g11 g12 - 2 g12^2} \sqrt{b12^2 + g12^2} + 4 g11 g12^{10} \sqrt{g11^2 + g11 g12 - 2 g12^2} \sqrt{b12^2 + g12^2} + \\
& 8 g12^{11} \sqrt{g11^2 + g11 g12 - 2 g12^2} \sqrt{b12^2 + g12^2} \Big) / \\
& \left( (g11 - g12) (g11 + 2 g12) \right. \\
& \quad \left( -2 b11^2 b12^2 g11 - 2 b11 b12^3 g11 - 5 b12^4 g11 - 2 b12^3 g11^3 - b11^2 b12^2 g12 + 8 b11 b12^3 g12 + 2 b12^4 g12 - 3 b12^2 g11^2 g12 - \right. \\
& \quad \left. 2 b11^2 g11 g12^2 - 2 b11 b12 g11 g12^2 - 2 b12^2 g11 g12^2 - 2 g11^3 g12^2 - b11^2 g12^3 + 8 b11 b12 g12^3 + 4 b12^2 g12^3 - 3 g11^2 g12^3 + \right. \\
& \quad \left. 3 g11 g12^4 + 2 g12^5 + 2 b11^2 b12 \sqrt{g11^2 + g11 g12 - 2 g12^2} \sqrt{b12^2 + g12^2} + 2 b11 b12^2 \sqrt{g11^2 + g11 g12 - 2 g12^2} \sqrt{b12^2 + g12^2} - \right. \\
& \quad \left. 4 b12^3 \sqrt{g11^2 + g11 g12 - 2 g12^2} \sqrt{b12^2 + g12^2} - 2 b12 g11^2 \sqrt{g11^2 + g11 g12 - 2 g12^2} \sqrt{b12^2 + g12^2} + \right. \\
& \quad \left. 4 b11 g11 g12 \sqrt{g11^2 + g11 g12 - 2 g12^2} \sqrt{b12^2 + g12^2} + 2 b11 g12^2 \sqrt{g11^2 + g11 g12 - 2 g12^2} \sqrt{b12^2 + g12^2} - \right. \\
& \quad \left. 4 b12 g12^2 \sqrt{g11^2 + g11 g12 - 2 g12^2} \sqrt{b12^2 + g12^2} \right) \Big)^2 \Big) ; \\
& \quad \left( \star \text{ comparing x1 of soln2 from netwk and modal } \star \right) \\
& \quad \left( \star \text{ ee -- network, ff -- modal } \star \right) \\
& \text{ ee} = \left( -b12 g11 + b11 g12 + \sqrt{g11^2 + g11 g12 - 2 g12^2} \sqrt{b12^2 + g12^2} \right) / \left( -2 b11 b12 g11 - b12^2 g11 + b11^2 g12 + 2 b12^2 g12 - g11^2 g12 - g11 g12^2 + 2 g12^3 \right) ; \\
& \text{ ff} = \left( -b12 g11 + b11 g12 + \sqrt{g11^2 + g11 g12 - 2 g12^2} \sqrt{b12^2 + g12^2} \right) / \left( -2 b11 b12 g11 - b12^2 g11 + b11^2 g12 + 2 b12^2 g12 - g11^2 g12 - g11 g12^2 + 2 g12^3 \right) ; \\
& \quad \left( \star \text{ comparing b2 of soln2 from netwk and modal } \star \right) \\
& \quad \left( \star \text{ gg -- network, hh -- modal } \star \right)
\end{aligned}$$

$$\begin{aligned}
& - \left( (2 b_{11} b_{12} g_{11} + b_{12}^2 g_{11} - b_{11}^2 g_{12} - 2 b_{12}^2 g_{12} + g_{11}^2 g_{12} + g_{11} g_{12}^2 - 2 g_{12}^3) \wedge 2 \right. \\
& \quad \left( -2 b_{11}^2 b_{12} g_{11}^2 - 2 b_{11} b_{12}^2 g_{11}^2 + 4 b_{12}^3 g_{11}^2 + 2 b_{12} g_{11}^4 - 2 b_{11}^2 b_{12} g_{11} g_{12} - 2 b_{11} b_{12}^2 g_{11} g_{12} + 4 b_{12}^3 g_{11} g_{12} - \right. \\
& \quad 4 b_{11} g_{11}^3 g_{12} + 2 b_{12} g_{11}^3 g_{12} + 4 b_{11}^2 b_{12} g_{12}^2 + 4 b_{11} b_{12}^2 g_{12}^2 - 8 b_{12}^3 g_{12}^2 - 6 b_{11} g_{11}^2 g_{12}^2 + 6 b_{11} g_{11} g_{12}^3 + 4 b_{12} g_{11} g_{12}^3 + \\
& \quad 4 b_{11} g_{12}^4 - 8 b_{12} g_{12}^4 - 2 b_{11}^2 g_{11} \sqrt{g_{11}^2 + g_{11} g_{12} - 2 g_{12}^2} \sqrt{b_{12}^2 + g_{12}^2} - 2 b_{11} b_{12} g_{11} \sqrt{g_{11}^2 + g_{11} g_{12} - 2 g_{12}^2} \sqrt{b_{12}^2 + g_{12}^2} - \\
& \quad 5 b_{12}^2 g_{11} \sqrt{g_{11}^2 + g_{11} g_{12} - 2 g_{12}^2} \sqrt{b_{12}^2 + g_{12}^2} - 2 g_{11}^3 \sqrt{g_{11}^2 + g_{11} g_{12} - 2 g_{12}^2} \sqrt{b_{12}^2 + g_{12}^2} - \\
& \quad b_{11}^2 g_{12} \sqrt{g_{11}^2 + g_{11} g_{12} - 2 g_{12}^2} \sqrt{b_{12}^2 + g_{12}^2} + 8 b_{11} b_{12} g_{12} \sqrt{g_{11}^2 + g_{11} g_{12} - 2 g_{12}^2} \sqrt{b_{12}^2 + g_{12}^2} + \\
& \quad 2 b_{12}^2 g_{12} \sqrt{g_{11}^2 + g_{11} g_{12} - 2 g_{12}^2} \sqrt{b_{12}^2 + g_{12}^2} - 3 g_{11}^2 g_{12} \sqrt{g_{11}^2 + g_{11} g_{12} - 2 g_{12}^2} \sqrt{b_{12}^2 + g_{12}^2} + \\
& \quad \left. \left. 3 g_{11} g_{12}^2 \sqrt{g_{11}^2 + g_{11} g_{12} - 2 g_{12}^2} \sqrt{b_{12}^2 + g_{12}^2} + 2 g_{12}^3 \sqrt{g_{11}^2 + g_{11} g_{12} - 2 g_{12}^2} \sqrt{b_{12}^2 + g_{12}^2} \right) \right) / \\
& \quad \left( 8 b_{11}^4 b_{12}^2 g_{11}^4 + 16 b_{11}^3 b_{12}^3 g_{11}^4 + 12 b_{11}^2 b_{12}^4 g_{11}^4 + 4 b_{11} b_{12}^5 g_{11}^4 + 41 b_{12}^6 g_{11}^4 + 36 b_{12}^4 g_{11}^6 + 8 b_{12}^2 g_{11}^8 + \right. \\
& \quad 16 b_{11}^4 b_{12}^2 g_{11}^3 g_{12} - 4 b_{11}^3 b_{12}^3 g_{11}^3 g_{12} - 30 b_{11}^2 b_{12}^4 g_{11}^3 g_{12} - 100 b_{11} b_{12}^5 g_{11}^3 g_{12} + 37 b_{12}^6 g_{11}^3 g_{12} + 16 b_{11}^3 b_{12} g_{11}^5 g_{12} + \\
& \quad 24 b_{11}^2 b_{12}^2 g_{11}^5 g_{12} - 60 b_{11} b_{12}^3 g_{11}^5 g_{12} - 74 b_{12}^4 g_{11}^5 g_{12} - 16 b_{11} b_{12} g_{11}^7 g_{12} + 24 b_{12}^2 g_{11}^7 g_{12} - 15 b_{11}^4 b_{12}^2 g_{11}^2 g_{12}^2 - \\
& \quad 84 b_{11}^3 b_{12}^3 g_{11}^2 g_{12}^2 + 18 b_{11}^2 b_{12}^4 g_{11}^2 g_{12}^2 - 48 b_{11} b_{12}^5 g_{11}^2 g_{12}^2 - 114 b_{12}^6 g_{11}^2 g_{12}^2 + 4 b_{11}^4 g_{11}^4 g_{12}^2 + 48 b_{11}^3 b_{12} g_{11}^4 g_{12}^2 + \\
& \quad 66 b_{11}^2 b_{12}^2 g_{11}^4 g_{12}^2 - 148 b_{11} b_{12}^3 g_{11}^4 g_{12}^2 - 51 b_{12}^4 g_{11}^4 g_{12}^2 + 24 b_{11}^2 g_{11}^6 g_{12}^2 - 32 b_{11} b_{12} g_{11}^6 g_{12}^2 + 25 b_{12}^2 g_{11}^6 g_{12}^2 + \\
& \quad 4 g_{11}^7 g_{12}^2 - 23 b_{11}^4 b_{12}^2 g_{11} g_{12}^3 + 8 b_{11}^3 b_{12}^3 g_{11} g_{12}^3 + 168 b_{11}^2 b_{12}^4 g_{11} g_{12}^3 + 272 b_{11} b_{12}^5 g_{11} g_{12}^3 - 20 b_{12}^6 g_{11} g_{12}^3 + \\
& \quad 8 b_{11}^4 g_{11}^3 g_{12}^3 - 52 b_{11}^3 b_{12} g_{11}^3 g_{12}^3 - 90 b_{11}^2 b_{12}^2 g_{11}^3 g_{12}^3 + 16 b_{11} b_{12}^3 g_{11}^3 g_{12}^3 - 89 b_{12}^4 g_{11}^3 g_{12}^3 + 72 b_{11}^2 g_{11}^5 g_{12}^3 - \\
& \quad 12 b_{11} b_{12} g_{11}^5 g_{12}^3 + 5 b_{12}^2 g_{11}^5 g_{12}^3 + 16 g_{11}^7 g_{12}^3 + 14 b_{11}^4 b_{12}^2 g_{12}^4 + 64 b_{11}^3 b_{12}^3 g_{12}^4 - 168 b_{11}^2 b_{12}^4 g_{12}^4 - 128 b_{11} b_{12}^5 g_{12}^4 + \\
& \quad 56 b_{12}^6 g_{12}^4 - 3 b_{11}^4 g_{11}^2 g_{12}^4 - 148 b_{11}^3 b_{12} g_{11}^2 g_{12}^4 - 96 b_{11}^2 b_{12}^2 g_{11}^2 g_{12}^4 + 288 b_{11} b_{12}^3 g_{11}^2 g_{12}^4 - 14 b_{12}^4 g_{11}^2 g_{12}^4 - \\
& \quad 18 b_{11}^2 g_{11}^4 g_{12}^4 - 88 b_{11} b_{12} g_{11}^4 g_{12}^4 - 99 b_{12}^2 g_{11}^4 g_{12}^4 + g_{11}^6 g_{12}^4 - 7 b_{11}^4 g_{11} g_{12}^5 + 72 b_{11}^3 b_{12} g_{11} g_{12}^5 + 240 b_{11}^2 b_{12}^2 g_{11} g_{12}^5 + \\
& \quad 160 b_{11} b_{12}^3 g_{11} g_{12}^5 - 60 b_{12}^4 g_{11} g_{12}^5 - 156 b_{11}^2 g_{11}^3 g_{12}^5 + 52 b_{11} b_{12} g_{11}^3 g_{12}^5 - 65 b_{12}^2 g_{11}^3 g_{12}^5 - 53 g_{11}^5 g_{12}^5 - 2 b_{11}^4 g_{12}^6 + \\
& \quad 64 b_{11}^3 b_{12} g_{12}^6 - 144 b_{11}^2 b_{12}^2 g_{12}^6 - 256 b_{11} b_{12}^3 g_{12}^6 + 104 b_{12}^4 g_{12}^6 - 18 b_{11}^2 g_{11}^2 g_{12}^6 + 336 b_{11} b_{12} g_{11}^2 g_{12}^6 + \\
& \quad 122 b_{12}^2 g_{11}^2 g_{12}^6 - 23 g_{11}^4 g_{12}^6 + 72 b_{11}^2 g_{11} g_{12}^7 - 112 b_{11} b_{12} g_{11} g_{12}^7 - 60 b_{12}^2 g_{11} g_{12}^7 + 61 g_{11}^3 g_{12}^7 + 24 b_{11}^2 g_{12}^8 - \\
& \quad 128 b_{11} b_{12} g_{12}^8 + 40 b_{12}^2 g_{12}^8 + 22 g_{11}^2 g_{12}^9 - 20 g_{11} g_{12}^9 - 8 g_{12}^{10} + 8 b_{11}^4 b_{12} g_{11}^3 \sqrt{g_{11}^2 + g_{11} g_{12} - 2 g_{12}^2} \sqrt{b_{12}^2 + g_{12}^2} + \\
& \quad 16 b_{11}^3 b_{12}^2 g_{11}^3 \sqrt{g_{11}^2 + g_{11} g_{12} - 2 g_{12}^2} \sqrt{b_{12}^2 + g_{12}^2} + 12 b_{11}^2 b_{12}^3 g_{11}^3 \sqrt{g_{11}^2 + g_{11} g_{12} - 2 g_{12}^2} \sqrt{b_{12}^2 + g_{12}^2} + \\
& \quad 4 b_{11} b_{12}^4 g_{11}^3 \sqrt{g_{11}^2 + g_{11} g_{12} - 2 g_{12}^2} \sqrt{b_{12}^2 + g_{12}^2} - 40 b_{12}^5 g_{11}^3 \sqrt{g_{11}^2 + g_{11} g_{12} - 2 g_{12}^2} \sqrt{b_{12}^2 + g_{12}^2} - \\
& \quad 36 b_{12}^3 g_{11}^5 \sqrt{g_{11}^2 + g_{11} g_{12} - 2 g_{12}^2} \sqrt{b_{12}^2 + g_{12}^2} - 8 b_{12} g_{11}^7 \sqrt{g_{11}^2 + g_{11} g_{12} - 2 g_{12}^2} \sqrt{b_{12}^2 + g_{12}^2} + \\
& \quad 12 b_{11}^4 b_{12} g_{11}^3 g_{12} \sqrt{g_{11}^2 + g_{11} g_{12} - 2 g_{12}^2} \sqrt{b_{12}^2 + g_{12}^2} - 12 b_{11}^3 b_{12}^2 g_{11}^2 g$$

$$\begin{aligned}
& 60 b_{11} b_{12}^6 g_{11}^2 g_{12}^2 + 8 b_{12}^9 g_{11}^2 g_{12}^2 - 14 b_{11}^4 b_{12}^3 g_{11}^4 g_{12}^2 + 52 b_{11}^3 b_{12}^4 g_{11}^4 g_{12}^2 + 6 b_{11}^2 b_{12}^5 g_{11}^4 g_{12}^2 - 40 b_{11} b_{12}^6 g_{11}^4 g_{12}^2 - \\
& 4 b_{12}^7 g_{11}^4 g_{12}^2 + 14 b_{11}^2 b_{12}^3 g_{11}^6 g_{12}^2 - 14 b_{11} b_{12}^4 g_{11}^6 g_{12}^2 - 6 b_{12}^5 g_{11}^6 g_{12}^2 - 2 b_{12}^3 g_{11}^8 g_{12}^2 + 2 b_{11}^6 b_{12}^3 g_{11} g_{12}^3 + \\
& 18 b_{11}^5 b_{12}^4 g_{11} g_{12}^3 + 28 b_{11}^4 b_{12}^5 g_{11} g_{12}^3 + 16 b_{11}^3 b_{12}^6 g_{11} g_{12}^3 + 24 b_{11}^2 b_{12}^7 g_{11} g_{12}^3 - 40 b_{11} b_{12}^8 g_{11} g_{12}^3 - 48 b_{12}^9 g_{11} g_{12}^3 - \\
& 4 b_{11}^5 b_{12}^2 g_{11}^3 g_{12}^3 - 38 b_{11}^4 b_{12}^3 g_{11}^3 g_{12}^3 - 40 b_{11}^3 b_{12}^4 g_{11}^3 g_{12}^3 - 154 b_{11}^2 b_{12}^5 g_{11}^3 g_{12}^3 + 56 b_{12}^6 g_{11}^3 g_{12}^3 + \\
& 24 b_{11}^3 b_{12}^2 g_{11}^5 g_{12}^3 + 78 b_{11}^2 b_{12}^3 g_{11}^5 g_{12}^3 + 18 b_{11} b_{12}^4 g_{11}^5 g_{12}^3 + 6 b_{12}^5 g_{11}^5 g_{12}^3 - 4 b_{11} b_{12}^2 g_{11}^7 g_{12}^3 - 10 b_{12}^3 g_{11}^7 g_{12}^3 - \\
& 4 b_{11}^6 b_{12}^3 g_{12}^4 - 4 b_{11}^5 b_{12}^4 g_{12}^4 - 8 b_{11}^4 b_{12}^5 g_{12}^4 - 16 b_{11}^3 b_{12}^6 g_{12}^4 + 16 b_{11}^2 b_{12}^7 g_{12}^4 - 16 b_{11} b_{12}^8 g_{12}^4 + 32 b_{12}^9 g_{12}^4 + \\
& 2 b_{11}^6 b_{12} g_{11}^2 g_{12}^4 + 12 b_{11}^5 b_{12}^3 g_{11}^2 g_{12}^4 - 12 b_{11}^4 b_{12}^4 g_{11}^2 g_{12}^4 + 12 b_{11}^3 b_{12}^5 g_{11}^2 g_{12}^4 + 240 b_{11} b_{12}^6 g_{11}^2 g_{12}^4 + \\
& 16 b_{12}^7 g_{11}^2 g_{12}^4 - 22 b_{11}^4 b_{12} g_{11}^4 g_{12}^4 + 16 b_{11}^3 b_{12}^2 g_{11}^4 g_{12}^4 - 30 b_{11}^2 b_{12}^3 g_{11}^4 g_{12}^4 - 88 b_{11} b_{12}^4 g_{11}^4 g_{12}^4 + 4 b_{12}^5 g_{11}^4 g_{12}^4 + \\
& 22 b_{11}^2 b_{12} g_{11}^6 g_{12}^4 + 8 b_{11} b_{12}^2 g_{11}^6 g_{12}^4 - 2 b_{12}^3 g_{11}^6 g_{12}^4 - 2 b_{12} g_{11}^8 g_{12}^4 + 2 b_{11}^6 b_{12} g_{11} g_{12}^5 + 12 b_{11}^5 b_{12}^2 g_{11} g_{12}^5 + \\
& 56 b_{11}^4 b_{12}^3 g_{11} g_{12}^5 + 16 b_{11}^3 b_{12}^4 g_{11} g_{12}^5 + 72 b_{11}^2 b_{12}^5 g_{11} g_{12}^5 - 128 b_{11} b_{12}^6 g_{11} g_{12}^5 - 192 b_{12}^7 g_{11} g_{12}^5 + 4 b_{11}^5 g_{11}^3 g_{12}^5 - \\
& 34 b_{11}^4 b_{12} g_{11}^3 g_{12}^5 - 36 b_{11}^3 b_{12}^2 g_{11}^3 g_{12}^5 - 242 b_{11}^2 b_{12}^3 g_{11}^3 g_{12}^5 - 28 b_{11} b_{12}^4 g_{11}^3 g_{12}^5 + 96 b_{12}^5 g_{11}^3 g_{12}^5 - 8 b_{11}^3 g_{11}^5 g_{12}^5 + \\
& 54 b_{11}^2 b_{12} g_{11}^5 g_{12}^5 + 12 b_{11} b_{12}^2 g_{11}^5 g_{12}^5 + 18 b_{12}^3 g_{11}^5 g_{12}^5 + 4 b_{11} g_{11}^7 g_{12}^5 - 6 b_{12} g_{11}^7 g_{12}^5 - 4 b_{11}^6 b_{12} g_{12}^6 - \\
& 8 b_{11}^5 b_{12}^2 g_{12}^6 - 16 b_{11}^4 b_{12}^3 g_{12}^6 - 48 b_{11}^3 b_{12}^4 g_{12}^6 + 48 b_{11}^2 b_{12}^5 g_{12}^6 - 64 b_{11} b_{12}^6 g_{12}^6 + 128 b_{12}^7 g_{12}^6 + 6 b_{11}^5 g_{11}^2 g_{12}^6 + \\
& 36 b_{11}^4 b_{12} g_{11}^2 g_{12}^6 + 60 b_{11}^3 b_{12}^2 g_{11}^2 g_{12}^6 + 60 b_{11}^2 b_{12}^3 g_{11}^2 g_{12}^6 + 360 b_{11} b_{12}^4 g_{11}^2 g_{12}^6 - 20 b_{11}^3 g_{11}^4 g_{12}^6 - \\
& 42 b_{11}^2 b_{12} g_{11}^4 g_{12}^6 - 112 b_{11} b_{12}^2 g_{11}^4 g_{12}^6 + 4 b_{12}^3 g_{11}^4 g_{12}^6 + 14 b_{11} g_{11}^6 g_{12}^6 + 2 b_{12} g_{11}^6 g_{12}^6 - 6 b_{11}^5 g_{11} g_{12}^7 + \\
& 28 b_{11}^4 b_{12} g_{11} g_{12}^7 - 16 b_{11}^3 b_{12}^2 g_{11} g_{12}^7 + 72 b_{11}^2 b_{12}^3 g_{11} g_{12}^7 - 144 b_{11} b_{12}^4 g_{11} g_{12}^7 - 288 b_{12}^5 g_{11} g_{12}^7 + 16 b_{11}^3 g_{11}^3 g_{12}^7 - \\
& 110 b_{11}^2 b_{12} g_{11}^3 g_{12}^7 - 16 b_{11} b_{12}^2 g_{11}^3 g_{12}^7 + 72 b_{12}^3 g_{11}^3 g_{12}^7 - 6 b_{11} g_{11}^5 g_{12}^7 + 10 b_{12} g_{11}^5 g_{12}^7 - 4 b_{11}^5 g_{12}^8 - 8 b_{11}^4 b_{12} g_{12}^8 - \\
& 48 b_{11}^3 b_{12}^2 g_{12}^8 + 48 b_{11}^2 b_{12}^3 g_{12}^8 - 96 b_{11} b_{12}^4 g_{12}^8 + 192 b_{12}^5 g_{12}^8 + 44 b_{11}^3 g_{11}^2 g_{12}^8 + 36 b_{11}^2 b_{12} g_{11}^2 g_{12}^8 + \\
& 240 b_{11} b_{12}^2 g_{11}^2 g_{12}^8 - 16 b_{12}^3 g_{11}^2 g_{12}^8 - 50 b_{11} g_{11}^4 g_{12}^8 - 16 b_{11}^3 g_{11} g_{12}^9 + 24 b_{11}^2 b_{12} g_{11} g_{12}^9 - 64 b_{11} b_{12}^2 g_{11} g_{12}^9 - \\
& 192 b_{12}^3 g_{11} g_{12}^9 + 2 b_{11} g_{11}^3 g_{12}^9 + 20 b_{12} g_{11}^3 g_{12}^9 - 16 b_{11}^3 g_{12}^{10} + 16 b_{11}^2 b_{12} g_{12}^{10} - 64 b_{11} b_{12}^2 g_{12}^{10} + 128 b_{12}^3 g_{12}^{10} + \\
& 60 b_{11} g_{11}^2 g_{12}^{10} - 8 b_{12} g_{11}^2 g_{12}^{10} - 8 b_{11} g_{11} g_{12}^{11} - 48 b_{12} g_{11} g_{12}^{11} - 16 b_{11} g_{12}^{12} + 32 b_{12} g_{12}^{12} + \\
& 8 b_{11}^4 b_{12}^4 g_{11}^3 \sqrt{g_{11}^2 + g_{11} g_{12} - 2 g_{12}^2} \sqrt{b_{12}^2 + g_{12}^2} + 16 b_{11}^3 b_{12}^5 g_{11}^3 \sqrt{g_{11}^2 + g_{11} g_{12} - 2 g_{12}^2} \sqrt{b_{12}^2 + g_{12}^2} + \\
& 30 b_{11}^2 b_{12}^6 g_{11}^3 \sqrt{g_{11}^2 + g_{11} g_{12} - 2 g_{12}^2} \sqrt{b_{12}^2 + g_{12}^2} + 22 b_{11} b_{12}^7 g_{11}^3 \sqrt{g_{11}^2 + g_{11} g_{12} - 2 g_{12}^2} \sqrt{b_{12}^2 + g_{12}^2} + \\
& 5 b_{12}^8 g_{11}^3 \sqrt{g_{11}^2 + g_{11} g_{12} - 2 g_{12}^2} \sqrt{b_{12}^2 + g_{12}^2} + 8 b_{11}^2 b_{12}^4 g_{11}^5 \sqrt{g_{11}^2 + g_{11} g_{12} - 2 g_{12}^2} \sqrt{b_{12}^2 + g_{12}^2} + \\
& 8 b_{11} b_{12}^5 g_{11}^5 \sqrt{g_{11}^2 + g_{11} g_{12} - 2 g_{12}^2} \sqrt{b_{12}^2 + g_{12}^2} + 2 b_{12}^6 g_{11}^5 \sqrt{g_{11}^2 + g_{11} g_{12} - 2 g_{12}^2} \sqrt{b_{12}^2 + g_{12}^2} - \\
& 8 b_{11}^5 b_{12}^3 g_{11}^2 g_{12} \sqrt{g_{11}^2 + g_{11} g_{12} - 2 g_{12}^2} \sqrt{b_{12}^2 + g_{12}^2} - 8 b_{11}^4 b_{12}^4 g_{11}^2 g_{12} \sqrt{g_{11}^2 + g_{11} g_{12} - 2 g_{12}^2} \sqrt{b_{12}^2 + g_{12}^2} - \\
& 68 b_{11}^3 b_{12}^5 g_{11}^2 g_{12} \sqrt{g_{11}^2 + g_{11} g_{12} - 2 g_{12}^2} \sqrt{b_{12}^2 + g_{12}^2} - 73 b_{11}^2 b_{12}^6 g_{11}^2 g_{12} \sqrt{g_{11}^2 + g_{11} g_{12} - 2 g_{12}^2} \sqrt{b_{12}^2 + g_{12}^2} + \\
& 64 b_{11} b_{12}^7 g_{11}^2 g_{12} \sqrt{g_{11}^2 + g_{11} g_{12} - 2 g_{12}^2} \sqrt{b_{12}^2 + g_{12}^2} - 22 b_{12}^8 g_{11}^2 g_{12} \sqrt{g_{11}^2 + g_{11} g_{12} - 2 g_{12}^2} \sqrt{b_{12}^2 + g_{12}^2} + \\
& 20 b_{11}^2 b_{12}^4 g_{11}^4 g_{12} \sqrt{g_{11}^2 + g_{11} g_{12} - 2 g_{12}^2} \sqrt{b_{12}^2 + g_{12}^2} + 20 b_{11} b_{12}^5 g_{11}^4 g_{12} \sqrt{g_{11}^2 + g_{11} g_{12} - 2 g_{12}^2} \sqrt{b_{12}^2 + g_{12}^2} + \\
& 5 b_{12}^6 g_{11}^4 g_{12} \sqrt{g_{11}^2 + g_{11} g_{12} - 2 g_{12}^2} \sqrt{b_{12}^2 + g_{12}^2} + 8 b_{11} b_{12}^3 g_{11}^6 g_{12} \sqrt{g_{11}^2 + g_{11} g_{12} - 2 g_{12}^2} \sqrt{b_{12}^2 + g_{12}^2} + \\
& 4 b_{12}^4 g_{11}^6 g_{12} \sqrt{g_{11}^2 + g_{11} g_{12} - 2 g_{12}^2} \sqrt{b_{12}^2 + g_{12}^2} + 2 b_{11}^6 b_{12}^2 g_{11} g_{12}^2 \sqrt{g_{11}^2 + g_{11} g_{12} - 2 g_{12}^2} \sqrt{b_{12}^2 + g_{12}^2} - \\
& 2 b_{11}^5 b_{12}^3 g_{11} g_{12}^2 \sqrt{g_{11}^2 + g_{11} g_{12} - 2 g_{12}^2} \sqrt{b_{12}^2 + g_{12}^2} + 43 b_{11}^4 b_{12}^4 g_{11} g_{12}^2 \sqrt{g_{11}^2 + g_{11} g_{12} - 2 g_{12}^2} \sqrt{b_{12}^2 + g_{12}^2} + \\
& 24 b_{11}^3 b_{12}^5 g_{11} g_{12}^2 \sqrt{g_{11}^2 + g_{11} g_{12} - 2 g_{12}^2} \sqrt{b_{12}^2 + g_{12}^2} + 92 b_{11}^2 b_{12}^6 g_{11} g_{12}^2 \sqrt{g_{11}^2 + g_{11} g_{12} - 2 g_{12}^2} \sqrt{b_{12}^2 + g_{12}^2} + \\
& 56 b_{11} b_{12}^7 g_{11} g_{12}^2 \sqrt{g_{11}^2 + g_{11} g_{12} - 2 g_{12}^2} \sqrt{b_{12}^2 + g_{12}^2} + 28 b_{12}^8 g_{11} g_{12}^2 \sqrt{g_{11}^2 + g_{11} g_{12} - 2 g_{12}^2} \sqrt{b_{12}^2 + g_{12}^2} + \\
& 6 b_{11}^4 b_{12}^2 g_{11}^3 g_{12}^2 \sqrt{g_{11}^2 + g_{11} g_{12} - 2 g_{12}^2} \sqrt{b_{12}^2 + g_{12}^2} + 12 b_{11}^3 b_{12}^3 g_{11}^3 g_{12}^2 \sqrt{g_{11}^2 + g_{11} g_{12} - 2 g_{12}^2} \sqrt{b_{12}^2 + g_{12}^2} - \\
& 16 b_{11}^2 b_{12}^4 g_{11}^3 g_{12}^2 \sqrt{g_{11}^2 + g_{11} g_{12} - 2 g_{12}^2} \sqrt{b_{12}^2 + g_{12}^2} - 22 b_{11} b_{12}^5 g_{11}^3 g_{12}^2 \sqrt{g_{11}^2 + g_{11} g_{12} - 2 g_{12}^2} \sqrt{b_{12}^2 + g_{12}^2} - \\
& 16 b_{12}^6 g_{11}^3 g_{12}^2 \sqrt{g_{11}^2 + g_{11} g_{12} - 2 g_{12}^2} \sqrt{b_{12}^2 + g_{12}^2} + 6 b_{11}^2 b_{12}^2 g_{11}^5 g_{12}^2 \sqrt{g_{11}^2 + g_{11} g_{12} - 2 g_{12}^2} \sqrt{b_{12}^2 + g_{12}^2} + \\
& 30 b_{11} b_{12}^3 g_{11}^5 g_{12}^2 \sqrt{g_{11}^2 + g_{11} g_{12} - 2 g_{12}^2} \sqrt{b_{12}^2 + g_{12}^2} + 9 b_{12}^4 g_{11}^5 g_{12}^2 \sqrt{g_{11}^2 + g_{11} g_{12} - 2 g_{12}^2} \sqrt{b_{12}^2 + g_{12}^2} + \\
& 2 b_{12}^2 g_{11}^7 g_{12}^2 \sqrt{g_{11}^2 + g_{11} g_{12} - 2 g_{12}^2} \sqrt{b_{12}^2 + g_{12}^2} + b_{11}^6 b_{12}^2 g_{12}^3 \sqrt{g_{11}^2 + g_{11} g_{12} - 2 g_{12}^2} \sqrt{b_{12}^2 + g_{12}^2} - \\
& 8 b_{11}^5 b_{12}^3 g_{12}^3 \sqrt{g_{11}^2 + g_{11} g_{12} - 2 g_{12}^2} \sqrt{b_{12}^2 + g_{12}^2} + 2 b_{11}^4 b_{12}^4 g_{12}^3 \sqrt{g_{11}^2 + g_{11} g_{12} - 2 g_{12}^2} \sqrt{b_{12}^2 + g_{12}^2} - \\
& 32 b_{11}^3 b_{12}^5 g_{12}^3 \sqrt{g_{11}^2 + g_{11} g_{12} - 2 g_{12}^2} \sqrt{b_{12}^2 + g_{12}^2} - 4 b_{11}^2 b_{12}^6 g_{12}^3 \sqrt{g_{11}^2 + g_{11} g_{12} - 2 g_{12}^2} \sqrt{b_{12}^2 + g_{12}^2} - \\
& 32 b_{11} b_{12}^7 g_{12}^3 \sqrt{g_{11}^2 + g_{11} g_{12} - 2 g_{12}^2} \sqrt{b_{12}^2 + g_{12}^2} - 8 b_{12}^8 g_{12}^3 \sqrt{g_{11}^2 + g_{11} g_{12} - 2 g_{12}^2} \sqrt{b_{12}^2 + g_{12}^2} - \\
& 8 b_{11}^5 b_{12} g_{11}^2 g_{12}^3 \sqrt{g_{11}^2 + g_{11} g_{12} - 2 g_{12}^2} \sqrt{b_{12}^2 + g_{12}^2} - 11 b_{11}^4 b_{12}^2 g_{11}^2 g_{12}^3 \sqrt{g_{11}^2 + g_{11} g_{12} - 2 g_{12}^2} \sqrt{b_{12}^2 + g_{12}^2} - \\
& 56 b_{11}^3 b_{12}^3 g_{11}^2 g_{12}^3 \sqrt{g_{11}^2 + g_{11} g_{12} - 2 g_{12}^2} \sqrt{b_{12}^2 + g_{12}^2} - 135 b_{11}^2 b_{12}^4 g_{11}^2 g_{12}^3 \sqrt{g_{11}^2 + g_{11} g_{12} - 2 g_{12}^2} \sqrt{b_{12}^2 + g_{12}^2} - \\
& 96 b_{11} b_{12}^5 g_{11}^2 g_{12}^3 \sqrt{g_{11}^2 + g_{11} g_{12} - 2 g_{12}^2} \sqrt{b_{12}^2 + g_{12}^2} - 36 b_{12}^6 g_{11}^2 g_{12}^3 \sqrt{g_{11}^2 + g_{11} g_{12} - 2 g_{12}^2} \sqrt{b_{12}^2 + g_{12}^2} + \\
& 15 b_{11}^2 b_{12}^2 g_{11}^4 g_{12}^3 \sqrt{g_{11}^2 + g_{11} g_{12} - 2 g_{12}^2} \sqrt{b_{12}^2 + g_{12}^2} - 15 b_{12}^4 g_{11}^4 g_{12}^3 \sqrt{g_{11}^2 + g_{11} g_{12} - 2 g_{12}^2} \sqrt{b_{12}^2 + g_{12}^2} + \\
& 8 b_{11} b_{12} g_{11}^6 g_{12}^3 \sqrt{g_{11}^2 + g_{11} g_{12} - 2 g_{12}^2} \sqrt{b_{12}^2 + g_{12}^2} + 11 b_{12}^2 g_{11}^6 g_{12}^3 \sqrt{g_{11}^2 + g_{11} g_{12} - 2 g_{12}^2} \sqrt{b_{12}^2 + g_{12}^2} + \\
& 2 b_{11}^6 g_{11} g_{12}^4 \sqrt{g_{11}^2 + g_{11} g_{12} - 2 g_{12}^2} \sqrt{b_{12}^2 + g_{12}^2} - 2 b_{11}^5 b_{12} g_{11} g_{12}^4 \sqrt{g_{11}^2 + g_{11} g_{12} - 2 g_{12}^2} \sqrt{b_{12}^2 + g_{12}^2} + \\
& 46 b_{11}^4 b_{12}^2 g_{11} g_{12}^4 \sqrt{g_{11}^2 + g_{11} g_{12} - 2 g_{12}^2} \sqrt{b_{12}^2 + g_{12}^2} + 48 b_{11}^3 b_{12}^3 g_{11} g_{12}^4 \sqrt{g_{11}^2 + g_{11} g_{12} - 2 g_{12}^2} \sqrt{b_{12}^2 + g_{12}^2} + \\
& 180 b_{11}^2 b_{12}^4 g_{11} g_{12}^4 \sqrt{g_{11}^2 + g_{11} g_{12} - 2 g_{12}^2} \sqrt{b_{12}^2 + g_{12}^2} + 168 b_{11} b_{12}^5 g_{11} g_{12}^4 \sqrt{g_{11}^2 + g_{11} g_{12} - 2 g_{12}^2} \sqrt{b_{12}^2 + g_{12}^2} + \\
& 80 b_{12}^6 g_{11} g_{12}^4 \sqrt{g_{11}^2 + g_{11} g_{12} - 2 g_{12}^2} \sqrt{b_{12}^2 + g_{12}^2} - 2 b_{11}^4 g_{11}^3 g_{12}^4 \sqrt{g_{11}^2 + g_{11} g_{12} - 2 g_{12}^2} \sqrt{b_{12}^2 + g_{12}^2} - \\
& 4 b_{11}^3 b_{12} g_{11}^3 g_{12}^4 \sqrt{g_{11}^2 + g_{11} g_{12} - 2 g_{12}^2} \sqrt{b_{12}^2 + g_{12}^2} - 42 b_{11}^2 b_{12}^2 g_{11}^3 g_{12}^4 \sqrt{g_{11}^2 + g_{11} g_{12} - 2 g_{12}^2} \sqrt{b_{12}^2 + g_{12}^2} - \\
& 110 b_{11} b_{12}^3 g_{11}^3 g_{12}^4 \sqrt{g_{11}^2 + g_{11} g_{12} - 2 g_{12}^2} \sqrt{b_{12}^2 + g_{12}^2} - 46 b_{12}^4 g_{11}^3 g_{12}^4 \sqrt{g_{11}^2 + g_{11} g_{12} - 2 g_{12}^2} \sqrt{b_{12}^2 + g_{12}^2} - \\
& 2 b_{11}^2 g_{11}^5 g_{12}^4 \sqrt{g_{11}^2 + g_{11} g_{12} - 2 g_{12}^2} \sqrt{b_{12}^2 + g_{12}^2} + 22 b_{11} b_{12} g_{11}^5 g_{12}^4 \sqrt{g_{11}^2 + g_{11} g_{12} - 2 g_{12}^2} \sqrt{b_{12}^2 + g_{12}^2} + \\
& 4 b_{12}^2 g_{11}^5 g_{12}^4 \sqrt{g_{11}^2 + g_{11} g_{12} - 2 g_{12}^2} \sqrt{b_{12}^2 + g_{12}^2} + 2 g_{11}^7 g_{12}^4 \sqrt{g_{11}^2 + g_{11} g_{12} - 2 g_{12}^2} \sqrt{b_{12}^2 + g_{12}^2} + \\
& b_{11}^6 g_{12}^5 \sqrt{g_{11}^2 + g_{11} g_{12} - 2 g_{12}^2} \sqrt{b_{12}^2 + g_{12}^2} - 8 b_{11}^5 b_{12} g_{12}^5 \sqrt{g_{11}^2 + g_{11} g_{12} - 2 g_{12}^2} \sqrt{b_{12}^2 + g_{12}^2} + \\
& 4 b_{11}^4 b_{12}^2 g_{12}^5 \sqrt{g_{11}^2 + g_{11} g_{12} - 2 g_{12}^2} \sqrt{b_{12}^2 + g_{12}^2} - 64 b_{11}^3 b_{12}^3 g_{12}^5 \sqrt{g_{11}^2 + g_{11} g_{12} - 2 g_{12}^2} \sqrt{b_{12}^2 + g_{12}^2} -
\end{aligned}$$



$$\begin{aligned}
& 12 b_{11}^2 b_{12}^4 g_{12}^5 \sqrt{g_{11}^2 + g_{11} g_{12} - 2 g_{12}^2} \sqrt{b_{12}^2 + g_{12}^2} - 96 b_{11} b_{12}^5 g_{12}^5 \sqrt{g_{11}^2 + g_{11} g_{12} - 2 g_{12}^2} \sqrt{b_{12}^2 + g_{12}^2} - \\
& 32 b_{12}^6 g_{12}^5 \sqrt{g_{11}^2 + g_{11} g_{12} - 2 g_{12}^2} \sqrt{b_{12}^2 + g_{12}^2} - 3 b_{11}^4 g_{11}^2 g_{12}^5 \sqrt{g_{11}^2 + g_{11} g_{12} - 2 g_{12}^2} \sqrt{b_{12}^2 + g_{12}^2} + \\
& 12 b_{11}^3 b_{12} g_{11}^2 g_{12}^5 \sqrt{g_{11}^2 + g_{11} g_{12} - 2 g_{12}^2} \sqrt{b_{12}^2 + g_{12}^2} - 51 b_{11}^2 b_{12}^2 g_{11}^2 g_{12}^5 \sqrt{g_{11}^2 + g_{11} g_{12} - 2 g_{12}^2} \sqrt{b_{12}^2 + g_{12}^2} + \\
& 24 b_{12}^4 g_{11}^2 g_{12}^5 \sqrt{g_{11}^2 + g_{11} g_{12} - 2 g_{12}^2} \sqrt{b_{12}^2 + g_{12}^2} - 5 b_{11}^2 g_{11}^4 g_{12}^5 \sqrt{g_{11}^2 + g_{11} g_{12} - 2 g_{12}^2} \sqrt{b_{12}^2 + g_{12}^2} - \\
& 20 b_{11} b_{12} g_{11}^4 g_{12}^5 \sqrt{g_{11}^2 + g_{11} g_{12} - 2 g_{12}^2} \sqrt{b_{12}^2 + g_{12}^2} - 45 b_{12}^2 g_{11}^4 g_{12}^5 \sqrt{g_{11}^2 + g_{11} g_{12} - 2 g_{12}^2} \sqrt{b_{12}^2 + g_{12}^2} + \\
& 7 g_{11}^6 g_{12}^5 \sqrt{g_{11}^2 + g_{11} g_{12} - 2 g_{12}^2} \sqrt{b_{12}^2 + g_{12}^2} + 3 b_{11}^4 g_{11} g_{12}^6 \sqrt{g_{11}^2 + g_{11} g_{12} - 2 g_{12}^2} \sqrt{b_{12}^2 + g_{12}^2} + \\
& 24 b_{11}^3 b_{12} g_{11} g_{12}^6 \sqrt{g_{11}^2 + g_{11} g_{12} - 2 g_{12}^2} \sqrt{b_{12}^2 + g_{12}^2} + 84 b_{11}^2 b_{12}^2 g_{11} g_{12}^6 \sqrt{g_{11}^2 + g_{11} g_{12} - 2 g_{12}^2} \sqrt{b_{12}^2 + g_{12}^2} + \\
& 168 b_{11} b_{12}^3 g_{11} g_{12}^6 \sqrt{g_{11}^2 + g_{11} g_{12} - 2 g_{12}^2} \sqrt{b_{12}^2 + g_{12}^2} + 72 b_{12}^4 g_{11} g_{12}^6 \sqrt{g_{11}^2 + g_{11} g_{12} - 2 g_{12}^2} \sqrt{b_{12}^2 + g_{12}^2} + \\
& 4 b_{11}^2 g_{11}^3 g_{12}^6 \sqrt{g_{11}^2 + g_{11} g_{12} - 2 g_{12}^2} \sqrt{b_{12}^2 + g_{12}^2} - 66 b_{11} b_{12} g_{11}^3 g_{12}^6 \sqrt{g_{11}^2 + g_{11} g_{12} - 2 g_{12}^2} \sqrt{b_{12}^2 + g_{12}^2} - \\
& 24 b_{12}^2 g_{11}^3 g_{12}^6 \sqrt{g_{11}^2 + g_{11} g_{12} - 2 g_{12}^2} \sqrt{b_{12}^2 + g_{12}^2} - 3 g_{11}^5 g_{12}^6 \sqrt{g_{11}^2 + g_{11} g_{12} - 2 g_{12}^2} \sqrt{b_{12}^2 + g_{12}^2} + \\
& 2 b_{11}^4 g_{12}^7 \sqrt{g_{11}^2 + g_{11} g_{12} - 2 g_{12}^2} \sqrt{b_{12}^2 + g_{12}^2} - 32 b_{11}^3 b_{12} g_{12}^7 \sqrt{g_{11}^2 + g_{11} g_{12} - 2 g_{12}^2} \sqrt{b_{12}^2 + g_{12}^2} - \\
& 12 b_{11}^2 b_{12}^2 g_{12}^7 \sqrt{g_{11}^2 + g_{11} g_{12} - 2 g_{12}^2} \sqrt{b_{12}^2 + g_{12}^2} - 96 b_{11} b_{12}^3 g_{12}^7 \sqrt{g_{11}^2 + g_{11} g_{12} - 2 g_{12}^2} \sqrt{b_{12}^2 + g_{12}^2} - \\
& 48 b_{12}^4 g_{12}^7 \sqrt{g_{11}^2 + g_{11} g_{12} - 2 g_{12}^2} \sqrt{b_{12}^2 + g_{12}^2} + 11 b_{11}^2 g_{11}^2 g_{12}^7 \sqrt{g_{11}^2 + g_{11} g_{12} - 2 g_{12}^2} \sqrt{b_{12}^2 + g_{12}^2} + \\
& 32 b_{11} b_{12} g_{11}^2 g_{12}^7 \sqrt{g_{11}^2 + g_{11} g_{12} - 2 g_{12}^2} \sqrt{b_{12}^2 + g_{12}^2} + 68 b_{12}^2 g_{11}^2 g_{12}^7 \sqrt{g_{11}^2 + g_{11} g_{12} - 2 g_{12}^2} \sqrt{b_{12}^2 + g_{12}^2} - \\
& 25 g_{11}^4 g_{12}^7 \sqrt{g_{11}^2 + g_{11} g_{12} - 2 g_{12}^2} \sqrt{b_{12}^2 + g_{12}^2} - 4 b_{11}^2 g_{11} g_{12}^8 \sqrt{g_{11}^2 + g_{11} g_{12} - 2 g_{12}^2} \sqrt{b_{12}^2 + g_{12}^2} + \\
& 56 b_{11} b_{12} g_{11} g_{12}^8 \sqrt{g_{11}^2 + g_{11} g_{12} - 2 g_{12}^2} \sqrt{b_{12}^2 + g_{12}^2} + 16 b_{12}^2 g_{11} g_{12}^8 \sqrt{g_{11}^2 + g_{11} g_{12} - 2 g_{12}^2} \sqrt{b_{12}^2 + g_{12}^2} + \\
& g_{11}^3 g_{12}^8 \sqrt{g_{11}^2 + g_{11} g_{12} - 2 g_{12}^2} \sqrt{b_{12}^2 + g_{12}^2} - 4 b_{11}^2 g_{12}^9 \sqrt{g_{11}^2 + g_{11} g_{12} - 2 g_{12}^2} \sqrt{b_{12}^2 + g_{12}^2} - \\
& 32 b_{11} b_{12} g_{12}^9 \sqrt{g_{11}^2 + g_{11} g_{12} - 2 g_{12}^2} \sqrt{b_{12}^2 + g_{12}^2} - 32 b_{12}^2 g_{12}^9 \sqrt{g_{11}^2 + g_{11} g_{12} - 2 g_{12}^2} \sqrt{b_{12}^2 + g_{12}^2} + \\
& 30 g_{11}^2 g_{12}^9 \sqrt{g_{11}^2 + g_{11} g_{12} - 2 g_{12}^2} \sqrt{b_{12}^2 + g_{12}^2} - 4 g_{11} g_{12}^{10} \sqrt{g_{11}^2 + g_{11} g_{12} - 2 g_{12}^2} \sqrt{b_{12}^2 + g_{12}^2} - \\
& 8 g_{12}^{11} \sqrt{g_{11}^2 + g_{11} g_{12} - 2 g_{12}^2} \sqrt{b_{12}^2 + g_{12}^2} \Big) / \\
& \left( (g_{11} - g_{12}) (g_{11} + 2 g_{12}) \right. \\
& \quad \left( 2 b_{11}^2 b_{12}^2 g_{11} + 2 b_{11} b_{12}^3 g_{11} + 5 b_{12}^4 g_{11} + 2 b_{12}^2 g_{11}^3 + b_{11}^2 b_{12}^2 g_{12} - 8 b_{11} b_{12}^3 g_{12} - 2 b_{12}^4 g_{12} + 3 b_{12}^2 g_{11}^2 g_{12} + \right. \\
& \quad 2 b_{11}^2 g_{11} g_{12}^2 + 2 b_{11} b_{12} g_{11} g_{12}^2 + 2 b_{12}^2 g_{11} g_{12}^2 + 2 g_{11}^3 g_{12}^3 + b_{11}^2 g_{12}^3 - 8 b_{11} b_{12} g_{12}^3 - 4 b_{12}^2 g_{12}^3 + 3 g_{11}^2 g_{12}^3 - \\
& \quad 3 g_{11} g_{12}^4 - 2 g_{12}^5 + 2 b_{11}^2 b_{12} \sqrt{g_{11}^2 + g_{11} g_{12} - 2 g_{12}^2} \sqrt{b_{12}^2 + g_{12}^2} + 2 b_{11} b_{12}^2 \sqrt{g_{11}^2 + g_{11} g_{12} - 2 g_{12}^2} \sqrt{b_{12}^2 + g_{12}^2} - \\
& \quad 4 b_{12}^3 \sqrt{g_{11}^2 + g_{11} g_{12} - 2 g_{12}^2} \sqrt{b_{12}^2 + g_{12}^2} - 2 b_{12} g_{11}^2 \sqrt{g_{11}^2 + g_{11} g_{12} - 2 g_{12}^2} \sqrt{b_{12}^2 + g_{12}^2} + \\
& \quad 4 b_{11} g_{11} g_{12} \sqrt{g_{11}^2 + g_{11} g_{12} - 2 g_{12}^2} \sqrt{b_{12}^2 + g_{12}^2} + 2 b_{11} g_{12}^2 \sqrt{g_{11}^2 + g_{11} g_{12} - 2 g_{12}^2} \sqrt{b_{12}^2 + g_{12}^2} - \\
& \quad \left. \left. 4 b_{12} g_{12}^2 \sqrt{g_{11}^2 + g_{11} g_{12} - 2 g_{12}^2} \sqrt{b_{12}^2 + g_{12}^2} \right) \wedge 2 \right);
\end{aligned}$$

```

(* aa: x1 soln1 network *)
(* bb: x1 soln1 modal *)
(* cc: b2 soln1 network *)
(* dd: b2 soln1 modal *)
(* ee: x1 soln2 network *)
(* ff: x1 soln2 modal *)
(* gg: b2 soln2 network *)
(* hh: b2 soln2 modal *)

Simplify[aa - bb]

0

Simplify[cc - dd]

0

Simplify[ee - ff]

0

Simplify[gg - hh]

0

```

## **APPENDIX D**

### **PROGRAM CODE FOR 3-ELEMENT ARRAY**

This appendix contains the program code written in *Mathematica* software. The code evaluates the eigenvalues and eigenvectors of a 3-element circular array with generalized admittance parameters.

```

(* program for a 3-element array *)
(* Last modified: 7 Oct 02 *)
(* Comments:- orthonormal eigenvectors obtained. *)

ymat =  $\begin{pmatrix} y_{11} & y_{12} & y_{12} \\ y_{12} & y_{11} & y_{12} \\ y_{12} & y_{12} & y_{11} \end{pmatrix}$ ;

Eigenvalues[ymat]

{y11 - y12, y11 - y12, y11 + 2 y12}

evecs = Simplify[Eigenvectors[ymat]]

{{-1, 0, 1}, {-1, 1, 0}, {1, 1, 1}}

Det[evecs] (* if det* 0, eigenvectors are linearly independent. *)

-3

<< LinearAlgebra`Orthogonalization`

Simplify[GramSchmidt[evecs]]

 $\left\{ \left\{ -\frac{1}{\sqrt{2}}, 0, \frac{1}{\sqrt{2}} \right\}, \left\{ -\frac{1}{\sqrt{6}}, \sqrt{\frac{2}{3}}, -\frac{1}{\sqrt{6}} \right\}, \left\{ \frac{1}{\sqrt{3}}, \frac{1}{\sqrt{3}}, \frac{1}{\sqrt{3}} \right\} \right\}$ 

```

## **APPENDIX E**

### **PROGRAM CODE FOR 4-ELEMENT ARRAY**

This appendix contains the program code written in *Mathematica* software. The code evaluates the eigenvalues and eigenvectors of a 4-element circular array with generalized admittance parameters.

```

(* program for a 4-element array *)
(* Last modified: 7 Oct 02 *)
(* Comments:- orthonormal eigenvectors obtained. *)

ymat = 
$$\begin{pmatrix} y_{11} & y_{12} & y_{13} & y_{12} \\ y_{12} & y_{11} & y_{12} & y_{13} \\ y_{13} & y_{12} & y_{11} & y_{12} \\ y_{12} & y_{13} & y_{12} & y_{11} \end{pmatrix};$$


Eigenvalues[ymat]

{y11 - y13, y11 - y13, y11 - 2 y12 + y13, y11 + 2 y12 + y13}

evecs = Simplify[Eigenvectors[ymat]]

{{0, -1, 0, 1}, {-1, 0, 1, 0}, {-1, 1, -1, 1}, {1, 1, 1, 1}}

Det[evecs] (* if det* 0, eigenvectors are linearly independent. *)

8

<< LinearAlgebra`Orthogonalization`

Simplify[GramSchmidt[evecs]]

{{0,  $-\frac{1}{\sqrt{2}}$ , 0,  $\frac{1}{\sqrt{2}}$ }, {- $\frac{1}{\sqrt{2}}$ , 0,  $\frac{1}{\sqrt{2}}$ , 0}, {- $\frac{1}{2}$ ,  $\frac{1}{2}$ , - $\frac{1}{2}$ ,  $\frac{1}{2}$ }, { $\frac{1}{2}$ ,  $\frac{1}{2}$ ,  $\frac{1}{2}$ ,  $\frac{1}{2}$ }}

```

## **APPENDIX F**

### **PROGRAM CODE FOR 5-ELEMENT ARRAY**

This appendix contains the program code written in *Mathematica* software. The code evaluates the eigenvalues and eigenvectors of a 5-element circular array with generalized admittance parameters.

```

(*) program for a 5-element array
(*) Last modified: 7 Oct 02
(*)
(*) Comments:- eigenvalues complicated.
              - eigenvectors expression complicated.
              - eigenvectors takes too long to compute. *)

```

$$\mathbf{ymat} = \begin{pmatrix} y_{11} & y_{12} & y_{13} & y_{13} & y_{12} \\ y_{12} & y_{11} & y_{12} & y_{13} & y_{13} \\ y_{13} & y_{12} & y_{11} & y_{12} & y_{13} \\ y_{13} & y_{13} & y_{12} & y_{11} & y_{12} \\ y_{12} & y_{13} & y_{13} & y_{12} & y_{11} \end{pmatrix};$$

Eigenvalues[ymat]

$$\left\{ \frac{1}{2} (2 y_{11} - y_{12} - \sqrt{5} (y_{12} - y_{13}) - y_{13}), \frac{1}{2} (2 y_{11} - y_{12} - \sqrt{5} (y_{12} - y_{13}) - y_{13}), \right. \\ \left. \frac{1}{2} (2 y_{11} - y_{12} + \sqrt{5} (y_{12} - y_{13}) - y_{13}), \frac{1}{2} (2 y_{11} - y_{12} + \sqrt{5} (y_{12} - y_{13}) - y_{13}), y_{11} + 2 y_{12} + 2 y_{13} \right\}$$

Simplify[Eigenvectors[ymat]]

$$\left\{ \left\{ \frac{1}{2} (-1 - \sqrt{5}), \frac{1}{2} (1 + \sqrt{5}), -1, 0, 1 \right\}, \left\{ -1, \frac{y_{12} + \sqrt{5} y_{12} - y_{13} + \sqrt{5} y_{13}}{2 y_{12} + 3 y_{13} - \sqrt{5} y_{13}}, \frac{(1 + \sqrt{5}) y_{12} + (-1 + \sqrt{5}) y_{13}}{-2 y_{12} + (-3 + \sqrt{5}) y_{13}}, 1, 0 \right\}, \right. \\ \left. \left\{ \frac{1}{2} (-1 + \sqrt{5}), \frac{1}{2} (1 - \sqrt{5}), -1, 0, 1 \right\}, \left\{ -1, \frac{y_{12} - \sqrt{5} y_{12} - (1 + \sqrt{5}) y_{13}}{2 y_{12} + (3 + \sqrt{5}) y_{13}}, \frac{(-1 + \sqrt{5}) y_{12} + (1 + \sqrt{5}) y_{13}}{2 y_{12} + (3 + \sqrt{5}) y_{13}}, 1, 0 \right\}, \{1, 1, 1, 1, 1\} \right\}$$

<< LinearAlgebra`Orthogonalization`

Simplify[GramSchmidt[Eigenvectors[ymat]]]

$$\left\{ \left\{ \frac{-1 - \sqrt{5}}{2 \sqrt{5 + \sqrt{5}}}, \frac{1 + \sqrt{5}}{2 \sqrt{5 + \sqrt{5}}}, -\frac{1}{\sqrt{5 + \sqrt{5}}}, 0, \frac{1}{\sqrt{5 + \sqrt{5}}} \right\}, \right.$$

$$\left\{ \left( \sqrt{\frac{1}{10} (5 + \sqrt{5})} (2 \sqrt{5} y_{12} + (-5 + 3 \sqrt{5}) y_{13}) \right) / \left( 2 ((5 + \sqrt{5}) y_{12} - (-5 + \sqrt{5}) y_{13}) \sqrt{\frac{(5 + \sqrt{5}) y_{12}^2 - 2 (-5 + \sqrt{5}) y_{12} y_{13} + 2 (5 - 2 \sqrt{5}) y_{13}^2}{(-2 y_{12} + (-3 + \sqrt{5}) y_{13})^2}} \right), \right. \\ \left( \sqrt{\frac{1}{10} (5 + \sqrt{5})} (2 \sqrt{5} y_{12} + (-5 + 3 \sqrt{5}) y_{13}) \right) / \left( 2 ((5 + \sqrt{5}) y_{12} - (-5 + \sqrt{5}) y_{13}) \sqrt{\frac{(5 + \sqrt{5}) y_{12}^2 - 2 (-5 + \sqrt{5}) y_{12} y_{13} + 2 (5 - 2 \sqrt{5}) y_{13}^2}{(-2 y_{12} + (-3 + \sqrt{5}) y_{13})^2}} \right), \\ \frac{(5 + 3 \sqrt{5}) y_{12} + 2 \sqrt{5} y_{13}}{10 (-2 y_{12} + (-3 + \sqrt{5}) y_{13}) \sqrt{\frac{(3 + \sqrt{5}) y_{12}^2 + 4 y_{12} y_{13} - (-3 + \sqrt{5}) y_{13}^2}{(-2 y_{12} + (-3 + \sqrt{5}) y_{13})^2}}}, \frac{\sqrt{\frac{1}{10} (5 + \sqrt{5})}}{\sqrt{\frac{(3 + \sqrt{5}) y_{12}^2 - 2 (-5 + \sqrt{5}) y_{12} y_{13} + 2 (5 - 2 \sqrt{5}) y_{13}^2}{(-2 y_{12} + (-3 + \sqrt{5}) y_{13})^2}}}, \\ \frac{(5 + 3 \sqrt{5}) y_{12} + 2 \sqrt{5} y_{13}}{10 (-2 y_{12} + (-3 + \sqrt{5}) y_{13}) \sqrt{\frac{(3 + \sqrt{5}) y_{12}^2 + 4 y_{12} y_{13} - (-3 + \sqrt{5}) y_{13}^2}{(-2 y_{12} + (-3 + \sqrt{5}) y_{13})^2}}}, \left\{ \frac{-1 + \sqrt{5}}{2 \sqrt{5 - \sqrt{5}}}, \frac{1 - \sqrt{5}}{2 \sqrt{5 - \sqrt{5}}}, -\frac{1}{\sqrt{5 - \sqrt{5}}}, 0, \frac{1}{\sqrt{5 - \sqrt{5}}} \right\}, \\ \left\{ \frac{\sqrt{2}}{-5 + \sqrt{5}}, \frac{\sqrt{2}}{-5 + \sqrt{5}}, \frac{\sqrt{2} ((-3 + \sqrt{5}) y_{12} - 2 y_{13})}{(-5 + \sqrt{5}) (2 y_{12} + (3 + \sqrt{5}) y_{13})}, \sqrt{\frac{2}{5}}, \frac{\sqrt{2} ((-3 + \sqrt{5}) y_{12} - 2 y_{13})}{(-5 + \sqrt{5}) (2 y_{12} + (3 + \sqrt{5}) y_{13})}, \left\{ \frac{1}{\sqrt{5}}, \frac{1}{\sqrt{5}}, \frac{1}{\sqrt{5}}, \frac{1}{\sqrt{5}}, \frac{1}{\sqrt{5}} \right\} \right\}$$

## **APPENDIX G**

### **PROGRAM CODE OF 6-ELEMENT ARRAY**

This appendix contains the program code written in *Mathematica* software. The code evaluates the eigenvalues and eigenvectors of a 6-element circular array with generalized admittance parameters.



```

(* program for a 6-element array *)
(* Last modified: 7 Oct 02 *)
(* Comments:- orthonormal eigenvectors obtained. *)

ymat = 
$$\begin{pmatrix} y_{11} & y_{12} & y_{13} & y_{14} & y_{13} & y_{12} \\ y_{12} & y_{11} & y_{12} & y_{13} & y_{14} & y_{13} \\ y_{13} & y_{12} & y_{11} & y_{12} & y_{13} & y_{14} \\ y_{14} & y_{13} & y_{12} & y_{11} & y_{12} & y_{13} \\ y_{13} & y_{14} & y_{13} & y_{12} & y_{11} & y_{12} \\ y_{12} & y_{13} & y_{14} & y_{13} & y_{12} & y_{11} \end{pmatrix};$$


Eigenvalues[ymat]

{y11+y12-y13-y14, y11+y12-y13-y14, y11-2 y12+2 y13-y14, y11-y12-y13-y14, y11-y12-y13+y14, y11+2 y12+2 y13+y14}

evecs = Simplify[Eigenvectors[ymat]]

{{1, 0, -1, -1, 0, 1}, {-1, -1, 0, 1, 1, 0}, {-1, 1, -1, 1, -1, 1}, {-1, 0, 1, -1, 0, 1}, {-1, 1, 0, -1, 1, 0}, {1, 1, 1, 1, 1, 1}}

Det[evecs] (* if det≠ 0, eigenvectors are linearly independent. *)

-72

<< LinearAlgebra`Orthogonalization`

Simplify[GramSchmidt[evecs]]


$$\left\{ \left\{ \frac{1}{2}, 0, -\frac{1}{2}, -\frac{1}{2}, 0, \frac{1}{2} \right\}, \left\{ -\frac{1}{2\sqrt{3}}, -\frac{1}{\sqrt{3}}, -\frac{1}{2\sqrt{3}}, \frac{1}{2\sqrt{3}}, \frac{1}{\sqrt{3}}, \frac{1}{2\sqrt{3}} \right\}, \left\{ -\frac{1}{\sqrt{6}}, \frac{1}{\sqrt{6}}, -\frac{1}{\sqrt{6}}, \frac{1}{\sqrt{6}}, -\frac{1}{\sqrt{6}}, \frac{1}{\sqrt{6}} \right\}, \right.$$


$$\left. \left\{ -\frac{1}{2}, 0, \frac{1}{2}, -\frac{1}{2}, 0, \frac{1}{2} \right\}, \left\{ -\frac{1}{2\sqrt{3}}, \frac{1}{\sqrt{3}}, -\frac{1}{2\sqrt{3}}, -\frac{1}{2\sqrt{3}}, \frac{1}{\sqrt{3}}, -\frac{1}{2\sqrt{3}} \right\}, \left\{ \frac{1}{\sqrt{6}}, \frac{1}{\sqrt{6}}, \frac{1}{\sqrt{6}}, \frac{1}{\sqrt{6}}, \frac{1}{\sqrt{6}}, \frac{1}{\sqrt{6}} \right\} \right\}$$


```

## **APPENDIX H**

### **PROGRAM CODE FOR INTERDIGITAL CAPACITORS**

This appendix contains the program code written in *Mathematica* software. The code uses the design equations in [30] to produce a set of curves for the design of interdigital capacitors.

```

(* program to compute equivalent capacitances of an interdigital capacitor *)
(* equations adapted from paper by she & chow *)
(* program plots graphs of capacitances for range of N and l *)

(* input parameters are: *)
(* - number of fingers, N *)
(* - length of overlap of fingers, l *)
(* - width of fingers or gap spacing, x *)

(* note: we let width of fingers = finger spacing = x *)

(* input parameters *)
er = 2.31; (* dielectric constant of substrate *)
h = 31; (* height of substrate, in mil *)
widfing = h/12.0; (* to maintain x/h = 1/12 *)
c0 = 3.0*10^8; (* speed of light *)
e0 = 8.85*10^-12; (* permittivity of air *)
d = 2*widfing; (* d=2x *)

(* lists to store range of N and l *)
numfinglist = {24, 30, 36, 42, 48, 54, 60, 66};
lenfinglist = Table[i, {i, 100, 500, 20}];

(* get the length of the N and l lists *)
numfingcount = Length[numfinglist];
lenfingcount = Length[lenfinglist];

(* arrays to store capacitance data and equivalent length of TL *)
cmlist = Array[x, {numfingcount, lenfingcount}];

cglist = Array[x, {numfingcount, lenfingcount}];
ctlist = Array[x, {numfingcount, lenfingcount}];
dllist = Array[x, {numfingcount, lenfingcount}];

General::spell1 : Possible spelling error: new symbol name "cglist" is similar to existing symbol "cmlist".
General::spell : Possible spelling error: new symbol name "ctlist" is similar to existing symbols {cglist, cmlist}.

(* arrays to store xy-coordinate pairs for plotting *)
xycm = Array[xy, lenfingcount];
xycg = Array[xy, lenfingcount];
xyct = Array[xy, lenfingcount];
xydl = Array[xy, lenfingcount];

General::spell1 : Possible spelling error: new symbol name "xycg" is similar to existing symbol "xycm".
General::spell : Possible spelling error: new symbol name "xyct" is similar to existing symbols {xycg, xycm}.

(* arrays to store plots and labels of cm, cg and ct for different N *)
cmplotlist = Array[y, numfingcount];
cgplotlist = Array[y, numfingcount];
ctplotlist = Array[y, numfingcount];
dlplotlist = Array[y, numfingcount];
cmlabels = Array[z, numfingcount];
cglabels = Array[z, numfingcount];
ctlables = Array[z, numfingcount];
dllabels = Array[z, numfingcount];

General::spell1 : Possible spelling error: new symbol name "cgplotlist" is similar to existing symbol "cmplotlist".
General::spell : Possible spelling error: new symbol name "ctplotlist" is similar to existing symbols {cgplotlist, cmplotlist}.
General::spell1 : Possible spelling error: new symbol name "cglabels" is similar to existing symbol "cmlabels".
General::spell : Possible spelling error: new symbol name "ctlables" is similar to existing symbols {cglabels, cmlabels}.

```

```

(* convert parameters in mils to meters *)
(* 1 mil = 0.000254 meter *)
milimeter = 0.000254;
lenfinglist = lenfinglist * milimeter;
widfing = widfing * milimeter;
h = h * milimeter;
d = d * milimeter;

(* use iterations to compute capacitances for range of N and l *)
index1 = 1;

While[ index1 ≤ numfingcount,

  (* width of interdigital capacitor *)
  numfing = numfinglist[[index1]];
  w = (2 * numfing - 1) * widfing;

  (* even and odd mode effective dielectric constant *)
  evenereff =  $\frac{\epsilon_r + 1}{2} + \frac{\epsilon_r - 1}{2} * \left(1 + 10 * \frac{h}{w}\right)^{-1/2}$ ;
  oddereff =  $\frac{\epsilon_r + 1}{2}$ ;

  (* characteristic impedance of microstripline *)
  If[  $\frac{w}{h} \leq 1$ ,
    zw =  $\frac{60}{\sqrt{\text{evenereff}}} * \text{Log}\left[\frac{8 * h}{w} + \frac{w}{4 * h}\right]$ ,
    zw =  $\frac{120 * \text{Pi}}{\sqrt{\text{evenereff}}} * \left(\frac{w}{h} + 1.393 + 0.667 * \text{Log}\left[\frac{w}{h} + 1.444\right]\right)^{-1}$  ];

  (* distributed capacitance of microstripline *)
  cw =  $\frac{\sqrt{\text{evenereff}}}{zw * c0}$ ;

  (* compute capacitance of one terminal strip to ground, ct *)
  ct = (cw * w) / 2; (* divide by 2 because there are 2 terminal strips *)

  (* even mode averaged distributed capacitance per finger *)
  ceven =  $\frac{cw}{\text{numfing}}$ ;

  (* odd mode averaged distributed capacitance per finger *)
  coddinf =  $\frac{2 * \text{Pi} * \text{oddereff} * \epsilon_0}{\text{Log}\left[\frac{8 * d}{\text{Pi} * \text{widfing}}\right]}$ ; (* for infinite number of fingers *)
  a =  $\frac{25.5 + 15.5 * \text{Log}[d / \text{widfing}]}{37.3 + 48.7 * \text{Log}[d / \text{widfing}] + 12.6 * (\text{Log}[d / \text{widfing}])^2}$ ; (* a positive number *)
  codd = coddinf *  $\left(1 - \frac{a}{\text{numfing}}\right)$ ;

  (* compute capacitance per meter of each finger to ground, c1, *)
  (* and mutual capacitance per meter between two fingers, c2 *)
  c1 = ceven;
  c2 =  $\frac{1}{2} * (codd - ceven)$ ;

  index2 = 1;

  While[ index2 ≤ lenfingcount,

    lenfing = lenfinglist[[index2]];

    (* compute equivalent capacitance to ground, cq, and mutual capacitance, cm *)

```

```

        cglist[[index1, index2]] =  $\frac{\text{numfing}}{2} * c1 * \text{lenfing};$ 
        cmlist[[index1, index2]] =  $\frac{\text{numfing}}{2} * c2 * \text{lenfing};$ 

        (* store capacitance of terminal strip to ground *)
        (* note: ct independent of length of fingers *)
        ctlist[[index1, index2]] = ct;

        (* compute equivalent length of TL required for the shunt capacitances, cg and ct *)
        (* dllist is in meters *)
        dllist[[index1, index2]] = (cglist[[index1, index2]] + ctlist[[index1, index2]]) / cw;

        index2 = index2 + 1;
    ];

    index1 = index1 + 1;
}

lenfinglist = lenfinglist / milimeter; (* convert back to mils *)

(* plot graphs of cm, cg, ct for different N and l *)
pF = 1 * 10^-12;
index1 = 1;

While[ index1 ≤ numfingcount,
    (* values in pico Farad *)
    cmlistcurr = cmlist[[index1]] / pF;
    cglistcurr = cglist[[index1]] / pF;
    ctlistcurr = ctlist[[index1]] / pF;

    (* values in mils *)
    dllistcurr = dllist[[index1]] / milimeter;

    (* arrange data in (x,y) pairs for plotting *)
    index2 = 1;
    While[ index2 ≤ lenfingcount,
        xycm[[index2]] = {lenfinglist[[index2]], cmlistcurr[[index2]]};
        xycg[[index2]] = {lenfinglist[[index2]], cglistcurr[[index2]]};
        xyct[[index2]] = {lenfinglist[[index2]], ctlistcurr[[index2]]};
        xydl[[index2]] = {lenfinglist[[index2]], dllistcurr[[index2]]};

        index2 = index2 + 1;
    ];

    cmplotlist[[index1]] = ListPlot[xycm, PlotJoined → True, DisplayFunction → Identity];
    cgplotlist[[index1]] = ListPlot[xycg, PlotJoined → True, DisplayFunction → Identity];
    ctplotlist[[index1]] = ListPlot[xyct, PlotJoined → True, DisplayFunction → Identity];
    dlplotlist[[index1]] = ListPlot[xydl, PlotJoined → True, DisplayFunction → Identity];

    (* text labels for N, with left alignment given by offset {-1.2,0} *)
    cmlabels[[index1]] = Graphics[Text["N = " <> ToString[numfinglist[[index1]]],
        Last[xycm], {-1.2, 0}]];
    cglabels[[index1]] = Graphics[Text["N = " <> ToString[numfinglist[[index1]]],
        Last[xycg], {-1.2, 0}]];
    ctlabels[[index1]] = Graphics[Text["N = " <> ToString[numfinglist[[index1]]],
        Last[xyct], {-1.2, 0}]];
    dllabels[[index1]] = Graphics[Text["N = " <> ToString[numfinglist[[index1]]],
        Last[xydl], {-1.2, 0}]];

    index1 = index1 + 1;
}

```

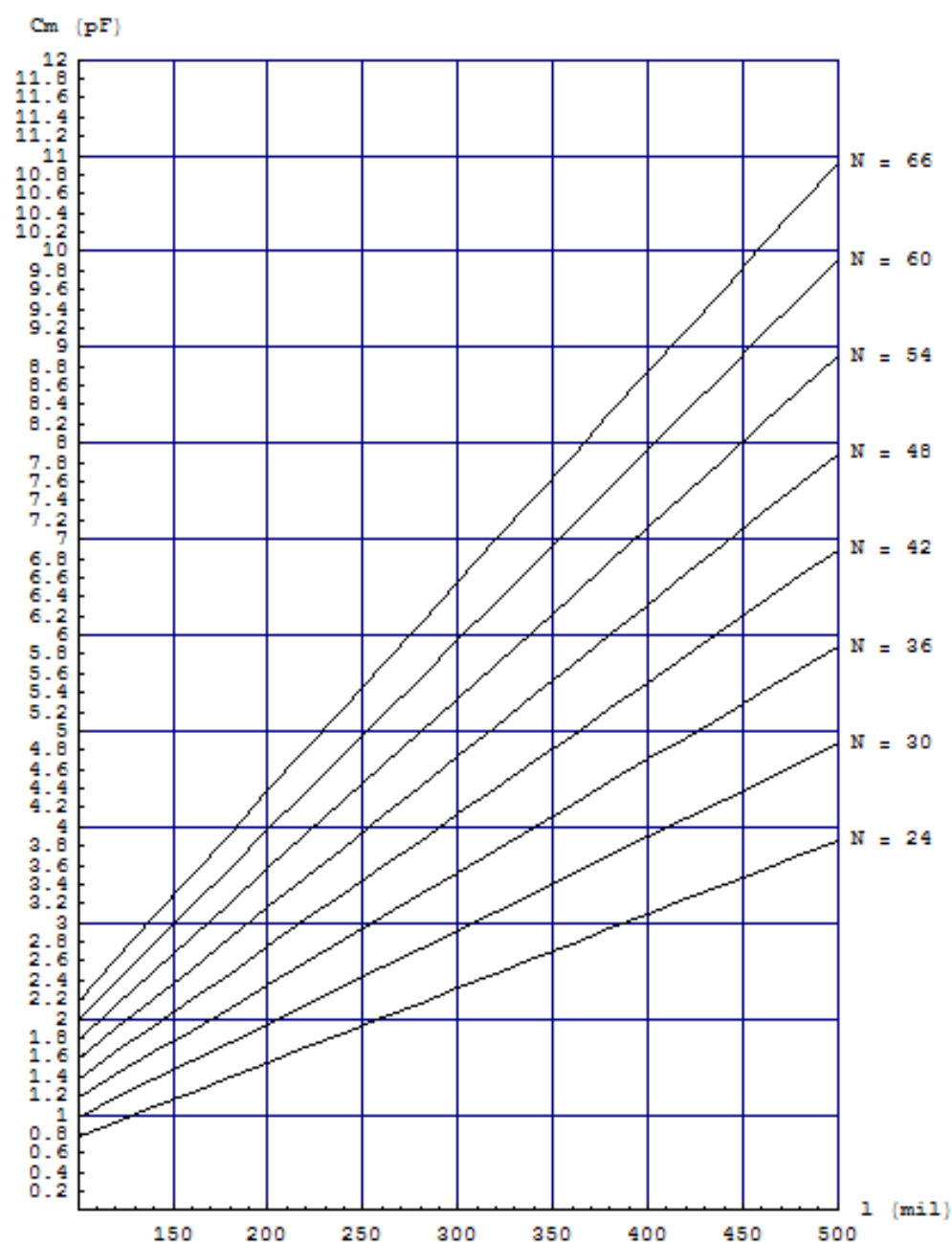
```

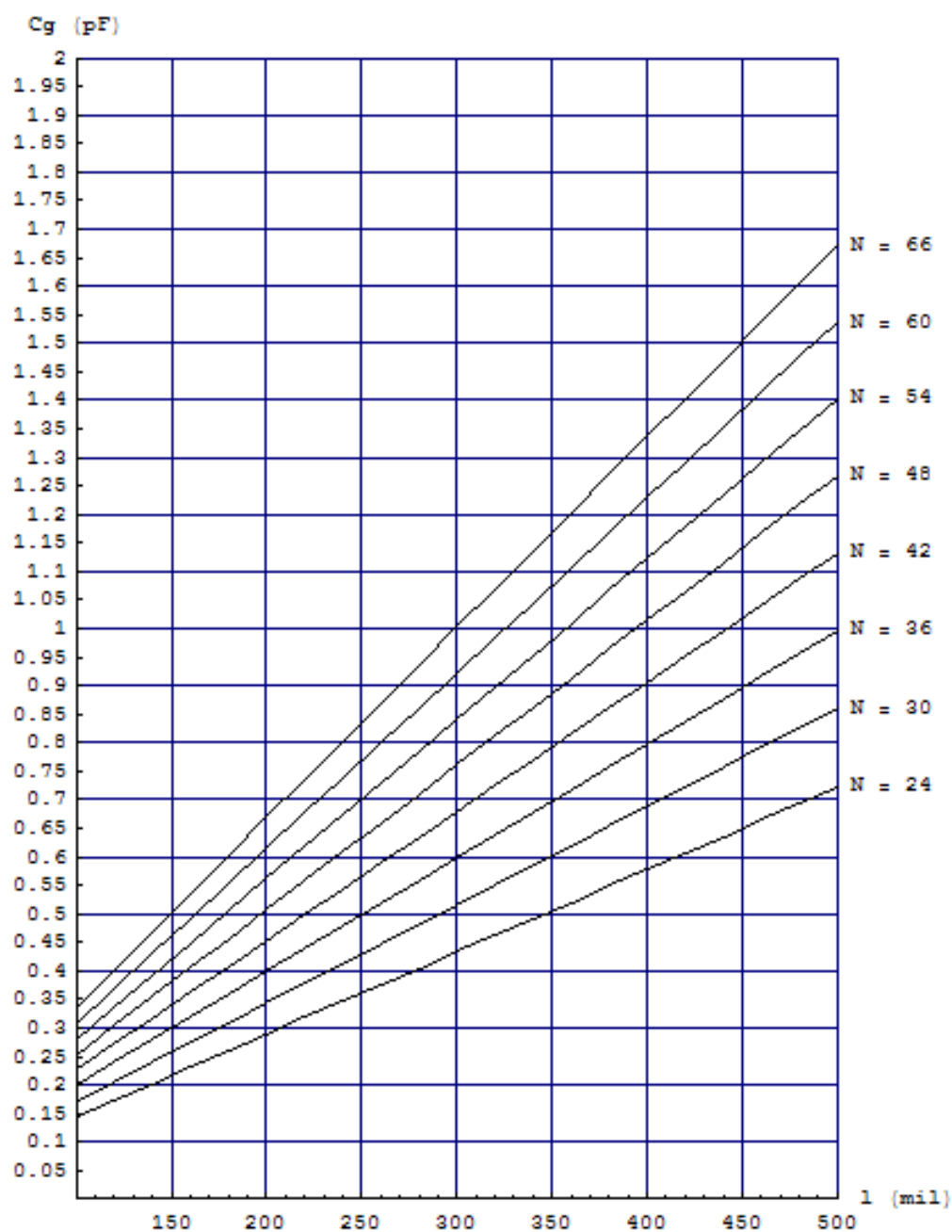
General::spell1 : Possible spelling error: new symbol name "cglistcurr" is similar to existing symbol "cmlistcurr".
General::spell : Possible spelling error: new symbol name "ctlstcurr" is similar to existing symbols {cglistcurr, cmlistcurr}.

(* display the plots *)
yticks1 = Table[j, {j, 0, 12, 0.2}];
ygridlines1 = Table[k, {k, 0, 12, 1}];
yticks2 = Table[j, {j, 0, 2, 0.05}];
ygridlines2 = Table[k, {k, 0, 2, 0.1}];
yticks3 = Table[j, {j, 0, 1.2, 0.02}];
yticks4 = Table[j, {j, 100, 500, 10}];

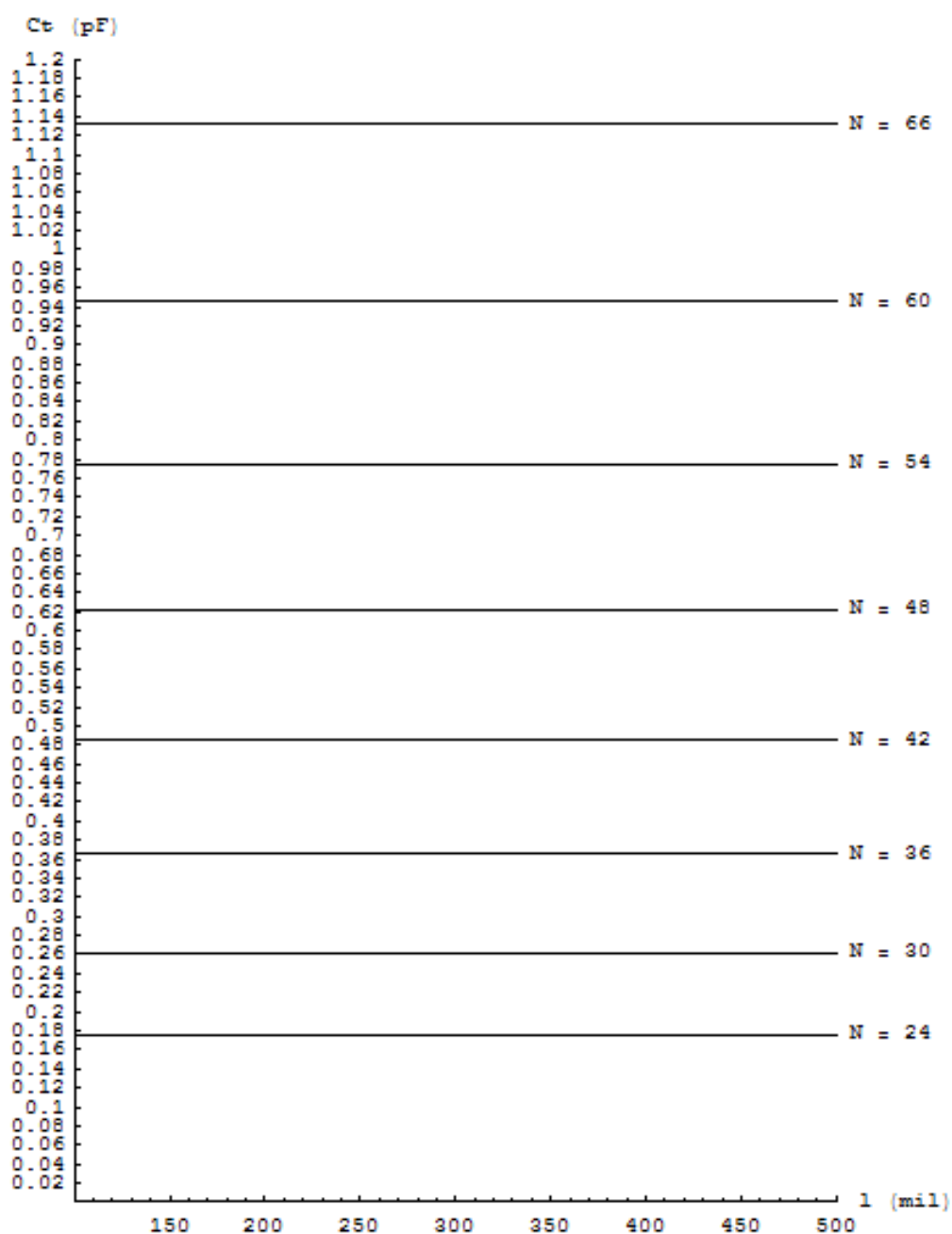
cmplot = Show[cmplotlist, cmlabels, AspectRatio -> 1.5, AxesLabel -> {"l (mil)", "Cm (pF)"}, AxesOrigin -> {100, 0},
  PlotRange -> {{100, 500}, {0, 12}}, Ticks -> {Automatic, yticks1}, GridLines -> {Automatic, ygridlines1},
  DisplayFunction -> $DisplayFunction];
cgplot = Show[cgplotlist, cglabels, AspectRatio -> 1.5, AxesLabel -> {"l (mil)", "Cg (pF)"}, AxesOrigin -> {100, 0},
  PlotRange -> {{100, 500}, {0, 2}}, Ticks -> {Automatic, yticks2}, GridLines -> {Automatic, ygridlines2},
  DisplayFunction -> $DisplayFunction];
ctplot = Show[ctplotlist, ctlabels, AspectRatio -> 1.5, AxesLabel -> {"l (mil)", "Ct (pF)"}, AxesOrigin -> {100, 0},
  PlotRange -> {{100, 500}, {0, 1.2}}, Ticks -> {Automatic, yticks3}, DisplayFunction -> $DisplayFunction];
dlplot = Show[dlplotlist, dllabels, AspectRatio -> 1.5, AxesLabel -> {"l (mil)", "dl (mil)"}, AxesOrigin -> {100, 100},
  PlotRange -> {{100, 500}, {100, 500}}, Ticks -> {Automatic, yticks4}, GridLines -> {Automatic, Automatic},
  DisplayFunction -> $DisplayFunction];

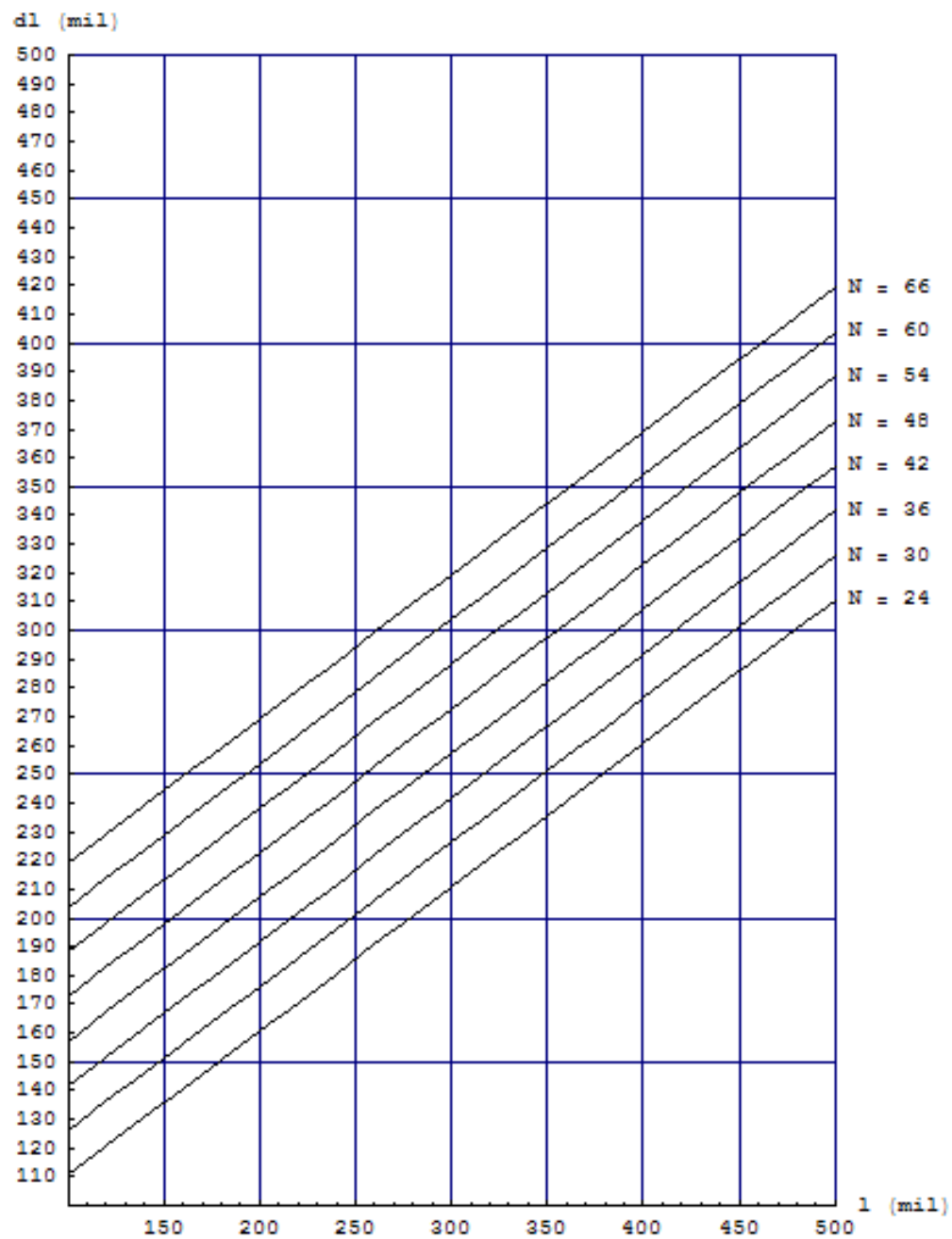
```











```
(* generate headings for tables *)
rowlabel = Table["(N=" <> ToString[numfinglist[[i]] <> ") ", {i, numfingcount}];
collabel = Table["(l=" <> ToString[lenfinglist[[i]] <> "mil) ", {i, lenfingcount}];
```

```
TableForm[cmlist / pF, TableHeadings -> {rowlabel, collabel}, TableSpacing -> {2, 1}, TableDirections -> Row]
```

	(N=24)	(N=30)	(N=36)	(N=42)	(N=48)	(N=54)	(N=60)	(N=66)
(l=100.mil)	0.772405	0.974061	1.17581	1.37762	1.57949	1.7814	1.98334	2.18531
(l=120.mil)	0.926886	1.16887	1.41097	1.65315	1.89539	2.13767	2.38	2.62237
(l=140.mil)	1.08137	1.36369	1.64613	1.92867	2.21128	2.49395	2.77667	3.05943
(l=160.mil)	1.23585	1.5585	1.88129	2.2042	2.52718	2.85023	3.17334	3.49649
(l=180.mil)	1.39033	1.75331	2.11645	2.47972	2.84308	3.20651	3.57001	3.93355
(l=200.mil)	1.54481	1.94812	2.35162	2.75524	3.15898	3.56279	3.96667	4.37062
(l=220.mil)	1.69929	2.14293	2.58678	3.03077	3.47487	3.91907	4.36334	4.80768
(l=240.mil)	1.85377	2.33775	2.82194	3.30629	3.79077	4.27535	4.76001	5.24474
(l=260.mil)	2.00825	2.53256	3.0571	3.58182	4.10667	4.63163	5.15668	5.6818
(l=280.mil)	2.16273	2.72737	3.29226	3.85734	4.42257	4.98791	5.55334	6.11886
(l=300.mil)	2.31721	2.92218	3.52742	4.13287	4.73846	5.34419	5.95001	6.55592
(l=320.mil)	2.4717	3.117	3.76259	4.40839	5.05436	5.70046	6.34668	6.99299
(l=340.mil)	2.62618	3.31181	3.99775	4.68391	5.37026	6.05674	6.74335	7.43005
(l=360.mil)	2.78066	3.50662	4.23291	4.95944	5.68616	6.41302	7.14001	7.86711
(l=380.mil)	2.93514	3.70143	4.46807	5.23496	6.00205	6.7693	7.53668	8.30417
(l=400.mil)	3.08962	3.89624	4.70323	5.51049	6.31795	7.12558	7.93335	8.74123
(l=420.mil)	3.2441	4.09106	4.93839	5.78601	6.63385	7.48186	8.33002	9.17829
(l=440.mil)	3.39858	4.28587	5.17356	6.06154	6.94975	7.83814	8.72668	9.61536
(l=460.mil)	3.55306	4.48068	5.40872	6.33706	7.26564	8.19442	9.12335	10.0524
(l=480.mil)	3.70754	4.67549	5.64388	6.61259	7.58154	8.5507	9.52002	10.4895
(l=500.mil)	3.86202	4.8703	5.87904	6.88811	7.89744	8.90698	9.91669	10.9265

```
TableForm[cglist / pF, TableHeadings -> {rowlabel, collabel}, TableSpacing -> {2, 1}, TableDirections -> Row]
```

	(N=24)	(N=30)	(N=36)	(N=42)	(N=48)	(N=54)	(N=60)	(N=66)
(l=100.mil)	0.144579	0.17205	0.19934	0.226496	0.253548	0.280517	0.307417	0.334259
(l=120.mil)	0.173495	0.206461	0.239208	0.271795	0.304258	0.336621	0.368901	0.40111
(l=140.mil)	0.202411	0.240871	0.279076	0.317094	0.354968	0.392724	0.430384	0.467962
(l=160.mil)	0.231326	0.275281	0.318944	0.362394	0.405677	0.448828	0.491868	0.534814
(l=180.mil)	0.260242	0.309691	0.358812	0.407693	0.456387	0.504931	0.553351	0.601666
(l=200.mil)	0.289158	0.344101	0.39868	0.452992	0.507097	0.561035	0.614834	0.668517
(l=220.mil)	0.318074	0.378511	0.438548	0.498291	0.557806	0.617138	0.676318	0.735369
(l=240.mil)	0.34699	0.412921	0.478416	0.543591	0.608516	0.673242	0.737801	0.802221
(l=260.mil)	0.375905	0.447331	0.518284	0.58889	0.659226	0.729345	0.799285	0.869073
(l=280.mil)	0.404821	0.481741	0.558152	0.634189	0.709935	0.785448	0.860768	0.935924
(l=300.mil)	0.433737	0.516151	0.59802	0.679488	0.760645	0.841552	0.922252	1.00278
(l=320.mil)	0.462653	0.550561	0.637888	0.724787	0.811355	0.897655	0.983735	1.06963
(l=340.mil)	0.491568	0.584972	0.677757	0.770087	0.862064	0.953759	1.04522	1.13648
(l=360.mil)	0.520484	0.619382	0.717625	0.815386	0.912774	1.00986	1.1067	1.20333
(l=380.mil)	0.5494	0.653792	0.757493	0.860685	0.963484	1.06597	1.16819	1.27018
(l=400.mil)	0.578316	0.688202	0.797361	0.905984	1.01419	1.12207	1.22967	1.33703
(l=420.mil)	0.607232	0.722612	0.837229	0.951283	1.0649	1.17817	1.29115	1.40389
(l=440.mil)	0.636147	0.757022	0.877097	0.996583	1.11561	1.23428	1.35264	1.47074
(l=460.mil)	0.665063	0.791432	0.916965	1.04188	1.16632	1.29038	1.41412	1.53759
(l=480.mil)	0.693979	0.825842	0.956833	1.08718	1.21703	1.34648	1.4756	1.60444
(l=500.mil)	0.722895	0.860252	0.996701	1.13248	1.26774	1.40259	1.53709	1.67129

```
TableForm[ctlist / pF, TableHeadings -> {rowlabel, collabel}, TableSpacing -> {2, 1}, TableDirections -> Row]
```

	(N=24)	(N=30)	(N=36)	(N=42)	(N=48)	(N=54)	(N=60)	(N=66)
(l=100.mil)	0.175543	0.262234	0.365623	0.485645	0.62225	0.775397	0.945052	1.13119
(l=120.mil)	0.175543	0.262234	0.365623	0.485645	0.62225	0.775397	0.945052	1.13119
(l=140.mil)	0.175543	0.262234	0.365623	0.485645	0.62225	0.775397	0.945052	1.13119
(l=160.mil)	0.175543	0.262234	0.365623	0.485645	0.62225	0.775397	0.945052	1.13119
(l=180.mil)	0.175543	0.262234	0.365623	0.485645	0.62225	0.775397	0.945052	1.13119
(l=200.mil)	0.175543	0.262234	0.365623	0.485645	0.62225	0.775397	0.945052	1.13119
(l=220.mil)	0.175543	0.262234	0.365623	0.485645	0.62225	0.775397	0.945052	1.13119
(l=240.mil)	0.175543	0.262234	0.365623	0.485645	0.62225	0.775397	0.945052	1.13119
(l=260.mil)	0.175543	0.262234	0.365623	0.485645	0.62225	0.775397	0.945052	1.13119
(l=280.mil)	0.175543	0.262234	0.365623	0.485645	0.62225	0.775397	0.945052	1.13119
(l=300.mil)	0.175543	0.262234	0.365623	0.485645	0.62225	0.775397	0.945052	1.13119
(l=320.mil)	0.175543	0.262234	0.365623	0.485645	0.62225	0.775397	0.945052	1.13119
(l=340.mil)	0.175543	0.262234	0.365623	0.485645	0.62225	0.775397	0.945052	1.13119
(l=360.mil)	0.175543	0.262234	0.365623	0.485645	0.62225	0.775397	0.945052	1.13119
(l=380.mil)	0.175543	0.262234	0.365623	0.485645	0.62225	0.775397	0.945052	1.13119
(l=400.mil)	0.175543	0.262234	0.365623	0.485645	0.62225	0.775397	0.945052	1.13119
(l=420.mil)	0.175543	0.262234	0.365623	0.485645	0.62225	0.775397	0.945052	1.13119
(l=440.mil)	0.175543	0.262234	0.365623	0.485645	0.62225	0.775397	0.945052	1.13119
(l=460.mil)	0.175543	0.262234	0.365623	0.485645	0.62225	0.775397	0.945052	1.13119
(l=480.mil)	0.175543	0.262234	0.365623	0.485645	0.62225	0.775397	0.945052	1.13119
(l=500.mil)	0.175543	0.262234	0.365623	0.485645	0.62225	0.775397	0.945052	1.13119

TableForm[dllist/milimeter, TableHeadings -> {rowlabel, collabel}, TableSpacing -> {2, 1}, TableDirections -> Row]

	(N=24)	(N=30)	(N=36)	(N=42)	(N=48)	(N=54)	(N=60)	(N=66)
(l=100.mil)	110.708	126.208	141.708	157.208	172.708	188.208	203.708	219.208
(l=120.mil)	120.708	136.208	151.708	167.208	182.708	198.208	213.708	229.208
(l=140.mil)	130.708	146.208	161.708	177.208	192.708	208.208	223.708	239.208
(l=160.mil)	140.708	156.208	171.708	187.208	202.708	218.208	233.708	249.208
(l=180.mil)	150.708	166.208	181.708	197.208	212.708	228.208	243.708	259.208
(l=200.mil)	160.708	176.208	191.708	207.208	222.708	238.208	253.708	269.208
(l=220.mil)	170.708	186.208	201.708	217.208	232.708	248.208	263.708	279.208
(l=240.mil)	180.708	196.208	211.708	227.208	242.708	258.208	273.708	289.208
(l=260.mil)	190.708	206.208	221.708	237.208	252.708	268.208	283.708	299.208
(l=280.mil)	200.708	216.208	231.708	247.208	262.708	278.208	293.708	309.208
(l=300.mil)	210.708	226.208	241.708	257.208	272.708	288.208	303.708	319.208
(l=320.mil)	220.708	236.208	251.708	267.208	282.708	298.208	313.708	329.208
(l=340.mil)	230.708	246.208	261.708	277.208	292.708	308.208	323.708	339.208
(l=360.mil)	240.708	256.208	271.708	287.208	302.708	318.208	333.708	349.208
(l=380.mil)	250.708	266.208	281.708	297.208	312.708	328.208	343.708	359.208
(l=400.mil)	260.708	276.208	291.708	307.208	322.708	338.208	353.708	369.208
(l=420.mil)	270.708	286.208	301.708	317.208	332.708	348.208	363.708	379.208
(l=440.mil)	280.708	296.208	311.708	327.208	342.708	358.208	373.708	389.208
(l=460.mil)	290.708	306.208	321.708	337.208	352.708	368.208	383.708	399.208
(l=480.mil)	300.708	316.208	331.708	347.208	362.708	378.208	393.708	409.208
(l=500.mil)	310.708	326.208	341.708	357.208	372.708	388.208	403.708	419.208

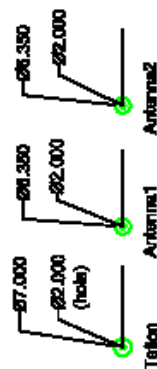
# **APPENDIX I**

## **CAD DRAWINGS OF THE ARRAY STRUCTURES**

This appendix contains the CAD drawings of the array structures manufactured for both microstrip (Part ID: PT-Hexaround) and stripline (Part ID: PT-Hexatuning) designs.

Part No: PT-HEXAROUND  
 Name: Chua Ping Tying  
 Mobile: 87363551  
 Email: g0202328@nus.edu.sg  
 Supervisor: Dr Jacob C. Costelloe

### Antenna and Teflon pieces

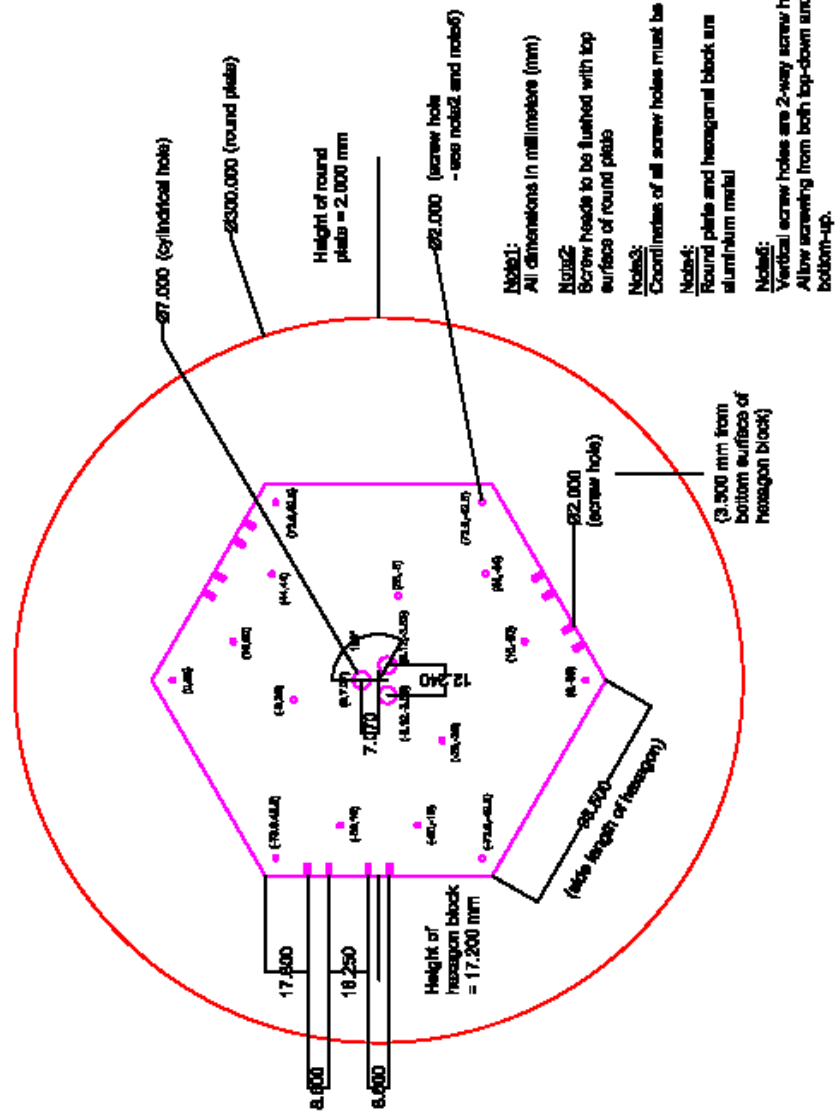


**Teflon (x 3 pcs):**  
 Height of teflon = 19.2 mm

**Antenna1 (x 3 pcs - copper rods):**  
 Height of thin section = 21 mm  
 Height of thick section = 30.5 mm

**Antenna2 (x 3 pcs - copper rods):**  
 Height of thin section = 20 mm  
 Height of thick section = 30.5 mm

### Round Plate and Hexagon Block



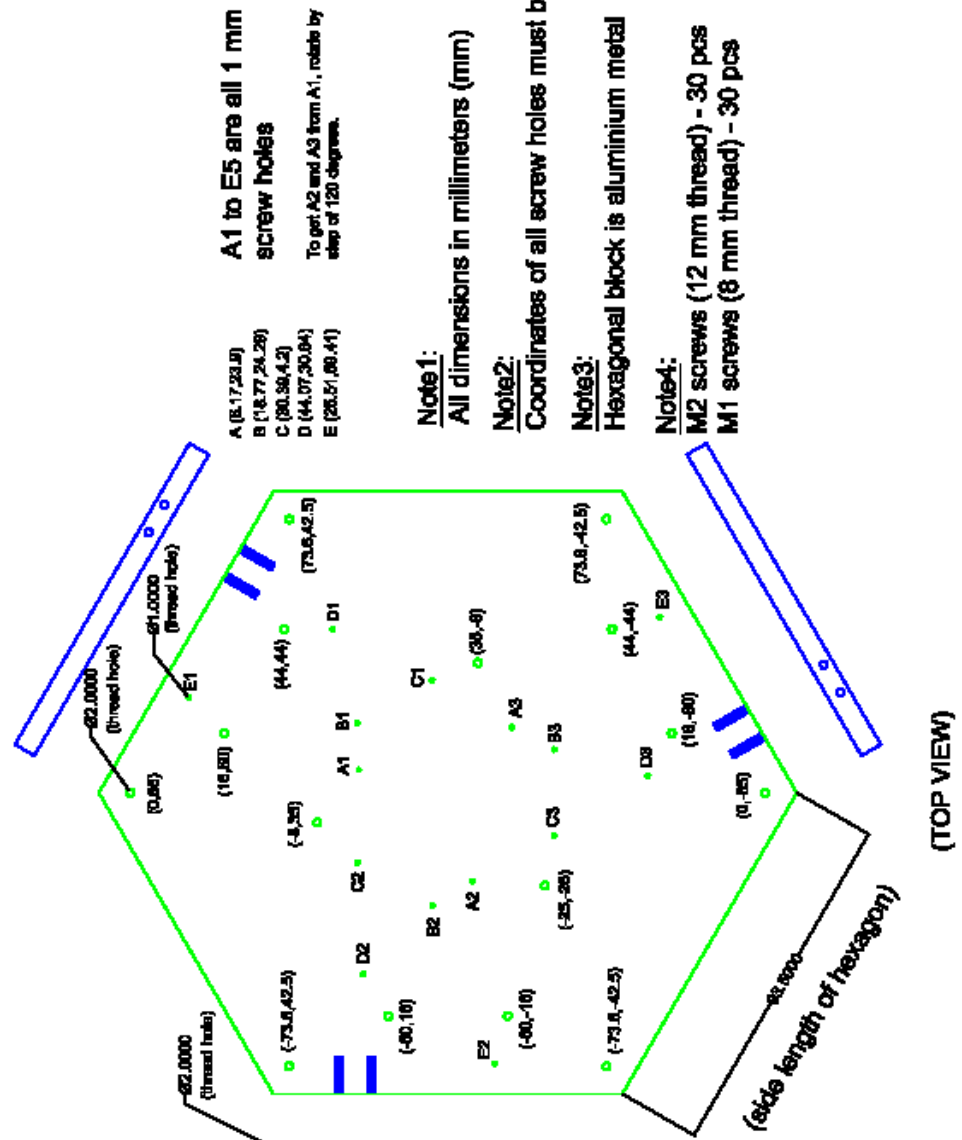
(TOP VIEW)



Part No: PT-HexaTuning  
 Name: Chua Ping Tyng  
 Mobile: 97363551  
 Email: g0202328@nus.edu.sg  
 Supervisor: Dr Jacob C. Coetzee

(M2 screw hole  
 3.500 mm from  
 top surface of  
 hexagon block)

Height of  
 hexagon block  
 = 6.000 mm



A1 to E5 are all 1 mm  
 screw holes

To get A2 and A3 from A1, rotate by  
 step of 120 degrees.

**Note1:**

All dimensions in millimeters (mm)

**Note2:**

Coordinates of all screw holes must be exact

**Note3:**

Hexagonal block is aluminium metal

**Note4:**

M2 screws (12 mm thread) - 30 pcs

M1 screws (8 mm thread) - 30 pcs



